

# Development of an adaptive shading device using a biomimetic approach

Redesign of the south facade of the Arab World Institute

Erik Pelicaen

*Master thesis submitted under the supervision of*

prof. dr. ir. arch. urb. Ahmed Z. Khan

prof. dr. ir. arch. Niels De Temmerman

*with the advices of*

ir. arch. François Denis

*Brussels Faculty of Engineering*

*Academic year*

*in order to be awarded the Master's Degree in*

2017-2018

Architectural Engineering



# Acknowledgements

The development of this master thesis research has been a long procedure in which many people have contributed to its realization and therefore deserve a word of thanks.

First of all, I would like to express my gratitude towards my supervisors Ahmed Z. Khan and Niels De Temmerman for their guidance, inspiring ideas and encouraging conversations. A special word of thanks goes to my advisor François Denis who followed up this work very closely and assisted to many problem-solving obstacles in the design process. Thank you Stijn Brancart for your advice on laser-cutting curved-line folding elements and Albert De Beir for your recommendations on 3D-printing. I would also like to acknowledge the research departments of MeMC and MECH for consultations and for borrowing equipment and measurement tools. Additional recognitions go to my fellow students at ARCH for being helpful with my models and patient with the many retakes of photos and videos. I also want to thank the supervisors and students at Fablab Brussels for their kind assistance in the prototyping process.

Secondly, I would like to thank my family – especially my mother and my grandparents – without whom this dissertation would not have been possible. Thank you for believing in me, for stimulating my motivation and for your financial support during the entirety of my academic career. Also, a big thanks to my brother to back me up in difficult times and encouraging my perseverance.

I would explicitly like to thank my housemates and my other friends for their humoristic distractions and enthusiastic interest and optimism towards my work. Last but not least, I want to thank our cat, Moris, who has been completely unaware of this event but is nevertheless unconditionally caring and affectionate.





# Abstract

The vast majority of existing buildings incorporating static facade systems are unable to regulate the energy metabolism of a building to changing environmental conditions. As there is an urgent demand for sustainable project developments and the building sector accounts for almost half of our total energy consumption, climate adaptive facades that are able to respond to varying weather conditions may contribute to meeting future energy targets. One of the first documented buildings integrating a kinetic shading system was the Arab World Institute (AWI) in Paris (1987). However, due to multiple failures and intensive maintenance, the mechanism was abandoned within six years after its inauguration. So far, no simplified mechanism has been proposed to substitute the AWI's rotating iris-like diaphragms relying on high-tech machinery.

Since nature has proven to be a valuable inspiration source for efficient design through millions of years of evolution, this master thesis investigates the potential of responsive biological systems to come up with biomimetic solutions in order to reduce the mechanical complexity of the diaphragms of the AWI. First, the south facade is given a coherent description by scanning literature on the classification of climate adaptive facades and the latest theories and developments of biomimetic building envelopes. Then follows an in-depth analysis of the south facade from an engineering as well as an architectural point of view, tackling technical problems, energy-related issues, and aesthetic qualities. The analysis is boiled down to a list of design parameters that serve as a set of verification and validation rules for the redesign of the facade. Next, five relevant case studies incorporating biomimetic adaptive facade systems are studied and compared to the AWI, providing a source of inspiration for the redesign and its practical execution. Subsequently, two biomimetic solutions are explored: thermo-bimetal curling and curved-line folding. Although the latter technique is studied more profoundly, both methods are inspected by predictions on energy performance, via simulation methods and by presenting a proof of concept through a prototyping process. Finally, the redesigns are verified and validated with respect to the pre-defined design parameters.

An innovative biomimetic solution using curved-line folding elements actuated by smart materials will be regarded as having great potential to replace the diaphragms of the AWI. Moreover, the implementation of dynamic elements in the facade may introduce a new period in Arabic architecture integrating traditional Islamic star patterns. Furthermore, a first step towards retrofitting climate adaptive facades is proposed through the development of a retrofitting methodology. By providing guidelines and recommendations for future research, the development of innovative adaptive facade systems is encouraged.



# Table of contents

Acknowledgements.....	i
Abstract.....	iii
Table of contents.....	v
List of figures .....	ix
List of tables.....	xix

## Chapter 1: Introduction

1.1	Problem statement.....	1
1.2	Research goals .....	4
1.3	Research methodology.....	5
1.4	Master thesis outline .....	5

## Chapter 2: State of the art

2.1	Arab World Institute .....	7
2.1.1	Location and implementation.....	8
2.1.2	Architectural concept .....	8
2.1.3	South facade.....	10
2.2	Climate adaptive facades.....	10
2.2.1	Definitions .....	11
2.2.2	Modulation and stimulus .....	11
2.2.3	Time- and adaptation scales.....	12
2.2.4	Control types.....	13
2.2.5	Adaptive shading systems.....	14
2.2.6	Retrofitting .....	15

2.3	Biomimicry in architecture.....	16
2.3.1	Biomimetic approaches.....	16
2.3.2	Biological role models.....	18
2.3.3	Transfer processes.....	19

## Chapter 3: Analysis

3.1	Arab World Institute.....	25
3.1.1	Control system .....	25
3.1.2	Mechanism and operability.....	26
3.1.3	Maintenance and failure.....	28
3.1.4	Energy performance .....	30
3.1.5	Biological inspiration.....	32
3.1.6	Aesthetics and Arabic references.....	33
3.1.7	Redesign parameters.....	35
3.2	Relevant case studies.....	37
3.2.1	Al Bahr Towers .....	37
3.2.2	HygroSkin .....	39
3.2.3	Air Flower .....	41
3.2.4	Flectofin®.....	43
3.2.5	Flectofold .....	45
3.2.6	Discussion.....	47

## Chapter 4: Exploration

4.1	Thermo-bimetal curling.....	49
4.1.1	State of the art.....	49
4.1.2	Redesign.....	51
4.1.3	Prototyping.....	55
4.2	Curved-line folding .....	58
4.2.1	State of the art.....	58
4.2.2	Redesign.....	60
4.2.3	Prototyping.....	66

## Chapter 5: Results and discussion

5.1	Verification.....	77
5.2	Validation.....	79

## Chapter 6: Conclusions

6.1	General overview.....	83
6.2	Review on two explorations.....	84
6.3	Proposal for a retrofitting methodology .....	86
6.4	Future Research.....	88

Bibliography.....	91
-------------------	----

Appendix .....	99
----------------	----

A Arab World Institute.....	99
-----------------------------	----

B Relevant case studies.....	103
------------------------------	-----

C Thermo-bimetal curling.....	110
-------------------------------	-----

D Curved-line folding.....	116
----------------------------	-----



## List of figures

<b>Figure 1:</b> The south facade of the Arab World Institute, counting 240 ‘mashrabiya’ modules, each containing 73 diaphragms ( ‘AD Classics: Institut Du Monde Arabe / Enrique Jan + Jean Nouvel + Architecture-Studio’ 2011).....	3
<b>Figure 2:</b> Biological role model (left), working principle (middle) and prototype (right) of the Flectofin® system (Lienhard et al. 2011). .....	3
<b>Figure 3:</b> <i>Left:</i> Location of the Institut du Monde Arabe, adjacent to the Seine river. <i>Right:</i> Plan of the first floor in its surroundings ( ‘Institut Du Monde Arabe   B&W Drawing, Site Plan’ n.d.). Remarkable is the courtyard which takes in about two thirds of the building site, allowing visitors to behold the south facade from any desired distance. ....	8
<b>Figure 4:</b> <i>Left:</i> In a London-based lecture in 1995, Jean Nouvel elucidated the importance of light entering the building through the south facade: “ <i>I began to consider the question of light at the Arab World Institute. The theme of light is reflected in the southern wall consisting entirely of camera-like diaphragms, and reappears in the stacking of stairs, the blurring of contours, the superimpositions, in reverberations, reflections and shadows</i> ” (Morgan 1998). <i>Right:</i> Traditional arabesque mashrabiya window. ....	9
<b>Figure 5:</b> <i>Left:</i> Venn-diagram classifying the fifteen areas of relevant physics of each CABS (Loonen et al. 2013). <i>Right:</i> Diagram illustrating the responsiveness types for an AKE (Wang, Beltran, and Kim 2012). Highlighted in yellow is the relevant domain for the south facade of the AWI.....	12
<b>Figure 6:</b> Diagram showing the classification of adaptive shading systems. The south facade of the AWI does not fit here as it is a kinetic ‘internal’ shading system instead of external.....	15
<b>Figure 7:</b> Biomimetic research methodologies: Bottom-up or ‘biology push’ (left) and top-down or ‘technology pull’ (right) process sequence (Knippers and Speck 2012). .....	17
<b>Figure 8:</b> <i>Left:</i> Visual representation of the biomimetic design concept generation (BioGen) methodology. <i>Right:</i> Demonstration of the theoretical application of the methodology by a water-harvesting envelope, inspired by the Namib Desert beetle. It relies on the morphological characteristics of this elytra, featuring hydrophilic (bumps) and hydrophobic (grooves) characteristics to capture condensation droplets (Badarnah and Kadri 2015). .....	21

<b>Figure 9:</b> Push-pull diagram for transferring bio-inspired motion principles into technical kinetic structures (Schleicher et al. 2015). It combines the bottom-up (biology push) and top-down (technology-pull) approaches in such a way that the actual transfer method resides in between them. The sizes of the circles reflect the range of possibilities for each step in the method.....	22
<b>Figure 10:</b> Biological role models investigated using the push-pull method (Schleicher 2015). The diagram shows the principles of movement and the conception of bio-inspired facade systems. Some of the nastic structures, such as the ones found in <i>Strelitzia reginae</i> and <i>Aldrovanda vesiculosa</i> have already been prototyped successfully. ....	23
<b>Figure 11:</b> Sequential operation of the panels in the following order: A1-I, B1-I, C1-I, D1-I, A2-I... A6-II, B6-II, C6-II, D6-II (adapted from 'ARCHITECTURE STUDIO - Arab World Institute' n.d.).....	27
<b>Figure 12:</b> <i>Left:</i> Rear view of a south facade module of the AWI. The opening and closure of the diaphragms occurs by actuation of two servomotors. <i>Middle:</i> Open and closed configuration of the central diaphragm. <i>Right:</i> Open and closed configuration of one of the small diaphragms, accentuating an 8-pointed Islamic star ('Architecture' 2016). ....	27
<b>Figure 13:</b> Mechanism of one of the shutters. Similar to camera diaphragms, the metal plates undergo a rotational movement by an actuated movement of adjustable sliders (Sharaidin 2014).....	28
<b>Figure 14:</b> <i>Left:</i> A south facade panel containing 57 out of 73 operable diaphragms. The non-functional diaphragms are shown in red and the ones actuated by the two servomotors are indicated in yellow and blue (Meagher 2015). <i>Right:</i> Detailed elevation of the rear view of a mashrabiya module. The right servomotor actuates the largest and the medium-sized diaphragms, while the left activates the small ones ('Moucharabiehs de l' Institut Du Monde Arabe à Paris' n.d.). ....	28
<b>Figure 15:</b> <i>Left:</i> Servomotor actuating a piston connected to rods. <i>Middle:</i> Actuator moving freely after the failure of a mechanical pin. <i>Right:</i> Damage of the arm transmitting the force of the servomotor to the diaphragm mechanism (the author 2016).....	29
<b>Figure 16:</b> Open (left) and closed (right) configuration of one south facade module of the Arab World Institute (the author 2017). The total aperture area ratio of the module is calculated by multiplying the aperture area ratio for each component by the number of components in the module, divided by the total surface area of the 210 x 210 cm module. ....	30
<b>Figure 17:</b> Biomimetic analogy of the human eye with the diaphragm of a camera (Quemere 2007).....	32
<b>Figure 18:</b> Two-dimensional iris mechanism in open (left), intermediate (middle) and closed (right) configuration (adapted from You and Pellegrino 1997).....	33
<b>Figure 19:</b> <i>Left:</i> Geometric study for the design of the diaphragms. An analysis was made for the two-dimensional rotation of the diaphragm blades to evoke Arabic geometric shapes such as the 8-pointed star, the hexagon, the circle and the square (Tonka and Fessy 1988). <i>Right:</i> Digital reconstruction of the hexagonal and 8-pointed star perforations in the module periphery (the author 2018).....	34
<b>Figure 20:</b> <i>Left:</i> Representation of a 'blank' module of the AWI, leaving out the diaphragms. <i>Right:</i> With the periphery of perforations left untouched, the only focus area left for the redesign becomes the square components inside the framework: 1 large component. 16 medium-sized and 64 small ones. ....	35



<b>Figure 21:</b> <i>Left and middle:</i> Views of the Al Bahr Towers in Abu Dhabi (Karanouh and Kerber 2015). <i>Right:</i> Hexagonal composition of triangular origami units in open and closed configurations ( ‘Al Bahr Towers   Aedas - Arch20.Com’ n.d.).	37
<b>Figure 22:</b> <i>Left:</i> Section illustrating the connection to the facade ( ‘Al Bahar Towers - Data, Photos & Plans - WikiArquitectura’ n.d.). <i>Right:</i> Operation scheme of one unit of the Al Bahr Towers (the author 2018).	38
<b>Figure 23:</b> Representation of the Al Bahr Towers components in open (left) and closed (right) configurations, inserted in a blank module of the AWI.	39
<b>Figure 24:</b> <i>Left:</i> A temporary outdoor exhibition of the HygroSkin Pavilion in Stuttgart, Germany (Reichert, Menges, and Correa 2015). <i>Right:</i> A conifer cone opening up its scales when the moisture content decreases (Holstov, Farmer, and Bridgens 2017).	40
<b>Figure 25:</b> <i>Left:</i> Bending of a hygromorphic composite due to differential hygroexpansion of the layers (Holstov, Bridgens, and Farmer 2015). <i>Right:</i> Operation scheme of one unit of the HygroSkin Pavilion (the author 2018).	40
<b>Figure 26:</b> Representation of the HygroSkin components in open (left) and closed (right) configurations, inserted in a blank module of the AWI.	41
<b>Figure 27:</b> <i>Left:</i> Rendering of the Air Flower prototype in a single or double facade system. <i>Right:</i> A yellow crocus opening its petals in response to an increase in temperature ( ‘Air Flower’ n.d.).	42
<b>Figure 28:</b> <i>Left:</i> Diagram illustrating the shape memory effect of the custom-made SMA wire ( ‘Air Flower’ n.d.). <i>Right:</i> Operation scheme of one unit of the Air Flower (the author 2018).	42
<b>Figure 29:</b> Representation of the Air Flower components in open (left) and closed (right) configurations, inserted in a blank module of the AWI.	43
<b>Figure 30:</b> <i>Left:</i> The Flectofin® facade in a full-scale prototype (Lienhard et al. 2011). <i>Right:</i> Pollination of the Bird-of-Paradise flower by a weaver bird (Schleicher 2015). The mechanical force of the bird’s weight is transferred to a flapping motion of two petal wings.	43
<b>Figure 31:</b> <i>Left:</i> Physical model (top) showing the working principle of the pollination mechanism and prototype (bottom) illustrating the location of glass fibre reinforcements (Lienhard et al. 2010). <i>Right:</i> Operation scheme of one Flectofin unit (the author 2018).	44
<b>Figure 32:</b> Representation of the Flectofin® components in open (left) and closed (right) configurations, inserted in a blank module of the AWI.	45
<b>Figure 33:</b> <i>Left:</i> Flectofold Large Scale Demonstrator at the Baubionik Exhibition 2017 (Saffarian 2017). <i>Right:</i> The trap leaves of the waterwheel plant are closing when small prey trigger its sensory hairs (Schleicher et al. 2015).	46
<b>Figure 34:</b> <i>Left:</i> Exploded composition scheme of the layered build-up of a Flectofold unit (Körner et al. 2016). <i>Right:</i> Operation scheme of the one Flectofold unit (the author 2018).	46
<b>Figure 35:</b> Representation of the Flectofold components in open (left) and closed (right) configurations, inserted in a blank module of the AWI.	47

<b>Figure 36:</b> <i>Left:</i> Inward bending of flower caused by rapid growth of the outer petals. <i>Middle:</i> Outward bending due to the rapid growth of the inner petals. <i>Right:</i> Bending of a cantilevered thermo-bimetal strip at a raised temperature (adapted from Foged and Pasold 2010).	50
<b>Figure 37:</b> <i>Left:</i> More deformation occurs in the cantilevered thermo-bimetal than the centre-pinned due to more operable length. <i>Middle:</i> Street view of the Bloom Pavilion, containing over 9000 unique pieces of thermo-bimetal, each designated to a different performance benchmark. <i>Right:</i> A select fraction of the strips curl a pre-defined amount to shade or ventilate when exposed to solar radiation (adapted from D. Sung 2016).	51
<b>Figure 38:</b> <i>Top:</i> Two rays growing from the midpoint of a polygon's side. The ray origins can be separated by distance $\delta$ to form overlapping star patterns. <i>Bottom:</i> Demonstration of Hankin's method, applied to a 4.8.8 tessellation (adapted from Kaplan 2005).	52
<b>Figure 39:</b> <i>Top:</i> Possible intermediate (left) and closed (right) configurations of the central component of the AWI, substituted by a 4.8.8 tessellation with bimetal strips. The triangular (red) and quadrangular (blue) pieces are split in two for enhanced performance. <i>Bottom:</i> Discrete representation of the whole range of intermediate states in a 4.8.8 tessellation, for various contact angles $\theta$ , the demonstrating the potential for dynamic elements in an adaptive facade system (adapted from Lee, Kim, and Jeon 2015).	53
<b>Figure 40:</b> Simulation of an intermediate state occurring at 30°C (left) and a fully opened configuration at 45°C (right). The inner edges of the bimetal strips show the surface subdivisions and thus the degree of accuracy of the geometric simulation.	54
<b>Figure 41:</b> Closed (left) at room temperature and open (right) at $\pm 100^\circ\text{C}$ configuration of the component with uncut bimetal sheets.	56
<b>Figure 42:</b> Closed (left) at room temperature and open (right) at $\pm 100^\circ\text{C}$ configuration of the component with cut bimetal sheets.	56
<b>Figure 43:</b> Open (left) at room temperature and closed (right) at $\pm 100^\circ\text{C}$ configuration of the component with perpendicular sheets.	56
<b>Figure 44:</b> Illustrations of one triangular bimetal sheet that is pre-bent by an elastic cord.	57
<b>Figure 45:</b> Open (left) at room temperature and closed (right) at $\pm 100^\circ\text{C}$ configuration of the component with pre-bent sheets.	57
<b>Figure 46:</b> A curved-line folding element with three concave creases. The flaps fold upwards around the creases when the spine is bent (Vergauwen 2016).	59
<b>Figure 47:</b> <i>Top:</i> Horizontal actuation using a winch and three cables. <i>Middle:</i> Vertical actuation using a central actuator bar and three sliding bars. <i>Bottom:</i> Combined actuation using a central actuator bar and a double layer (adapted from Vergauwen 2016).	61
<b>Figure 48:</b> From left to right: two concave creases, two convex creases, three concave creases, three convex creases, four concave creases (Goetschalckx 2015).	61
<b>Figure 49:</b> Open (top), intermediate (middle) and closed (bottom) configuration of the redesign of the AWI's south facade with curved-line folding elements.	64

<b>Figure 50:</b> Simulation of two intermediate configurations of the redesign of the AWI's south facade with curved-line folding elements.....	66
<b>Figure 51:</b> Folding force measurement set-up of the five curved-line folding elements with a thickness of 0,5 mm. The same set-up was made for elements with a thickness of 0,8 mm. ....	67
<b>Figure 52:</b> Measurements of the folding force $F_f$ of a 3-crease 6.6.6 element (left) and a 2-crease convex 4.4.4.4 element (right) using an analogue dynamometer. ....	67
<b>Figure 53:</b> Small difference in folding position between the element in its folded position (left) and unfolded position (right).....	69
<b>Figure 54:</b> Scheme of the forces operating on the conical pressure spring. The folding force $F_f$ will cause the spring to compress to from length $L_0$ to length $L_1$ . A vertical point load $F_p$ compresses the spring to length $L_2$ . ....	69
<b>Figure 55:</b> <i>Left:</i> Visualization of the conical spring. <i>Middle:</i> Element in folded position. <i>Right:</i> Unfolding under a vertical point load. ....	69
<b>Figure 56:</b> Variations of the elastic spine's dimensions by shorter boundary segments. From left to right: 5, 10, 15 and 20 mm indent.....	70
<b>Figure 57:</b> <i>Left:</i> Front view of the pre-bent layer where the height should at least be equal to the interlayer height $L_i$ . <i>Right:</i> Visualization of the crease length $L_c$ of the pre-bent spine and the flat element.....	71
<b>Figure 58:</b> <i>Left:</i> Visualization of the pre-bent spine. <i>Middle:</i> Element in folded position. <i>Right:</i> Unfolding under a vertical point load. ....	71
<b>Figure 59:</b> Closed (left) and open (right) element when applying an electrical current to the Nitinol wire..	73
<b>Figure 60:</b> Front (left) and rear (right) view of a 6.6.6 component frame for the actuation of one curved-line folding element. The SMA wire (blue) is guided around a series of pulleys to minimize friction. The empty holes in the frame indicate the location of the other elements and the extended actuation system for six elements. ....	73
<b>Figure 61:</b> Closed (left) and open (right) element in a 6.6.6 component when applying an electrical current to the Nitinol wire.....	73
<b>Figure 62:</b> <i>Top:</i> Closed (left) at room temperature and intermediate (right) at $\pm 60^\circ\text{C}$ configuration of one element actuated by ambient heat. <i>Bottom:</i> Open (left) at $\pm 70^\circ\text{C}$ and closed (right) configuration at room temperature. The element is visibly less pre-folded after one actuation by ambient heat. ....	75
<b>Figure 63:</b> Visual representation of the aperture area ratio for the Arab World Institute (AWI), the thermo-bimetal curling (TBC) and the curved-line folding (CLF) design. The left (lower) boundaries show the values for the closed configurations while the right (upper) boundaries show the values for the open configurations. The dashed line corresponds to the central component, the filled line to the entire module and the zigzagged line is an assumption on the prototype.....	81

**Figure 64:** Diagram of the retrofitting methodology proposal representing the steps to be taken for retrofitting a climate adaptive facade (CAF). The grey parts depict the specific case for this thesis, while the black parts reveal the general methodology.....87

**Figure A - 1:** *Top-left:* Axonometric drawing. *Top-right:* Plan of the first floor ( ‘Institut Du Monde Arabe - Data, Photos & Plans’ n.d.). *Bottom:* North-south section ( ‘Équerre d’ argent 1987 / Jean Nouvel Architecture Studio – Institut du monde arabe – Paris V’ n.d.)......99

**Figure A - 2:** Summary of plans and sections ( ‘Featured Design - SlideShare’ n.d.). .....100

**Figure A - 3:** Constuction details of the mashrabiya modules of the south facade (Croquis 1994). .....100

**Figure A - 4:** Open (top) and closed (bottom) configurations of one module of the Arab World Institute (the author 2017).....101

**Figure A - 5:** View of one module from the outside (top) and inside (bottom) of the building (Aðalheiðr 2011). .....102

**Figure B - 1:** Conceptual diagram of the Al Bahr Towers illustrating the various inspiration sources from biological systems and traditional Arabic architecture (Karanouh and Kerber 2015).....103

**Figure B - 2:** Dynamic origami shading device inspired from the traditional mashrabiya window and the opening and closing sequences of blooming flowers (Karanouh and Kerber 2015).....104

**Figure B - 3:** Six triangular units inserted in an AWI component in open (left) and closed (right) configurations (the author 2018).....104

**Figure B - 4:** Visualization of the HygroSkin Paviliion from outside and inside (top) and the opening and closing of the hygroscopic wooden veneer sheets under influence of relative humidity changes (Reichert, Menges, and Correa 2015).....105

**Figure B - 5:** Demonstration of the shape-dependency of hygroscopic elements in relation to deformation under relative humidity changes. Generally, the curling is the largest for long and narrow strips (Reichert, Menges, and Correa 2015).....105

**Figure B - 6:** Six triangular sheets inserted in an AWI component in open (left) and closed (right) configurations (the author 2018).....106

**Figure B - 7:** Opening of the Air Flower by contraction of an SMA wire through application of a heat source ( ‘Air Flow(Er) - Thermally Active Architectural Skin’ n.d.). The contraction overcomes the tension of the elastic cords, making the panels rotate around tubes.....106

**Figure B - 8:** Exploded axonometry of the prototype’s assembly; 8 are the elastic cords and 9 is the SMA wire ( ‘Air Flower’ n.d.). .....106

**Figure B - 9:** Air Flower unit inserted in an AWI component in open (left) and closed (right) configurations (the author 2018).....107

<b>Figure B - 10:</b> Top: Non-autonomous movement of the pollination mechanism in <i>Strelitzia reginae</i> . Bottom: Abstracted working principle by means of a simple physical model. The bending of the backbone causes lateral torsional buckling in the attached fin and results in a sideways deflection of 90° (Lienhard et al. 2011).	107
<b>Figure B - 11:</b> Three Flectofin® units inserted in an AWI component in open (left) and closed (right) configurations (the author 2018).	108
<b>Figure B - 12:</b> Top: Kinematic model of the abstracted folding mechanism using a rigid origami simulator (Körner et al. 2016). Bottom: Kinetic model of the abstracted folding mechanism using finite element modelling (FEM) (Schleicher et al. 2015).	108
<b>Figure B - 13:</b> Actuation of the Flectofold prototype by a pneumatic cushion between the midrib and the backbone (Körner et al. 2018).	109
<b>Figure B - 14:</b> Open (left), intermediate (middle) and closed (right) configurations of one square framed component consisting of four Flectofolds. The intermediate state clearly accentuates a 4-pointed Islamic star pattern (the author 2018).	109
 <b>Figure C - 1:</b> Star patterns originating from different tessellations by implementation of Hankin's method for polygons in contact. Each row represents a tessellation that is transformed into an Islamic star pattern by changing the contact angle $\theta$ . The larger the contact angle, the more the stars are accentuated (Kaplan 2005).	110
<b>Figure C - 2:</b> Selection of the Grasshopper script for the parametric geometric simulation of thermo-bimetal curling for a 4.8.8 tessellation frame. From top to bottom: 1) Drawing of the tessellation (octagon part). 2) Calculation of the radius of curvature. 3) Definition for the central arc running through the middle of the triangular bimetal sheets. 4) Approximation of the movement for the triangle edges by a helicoidal transformation. The definition for the squares is similar as for the octagons.	111
<b>Figure C - 3:</b> Geometric simulation of the thermo-bimetal curling in a square 4.8.8 tessellation frame of 60 by 60 cm (central component of the AWI). Motion sequence starting at 20 °C (top-left) and ends at 70 °C (bottom-right) with an interval of 10 °C.	112
<b>Figure C - 4:</b> Comparison of four thermo-bimetal strips from room temperature (left) to $\pm 80$ °C (right). From left to right: 1) Strip proportions 1:5. 2) Strip with proportions 1:5/2. 3) Pre-bent strip with elastic cord flipping into a bi-stable position at $\pm 80$ °C. 4) Pre-bent strip by plastic deformation.	113
<b>Figure C - 5:</b> Motion sequence of the in-the-plane positioning of bimetal sheets in a 4.4.4.4 tessellation component of 15 by 15 cm. The experiment starts at room temperature and ends at $\pm 120$ °C.	113
<b>Figure C - 6:</b> Motion sequence of the out-of-plane positioning of bimetal sheets in a 4.4.4.4 tessellation component of 15 by 15 cm. The experiment starts at room temperature and ends at $\pm 110$ °C.	114
<b>Figure C - 7:</b> Wooden frames used for the prototypes. Left: In-the-plane positioning. This one was also used for the tests with pre-bent sheets by plastic deformation. Right: Out-of-plane positioning.	114

<b>Figure C - 8:</b> Motion sequence of bimetal sheets pre-bent by plastic deformation in a 4.4.4.4 tessellation component of 15 by 15 cm. The experiment starts at room temperature and ends at $\pm 120^{\circ}\text{C}$ .....	115
<b>Figure C - 9:</b> Datasheet of the thermostatic bimetal purchased from Auerhammer Metallwerk GmbH (‘Datasheets’ n.d.). The one used for the prototypes is highlighted and has one of the highest specific thermal curvatures available on the market.....	115
<b>Figure D - 1:</b> Section of the adaptive shading system developed by (Roger 2014) and adapted by (Vergauwen 2016). When the motor is activated, the threaded rod is either pushed upwards or pulled downwards. By connection of the additional spine to the threaded rod by means of a nut, the element performs a folding and unfolding movement. ....	116
<b>Figure D - 2:</b> Motion sequence of the medium-scale prototype developed by (Vergauwen 2016). The side length of the triangular curved-line folding element with 3 concave creases is 0,89 m and the spine width at the boundaries is 0,03 m.....	116
<b>Figure D - 3:</b> Representation a redesigned module of the AWI with curved-line folding elements in open (top) and intermediate (bottom) configurations, showing more polygons and Islamic star patterns than in the original design with diaphragms.....	117
<b>Figure D - 4:</b> From top to bottom: 1) Global view of the Grasshopper script for the kinematic simulation of the entire redesigned module of the AWI with curved-line folding elements. By clicking one Boolean toggle unit, all the elements in the module can be activated at once. The long vertical series of units are needed to copy the components to all the corresponding locations within the module. 2) Script for the simulation of the central component. 3) Daniel Piker’s definition for the kinematic simulation of origami elements. The folding pattern mesh is modelled in Rhinoceros and goes to the input of an Origami cluster unit along with the defined mountain folds and folding angles. The output is a set of forces and a new mesh, which serve as the input for the Kangaroo Live Physics unit to simulate the folding process.....	118
<b>Figure D - 5:</b> Motion sequence of the redesigned module with curved-line folding elements. The unfolding movement starts in the open configuration (top-left) and ends in the closed configuration (bottom-right) of the module.....	119
<b>Figure D - 6:</b> Datasheets for the Flexinol® actuator wire purchased from Dynalloy Inc. (‘DYNALLOY, Inc. Makers of Dynamic Alloys’ n.d.). From top to bottom: 1) Summary of the physical properties. 2) Electrical guidelines. The wire used for the prototypes is highlighted. 3) Stroke and available forces for some basic structures. The structure used in the prototypes is highlighted. ....	120
<b>Figure D - 7:</b> From top to bottom: 1) Wooden frame used for the pre-folding methods (left) and for the actuation methods with the Nitinol wire (right). The corners are round off to reduce stresses when the curved-line folding element is pushed to unfold. 2) Front (left) and rear (right) view of the 6.6.6 component frame with one curved-line folding element actuated by a Nitinol wire of $\pm 1$ m long. 3) Experimental set-up for the folding force measurements (left) and poor printing results for the elastic spine with nylon and plasticized copolyamide thermoplastic elastomer (PCTPE) filaments (right). 4) Evolution process for the pre-	

bent spine with polylactic acid (PLA) filament. A compromise between thickness and curvature was required to obtain a sufficiently strong spine that would not break when actuated by the Nitinol actuator wire. .... 121

**Figure D - 8:** Motion sequence of the curved-line folding element with a pre-bent spine under a vertical point load in frontal and top view. The bottom-right image shows the bi-stable position from which the element cannot return without mechanical effort..... 122

**Figure D - 9:** Motion sequence of the curved-line folding element actuated by electrical current. The time interval between the pictures is 10 s and the bottom-right is taken at 30 s after application of current..... 123

**Figure D - 10:** Burning of the heated actuator wire in the central hole of the pre-bent spine. The right image shows the plastic deformation of the spine due to excessive pulling of the wire when actuated. .... 123

**Figure D - 11:** Motion sequence of the curved-line folding element actuated by ambient heat in an acrylic glass box. The experiment starts at room temperature, the element starts to unfold at  $\pm 50\text{ }^{\circ}\text{C}$  and reaches a bi-stable state at  $\pm 70\text{ }^{\circ}\text{C}$ . At this point, the element requires mechanical effort to return to its folded state. .... 124





## List of tables

<b>Table 1:</b> Summary of the results for the aperture area ratio in open and closed configurations of one module of the AWI. ....	31
<b>Table 2:</b> Summary of the biomimetic principles.....	47
<b>Table 3:</b> Summary of the climate adaptive properties. ....	48
<b>Table 4:</b> Summary of the mechanical characteristics and energy performance predictions.....	48
<b>Table 5:</b> Results of the aperture area ratio for the central component of the thermo-bimetal-based redesign of the AWI. ....	55
<b>Table 6:</b> Demonstration of the method for framing tessellations with curved-line folding elements. The steps to be taken were explained earlier in this section and are included in the titles. The two right columns are showing the rear view of the component. The red indicates geometric shapes recurring in the AWI, the yellow depicts new Arabic references. ....	63
<b>Table 7:</b> Calculation of the aperture area ratio for one module of the curved-line folding based redesign of the AWI. ....	65
<b>Table 8:</b> Experimentally determined values of the folding force $F_f$ and the interlayer distance $L_i$ for two thicknesses $t$ . ....	68



## Chapter 1

# Introduction

*This master thesis in the field of architectural engineering explores the potential of biological responsive systems as an inspiration source for the development of climate adaptive facade systems. It focuses on the kinetic shading devices of the south facade modules of the Arab World Institute in Paris and proposes an alternative solution to its premature deficiency, based on responsive systems in nature.*

### 1.1 Problem statement

Since climate change, global overpopulation and urban migration are topics that have steadily gained awareness over the last few decades, the demand for sustainable solutions has increased significantly. Tackling environmental issues by lowering the ecological footprint on our planet is one of the greatest challenges we face today. As we are striving towards design for the Ecological Age (Khan, Vandevyvere, and Allacker 2013), it is paramount to develop new strategies and undertake paradigm shifts in order to achieve a low-energy future.

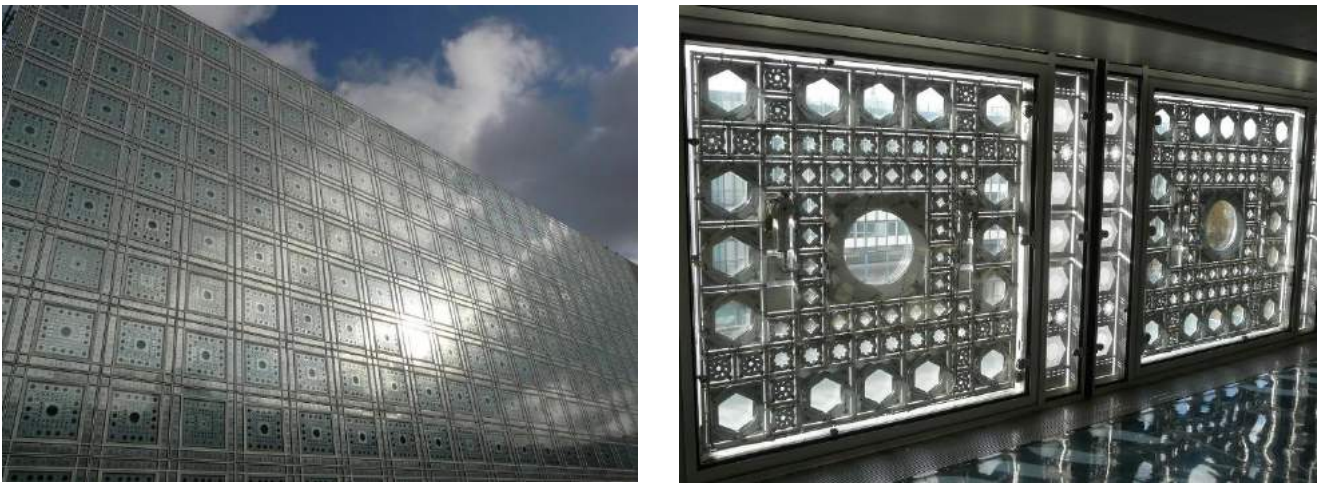
Recent recordings indicate that the building sector is responsible for the highest energy consumption, almost as large as the transportation and the industrial sector combined. Moreover, building envelopes account for more than 40% of heat losses during winter and overheating in the summertime (Barozzi et al. 2016). Furthermore, new studies reveal that on average 90% of the time spent by people in developed countries is in the indoor environment, which emphasizes the requirements for the well-being of people inside buildings (Aelenei, Aelenei, and Vieira 2016). Therefore, reductions of energy consumptions and CO<sub>2</sub>-emissions in the building industry must be addressed without compromising user comfort and welfare. Positioned at the interface of energy transmissions in buildings, facades can play a key role in the evolution towards energy-neutral buildings (Loonen et al. 2015). As the European Directive of 2010 aims at improving the energy efficiency of buildings by introducing Nearly Zero Energy Buildings (nZEBs) (‘Adaptive Facade Network – Europe’ n.d.), and building envelopes have a prevailing impact on energy performance, it is evident that facade technology awaits a design transition for the years to come. In order to meet our future energy targets, the

excessive reliability of mechanical devices to actively acclimate the indoor environment must be made redundant. Besides, such highly conditioned buildings “*may make the building insensitive to its environment and uncouple the building envelope from its role as an environmental moderator*” (Wang, Beltran, and Kim 2012). Although good progress is at hand in current facade design, conventional ‘static’ building shells dominate in a dynamic environmental landscape, meaning they are not able to respond to changing weather conditions and varying preferences of building occupants (Loonen, Trčka, and Hensen 2011). Therefore, “*multifunctional, adaptive, and dynamic facades can be considered the next big milestone in facade technology*” and may contribute to meeting the EU climate and energy sustainability goals (‘Adaptive Facade Network – Europe’ n.d.). Adaptive facade systems have the potential of working as a selective energy regulator, meaning it is able to alter its behaviour in response to external stimuli and thus only activates shading, lighting, ventilation, insulation etc., when passive energy saving or enhanced indoor comfort is demanded. Despite of advancements in technology, simulation tools and testing methods, few projects incorporating adaptive building skins have been realised (Alotaibi 2015).

The energy metabolism of a building, also known as thermoregulation, is done by an interaction of conduction, convection, evaporation, and radiation. The latter, when originating from solar rays, is essential for passive heating in cold climate conditions. However, in a warm environment, blocking the sun by means of shading devices is fundamental for a building’s prevention of heat gains. It is of crucial importance for obtaining thermal comfort in summer and as a part of the heat avoidance strategy, it is “*tier one of the three-tier design approach to cooling a building. The second tier consists of passive cooling, and the third uses mechanical equipment to cool whatever the strategies of tiers one and two could not accomplish*” (Lechner 2014). Since direct solar radiation can present local discomfort and overheating even in relatively cold climates, shading may be the most important passive design approach as it could be more energy efficient than any other solar strategy (Almusaed 2010). Hence, the focus of this master thesis resides in adaptive shading methods as a part of passive cooling strategies.

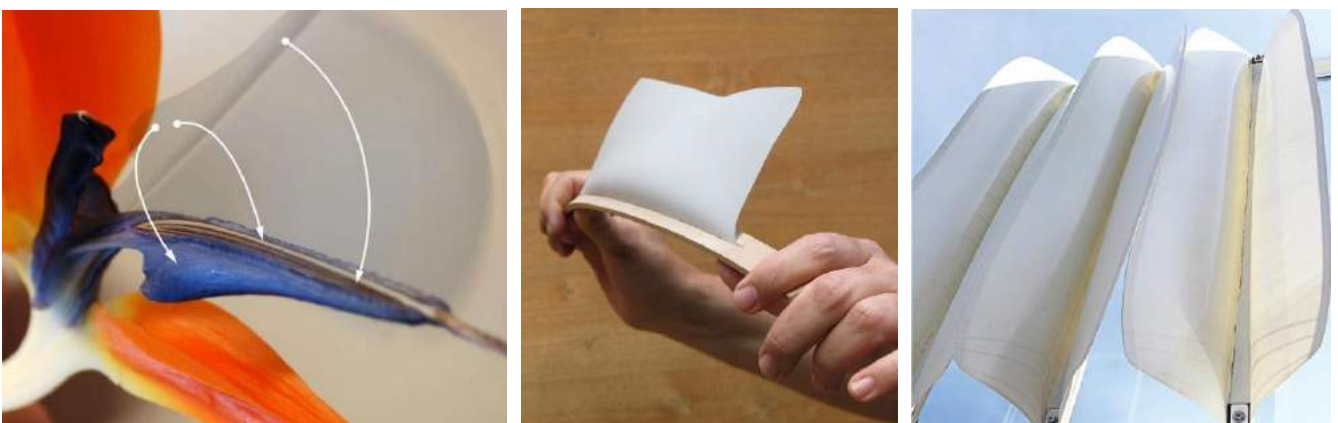
As the Arab World Institute (1987) is one of the first realizations of adaptive, kinetic architecture and a landmark in the heart of Paris, it is a quite famous building among architects, engineers, historians, and anthropologists. As illustrated in **Figure 1**, the south facade is entirely clad with modernized mashrabiya (traditional arabesque window) modules, consisting of iris-like diaphragms that open and close to passively regulate lighting and thermal comfort. Sadly, the diaphragms had become inoperable within six years after its inauguration, due to early failures of the mechanism and costly maintenance schemes. Now, with the celebration of its 30th anniversary, the building was renovated in 2017 by, amongst other things, repairing the mashrabiya modules and adding LEDs for a dynamic lighting display at night (‘Architecture’ 2016). However, replacing the modules by the exact same thing, only with newer materials, will probably result in a repeated scenario of the diaphragms ceasing to function prematurely. Strangely, retrofitting the modules by another, more reliable mechanism has not yet been explored. Moreover, reducing the complexity of the system by making use of hinge-less mechanisms instead of conventional rigid-body mechanics, has not been investigated.

It is therefore the objective of this thesis to examine the potential of biological responsive systems functioning by means of energy-efficient mechanisms, or in other words, to find an intelligent transformation from a complex organic system into a simplified mechanical solution.



**Figure 1:** The south facade of the Arab World Institute, counting 240 'mashrabiya' modules, each containing 73 diaphragms ('AD Classics: Institut Du Monde Arabe / Enrique Jan + Jean Nouvel + Architecture-Studio' 2011).

For 3.8 billion years, nature has gained experience in doing research and developing a vast collection of species that symbolize evolutionary success stories. This is why biological organisms can be interpreted as embodying technologies, waiting to be discovered in order to help humanity achieve the same or even greater efficiency by fewer means. Since the Ecological Age strives for sustainable, low-energy design, there is an urgent demand for innovative design solutions for which many lessons can be found in our natural environment. Biomimicry or biomimetic design can thus simply be formulated as "*the abstraction of good design from nature*", or more specifically as "*mimicking the functional basis of biological forms, processes and systems to produce sustainable solutions*" (Pawlyn 2011). Hence, the aim is to inspect ways of transferring evolutionary adaptations from biology into solutions for architectural design. Previous developments, such as the Flectofin<sup>®</sup> shading system (**Figure 2**), have been promising in their application and biomimetic transfer method and deliver a new view on innovative architectural accomplishments that have not yet been exploited extensively.



**Figure 2:** Biological role model (left), working principle (middle) and prototype (right) of the Flectofin<sup>®</sup> system (Lienhard et al. 2011).

## 1.2 Research goals

As mentioned in the previous paragraph, adaptive shading systems inspired by biological systems is an up-and-coming research field that has not yet been studied in depth. Furthermore, the kinetic facade of the Arab World Institute (AWI) is an interesting case study to investigate the potential of biomimetic shading devices. By cause of high mechanical complexity and difficult maintenance, the lifetime of the diaphragm mechanism remained very short. An alternative solution with reduced complexity, increased performance and a longer lifetime expectancy has not yet been proposed nor investigated. Hence, the main goal of this master thesis is to find a suitable biologically inspired mechanism to design a new module to retrofit those of the AWI's south facade. As the master thesis is done in the field of architectural engineering, the redesign comes along with care for aesthetics and with respect for the architectural concept of the building and its historic context. By combining both the architectural background and technical know-how a redesign for the south facade of the AWI can be proposed, which leads us to the central research question of this thesis:

*How can the south facade of the Arab World Institute be redesigned and redeveloped with a simplified kinetic shading device by searching for inspiration in biological responsive systems?*

The south facade of the AWI represents the focal point of this research, as it helps to frame the thesis to a more specific design problem. From this starting point, the extrapolation to other case studies may be initiated, as it provides a reference basis for the problem-solving of mechanical complexities of kinetic shading systems using a biomimetic approach. By studying several responsive systems in nature, it is examined whether they can answer to the mechanical challenges within the development of climate adaptive facades, which brings us to a more general research question:

*Can responsive systems in nature provide a valuable inspiration source for the development of climate adaptive shading systems?*

The outcome of this research will provide further insight into biomimetic shading systems and facilitate the design process of future kinetic facade retrofitting projects. Additionally, recommendations on the design and actuation of two explored bio-inspired shading techniques will assist the progress of future projects investigating the proposed methods. The idea is that other researchers and designers can use this master thesis as a reference work if they are to develop a bio-inspired kinetic shading system. Considering the aspect of renovating the south facade of the AWI, it is also a first step towards retrofitting existing climate adaptive building shells. As realized projects incorporating kinetic facades using conventional rigid-body mechanics will probably not last very long, this research can be used to find new, biologically inspired solutions suiting the architectural context. Moreover, the retrofitting methodology can be adapted and expanded to buildings with static facades. This may contribute to the prevention of buildings from being demolished due to their low energy performance and instead, to be retrofitted with an additional climate adaptive layer, lowering the energy demands for active thermoregulation.

## 1.3 Research methodology

The previous paragraphs introduced the notion of biomimicry and responsive systems. Nature provides a broad range of efficient self-activating mechanisms reactive to changing weather conditions, developed through billions of years of evolution by natural selection. Therefore, the main idea in the research methodology is to find a suitable biomimetic alternative design to solve the problem of mechanical deficiency of the diaphragms of the Arab World Institute. However, the analysis of such responsive systems requires a considerable amount of knowledge in the fields of biology, chemistry, and biomechanics. Thus, adaptive organisms in nature will not be investigated thoroughly within the scope of this thesis by means of biomechanical research methods. Instead, existing research on biological responsive systems will be used as a concept generator for the development of an adaptive shading device.

First, the modules of the south facade of the AWI are analysed from both an architectural as well as an engineering point of view. The aesthetics and references to traditional Arabic architecture are studied and the operation and mechanics of the diaphragms are examined more profoundly. This is boiled down to a list of design parameters that need to be taken into account for the redesign. Then, a series of relevant case studies are selected and compared to the AWI in order to comprehend the steps to be taken in the development of the adaptive shading system. The most promising bio-inspired techniques are tested in a preliminary way for the modules of the AWI. Once the most promising biomimetic solution is chosen, a parametric model is developed in which the kinetic movement is described and tested at the hand of geometric and kinematic simulations. In a preparatory way, this is evaluated in terms of aesthetics, energy performance and mechanical complexity. Then follows an exploratory procedure of physical modelling and prototyping, which determines the quality of the system from a mechanical perspective. The various approaches are scientifically documented to inform future researchers of design obstacles that can occur during the prototyping process. Finally, the results are discussed and an assessment of the design is made through validation and verification with regard to the redesign parameters.

## 1.4 Master thesis outline

Three principal sections build up the master thesis: (a) the state of the art, (b) the analysis and (c) the exploration. Chapter 2 gives a literature review about climate adaptive facades to provide a classification of the AWI's south facade and a general overview of biomimicry in architecture and potential transfer processes. In Chapter 3 follows a detailed analysis of the kinetic shading devices of the AWI. The modules are evaluated in relation to their control, operability, mechanism, energy performance, biological inspiration, and aesthetics. Then, the analysis is compressed into design parameters to be considered in the next chapter. The second part of Chapter 3 is a review of five case studies of biologically inspired adaptive facade systems that exist in a prototyped state. It will become clear in this section that compliant mechanisms in plant movements show

great potential for kinetic shading devices. In Chapter 4, two biomimetic techniques are explored: thermo-bimetal curling and a curved-line folding. The choice of the biomimetic systems is motivated and a state of the art on the current developments are summed up. The modules of the AWI are then redesigned and tested with simulations and a prediction on energy performance. It will be discovered that dynamic shading elements can cover a wide domain of Islamic star patterns, conceivably introducing a new period in Arabic architecture. Next, the bio-inspired kinetic shading devices are tested with physical models in a prototyping development process. Several prototypes will successfully be developed, either powered by electrical current or passively activated by ambient heat. In Chapter 5, the two explorations are assessed by discussing the results and by verification and validation with regard to the redesign parameters. Chapter 6 concludes this master thesis with a general overview, a review on the potential of the two bio-inspired techniques, a proposal for a retrofitting methodology and a summary of future research topics.



## Chapter 2

# State of the art

*The second chapter provides a brief summary of the architectural concept and qualities of the Arab World Institute, followed by an overview of the latest studies on the categorisation of climate adaptive facades. In this order, the adaptive behaviour of the south facade of the AWI can be assigned a more precise definition. Subsequently, the recent developments in biomimetic design methodologies are described, as well as the potential biological role models and transfer processes from responsive systems in biology to adaptive facade technologies.*

## 2.1 Arab World Institute

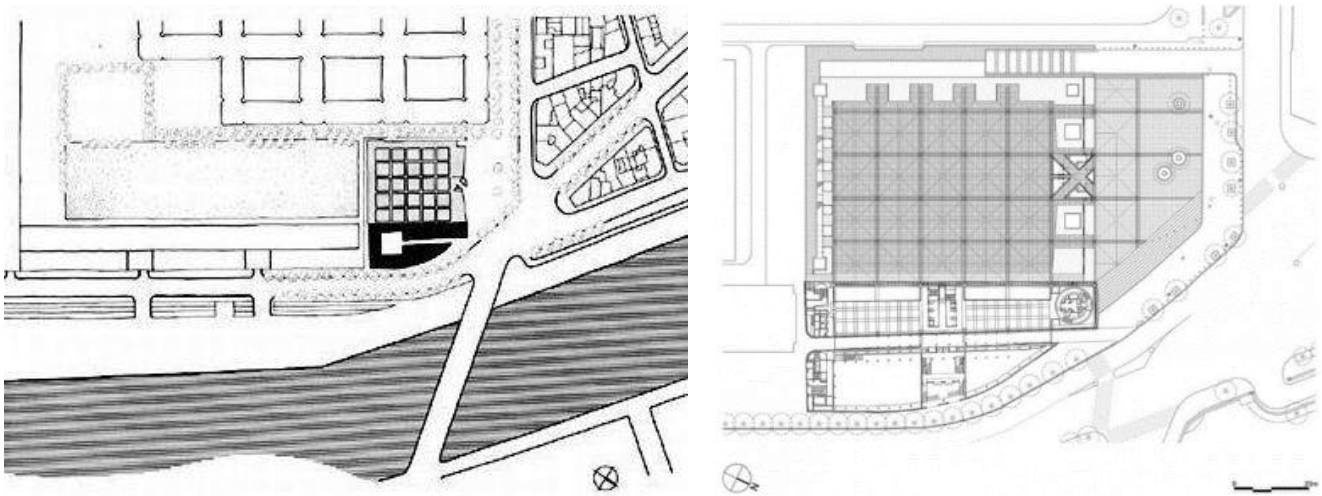
It was brought up in Chapter 1 that one of the first realized adaptive building skins was the south facade of the Arab World Institute (AWI) and it is selected as the principal case study for this master thesis for several reasons. Firstly, it is a renowned building amongst architects and engineers as it manifested a revolutionary facade technology on a large scale. Secondly, the facade is responsive to changing weather conditions and adapts its apertures to achieve thermal and visual comfort and reduce energy demands by means of shading, which was also indicated as a focus point for this master thesis. Thirdly, the building adopts a biomimetic approach by altering its kinetic system in a similar way the iris of the human eye does when exposed to changes in light intensity. Finally, due to its complex mechanism and operation, it was condemned to a premature failure.

An alternative biomimetic solution to replace the modules by a more durable and efficient system has not been speculated nor proposed in literature, which stimulates the objective of this thesis. Furthermore, it was also pointed out in Chapter 1 that the architectural qualities of the building needed to be taken into account for the redesign. Hence, a summary of the architectonic features of the building is given in this section, with special attention to the kinetic south facade. In Chapter 2, the adaptive behaviour and causes of failure of the mechanism, amongst other things, will be studied more in depth.

### 2.1.1 Location and implementation

The project competition for the AWI was won by Jean Nouvel in 1981, six years before its official opening. Funded by the French government and several Arab countries, the building was envisioned as a cultural hub in Paris expressing the partnership between France and the Middle-East. Accommodating a museum of Arabic history and culture, a library, conference rooms, meeting spaces, a resource centre, a cinema and a restaurant located on the roof, it remains one of the most visited edifices in Paris (Morgan 1998).

The museum is located in the quarter of Saint-Germain, on the border of the Jussieu University campus. Positioned at this interchange, its urban qualities form an easy transition between traditional Parisian architecture and the brutalist appearance of the campus. The north and south sections of the building are sliced in the middle by a narrow passage leading to a deep patio (Boissiere 1997). As illustrated in **Figure 3**, the triangular site on the south bank of the Seine river is curved to the north, following the streamline towards the Ile de la Cité. The northwest part of the building ends in a sharp prism pointing towards the Notre Dame Cathedral, emphasizing the entrance from the west side. The east part faces an open, paved area affiliated with the Jussieu campus, whereas the generous courtyard to the south confronts the university's built zone (Morgan 1998).



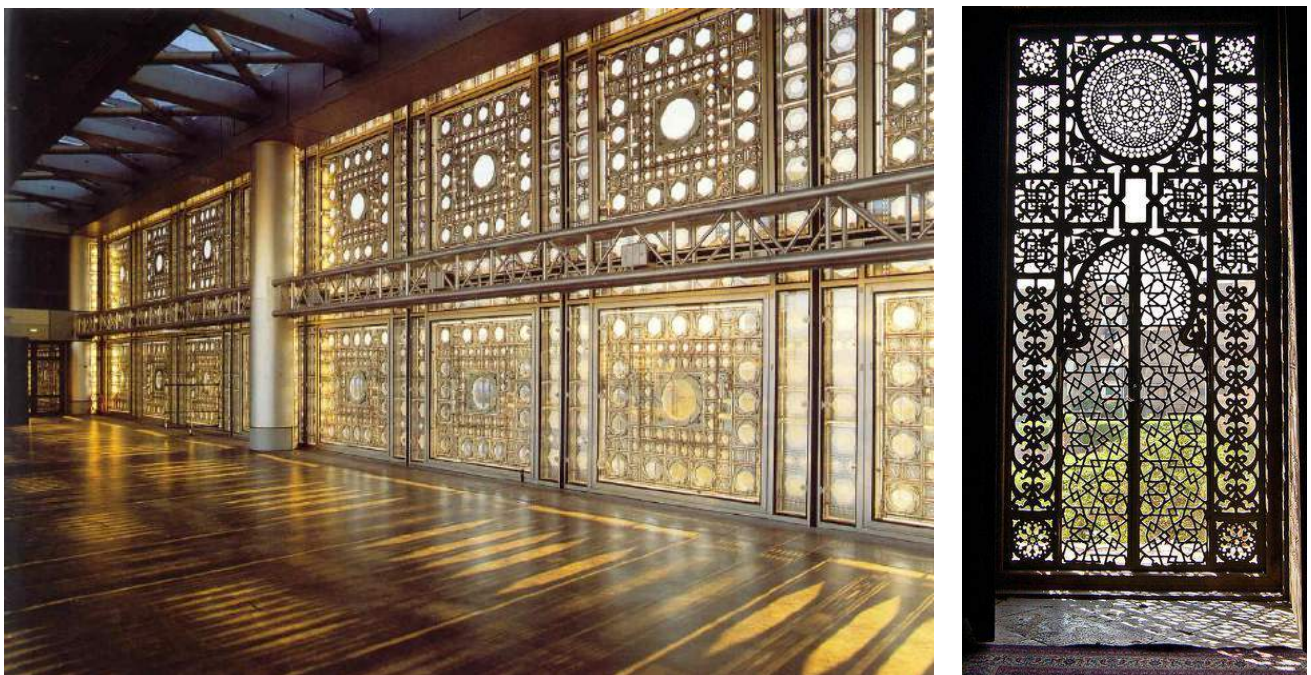
**Figure 3:** *Left:* Location of the Institut du Monde Arabe, adjacent to the Seine river. *Right:* Plan of the first floor in its surroundings (‘Institut Du Monde Arabe | B&W Drawing, Site Plan’ n.d.). Remarkable is the courtyard which takes in about two thirds of the building site, allowing visitors to behold the south facade from any desired distance.

### 2.1.2 Architectural concept

In several interviews, Nouvel underlines that the Arab World Institute is not an oriental building but a contemporary, occidental building using contemporary materials (Morgan 1998). Moreover, the building reflects an urban pivot between two different cultures and histories. *“If the south side of the building, with its motorized diaphragms, is a contemporary expression of eastern culture, the north side is a literal mirror of western culture: images of the Parisian cityscape across the Seine are enamelled on the exterior glass like chemicals over a photographic plate”* (‘Arab World Institute (AWI)’ n.d.). On the south facade, the geometric

patterns in the modern interpretation of the mashrabiya recall Arabic designs like the Alhambra in Granada (Morgan 1998). Other essential references to Arab culture are the spiral ramp and the patio, although the design preserves a humble distance to these allusions by redefining them with contemporary techniques and by approaching them in a Western way (Tonka 1990). The high-tech mechanical diaphragms in the south facade react to changes in light conditions and mimic the iris dilation and contraction (Figure 4). It is like a gazing facade with thousands of eyes controlling light levels and transparency.

The AWI can be considered as a modern metal building enveloped with glass, in which the supporting structure is concealed from the outside and revealed on the inside. The rigorous geometric approach is elaborated at the macro-scale in the space definitions and at the micro-scale in the continuous encounter of patterns evoking traditional Arabic architecture. The latter's characteristics are continually reappearing through an interaction of light and shadow by the ever-changing configuration of the south facade modules, arousing the aspect of privacy of the mashrabiya. For many, the success of the building lies in the dynamic features, or as Olivier Boissière beautifully describes: *"Expanding and confined spaces alternate in an otherworldly atmosphere created by the successive filters of the facades, the backlit shadows of the slim, criss-crossing staircases, and by the teeming geometrical motifs – squares, circles, hexagons – reflected, refracted, diffracted, and projected onto the walls, floors and ceilings in a swirling kaleidoscope like a shower of shooting stars."* (Boissière 1997). Besides, Nouvel describes it as being inside a film. As you walk through the building, the change of light levels and volumes can be experienced as an itinerary of different camera angles and diaphragm apertures. Through the dynamic perception of aperture and closure, the design is able to intensify a close relationship between architecture and cinematography (Morgan 1998).



**Figure 4:** Left: In a London-based lecture in 1995, Jean Nouvel elucidated the importance of light entering the building through the south facade: *"I began to consider the question of light at the Arab World Institute. The theme of light is reflected in the southern wall consisting entirely of camera-like diaphragms, and reappears in the stacking of stairs, the blurring of contours, the superimpositions, in reverberations, reflections and shadows"* (Morgan 1998). Right: Traditional arabesque mashrabiya window.

### 2.1.3 South facade

The major oriental depiction of the building was bound to be on the south side as it captures the most of sunlight. Moreover, the filtered view from the inside blurs the mediocre sight of the university campus and its attention to visitors is diverted from the outside by its monumentality (Tonka 1990). It must have been an extraordinary event in the first years of its existence to stand in the courtyard and behold the countless mechanical irises, clicking into different configurations across the glazed facade in response to the shifting intensities of sunlight (Meagher 2015). Aside from the iris imitation, it was also Nouvel's intention to evoke the mashrabiya, a wooden latticework window that regularly occurs in traditional Arabic architecture. The diaphragms can be interpreted as a “*sheer synthesis of ordinary modernity (photography and light), of Arab interiority (light variations), and of Arab essentiality (geometric patterns)*” (Tonka 1990). Used since the Middle Ages until the 20<sup>th</sup> century, the mashrabiya's primary function was to serve as a moderator of light, heat and ventilation: the dense geometric patterns provided privacy while retaining visibility, protected occupants from the hot desert sun and allowed cool winds to flow through. In the Arab World Institute, the diaphragms serve as a reference to this architectural tradition and maintain the ornamental quality as well as its ability to filter daylight and shade (Heylighen and Martin 2004).

The south facade consists of 240 identical, square mashrabiya modules with a side length of about three meters, sandwiched between two glass panes. Each of the modules contains a hierarchical composition of 73 diaphragms, set to execute 18 movements in a day (‘Architecture’ 2016), regulating the sunlight coming into the building by modifying the apertures. The techno-centricity of the facade is embodied in the vast amount of electrical parts such as sensors, processors and actuators, interconnected in a network of metallic elements, shifting and rotating to perform iris-like movements (Holstov, Farmer, and Bridgens 2017). However, due to exorbitant maintenance costs, regular replacement of components and numerous mechanical deficiencies, the kinetic operation of the system was abandoned in less than six years (Chaslin 2008). Then again, even with the mechanism being currently inactive, it still remains an emblematic instance of its kind and a valuable case study in understanding climate adaptive facades (Meagher 2015).

## 2.2 Climate adaptive facades

The necessity of integrating climate adaptive facades in buildings is a consequence of the increasing interest for sustainable design to lower energy demands for economic and ecological reasons. These energy demands are a fundamental effect of our survival behaviour: to build shelters for protection and for maintaining a constant body temperature. By continually modifying indoor climate conditions, either manually (windows, shades, blinds...) or mechanically (fans, air conditioning, heating...), we actively pursue equilibrium to counteract changing environmental conditions (Meagher 2015). Passive, adaptive facade systems provide a potential solution to maintain a stable indoor comfort whilst reducing the need for active adjustments by energy-consuming devices.

### 2.2.1 Definitions

Recent developments and realizations of building skins that interact with their environment have repeatedly been documented as promising and innovative (Wang, Beltran, and Kim 2012). In literature, many terms have been used to describe the nature of climate adaptive facades. Especially the adaptive behaviour has known many equivalents such as responsive, dynamic, kinetic, multifunctional, active, smart... to name a few (Loonen et al. 2013). The ambiguity of the terminology has triggered many researchers to conceive a precise definition of climate adaptive facades. Wang, Beltran and Kim described them as follows:

*“Acclimated Kinetic Envelopes (AKE) respond to the variable climatic environment by means of visible physical behaviours of building envelope components.”* (Wang, Beltran, and Kim 2012)

Interestingly, both terms are related to biology: ‘acclimated’ refers to the gradual adaptation of an organism to its changing environment by altering its behaviour or appearance; ‘kinetic’ originates from motion and signifies an organism’s response to a stimulus (Wang, Beltran, and Kim 2012). Another, the more detailed definition is given by Loonen et al.:

*“A Climate Adaptive Building Shell (CABS) has the ability to repeatedly and reversibly change its functions, features or behaviour over time in response to changing performance requirements and variable boundary conditions. By doing this, the building shell effectively seeks to improve overall building performance in terms of primary energy consumption while maintaining acceptable thermal and visual comfort conditions.”* (Loonen et al. 2013)

The latter interpretation provides a better understanding of the function and aim of climate adaptive facades. Aside from these definitions, many more such as Climate Adaptive Skin (CAS) and Intelligent Building Skins (IBS) exist. For this reason and for the sake of literary variation, several synonyms of this term will be used in this thesis. The following paragraphs discuss the various parameters that define a type of climate adaptive facade in order to get a better understanding of how it works. This way the case study of this thesis, the south facade of the Arab World Institute (AWI), can be defined in a precise manner.

### 2.2.2 Modulation and stimulus

The skin of a building sets the border between indoor and outdoor environments and attempts to regulate the energy metabolism of the building. It is an intersection where diverse physical interactions occur. By *“blocking, filtering, converting, collecting, storing or passing through the various energy fields”* (Loonen et al. 2013), each climate adaptive facade has its specific way of controlling its multi-physical nature. Loonen et al. define four overlapping domains of relevant physics for a CABS, which is visualized **Figure 5**. The diagram comprises fifteen unique possibilities of multi-physical interactions that can take place in a CABS design. The four physical domains are described this way:

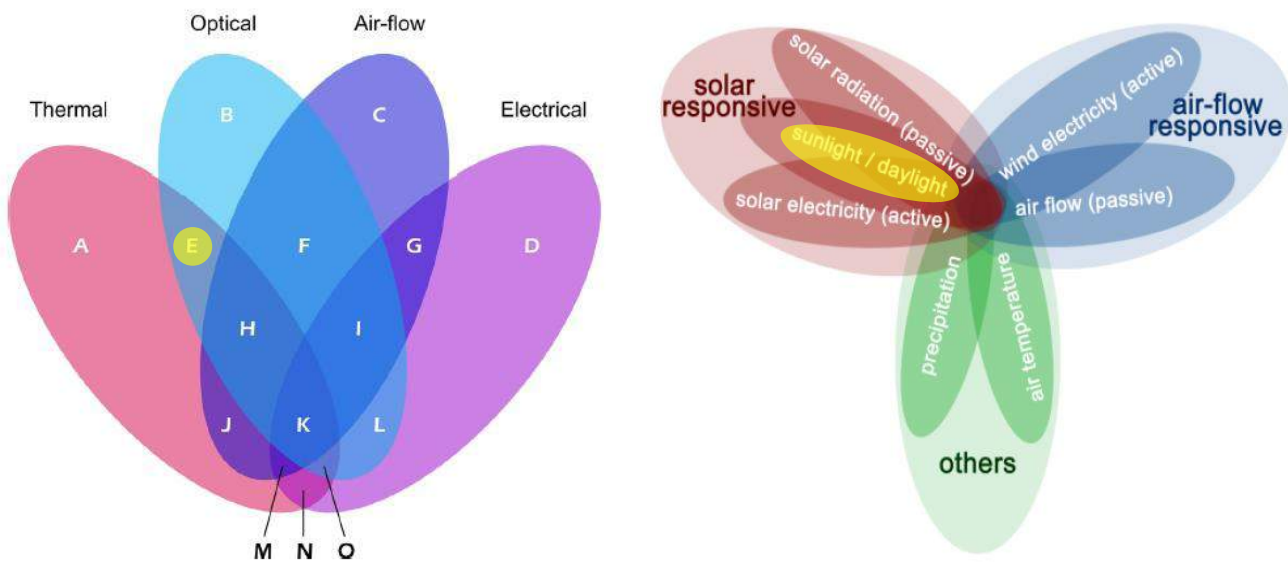


- Thermal** By convection, conduction and radiation the adaptive behaviour alters the energy balance.
- Optical** Adaptation changes the visual perception of occupants through transparent surfaces.
- Air-flow** The speed and direction of winds influence the adaptive nature.
- Electrical** The facade integrates energy generation mechanisms or electricity drives the adaptation.

A slightly different, simplified categorization was developed by Wang, Beltran and Kim. They subdivided adaptive facades by their response to a climatic source in three regions: solar responsive, air-flow responsive facades and others (precipitation or air temperature responsive). The two main categories can be interpreted as follows:

- Solar** Responsiveness is caused by solar radiation, daylight or to collect solar electricity.
- Air-flow** The facade responds to air exchange and circulation or convert wind energy into electricity.

Although the latter approach is more confined, the classification used by Loonen et al. provides a more general overview. As this method used a more exhaustive list of case studies, some climate adaptive facades cannot be categorized by with the model used by Wang, Beltran and Kim. Considering the physical domains explained above, it can be concluded that the south facade of the AWI uses ‘solar’ or ‘thermal and optical’ adaptation to control heat gains and maintain visual comfort.



**Figure 5:** *Left:* Venn-diagram classifying the fifteen areas of relevant physics of each CABS (Loonen et al. 2013). *Right:* Diagram illustrating the responsiveness types for an AKE (Wang, Beltran, and Kim 2012). Highlighted in yellow is the relevant domain for the south facade of the AWI.

### 2.2.3 Time- and adaptation scales

The miscellaneous environmental influences to which buildings are exposed occur at a certain timespan. The time domain of these effects can range from less than seconds to changes that can only be noticeable during the lifespan of a building. The most important time-scales for CABS are described by Loonen et al. in the following overview:

<b>Seconds</b>	Adaptation within the range of seconds occurs at very rapid changes in the environment, such as the abrupt alteration in wind direction and speed that trigger movement in kinetic facades using wind pressure as a stimulus.
<b>Minutes</b>	Sunlight availability and cloud cover can change over a timespan of minutes. Climate adaptive facades that make use of daylight optimization and shading strategies need to adjust their obstruction degree at this rate.
<b>Hours</b>	Adaptive facades that respond to changes in air temperature or track the sun's trajectory are typically required to adapt in the order of hours.
<b>Diurnal</b>	A rarely occurring time-scale adaptation is one following day-night cycles. Some constraints like solar exposure or ambient air temperature can be preconditions for changes at this rate.
<b>Seasons</b>	Especially for regions with high climate variations over seasonal changes, this is an interesting time-rate and can result in considerable profits regarding energy performance.

Since most kinetic facades are designed to respond to changes in solar radiation, the majority of climate adaptive facades fits in the category of the adaptation at the rate of minutes. As the south facade of the AWI responds to changes in light conditions, it can be considered to suit this classification as well. From a physical perspective, the adaptive behaviour of climate adaptive facades can be divided into two classes: adaptability at the micro scale or at the macro scale. They depend on the spatial resolution at which adaption takes place over a certain time-scale (Loonen et al. 2013). Adopting the categorization developed by Loonen et al., the difference in properties of the mechanisms is explained below:

<b>Macro</b>	The most known form of adaptive behaviour occurs at the macro scale through the integration of kinetic parts, indicating that there is an observable adaptation by moving parts. This can be obtained by altering the configuration of the facade via subsystems, components, subcomponents or motion of the entire facade.
<b>Micro</b>	Adaptive behaviour at the micro scale is achieved by altering the characteristics of a material at a molecular level. This can either be done by changing the thermophysical behaviour or by modifying the optical properties, which is more common for this adaptation scale. By shifting through a set of material states, the latter is able to regulate daylight and solar radiation.

By controlling daylight and regulating solar radiation using kinetic components (diaphragms), the south facade of the AWI clearly fits in the category of adaptive behaviour at a macro scale. Moreover, it can be said that it exploits the motion of subcomponents (diaphragm blades) to obtain its adaptive behaviour.

## 2.2.4 Control types

The use of an efficient system to control a climate adaptive facade is essential to a favourable operability and optimized occupant comfort. According to Loonen et al., the control systems can be subdivided into two categories: extrinsic and intrinsic control. A general description of both approaches along with their benefits and drawbacks is given hereunder.

- Extrinsic** The adaptive behaviour is obtained by a communication process between sensors, processors, and actuators. The control system can either be centralized by an all-encompassing mechanism or distributed through integration in local processors. The essence of an extrinsically controlled system is feedback: comparing a current situation (action) to a requested state (set-point).
- Intrinsic** Also called 'direct control', this type relies on the inherent characteristics of subcomponents. The adaptation is instantly triggered by changing environmental conditions, without the need for a signal coming from an external control unit. The elements composing the adaptive facade are acting like a sensor, processor and actuator simultaneously. In most cases, this is obtained by the introduction of smart materials in the kinetic device.

The principal disadvantage of intrinsic control is that intervention by building occupants is impossible. The materials were tailored in the design process to respond to a specific environmental state, meaning that unexpected disturbances can cause the system to not be as performative as intended. However, one of the main assets of this control system is the elimination of reliance on high-tech equipment such as sensor cells, computational processing tools and motorizing units. Furthermore, the energy required to activate the mechanism is made redundant as the elements immediately alter their configuration through a modified material state (Loonen et al. 2013). To conclude this paragraph, it can be deduced that the south facade of the AWI uses an extrinsic control system, depending on a large-scale interaction of sensors, processors and actuators.

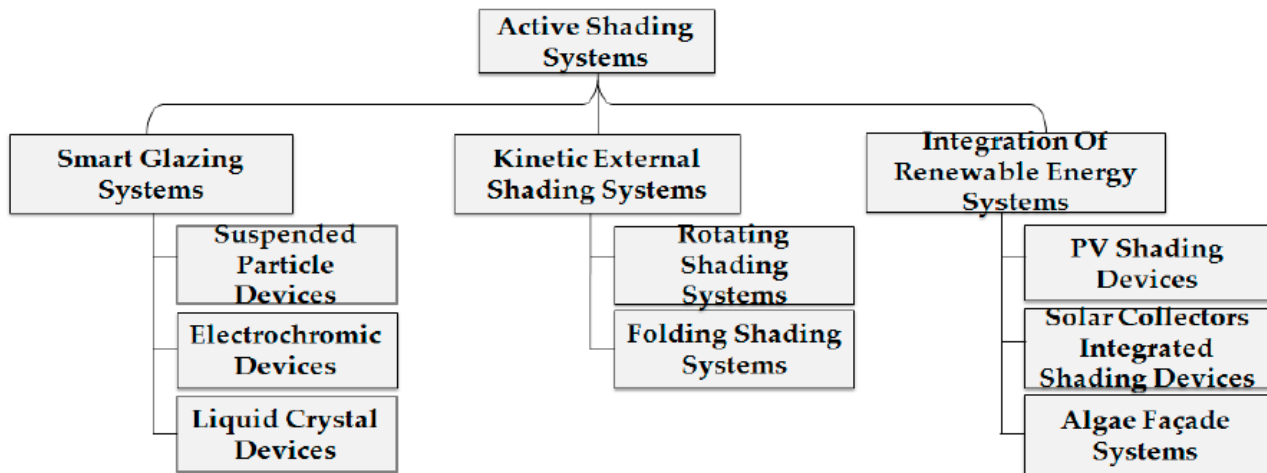
### 2.2.5 Adaptive shading systems

From 2010 until now, the increase of literature reporting on dynamic shading systems is remarkable. Automated daylighting and shading systems have more potential than static ones as the energy efficiency of a building is enhanced through equilibration of daylighting levels and solar obstruction (Konstantoglou and Tsangrassoulis 2016). Since the south facade of the AWI actively regulates daylight levels and aims to block solar radiation to maintain indoor comfort by means of shading, it can be considered as an adaptive shading system. As reported by Al Dakheel and Tabet Aoul, these devices can be subdivided into three classes: smart glazing systems, kinetic external shading systems and shading systems that integrate renewable energy (Al Dakheel and Tabet Aoul 2017). Visualized in **Figure 1**, each of these categories has a number of subcategories including the most common types.

Regarding kinetic shading systems, several interesting developments have been made in recent years. Firstly, hinge-less, biologically inspired devices show great potential and have not extensively been studied yet. Biomimetic approaches could solve engineering problems such as the improved distribution of materials and elastic reversible movements. Secondly, smart materials prove to be efficient actuators due to their shape memory properties and actuation velocity. Especially Shape Memory Alloys (SMA's) are promising because they have been investigated widely and present excellent results to fatigue tests, which is fundamental for cyclic movements in kinetic systems. Thirdly, elastic and light-weight materials are up-and-coming for the



application of kinetic elements, as they allow anisotropic compositions in order to optimize motion through reduced stresses and reversibility (Fiorito et al. 2016).



**Figure 6:** Diagram showing the classification of adaptive shading systems. The south facade of the AWI does not fit here as it is a kinetic ‘internal’ shading system instead of external.

Using the classification developed by Al Dakheel and Tabet Aoul, it is obvious to classify the south facade of the AWI within the kinetic shading systems, although it is internal instead of external as the diaphragm modules are sandwiched between two glass panes. Kinetic shading systems depend on “*mechanical, chemical and electrical engineering where folding, sliding, expanding, shrinking and transforming in the shading devices takes place*” (Moloney 2011). Since the AWI’s modules contain a composition of diaphragms blades rotating in two dimensions, it can be defined as a rotating shading system. To complete this section, the previous paragraphs have provided a more rigorous description of the main case study of this thesis:

*The south facade of the AWI is a climate adaptive facade responding to changes in light conditions over a time-scale of minutes, regulating incoming daylight and solar radiation by using a kinetic rotating shading system at a macro-scale through an extrinsic control system.*

## 2.2.6 Retrofitting

Many cities struggle with energy-consuming, outdated buildings due to aging structures and materials, old-fashioned technologies and facades with minimal amounts of insulation or prone to overheating. A common approach to cope with these issues is to demolish those buildings and replace them with modern sustainable constructions. However, this procedure is not always consistent regarding economic and environmental concerns. Therefore, the challenge to adapt these buildings to match current building standards, which can be done by retrofitting existing building skins with innovative climate responsive attachments. Moreover, the ease with which veteran facades can be retrofitted seems promising, as prefabricated units can be assembled ex-situ to result in a sped up in-situ connection (Dubois and de Bouw 2015). The Adaptive Facade Network in Europe reports that buildings with low energy performance have been successfully retrofitted with additional climate adaptive layers. It is considered a critical opportunity to retrofit building envelopes with facade

technologies that not existed at the time of the original design, in order to achieve increased energy efficiency to meet modern performance criteria ( 'Adaptive Facade Network – Europe' n.d.).

## 2.3 Biomimicry in architecture

As previously mentioned in Chapter 1, the aim of this thesis is to investigate biological responsive systems as a potential inspiration source for the development of an adaptive shading system to replace the defective diaphragms of the south facade of the AWI. Moreover, it was discussed in **Paragraphs 2.1.2 and 2.1.3** that the shutters of the AWI were inspired by the movement of the iris. Therefore, a literature review on the latest theories regarding biomimetic research in architecture, focusing on adaptive systems, is given in this section.

### 2.3.1 Biomimetic approaches

'Biomimicry', 'biomimetics' or 'bionics', is a concept that was firstly introduced in 1969 by Otto Schmitt. Assembled from the terms 'biology' and 'mimesis' or 'technics', it was essentially defined as "*the science that studies the replication in human's design of natural methods and processes*" (Schmitt 1969). A more recent definition describes biomimetics as "*the realization of technical applications based on insights resulting from fundamental biological research*" (Speck and Speck 2008). Nature provides a limitless source of efficient systems that have evolved over millions of years of evolution by natural selection (Bar-Cohen 2005). In biomimetic research, a collaboration between biologists, physicists, chemists, engineers and architects amongst others, can determine a very interdisciplinary mechanism for research and development projects (Knippers, Nickel, and Speck (eds.) 2016). At the basis of this kind of research stands the examination of biological organisms with regard to their relationships between form, structure and function, a study field called technical biology. By quantitative experimentation, it allows for a better comprehension of biological phenomena and sets the fundamentals for transfer processes towards technical applications (Speck and Speck 2008). As this is a final project in the field of architectural engineering, technical biology is not studied within the scope of this master thesis. Instead, knowledge on this topic will be derived from current research. According to their process sequences, two main methods of biomimetic R&D-projects can be distinguished, both of which are explained below and visualized in **Figure 7**.

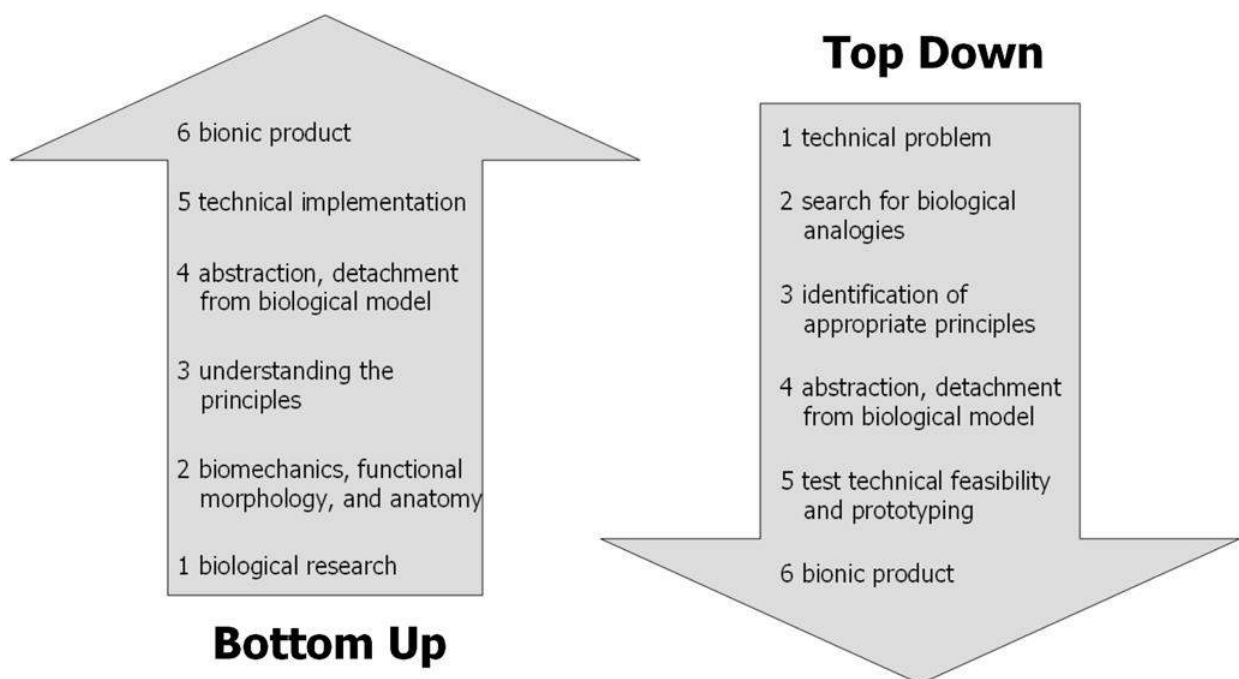
#### 2.3.1.1 Bottom-up

When the process starts from promising biological research to provide a range of solutions in fields like architecture or engineering, it is called a bottom-up approach (Vincent et al. 2006). The process starts with examination of the physiology and biomechanics of an organism. Subsequently, an accurate knowledge of the form-structure-function relations is derived from the quantitative analysis. Next, the working principles are isolated from the organism in the abstraction phase. Then follows a sequence of laboratory tests and engineering work using existing techniques to find a technical application. Finally, the product is optimized regarding the production process and cost (Speck and Speck 2008). In general, the bottom-up approach is

rather slow as it takes time (3-7 years) to discover technical functions, but it has high potential to uncover innovative applications (Vincent et al. 2006). Successful abstraction may lead to widely applied technical solutions, but it is a risky process as it must be originating from a sufficiently potential biological template and result in a viable technical application (Speck and Speck 2008).

### 2.3.1.2 Top-down

In the top-down process, research initiates from a well-defined technical problem and attempts to resolve it by using nature as a source to be mimicked (Vincent et al. 2006). The first stage is to define the problem from an engineering point of view and to determine boundary conditions. Later, a set of organisms that can provide a solution to the technical problem is explored by biologists and engineers. Then, the organisms with highest potential are chosen to be analysed in depth in order to abstract the working principle. Next, the engineers follow a transfer model and evaluate the feasibility to solve the problem. Ultimately, biomimetic prototypes are constructed, tested and industrialized in the case of success<sup>1</sup> (Speck and Speck 2008). Although this process is faster due to a reduced timespan (6-18 months) for the technical implementation phase, the confined technical problem may not present a high level of innovation (Vincent et al. 2006).



**Figure 7:** Biomimetic research methodologies: Bottom-up or 'biology push' (left) and top-down or 'technology pull' (right) process sequence (Knippers and Speck 2012).

As to the south facade of the AWI, neither of these processes corresponds to the approach of Jean Nouvel. The diaphragms were presumably developed as a mere evocation of the iris, and not as an investigated biomimetic product. This will be discussed more deeply in Chapter 3. Since the mechanical deficiency and maintenance-

<sup>1</sup> In an extended top-down process, several iterations of the basic research cycles are needed in order to increase the biomimetic improvement. (Speck and Speck 2008).

intensity of the modules clearly define a technical problem, the biomimetic top-down process will be the basis of inspiration in order to obtain an improved technological product.

### **2.3.2 Biological role models**

In both approaches that were discussed in the previous section, an essential phase is the investigation of suitable biological role models for a technical application. Knippers and Speck subdivided biological organisms into four categories with relation to their basic principles that can be transferred to architectural applications: Multifunctionality, anisotropy, heterogeneity and hierarchy (Knippers and Speck 2012). For the implementation of climate adaptive shading systems through a biomimetic approach, multifunctionality and anisotropy are the two most relevant characteristics. Multifunctionality indicates the combination of different elements with different functions into one entity, which can, for instance, be obtained with the integration of smart materials that can function both as a sensing and an actuating mechanism. Anisotropy is a property in natural systems essential for motion and deformation, that allows for optimal stress distribution by spatial distribution and orientation of fibres, which can in practice be obtained by fibre reinforced composites (Fiorito et al. 2016). In the following paragraphs, two types of biological responsive systems will be presented in which these features will occur.

#### **2.3.2.1 Adaptive surfaces – animals**

Through millions of years of evolution typified by extreme conditions, animals have progressively developed a vast array of skin structures to survive in these severe environments. Aside from harsh climates and geographical conditions, the drive for reproduction, the avoidance of predators and the hunting for prey have made animals cultivate fascinating multifunctional surfaces (Han et al. 2016). Lately, investigations from researchers in various disciplines have resulted in promising functional surfaces based on the involved interactions between physical and chemical characteristics and morphologies of animal skins (Al-Obaidi et al. 2017). Through particularities at both macro- and micro-scale resulting in hierarchical structures, animal skins obtain highly effective multifunctional surfaces to adapt to their environment. Recent biomimetic developments have succeeded in the adoption of these features for the fabrication of artificial functional surfaces (Han et al. 2016). Typical features are hydrophobicity, water capture, optical functions, anti-wear, low light reflection, anti-fog, self-cleaning, amongst others (Al-Obaidi et al. 2017). However, only few of these characteristics are interesting for the development of climate adaptive facades, such as water capture for evaporation purposes or low light reflection for insulation properties. Moreover, as the south facade of the AWI uses kinetic components at a macro-scale to provide shade, functional surfaces that adapt at a micro-scale are not the optimal source of inspiration for an adaptive shading system respecting the original design.

#### **2.3.2.2 Adaptive movements – plants**

As fauna relies on muscles to induce movement and flora produces metabolism-based motion, a promising branch in biomimicry regarding kinetic systems is the study of plant structures, also called phytomimetics

(Hensel and Menges 2008). Where animals produce motion by muscle contraction and relaxation, plants rely on the regulation of water pressure through their cells to allow for flexible movement, also termed nastic movements (Bar-Cohen 2005). Nastic movements or structures “*respond to an external stimulus regardless the direction of the stimuli inducing movement which is predominantly reversible*” (Fiorito et al. 2016) and exist in two different ways: autonomous movements, where the motorizing mechanism is integrated in the plant itself; and non-autonomous movements, where the motion is caused by an external mechanical force, which can occur in pollination by animals for instance (Hensel and Menges 2008). The reversibility of the movement is an important asset regarding kinetic architecture, as for example the folding/unfolding movements of plant leaves can provide inspiration for the conception of deployable systems (Al-Obaidi et al. 2017). Another feature of nastic structures is their anisotropy: the orientation and concentration of fibres can significantly improve the efficiency of the movement by minimal stresses (Fiorito et al. 2016).

Unlike animals using rigid-body mechanics to produce motion, the soft mechanics observed in flexible plant movements present a new paradigm in mechanical engineering. By successful transfer of motion principles into biomimetic devices, the use of technical hinges connecting rigid members can be replaced by living hinges allowing large elastic deformations (Schleicher et al. 2015). These flexible systems, also termed compliant mechanisms, are rarely used in classic mechanical engineering, they are abundantly present in nature. Especially when drawing inspiration from plants where compliant mechanisms occur in the form of folding and bending of flower petals and leaves, the mechanical complexity of bio-inspired devices can significantly be reduced by introducing hinge-less mechanisms with elastic properties (Lienhard et al. 2010).

Another important feature of compliant mechanisms in plant movements is the systematic exploitation of mechanical failure, diametrically opposed to classic engineering where these circumstances are consistently avoided. As the boundaries between material, structure and motion are blurred in plants, they are able to take advantage of failure mechanisms. For instance, interconnected parts can be triggered by a sequence of buckling failures to activate their deformation, resulting in the motion of the whole system (Schleicher 2015). Plant movements are therefore considered to be an up-and-coming research topic for the conception of climate adaptive facades, and more specifically on the development of kinetic shading elements. Concerning the south facade of the AWI, the overall complexity of the diaphragms can be highly reduced by searching for inspiration in compliant mechanisms found in plant movements.

### 2.3.3 Transfer processes

Another fundamental step in the bottom-up and top-down process is the transfer of the knowledge on a biological system to a technical application. It is the bottom line of biomimetic research, as it represents the intelligent abstraction of occurrences in nature towards the useful implementation of technology answering to human needs. A major challenge remains to define a clear methodology to be put into use for architectural design. In this section, two transfer methods are described: the BioGen method and the push-pull method.

Both approaches have proved to be valuable and have successfully managed to convert biological systems into concepts applicable to climate adaptive facades.

### 2.3.3.1 BioGen method

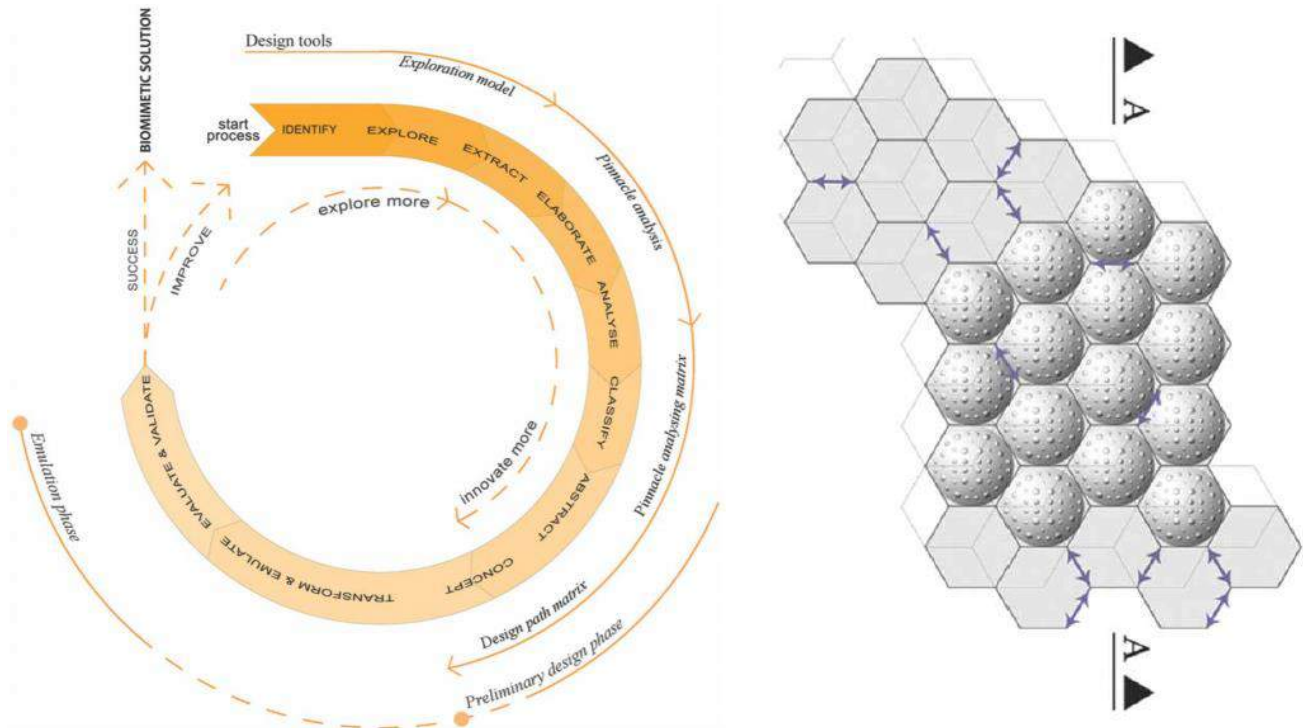
The BioGen method stands for ‘biomimetic design concept generation’, and its primary objective is to *“select dominant strategies that function simultaneously in nature and provide selective user-friendly tools, which facilitate the generation of preliminary design concepts”* (Badarnah and Kadri 2015). As part of a PhD research at Delft University of Technology, Badarnah and Kadri present a concept-generator for architectural design and is divided into three phases: the exploration model (1), which uses pre-defined design tools; the pinnacle<sup>2</sup> analysis (2), representing the biophysical investigation phase; and both the pinnacle analysing matrix and the design path matrix (3), which stand for the abstraction process. The exploration model starts by identifying the design problem and requirements, followed by an examination of natural (eco)systems and biological organisms and the isolation of the best-performing ones (pinnacles). In the pinnacle analysis, the pinnacles are investigated and elaborated more profoundly by examining their function according to their principles and strategies. The pinnacle analysing matrix performs a classification and abstraction on a combination of selected strategies and the design path matrix looks for a convergence in order to conceive a preliminary design, which is then evaluated. If the solution is not approved and further advancement is desired, the cycle is reinitiated by exploring other pinnacles. The application of this methodology was manifested by the conception of a water-harvesting building skin. Along with this development, the complete biomimetic transfer process of the BioGen method is illustrated in **Figure 8**.

Since the methodology starts with the definition of the design problem, it is considered to follow the top-down or ‘problem-based’ approach, in which the objective is to find a solution to a very specific design question (Badarnah and Kadri 2015). Although it serves as a convenient tool for problem-solving, it lacks a well-defined confined system for organizing and classifying gathered information (Al-Obaidi et al. 2017). Moreover, the complexity of the interdisciplinary procedure in the BioGen method can sometimes become too high and generate conflicts in between different strategies from a selection of pinnacles, which could arise only very lately (Badarnah and Knaack 2008). Another drawback of this process is the shortcoming of a clear transition from the abstracted biomimetic concept to the design and development phase (Al-Obaidi et al. 2017).

As the utilization of the BioGen methodology is limited to only one theoretical implementation, it is lacking reliability and feasibility for practical solutions. The transfer method presented in the following paragraph is supported by multiple adaptive concepts of which some have been prototyped successfully.

---

<sup>2</sup> A pinnacle is described in the BioGen method as a *“representative organism or system in nature for a particular adaptation strategy”* and features its significance and singularity as an abstraction source for adaptability (Badarnah and Kadri 2015).



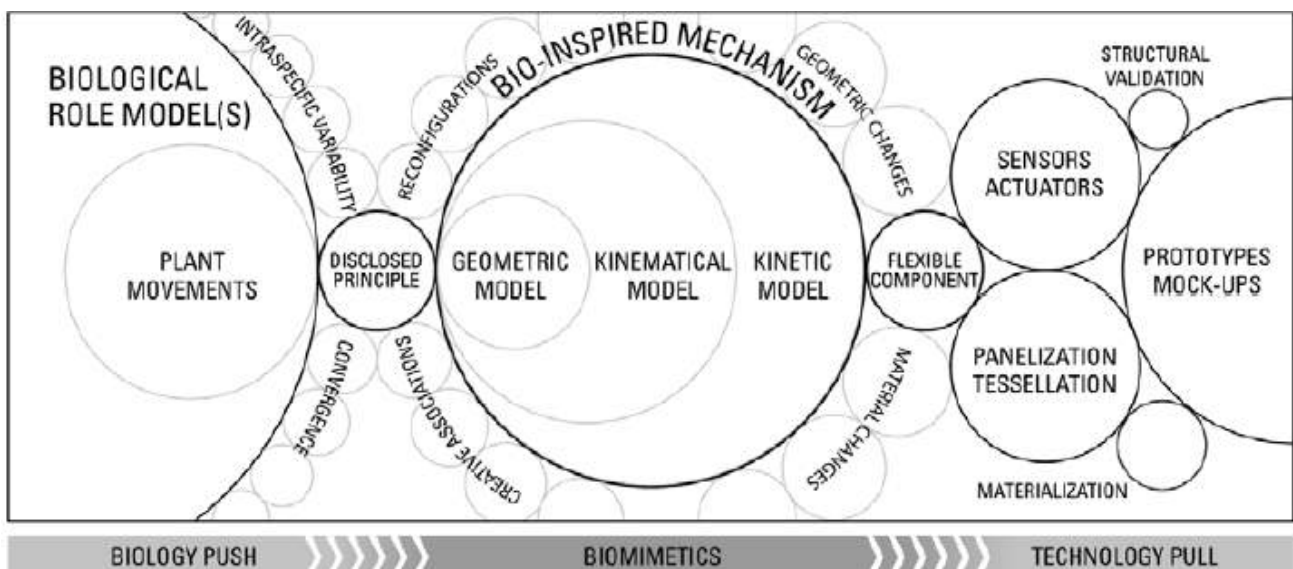
**Figure 8:** Left: Visual representation of the biomimetic design concept generation (BioGen) methodology. Right: Demonstration of the theoretical application of the methodology by a water-harvesting envelope, inspired by the Namib Desert beetle. It relies on the morphological characteristics of this elytra, featuring hydrophilic (bumps) and hydrophobic (grooves) characteristics to capture condensation droplets (Badarnah and Kadri 2015).

### 2.3.3.2 Push-pull method

It was discussed in Paragraph 2.3.2.2 that compliant mechanisms observed in plant movements show great potential for the application of climate adaptive shading systems. In this paragraph, a method for transferring motion principles from plants into technical devices will be explained. A clear linear development of the two main biomimetic research methods, as discussed in Paragraphs 2.3.1.1 and 2.3.1.2, is frequently difficult to obtain within the context of architectural developments. Therefore, a more detailed biomimetic research process was worked out as part of Schleicher's Ph.D. at the University of Stuttgart (Schleicher 2015), where the bottom-up (biology push) and top-down (technology pull) methods are both integrated into the development of kinetic structures based on plant movements. Figure 9 summarizes and visualizes this process, resulting from biomimetic studies on various nastic structures.

The first step in the push-pull methodology is to find a suitable biological role model (1), which in this case is restricted to the domain of plant movements responding to an external stimulus, also called nastic movements. Since the precise description of the moving organ through its composition requires anatomical and physiological expertise, this phase is usually done by biologists. Once the nastic structure is selected, the functional morphology (2) is described by identification and location of the essential parts responsible for the deformation. In this phase, a biomechanical analysis takes place by investigating the plants' actuation system, which can either be a consequence of hydraulic pressure changes in the cell tissue or resulting from the exploitation of elastic instabilities that enlarge or accelerate the movement, or by an external mechanical force.

The next step is to disclose the motion principle (3) by abstracting the plant organ's relationship between function and morphology by reducing the complexity of the nastic structure to a maximum extent in order to find the most elementary mechanism. Rather than literally mimicking the organism, the primary simplification of the mechanism may contribute to a greater design freedom on the long term, as the rearrangement of essential components can lead to the broad design exploration of simple or complex solutions. The following phase investigates the transformation of the working principle of the nastic structure to bio-inspired mechanisms (4). Instead of conventional rigid-body mechanics linking stiff parts with technical hinges, the compliant mechanisms detected in plant movements employ elastic deformation by flexible members through living hinges, able to significantly reduce the complexity of the biomimetic product. In order to develop a bio-inspired mechanism, the biological role model is reproduced in a series of computational models to obtain a better understanding of the mechanics at work. The accurate yet stationary geometric model (i) can be parametrized in order to generate a set of models varying in shape, size, and proportion. A kinematic model (ii) is able to describe the displacements and rotations of the mechanism by assigning degrees of freedom (DOF) and degrees of constraint (DOC). The kinetic model (iii) provides a full understanding of the motion by calculating the forms and forces when submitted to large elastic deformations, using Finite Element Analysis (FEA). A combined model (iv) would be able to integrate the three models in one simplified configuration for an enhanced information exchange and instantaneous feedback. Finally, conceptualizing the flexible component (5) consists in considering the application as a kinetic structure with regard to its requirements in terms of function, materials and loads. Concerning the spatial arrangements of the mechanism on a (double curved) surface tessellation and hereby the location possibilities of sensors and actuators, mock-ups or prototypes are developed to be tested and validated as a proof of concept (Schleicher et al. 2015).

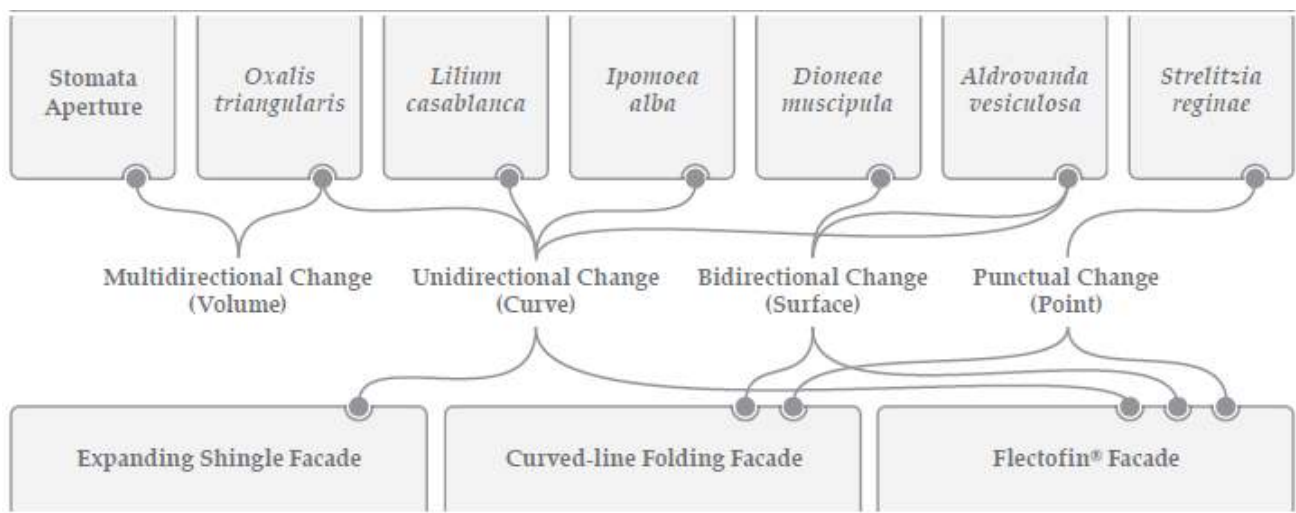


**Figure 9:** Push-pull diagram for transferring bio-inspired motion principles into technical kinetic structures (Schleicher et al. 2015). It combines the bottom-up (biology push) and top-down (technology-pull) approaches in such a way that the actual transfer method resides in between them. The sizes of the circles reflect the range of possibilities for each step in the method.

Following the methodology discussed above, the abstracted working principle of compliant mechanisms originating from nastic structures in plant movements shows promising results for the development of kinetic



shading systems. Multiple organisms (**Figure 10**) have been investigated using this approach, some of which have been prototyped successfully as adaptive shading systems such as the Flectofin® and Flectofold (Körner et al. 2018) mechanisms, which will be analysed in Chapter 3. Like in the BioGen method, one of the difficulties of this approach is the very interdisciplinary workflow, which is rather difficult to apply for this master thesis. For this reason, another method needs to be developed for the redesign of the south facade of the AWI, capable of bypassing the anatomical, physiological, chemical and biomechanical study of biological role models. A possible way of achieving this is to look into actual realizations of adaptive, biomimetic shading systems, from which concepts can be adopted and combined for the redesign. The next chapter provides an in-depth analysis of the AWI, along with five other case studies implementing biomimetic shading systems, from which inspiration will be drawn for the exploration phase of Chapter 4.



**Figure 10:** Biological role models investigated using the push-pull method (Schleicher 2015). The diagram shows the principles of movement and the conception of bio-inspired facade systems. Some of the nastic structures, such as the ones found in *Strelitzia reginae* and *Aldrovanda vesiculosa* have already been prototyped successfully.



## Chapter 3

# Analysis

*This chapter handles the south facade of the Arab World Institute more in detail, as well as several other adaptive facade systems. The mechanism, control, operation, maintenance and failure of the AWI's diaphragms are described, along with basic geometric performance calculations and a study of Arabic geometric references. Next, a series of relevant case studies are investigated with regard to their potential to substitute the existing modules. Finally, the analysis is boiled down to a summary of parameters that need to be taken into consideration for the redesign.*

### 3.1 Arab World Institute

In Chapter 2 a brief introduction to one of the first documented adaptive dynamic building enclosures was given. The Arab World Institute was discussed and summarized regarding its architectural concept and implementation in the environment. In this chapter, the south facade modules are treated more thoroughly, especially with reference to the cause of its early failure.

#### 3.1.1 Control system

The scale at which the south facade of the Arab World Institute was controlled was very ambitious at the time. All of the 13' 680 diaphragms were motorized, eliminating the opportunity for user control (Tonka and Fessy 1988). Using an extrinsic control system to operate its diaphragms, the facade was intended to activate each module independently by embedded photosensors. Counting a total of 240 modules, each containing two light sensors responsible for the activation of either half of its diaphragms by two groups of linear actuators demonstrates the motive of an accurate registration of fractioned light levels. Instead of opening or closing all the panels at once, it displayed a 'bitmap' with local variations of apertures across the vast rectangular facade. Visible in its entirety from the outside but also in large indoor spaces such as the library, it revealed a scattered play of light and shadow responsive to subtle environmental changes (Meagher 2015).

Sadly, the energizing of the individual modules did not even last three years after the building was opened to the public due to the excessive processing demands of the control unit. Later, one single exterior photo-sensitive sensor, located on the roof of the building, collected data of the current configuration (action) of solar intensity and outside temperature and sent it to a central computer. Upon receipt, the computer processed the information and provided feedback by comparing this state to the desired state (setpoint). If necessary, the apertures of the diaphragms were adjusted as the computer commanded the servomotors to actuate the mechanism. Besides, the servomotors relied on a digital signal from the central processor, which means that in this case there were no intermediate states and thus the diaphragms were either fully closed or fully opened (Tonka 1990). The current apertures of the static diaphragms are a mere aesthetic intention, as the mechanism ceased working.

The dominant physical property controlling the diaphragms is solar intensity. When sunlight levels get too high compared to the predefined setpoint, the light intensity of the interior spaces must be controlled and solar heat gain must be minimized. Hence, the processor sends a signal to the actuators, reducing the diaphragm's aperture. However, during winter with outside temperatures dropping below 5 °C, the central computer ignores the condition of solar intensity and calls the diaphragms to open in order to maximize solar heat gain. When temporary conditions occur such as passing clouds on a clear sky, the diaphragms will not operate instantly. This is due to an adjustable 10-minutes time delay of the data processing before any new operation is done, thus avoiding short cycles of the servomotor (Chaslin 2008).

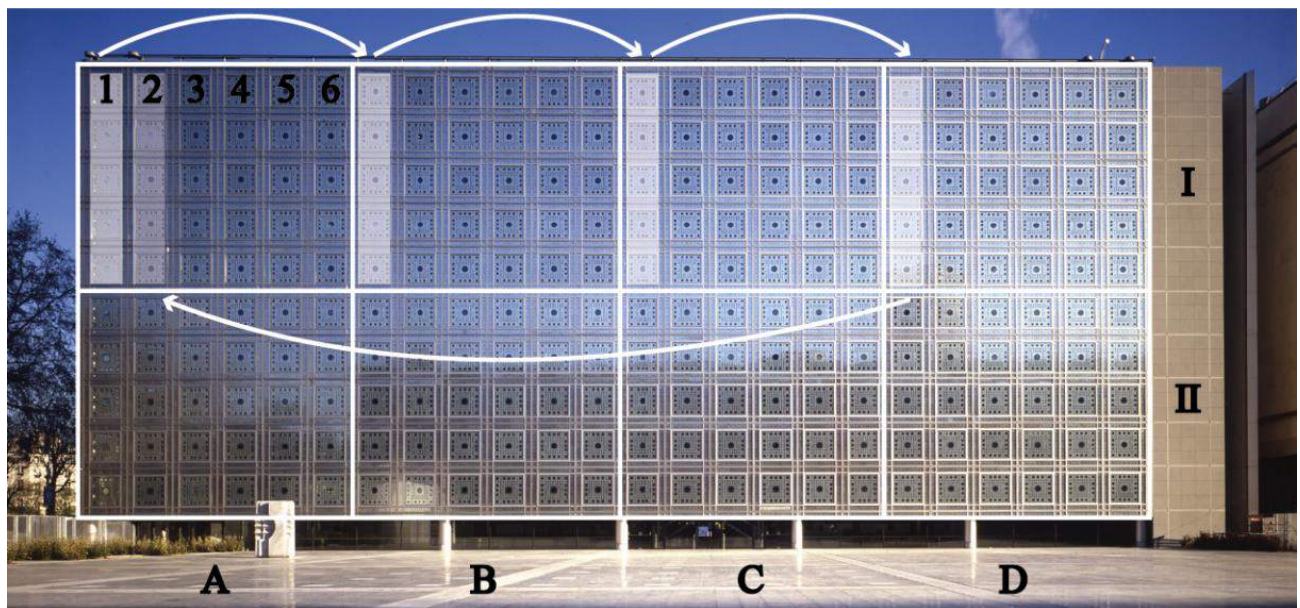
### 3.1.2 Mechanism and operability

As previously mentioned, the individual operation of each module was rapidly terminated and replaced by a central element bypassing the 480 embedded sensors. Although just one sensor stands in for the control of all the diaphragms, the panels do not operate as a whole. Alternatively, the 240 modules of the south facade are divided into eight sections of 30 modules, each of which is then subdivided into six columns of five modules, as shown in **Figure 11**. A sequential operation of these 5-module columns smoothens the movement and allows a progressive variation in the luminosity of the spaces (Casamonti 2009). This way, the visual comfort of visitors and occupants is enhanced and the amount of data that needs to be processed by the control unit is reduced.

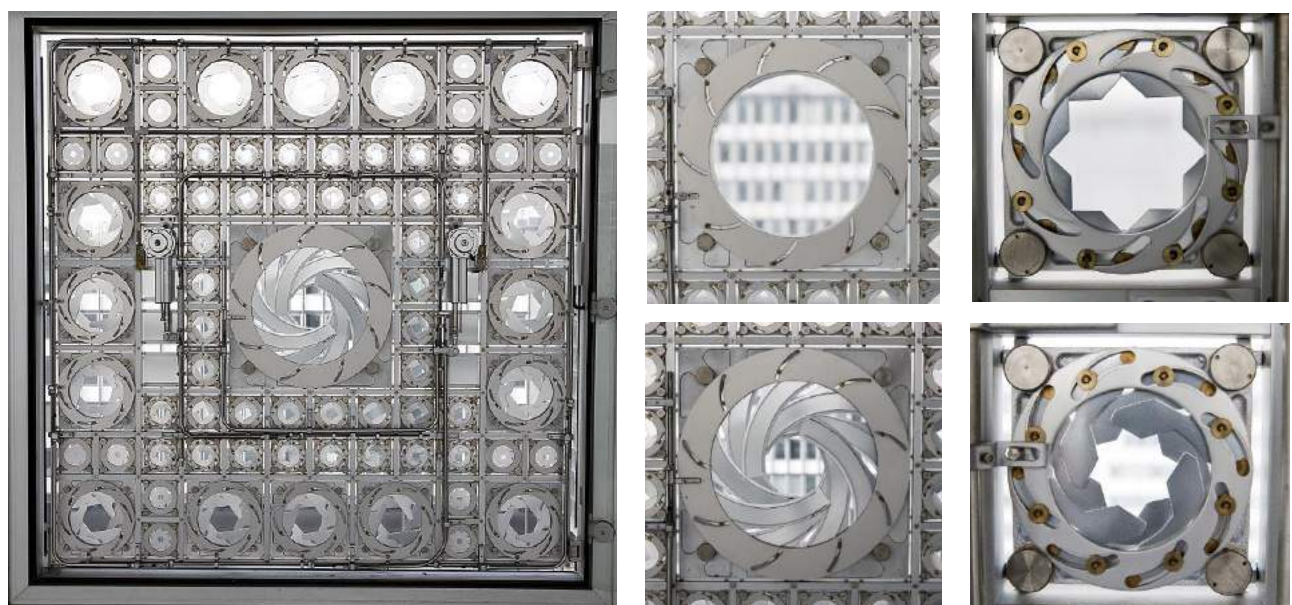
Each module is composed of 73 iris-like shutters that function in a comparable way to camera diaphragms, capturing or obstructing the amount of incoming light (**Figure 12** and **Figure 13**). A sequential interaction of two electrically driven pistons, stainless-steel rods and gliding cables allow the motion of metal slides, broadening or narrowing the aperture of each diaphragm (Tonka 1990). The central and largest iris contains nine rotating blades, the medium-sized six and the smaller diaphragms either eight or four. The number and the shape of the blades are well-thought of, as they produce geometric shapes recurring in traditional Arabic architecture. This will be analysed more profoundly in **Paragraph 3.1.6** of this chapter. On one hand, curved blades such as in the central component, produce an improved roundness of the iris opening. On the other

hand, straighter blades result in a polygon-shaped iris opening. Besides, an increased number of blades defines a more complex polygon.

However, as illustrated in **Figure 14**, some of the diaphragms are not operable. Four small filled squares on each side in stainless steel were used to hide the servomotors from the outside and eight of the smaller diaphragms in the periphery of the panel could not be reached by the actuators and thus remained in a static state with an invariable aperture. Thus, only 57 of the 73 shutters are capable of motion (Meagher 2015). One servomotor activates the central diaphragm and the 16 medium-sized diaphragms whereas the other activates the 40 smaller diaphragms. It has not been found in literature whether the motors require the same amount of energy to operate their individual group of diaphragms.

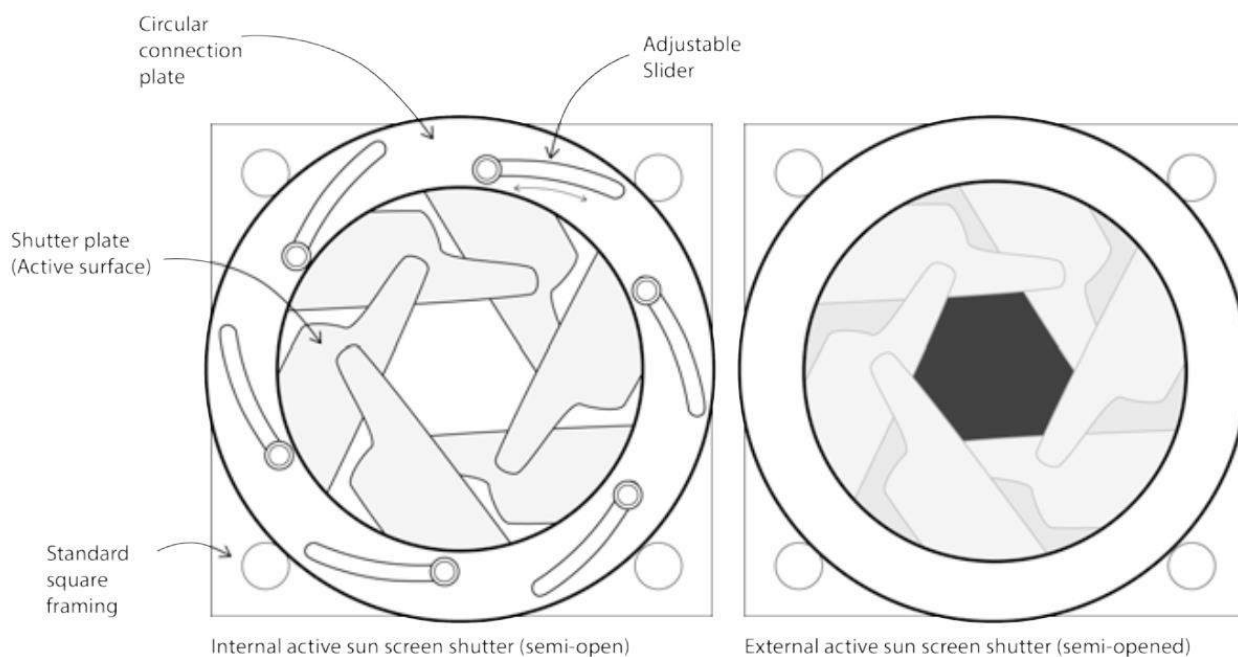


**Figure 11:** Sequential operation of the panels in the following order: A1-I, B1-I, C1-I, D1-I, A2-I... A6-II, B6-II, C6-II, D6-II (adapted from 'ARCHITECTURE STUDIO - Arab World Institute' n.d.).

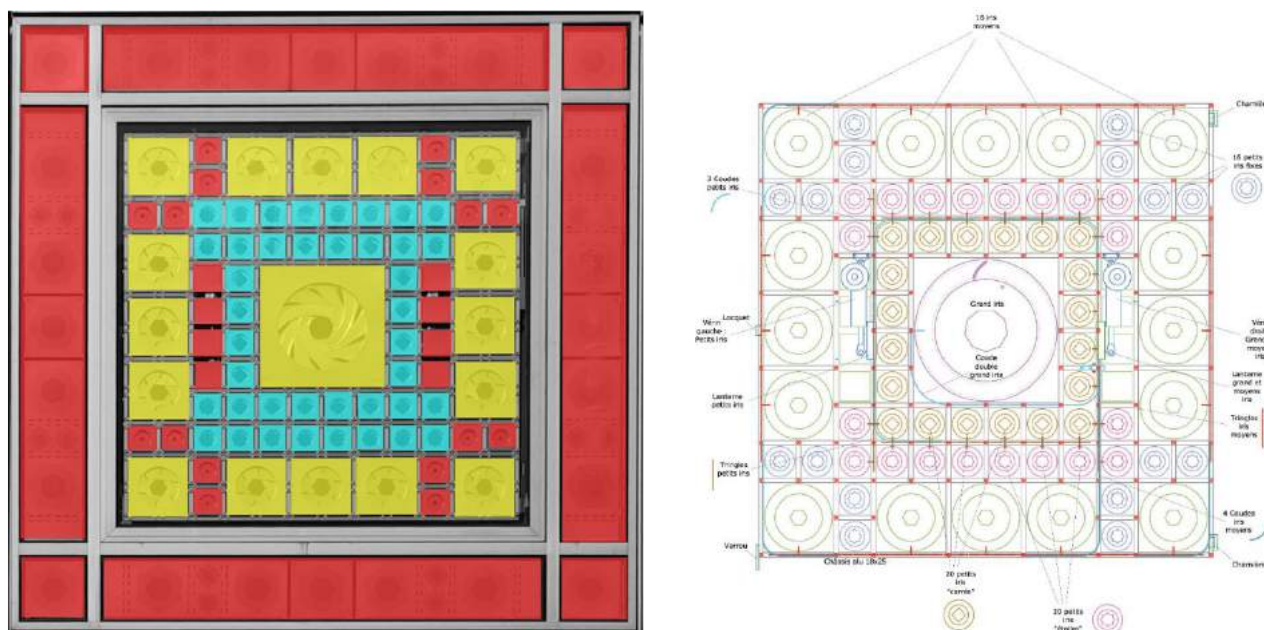


**Figure 12:** Left: Rear view of a south facade module of the AWI. The opening and closure of the diaphragms occurs by actuation of two servomotors. Middle: Open and closed configuration of the central diaphragm. Right: Open and closed configuration of one of the small diaphragms, accentuating an 8-pointed Islamic star ('Architecture' 2016).





**Figure 13:** Mechanism of one of the shutters. Similar to camera diaphragms, the metal plates undergo a rotational movement by an actuated movement of adjustable sliders (Sharaidin 2014).



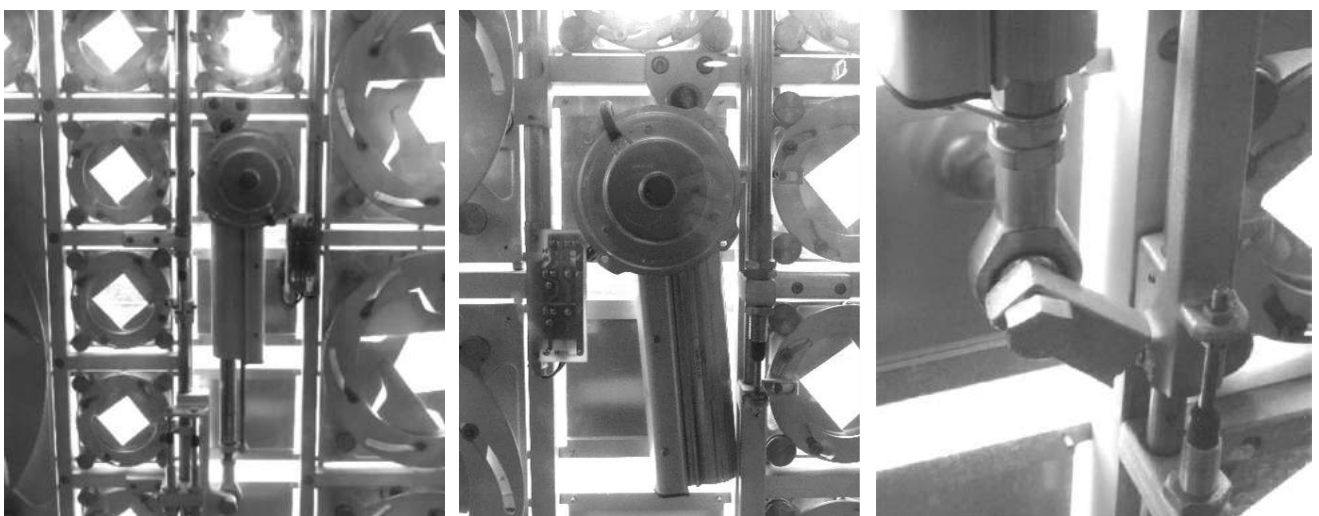
**Figure 14:** *Left:* A south facade panel containing 57 out of 73 operable diaphragms. The non-functional diaphragms are shown in red and the ones actuated by the two servomotors are indicated in yellow and blue (Meagher 2015). *Right:* Detailed elevation of the rear view of a mashrabiya module. The right servomotor actuates the largest and the medium-sized diaphragms, while the left activates the small ones (‘Moucharabiehs de l’ Institut Du Monde Arabe à Paris’ n.d.).

### 3.1.3 Maintenance and failure

Even before the inauguration of the building, it was already speculated that the diaphragms would not function as intended. At that time, the immense technology required for the monumental clockwork of manifold diaphragms may have been too ambitious or even pretentious. After only three years, the diaphragms ceased to be controlled by 480 individual sensors installed in the facade and became instead controlled by only one central cell on the roof. Within six years after the building was realized, the

diaphragms had stopped working entirely. Whether the early failure was due to inadequate design or a maintenance management that was not properly executed, still remains unclear to this day. However, the durability of the mechanism could have been improved by assigning a higher importance to the life-expectancy during the design process (Meagher 2015). The multiple actuators necessitated precise synchronization to prevent the intensification of residual stresses. Additionally, persistent replacement of components and constant maintenance caused by the frequent sliding and rotation of mechanical hinge constituents contributed to unusually high out-of-operation costs (Adriaenssens et al. 2014). Hence, the accumulating expenses of these factors were presumably the main reason to shut down the mechanism completely.

To sustain the desired visibility of the mechanism from the inside, a vast amount of the yearly maintenance budget of the panels goes to the inside glass panes, whereas the outside glass panes are cleaned once every year (Casamonti 2009). All of the modules are enclosed by a single glass pane on both sides and can be brought under maintenance by swinging the inside glass pane toward the interior (Meagher 2015). The diaphragms inside the double glass cover are often subject to overheating, generating a repeated expansion and contraction of the components, joints and moving elements. Obviously, this was causing failure of the mechanism when moving pieces got stuck due to exorbitant friction on the expanded articulations. When this situation occurred, the diaphragms could have been damaged by the actuators, each possessing enough force to deform the structural elements permanently. However, a mechanical pin connecting the servomotor with the rod that operates the mechanism prevents this from happening. As the material of the pin is of a notably lower strength than the rest of the panel's components, it will break upon excessive friction of the moving parts and joints (Goulet 1994). The actuator can then move freely, avoiding any permanent damage to the panels. In other words, the failure of a smaller mechanism prevents the damage of a larger mechanism. **Figure 15** illustrates two situations of failure, one where the failure of a larger part was prevented and another where a larger component must be replaced.

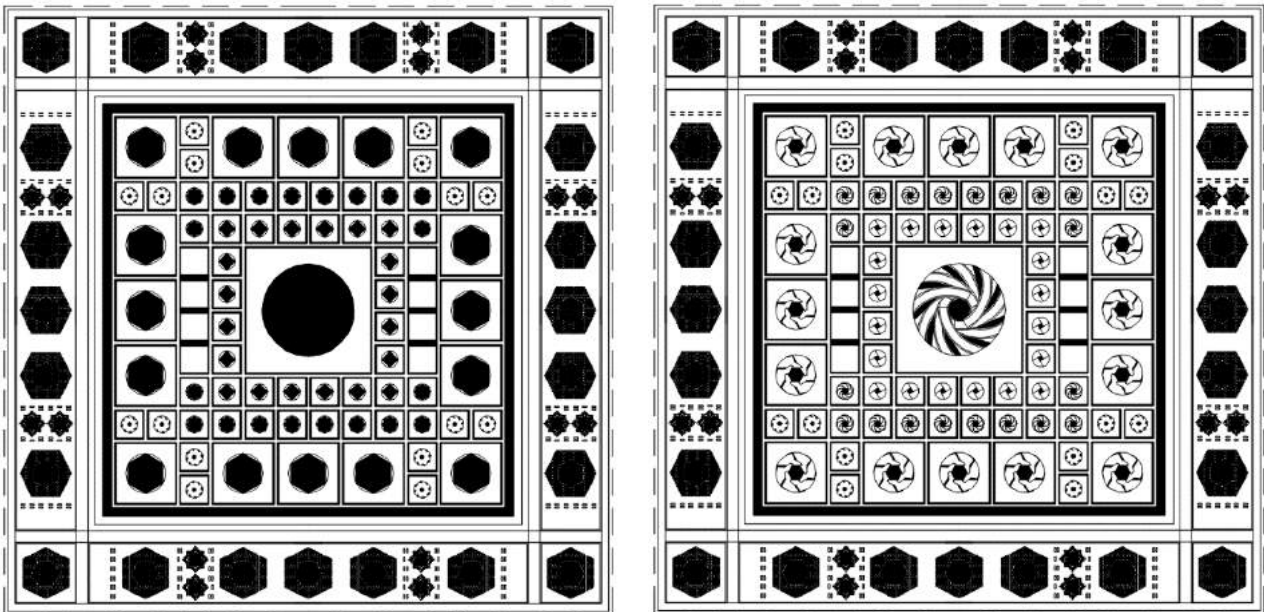


**Figure 15:** *Left:* Servomotor actuating a piston connected to rods. *Middle:* Actuator moving freely after the failure of a mechanical pin. *Right:* Damage of the arm transmitting the force of the servomotor to the diaphragm mechanism (the author 2016).

### 3.1.4 Energy performance

Despite being a renowned building amongst architects and engineers, little documentation exists on the thermal and optical performance of the adaptive modules of the AWI. Moreover, Adriaenssens et al. state that “the engineering of such shape shifting modules is often dictated by practical hinge and actuator related constraints such as allowable forces, available sizes and energy consumption rather than energy related performance criteria” (Adriaenssens et al. 2014), which means there may have been given too little attention to what the south facade was intended to achieve: reduce energy demands without compromising indoor comfort needs. While the latter requirement was relatively well achieved by avoiding solar glare and regulating the amount of illumination, the effectiveness regarding heat gain prevention was minimal. By positioning the shading device inside the glass panes, solar radiation is mainly absorbed and little is reflected to the outside (Decker and Zarzycki 2014). In order to get a rough idea of the energy performance of the AWI’s modules, the aperture area ratio of a module can be calculated. This is the area allowing frontal solar penetration in the building compared to the shading device’s frontal obstruction area and it gives us an idea of how much light, and thus thermal radiation, can infiltrate the south facade in its open and closed configurations. **Figure 16** illustrates a digital reconstruction of the south facade module, allowing fast calculations by measuring the surface areas in AutoCAD. In **Table 1**, for each of the components, the component area  $A_c$  is measured. The void area  $A_v$  is the glass area between the frame of the component and the framework of the module, whereas the aperture area  $A_a$  is the exposed glass area within the diaphragm. Thus, the obstruction area  $A_o$  is given by  $A_c - A_v - A_a$  and the aperture area ratio is calculated as follows:

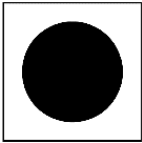

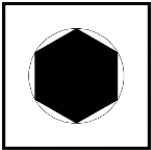
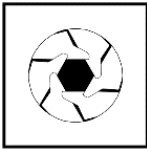
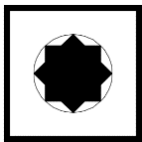


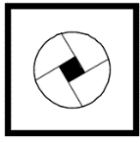

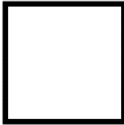
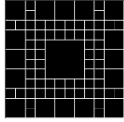

$$\text{aperture area ratio} = \frac{A_v + A_a}{A_c} \text{ or } \frac{A_c - A_o}{A_c}$$



**Figure 16:** Open (left) and closed (right) configuration of one south facade module of the Arab World Institute (the author 2017). The total aperture area ratio of the module is calculated by multiplying the aperture area ratio for each component by the number of components in the module, divided by the total surface area of the 210 x 210 cm module.



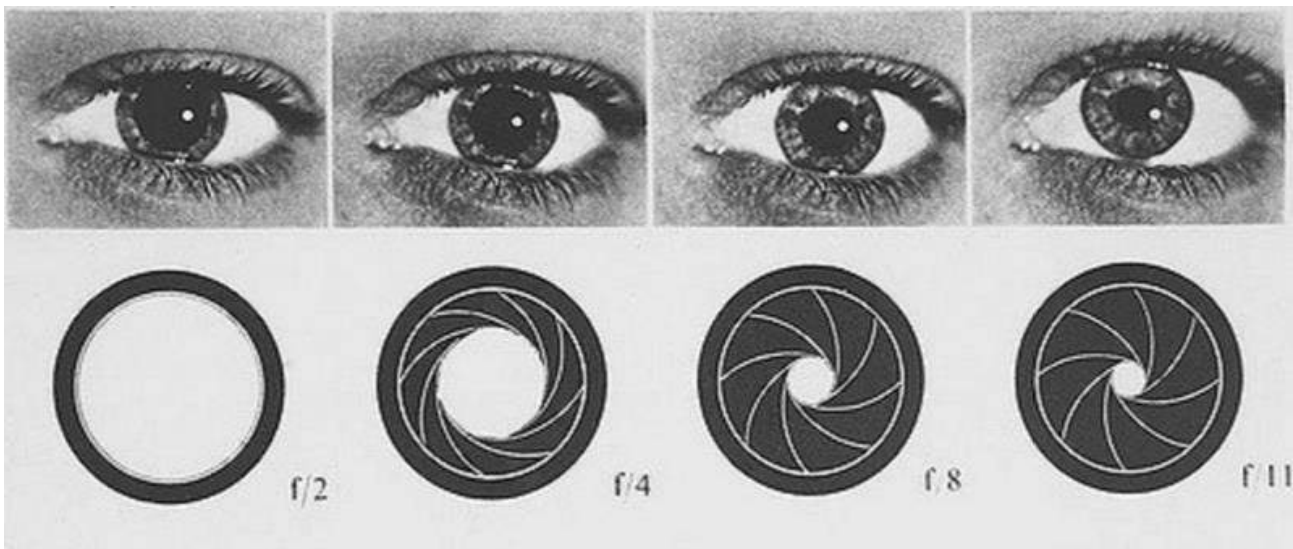
**Table 1:** Summary of the results for the aperture area ratio in open and closed configurations of one module of the AWI.

Component	#	Configuration	Component area $A_c$ [cm <sup>2</sup> ]	Void area $A_v$ [cm <sup>2</sup> ]	Aperture area $A_a$ [cm <sup>2</sup> ]	Obstruction area $A_o$ [cm <sup>2</sup> ]	Aperture area ratio (%)
Circular diaphragm	1	Open	3600.00	127.26	1500.44	2039.87	44
		Closed			322.04	3345.54	12
						Range	32
Component dimensions: 60 x 60 cm							
Hexagonal diaphragm	16	Open	900.00	61.00	234.40	574.32	34
		Closed			50.52	758.19	13
						Range	21
Component dimensions: 30 x 30 cm							
8-point star diaphragm I	20	Open	225.00	28.30	37.47	128.98	34
		Closed			8.25	158.20	19
						Range	15
Component dimensions: 15 x 15 cm							
Square diaphragm	20	Open	225.00	28.30	31.98	134.47	31
		Closed			3.79	162.66	16
						Range	15
Component dimensions: 15 x 15 cm							
8-point star diaphragm II	16	Invariable	225.00	28.30	4.52	161.93	17
							
Component dimensions: 15 x 15 cm							
Filled square	8	Invariable	225.00	28.30	0.00	166.45	15
							
Component dimensions: 15 x 15 cm							
Framework	1	Invariable	2800.00	132.31	0.00	2667.69	
							
Module dimensions: 200 x 200 cm							
Module	1	Invariable	44100.00	3071.97	35344.08	5683.95	
							
Module dimensions: 200 x 200 cm							
Total		Open		6118.70	6712.11	31269.43	29
		Closed			1443.52	36665.28	17
						Range	12

This table highlights that the smaller the component dimensions become, the smaller the range between the aperture area ratio in open and closed configuration gets. It can also be said that the overall performance is quite poor, as there is a total range of only 12% between the open and closed configuration. The upper boundary of this domain is only 29%, which means it allows little thermal radiation to penetrate the building. Hence, the south facade blocks more than two thirds of direct sunlight, which implies a significant reduction of thermal gains in wintertime.

### 3.1.5 Biological inspiration

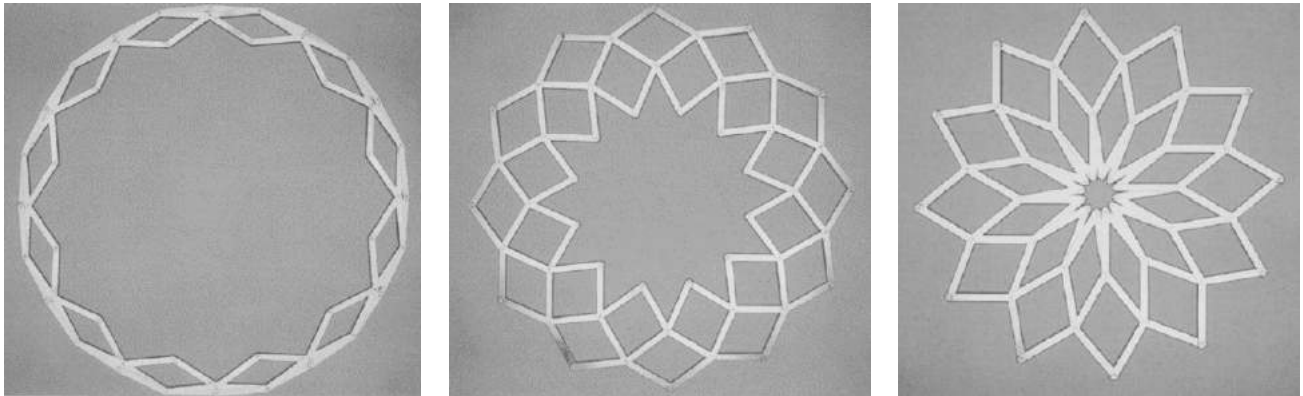
As previously mentioned in **Paragraph 3.1.2**, the mechanism of the AWI's south facade diaphragms can be described by a two-dimensional rotation of metal blades, widening or narrowing the aperture of the shutters. It was Jean Nouvel's intention to evoke the iris movement of the human eye or the diaphragms of a camera (Goulet 1994), illustrated in **Figure 17**. As the latter mechanism was inspired by the iris dilation and contraction, it exhibits a translation from biology to technology and can thus be considered as a biomimetic approach. Whether the architect investigated the anatomy and physiology of the iris, still remains unclear. Presumably, the design for the shutters was influenced by the mechanism of a camera diaphragm, rather than the complex sequential biochemical reactions resulting in muscle interactions from where the movement of the human iris originates.



**Figure 17:** Biomimetic analogy of the human eye with the diaphragm of a camera (Quemere 2007).

Although the camera diaphragm approximates the pupil dilation and contraction relatively well, it was discussed in **Paragraph 3.1.3** that the operation of many such components resulted in the early failure of the mechanism. However, another system mimicking the iris movement was discovered in 1994. Seven years after the inauguration of the Arab World Institute, the 'Iris Dome' by Chuck Hoberman was exposed at the Museum of Modern Art in New York. Inspired by the metamorphosis of biology and mathematics, he managed to fuse nature with technology in a kinetic construction performing a three-dimensional transformation. *"The opening of the dome resembles time-lapse photography of a flower in bloom or the iris*

of an eye adjusting to changes in the light” (Hoberman 1994). In a collaboration with Z. You and S. Pellegrino, he succeeded in creating an iris mechanism based on foldable scissor structures. The mechanism is an assembly of hinged couples of members attached to adjacent couples at hubs, allowing them to rotate smoothly like scissors around axes perpendicular to the dome. However, the large number of hubs and hinges in this system does not make it a potential substitution of the AWI’s components. The sheer number of actuators needed, the complex rigid-body mechanics combined with the precision at such a large scale would probably result in a similar scenario of high maintenance requirements and premature failure.



**Figure 18:** Two-dimensional iris mechanism in open (left), intermediate (middle) and closed (right) configuration (adapted from You and Pellegrino 1997).

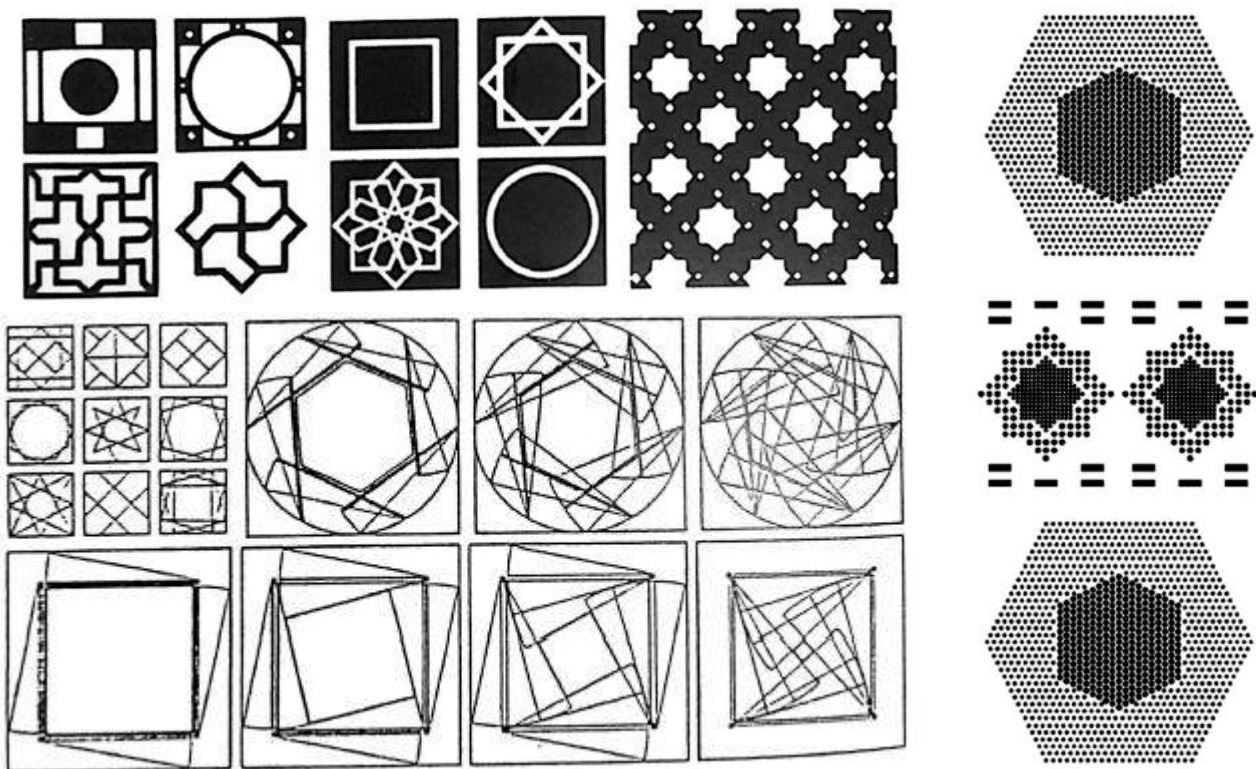
### 3.1.6 Aesthetics and Arabic references

Aside from measurable qualities such as energy performance, thermal and visual comfort, the tendency to implement poetic and eloquent dynamic features is a growing movement to achieve an aesthetic design. The characteristics of responsive elements contributing to the aesthetics of a building can be subdivided into two categories: the expressivity and the dynamics. The expressive potential is able to influence the experience through “colour, texture, hardness, form and transparency”, whereas the time-dependent properties such as “speed, behaviour and choreography” determines the dynamics (Meagher 2015). The appreciation of motion can be described by several factors and is dependent on the visual perception, i.e. the anticipation of action through our eyes. For instance, while in slow movements the motion itself can evolve into a design feature, fast movements assign importance to the transitioned state instead of the process of change. Serial repetitions can induce a more attractive appearance by pattern composition and by movement of individual components, the source and scale of motion alter our senses and even the perception of weight can be manipulated through movement (Fiorito et al. 2016).

Knowing these ‘parameters of aesthetics’ for kinetic elements, a description of the responsive elements in the south facade of the AWI can be given. In terms of expressivity, it can be said that the diaphragms demonstrate a harmonious integration in the building, especially in terms of materiality. The metallic irises dissolve in their complex machinery of sensors, motors, rods and cables and become an essential part of the glazed metal building, not an addition. Regarding dynamics, the movement of the iris-like shutters can be

evaluated by their speed, serial repetition and scale. As the diaphragms used to open or close quite rapidly, it could be said that the movement itself was of less importance. Yet, in this project, the movement was still slow and recognisable enough to perceive the typical rotation of blades when a photograph is taken. Moreover, the sudden 'click' sound it used to be accompanied by created an appealing noise map across the facade and coexisted with a playful surprise effect. Furthermore, the hierarchical arrangement of different iris sizes and the actuation of individual series of diaphragms definitely adds to the aesthetics of the kinetic facade.

It was briefly introduced in **Paragraph 2.1.2** of Chapter 2 that the modules of the AWI's south facade are representing a modern interpretation of the mashrabiya, a traditional arabesque window providing shade and privacy through a wooden lattice of dense geometric patterns. The hierarchical composition of the components within the aluminium frame reflects archetypical elements of traditional Arabic architecture. It was also mentioned in **Paragraph 3.1.2** that the blades of the diaphragms were shaped and sized to accentuate geometric shapes such as polygons and Islamic stars. **Figure 19** demonstrates how this was conceived for the dynamic elements in the diaphragms. The designers pulled off a neat little trick of engineering to create the correct form of the blades in order to produce the desired aperture contour. The geometric shapes generated by the diaphragms are circles, squares, hexagons, and the 8-pointed Islamic star. The latter two also exist as a static representation in the periphery of the modules by means of perforation, allowing a higher amount of daylight entering the edifice.

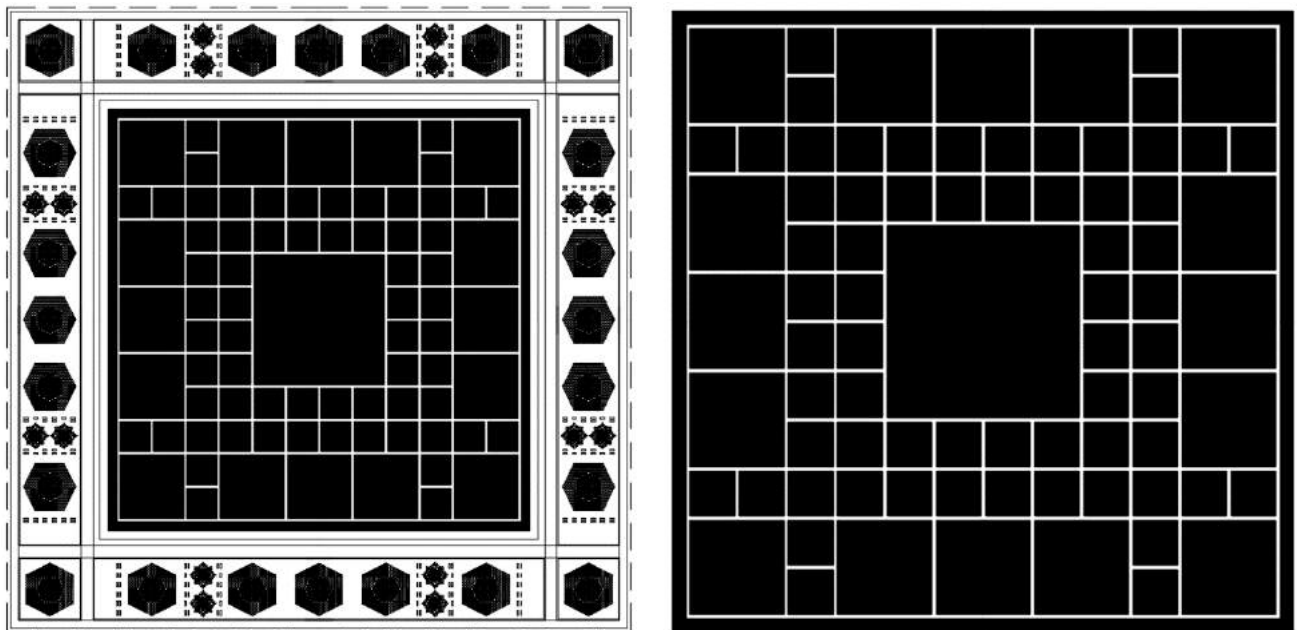


**Figure 19:** *Left:* Geometric study for the design of the diaphragms. An analysis was made for the two-dimensional rotation of the diaphragm blades to evoke Arabic geometric shapes such as the 8-pointed star, the hexagon, the circle and the square (Tonka and Fessy 1988). *Right:* Digital reconstruction of the hexagonal and 8-pointed star perforations in the module periphery (the author 2018).

### 3.1.7 Redesign parameters

The in-depth analysis of the south facade of the AWI that was elaborated in the previous paragraphs of this chapter provides a knowledge basis that can be boiled down to a set of parameters that need to be considered for the redesign of the modules. These can be evaluated later and compared to the original design, furnishing a solid reference-based assessment to conclude this thesis.

Regarding the architectural concept of the building and the south facade in particular, some fundamental ideas need to be brought into consideration for the redesign. One distinct factor is the reference to traditional Arabic architecture, or more specifically, the evocation of the mashrabiya. The formation of geometric shapes such as polygons and Islamic star patterns should be an important feature of the redesign. Moreover, in order to respect the original hierarchy and composition of the module, the framework should be left untouched. Furthermore, the geometric perforations in the perimetry of the module do not have any influence on the deficiency of the mechanism. Therefore, this part ought to be left unmodified as well. Besides, the hierarchical arrangement of the diaphragms and the geometric perforations are both references to Arabic architecture and essential elements of the conception of the south facade. **Figure 20** visualizes the south facade module without the diaphragms, where the newly designed components can thus be retrofitted inside the framework, obeying the structural conception of the module. Another key feature that defines the concept of the kinetic shading system is the biological analogy to the iris of the human eye. Although the physiology of this organism was presumably not studied but instead approximated by the diaphragms of a camera, it remains a remarkable essence of the design conception. Since it is one of the main objectives of this thesis to find a biomimetic solution using a less complex responsive mechanism, it is a predominant feature that needs to be considered for the redesign.



**Figure 20:** *Left:* Representation of a ‘blank’ module of the AWI, leaving out the diaphragms. *Right:* With the periphery of perforations left untouched, the only focus area left for the redesign becomes the square components inside the framework: 1 large component, 16 medium-sized and 64 small ones.

Naturally, the redesigned components need to possess an adaptive behaviour and respond to changing environmental conditions to shade at the desired moment to reduce energy demands and enhance indoor comfort. In terms of energy performance, this means that the newly designed adaptive system should require a low amount of energy to be activated and provide a considerable amount of shade to prevent overheating, without compromising the need for natural lighting and visual comfort. As these are a lot of factors to be included whose quantities are not being determined within the scope of this thesis, an alternative approximation was conceived in **Paragraph 3.1.4**. A very basic way of predicting the energy performance of the adaptive system is by calculating the aperture area ratio. As it represents the ratio of the surface area of openings in the components to the total area of the components, it gives a rough idea of the amount of sunlight able to penetrate the modules. The domain of the aperture area ratio between open and closed configurations gives the obstruction range of the shading elements and may be a good indicator of energy performance and indoor comfort in the primary design phase.

Concerning the mechanism, control and operability of the adaptive shading device, the redesign needs to present an effective and efficient solution to the problems occurring in the diaphragms of the AWI. As one of the primary concerns of the original design was its premature deficiency due to multiple mechanical failures and high maintenance requirements, the new kinetic system needs to demonstrate a simplified alternative with reduced complexity. As formerly discussed in **Paragraphs 3.1.1, 3.1.2 and 3.1.3**, the complex machinery of the diaphragms consisting of sensors, processors, actuators and mechanical parts using conventional rigid-body mechanics, caused the system to cease functioning within six years after the building's inauguration. Therefore, it is the aim to investigate the possibility of implementing alternative, hinge-less mechanisms that facilitate the movement and may lessen the necessity for maintenance. In terms of control and operability, it might also be interesting to consider means of a passive activation system through intrinsic control, bypassing the reliance on high-tech equipment. Hence, the set of parameters to be considered for the redesign can be summarized as follows:

- 1) *The redesign must recognize the aesthetic values of the AWI and incorporate a collection of references to Arabic architecture by means of introducing geometric patterns such as polygons and Islamic star patterns. The hierarchy of the mashrabiya module is respected and the new components must retrofit their original sizes and diversities.*
- 2) *The domain of the aperture area ratio must be expanded through an increase in the range of obstruction of sunlight by the kinetic shading elements between open and closed configurations.*
- 3) *The adaptive shading device must present a simplified alternative regarding its mechanism, control system and operability by mimicking a biological responsive system and thus obtain a biomimetic product with reduced technical complexity.*

## 3.2 Relevant case studies

The five selected case studies were chosen for two specific reasons related to the research question of this master thesis. One aspect they share is their design based on biological inspiration. Another feature they have in common is their physical development in either a prototype or in a built project. Studying these projects is essential for learning different processes in the biomimetic approach and physical development that needs to be taken into consideration for the redesign of the south facade of the Arab World Institute. For additional information, the reader is kindly requested to consult **Appendix B**.

### 3.2.1 Al Bahr Towers

This project was included in the case studies for its combination of a biological inspired shading mechanism and a modernized Mashrabiya system. The computational design team at Aedas is responsible for the development of the kinetic shading structure of the 145-meter-high twin towers in Abu Dhabi, completed in June 2012 (**Figure 21**). The fully automated, dynamic solar screen responds to the sun's angle, allowing control over energy use, solar radiation and glare (Attia 2017). The design team made use of a parametric script to simulate the operation of the panels in relation to the changing solar incidence angle over the year. The designers investigated natural systems where form adapts to local environments, as well as traditional building techniques that have provided comfort over many centuries in the arid climate of the desert. These two starting points established the form-finding process of a complex dynamic mashrabiya curtain wall (Karanouh and Kerber 2015).



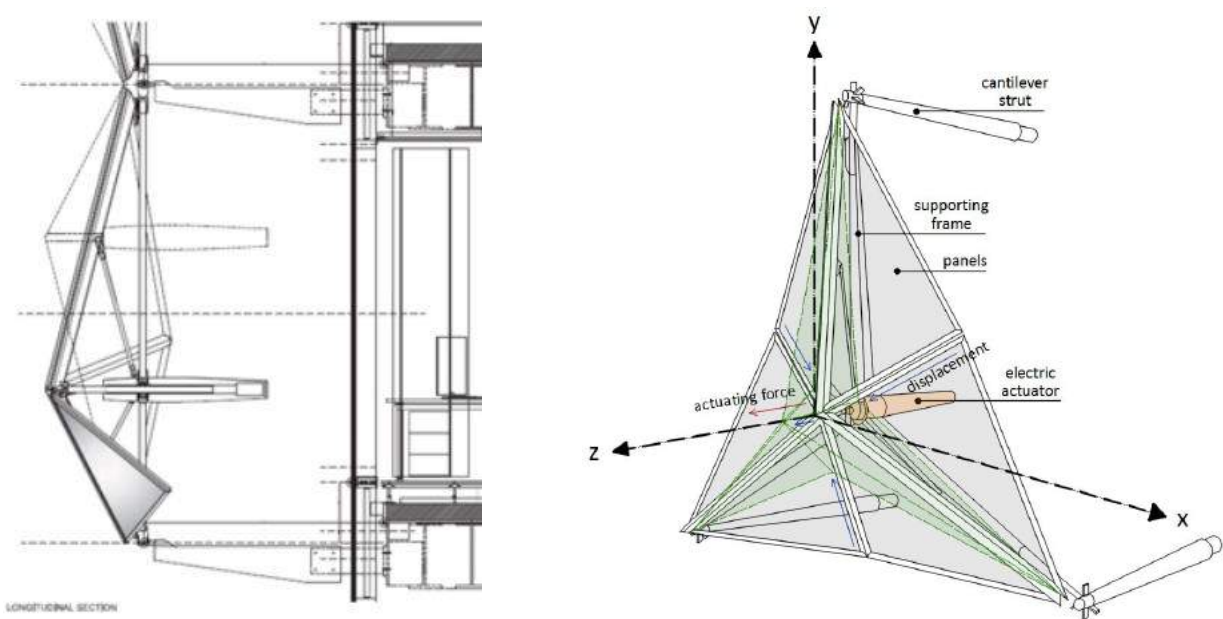
**Figure 21:** *Left and middle:* Views of the Al Bahr Towers in Abu Dhabi (Karanouh and Kerber 2015). *Right:* Hexagonal composition of triangular origami units in open and closed configurations (‘Al Bahr Towers | Aedas - Arch2O.Com’ n.d.).

The entire structural concept for the buildings was biologically inspired. A honeycomb-like design was developed as a supporting structure for the dynamic facade, while pineapples accounted for the hexagonal covering of a double-curved surface. Cacti function the same way umbrellas do to protect their fragile



membrane from extreme weather conditions. Lastly, flower opening and closing movements in response to temperature were the key inspiration for the design of the kinetic shading device (Karanouh and Kerber 2015). On the other hand, traditional Islamic architecture was the basic reference for the building's implementation in the context. The mashrabiya's geometric patterns provide shade to cope with the hot desert sun although enough diffused light is allowed to penetrate the building (Karanouh and Kerber 2015). As the light is scattered through the patterns, the spaces are filled with a shadow projection following the sun's trajectory, contributing to the aesthetics of the building. By merging the traditional shading screen technology with the adaptive nature of flower petals, a dynamic origami solar screen was developed. One triangular origami unit consists of six panels, folding and unfolding around three creases. Six of these units combined form a snowflake-like component, which is repeated over the entire double-curved envelope.

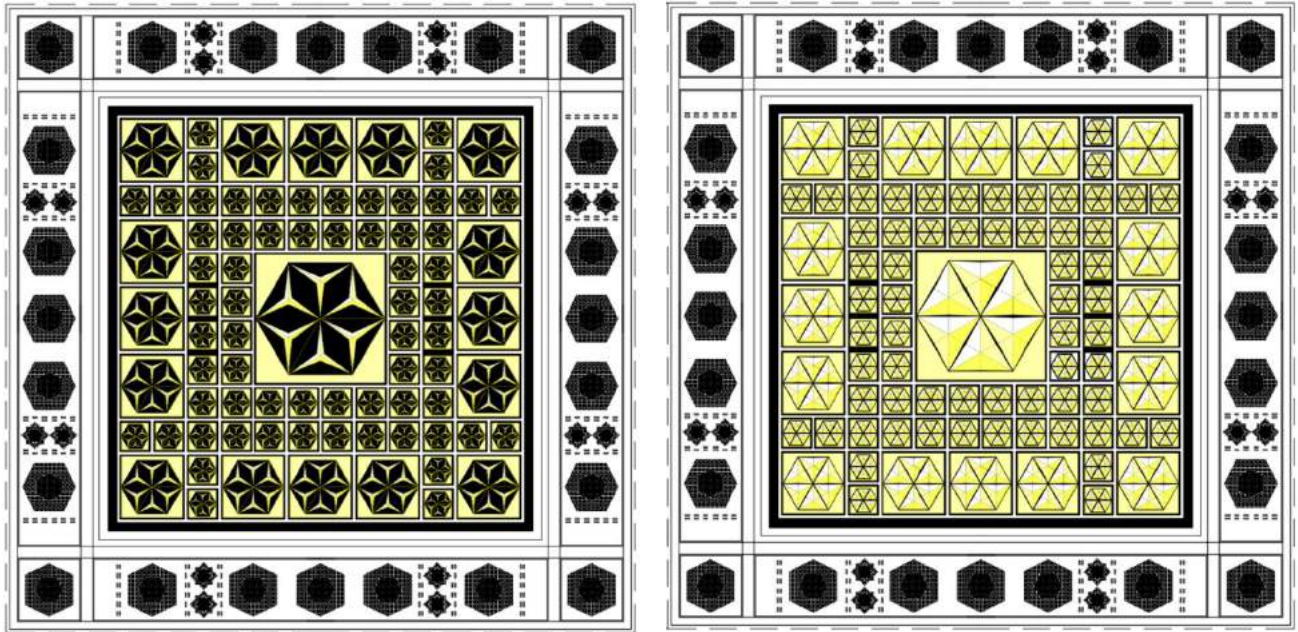
A sun tracking software controls the folding-unfolding sequence in order to maintain optimal solar and light conditions. The triangular origami units are grouped into computer-controlled hexagonal sectors. Each storey-sized unit has six PTFE coated fibre glass panels and is activated by a linear actuator and piston. Operation of a unit occurs once a day, based on a predefined sequence to block incident solar radiation. A central Building Management System (BMS) controls the 1049 units in a pre-set automated regulation, tracking the sun's angle throughout the year. An anemometer and a photometer on the roof cause the system to update every 15 minutes, while sensors integrated in the envelope pick up signals to open all units in case of overcast conditions or extreme weather events. The shading devices have a lifespan of 20 years and the actuators last a service life of 15 years (Attia 2017). **Figure 22** illustrates the connections of the units to the facade in which the supporting frame holding the mechanism together is attached to the facade with cantilever struts; and a triangular unit in closed configuration (grey), in which the linear actuation force causes the origami to fold into its open configuration (green).



**Figure 22:** Left: Section illustrating the connection to the facade ('Al Bahar Towers - Data, Photos & Plans - WikiArquitectura' n.d.). Right: Operation scheme of one unit of the Al Bahr Towers (the author 2018).



To assess this case study, **Figure 23** demonstrates a test of the hexagonal mashrabiya components incorporated in a blank module of the Arab World Institute. From an aesthetic point of view, the units blend in nicely, evoking traditional Islamic geometric patterns. Moreover, the frame area of each component is less than that of the AWI. Intuitively, from **Figure 23**, the total aperture area ratio range of an 'Al Bahr module' would be higher than that of the AWI. However, the complexity of each shading unit would require a huge amount of small parts, which would be difficult to assemble and to maintain. The module would count 486 actuators (six for all 81 components), which may skyrocket manufacturing costs.



**Figure 23:** Representation of the Al Bahr Towers components in open (left) and closed (right) configurations, inserted in a blank module of the AWI.

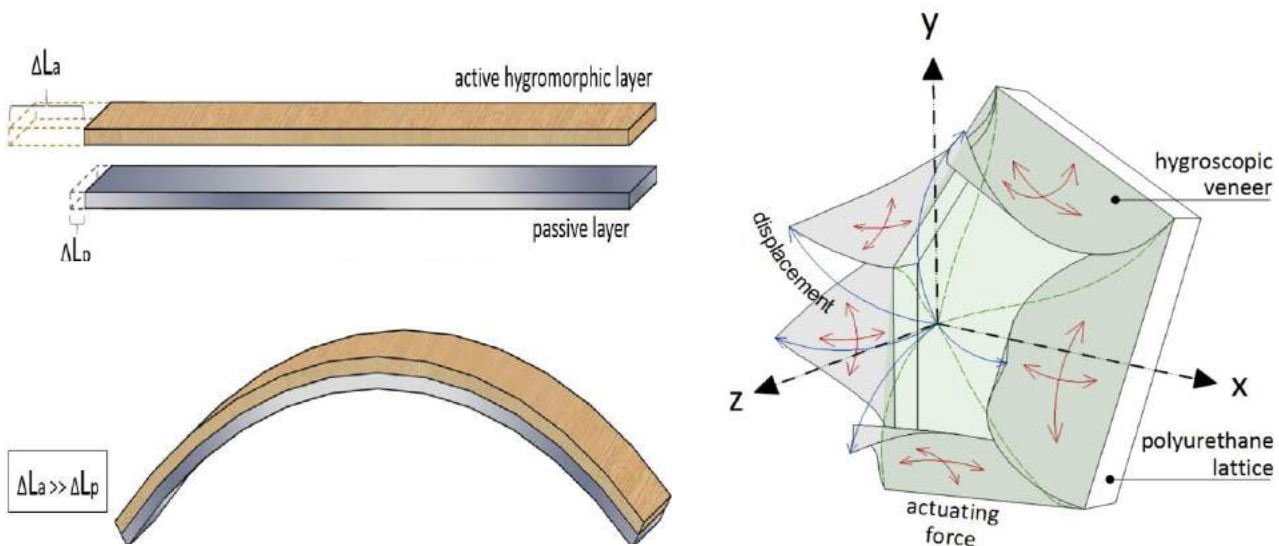
### 3.2.2 HygroSkin

Developed for the Archilab exhibition at Orléans (France) in 2013, the HygroSkin – Meteorosensitive Pavilion presents a daylighting and ventilation modulator for architectural applications. Inspired by the hygroscopic response of *Pinophyta* (conifer) cone scales, the construction incorporates compositions of wooden sheets that gradually open and close as a result of changing relative humidity levels (**Figure 24**). The primary function of conifer cones is to protect its reproductive seeds and when the cone is mature, the seeds are released as a result of the drying and opening of the scales. The scales have an anisotropic composition and consist of two different fibre layers responding differently to changes in moisture content. When the relative humidity alters, a process of swelling and shrinking causes the passive autonomous bending of the scales (Reichert, Menges, and Correa 2015). This movement can be reproduced by a thin lamination of an active hygroscopic wood layer to a natural or synthetic passive layer (Holstov, Farmer, and Bridgens 2017). The elastic deformation or curling is caused by stress dissipation of the bilayer material (**Figure 25**). As the movement is reversible for a high number of cycles and it requires no external actuation, it seems very promising for adaptive facade technologies (Reichert, Menges, and Correa 2015).



**Figure 24:** Left: A temporary outdoor exhibition of the HygroSkin Pavilion in Stuttgart, Germany (Reichert, Menges, and Correa 2015). Right: A conifer cone opening up its scales when the moisture content decreases (Holstov, Farmer, and Bridgens 2017).

In the HygroSkin Pavilion, the hygroscopically actuated veneer sheets are positioned in a polyurethane lattice like an oculus on each of the modularly assembled conical plywood panels. The linear actuation of the elements is geometrically controlled by the polygonal configuration of the latticework. Acting as an energy modulator between inside and outside, the components are calibrated to respond to very local environmental changes. Apart from enhancing aesthetic qualities, the configuration of the elements is optimized to regulate air flow, temperature, daylight and to block precipitation (Reichert, Menges, and Correa 2015).

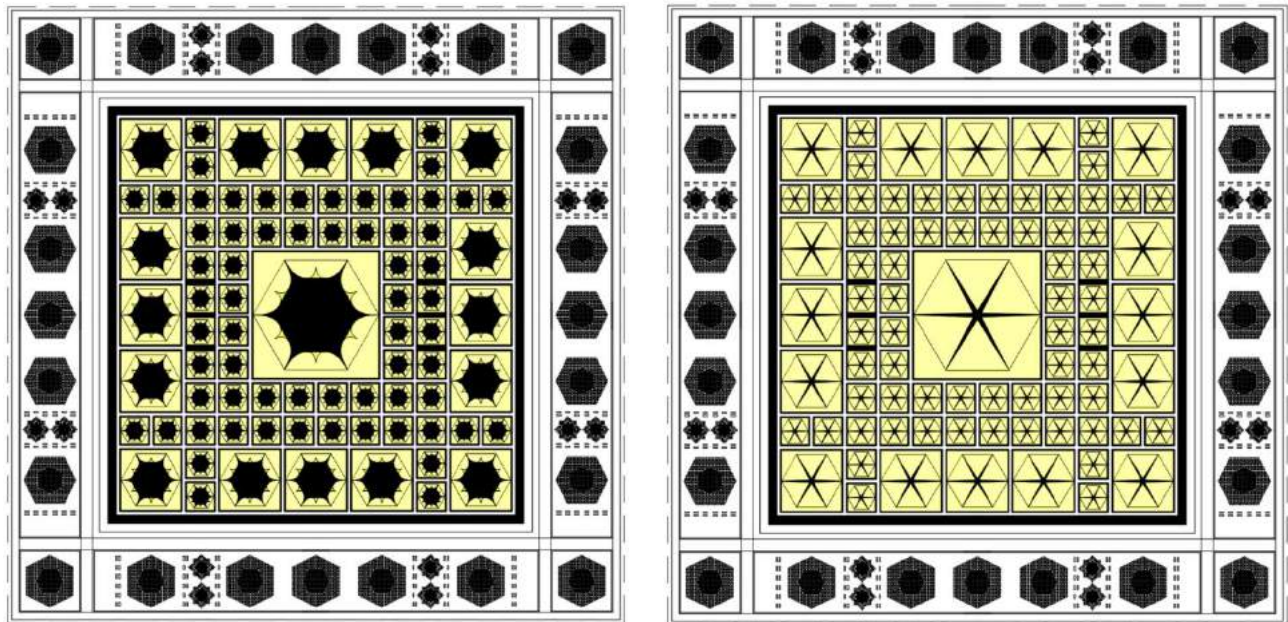


**Figure 25:** Left: Bending of a hygromorphic composite due to differential hygroexpansion of the layers (Holstov, Bridgens, and Farmer 2015). Right: Operation scheme of one unit of the HygroSkin Pavilion (the author 2018).

By slightly adapting the original configuration of the HygroSkin elements, the AWI's module can be substituted with hexagonal hygroscopic wood components (Figure 26). Although in open configuration there is not a clear accentuation of a polygonal shape due to the curling of the elements, the hexagonal components evoke 6-pointed Islamic star patterns. However, due to the additional framing and the limited curling of the



veneer sheets, the range of the aperture area ratio between open and closed configurations is probably similar to the original of the AWI. Then again, the entire module would consist of extremely lightweight, energy-independent kinetic elements that would probably require a minimum of maintenance. Moreover, the hygroscopic wooden sheets can be cut in a high variety of shapes which allows for a large design freedom.

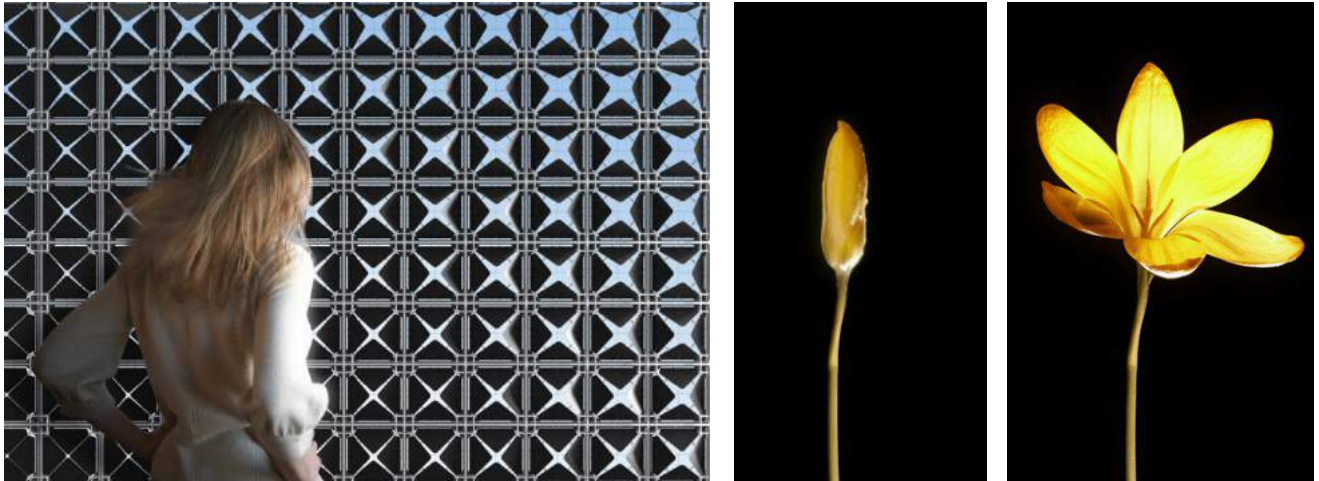


**Figure 26:** Representation of the HygroSkin components in open (left) and closed (right) configurations, inserted in a blank module of the AWI.

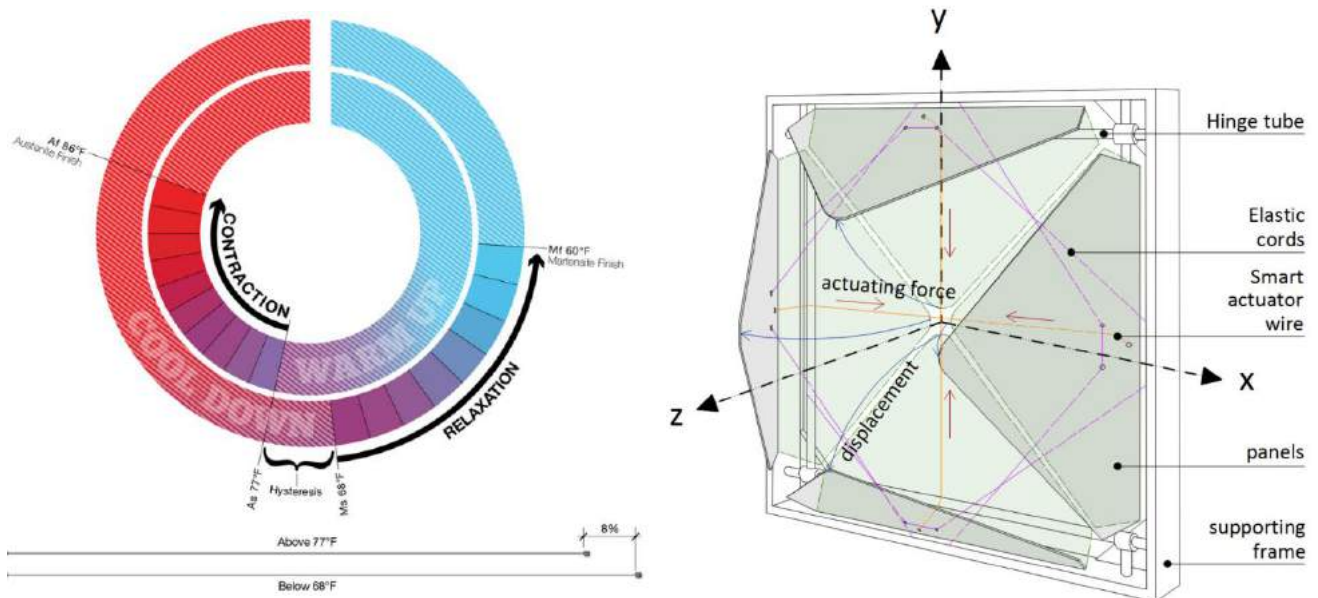
### 3.2.3 Air Flower

The Air Flower is a concept for an adaptive ventilation system developed in 2007 by a Boston-based firm called Lift Architects. The energy-independent device exists in a prototyped state and was inspired by the thermonastic behaviour of *Crocus flavus* (the yellow crocus). Responding to temperature changes, this flower opens its petals due to the differential expansion of two cell layers, similar to the conifer cone scales. When the temperature rises, the inside layer will expand more than the outer layer, causing the petals to bend outwards and thus the flower to bloom (**Figure 27**). The architects mimicked this movement by means of a Shape Memory Alloy (SMA) wire, which is more commonly known as a smart material. One of the main features of an SMA is its ability to recover its original shape by heating after deformation. Contrary to most materials, this nickel-titanium alloy contracts with great force at a warm temperature (austenite phase) and undergoes relaxation at a lower temperature (martensite phase) ('Air Flower' n.d.).

As illustrated in **Figure 28**, the SMA wire used in this project was custom-made in order to obtain a contraction of 8 % and an activation temperature of 80 °F ( $\pm 27$  °C). The Air Flower consists of four panels that are kept closed by elastic cords. When the air is heated, the SMA wire contracts and overcomes the tensional force of the elastic cords. As one SMA wire is connected to two panels, the contraction causes the panels to rotate around hinge tubes to allow ventilation through the building. However, the extent of the panel's movement is restricted by the limited contraction length of the wire (Fiorito et al. 2016).



**Figure 27:** *Left:* Rendering of the Air Flower prototype in a single or double facade system. *Right:* A yellow crocus opening its petals in response to an increase in temperature (‘Air Flower’ n.d.).



**Figure 28:** *Left:* Diagram illustrating the shape memory effect of the custom-made SMA wire (‘Air Flower’ n.d.). *Right:* Operation scheme of one unit of the Air Flower (the author 2018).

When the diaphragms of the AWI are substituted by the components of the Air Flower (**Figure 29**), the open configuration accentuates rotated 4-pointed Islamic star patterns. The modular nature of the Air Flower allows it to directly fit into the square-shaped component frames of the AWI. However, as the original scale of the prototype is relatively small, the larger components in of the AWI would require impractically strong SMA wires for their actuation or the module would lose its hierarchy by implementing equally-dimensioned components everywhere. Therefore, due to the limited aperture of the components, the range of the aperture area ratio between open and closed configurations is expected to be similar to or lower than the AWI. Then again, the module would be activated in a completely energy-independent way without the use of motorizing systems, significantly reducing energy demands and mechanical complexity respectively. Moreover, as the activation of the device solely depends on the material properties of the SMA wire, it can be calibrated to suit various environmental zones or different locations on a building.



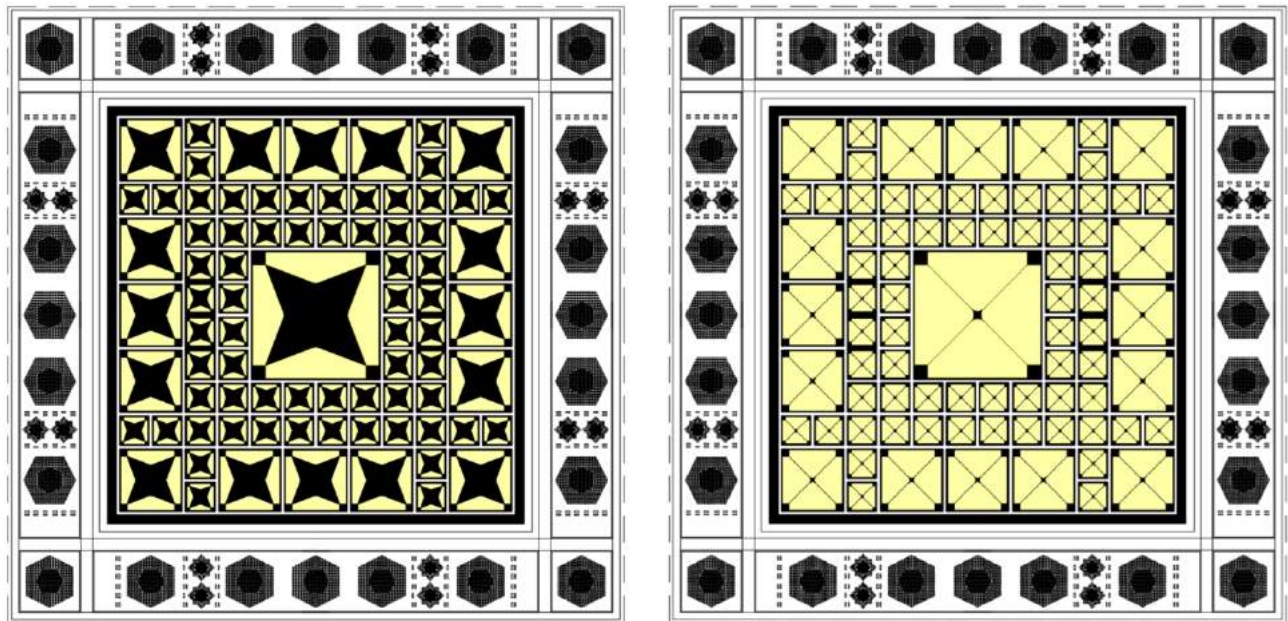


Figure 29: Representation of the Air Flower components in open (left) and closed (right) configurations, inserted in a blank module of the AWI.

### 3.2.4 Flectofin®

In 2010, the ITKE research team at the University of Stuttgart (Germany) developed a full-scale prototype of the award-winning Flectofin® Facade in collaboration with their industrial partner Clauss Markisen (Figure 30). The system features a compliant mechanism inspired by the elastic and reversible pollination mechanism of *Strelitzia reginae* (Bird-Of-Paradise flower). This passive, non-autonomous movement is caused by the landing of a bird on the perch of the flower, bending it downward and inducing a secondary sideways flapping movement of two petal wings. The bird is rewarded with the flower's nectar and the flower is recompensed by transferring pollen to the bird's feet. Once the bird leaves the perch takes back its original closed state to protect its reproductive organs, which means the movement is reversible and thus suitable for application in adaptive facade technology (Lienhard et al. 2011).

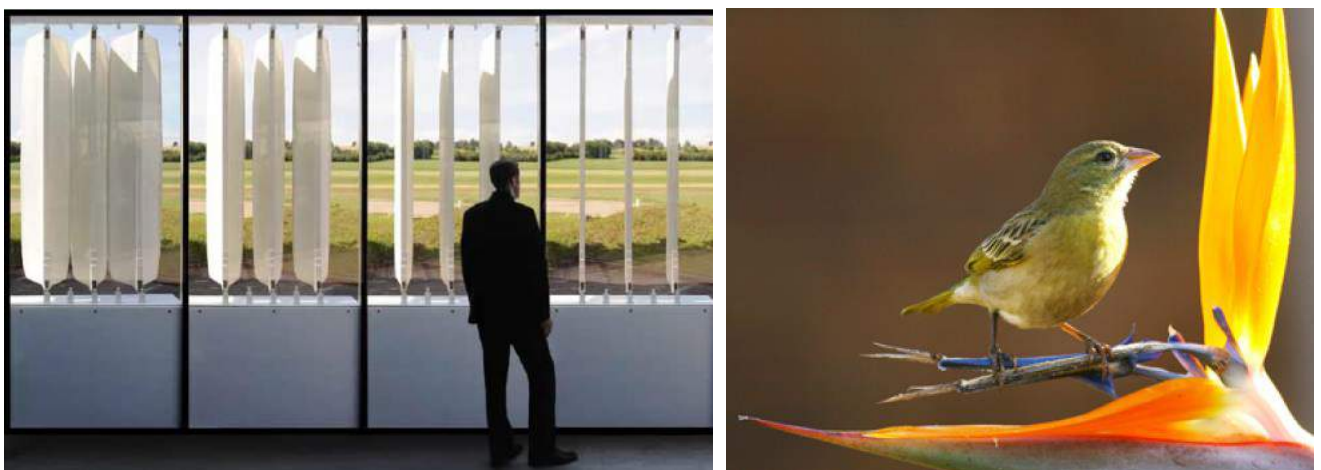
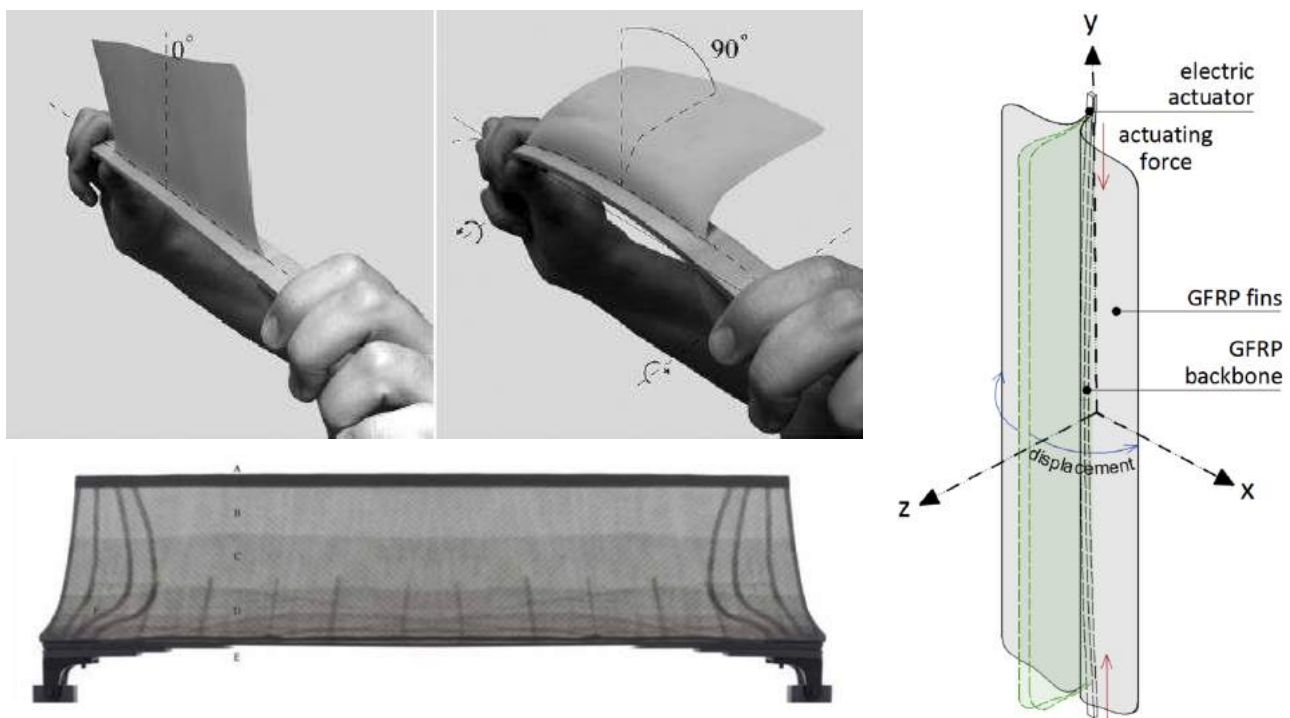


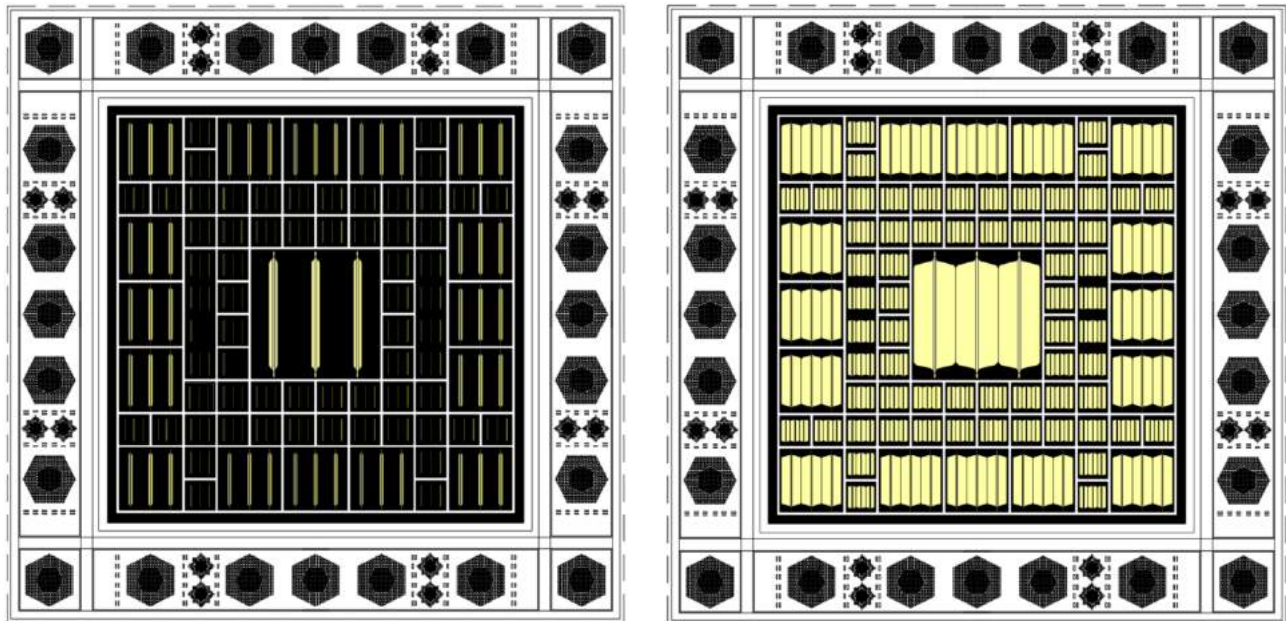
Figure 30: Left: The Flectofin® facade in a full-scale prototype (Lienhard et al. 2011). Right: Pollination of the Bird-of-Paradise flower by a weaver bird (Schleicher 2015). The mechanical force of the bird's weight is transferred to a flapping motion of two petal wings.

As illustrated in **Figure 31**, the underlying working principle of the pollination mechanism can efficiently be reproduced with a physical model using simple materials like paper and wood. The ‘lateral torsional buckling’ is the resulting movement of the uniaxial bending of a stiff beam member, which subsequently causes an out-of-plane bending due to built-up tension in a perpendicularly attached elastic fin. The elastic stress in the fin is released after a critical tension peak is reached, causing a deflection into a less strained equilibrium state (Schleicher 2015). Through kinetic simulations using finite element modelling (FEM), the mechanism was tested for two fins attached to one beam, flipping in opposite directions. The scaling of the model into a 2 m long prototype required the implementation of glass-fibre reinforced polymers (GFRP) in a matrix of ultra-flexible epoxy resin with local variations in fibre direction and orientation to reduce the stress loads in the fins. The fabric layers decrease from the backbone to the edges of the fin and the corners are additionally reinforced with glass rovings to avoid local stress concentrations. The backbone is made from a similar GFRP laminate with unidirectional fibres to take up longitudinal forces. A small, powerful electric motor is required to perform a displacement of only 25 mm in order to bend the backbone sufficiently to produce the flapping motion of the fins (Lienhard et al. 2011).

The substitution of Flectofin elements in the AWI’s module results in a poor evocation of the Arabic mashrabiya (**Figure 32**). However, the range between the aperture area ratio in open and closed configurations is promising as it seems much larger than the original of the AWI. Moreover, the simplicity of the hinge-less compliant mechanism can significantly reduce maintenance requirements and the chance of mechanical failures. Then again, as the original prototype is 2 m long, the severe downscaling would result in a large number of actuators for very small elements, which may lead to higher production costs.



**Figure 31:** Left: Physical model (top) showing the working principle of the pollination mechanism and prototype (bottom) illustrating the location of glass fibre reinforcements (Lienhard et al. 2010). Right: Operation scheme of one Flectofin unit (the author 2018).



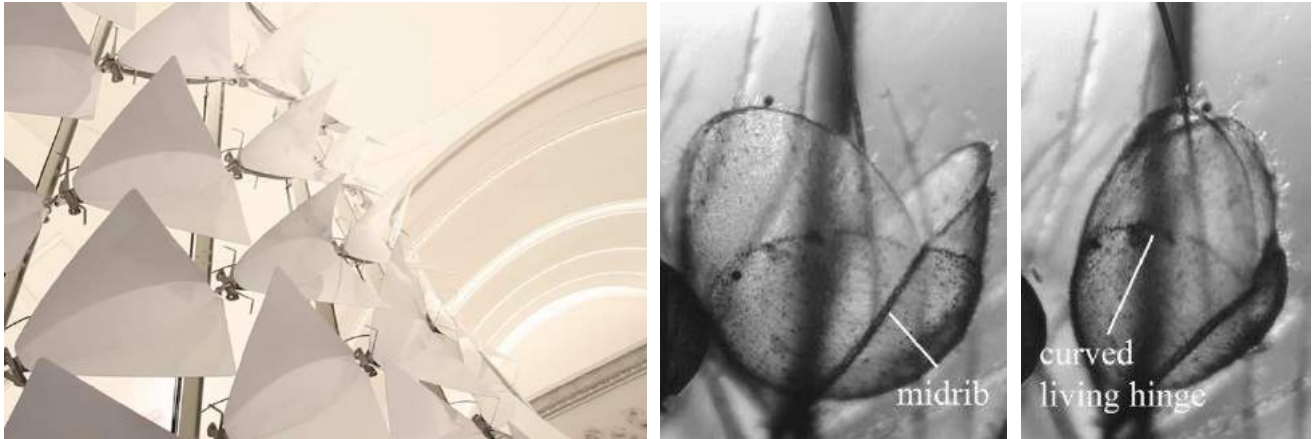
**Figure 32:** Representation of the Flectofin® components in open (left) and closed (right) configurations, inserted in a blank module of the AWI.

### 3.2.5 Flectofold

In 2017, the Flectofold Large Scale Demonstrator (**Figure 33**) was exposed as part of the Baubionik Exhibition at Schloss Rosenstein in Stuttgart, Germany. The 9-meter-high prototype consisting of 36 Flectofolds was developed by the ITKE research group at the University of Stuttgart. The reversible snapping motion found in *Aldrovanda vesiculosa* (the waterwheel plant) was the biological role model for the development of Flectofold. When small prey touches the sensory hairs of this aquatic carnivorous plant, its tiny leaves close with high speed. A curved living hinge connects the two lobes of the trap to the central part, allowing the conversion of a small initial displacement into a larger successive movement of the entire compliant mechanism. In fact, the movement is comparable yet inverse to the flapping motion of Flectofin®. The disclosed principle of this movement lies in a controlled sequence of intertwined deformations. Hydraulic pressure differences in motor cells cause the midrib and central portion to bend, which subsequently generates the out-of-plane bending of the adjacent laminae along the living hinge (Schleicher et al. 2015).

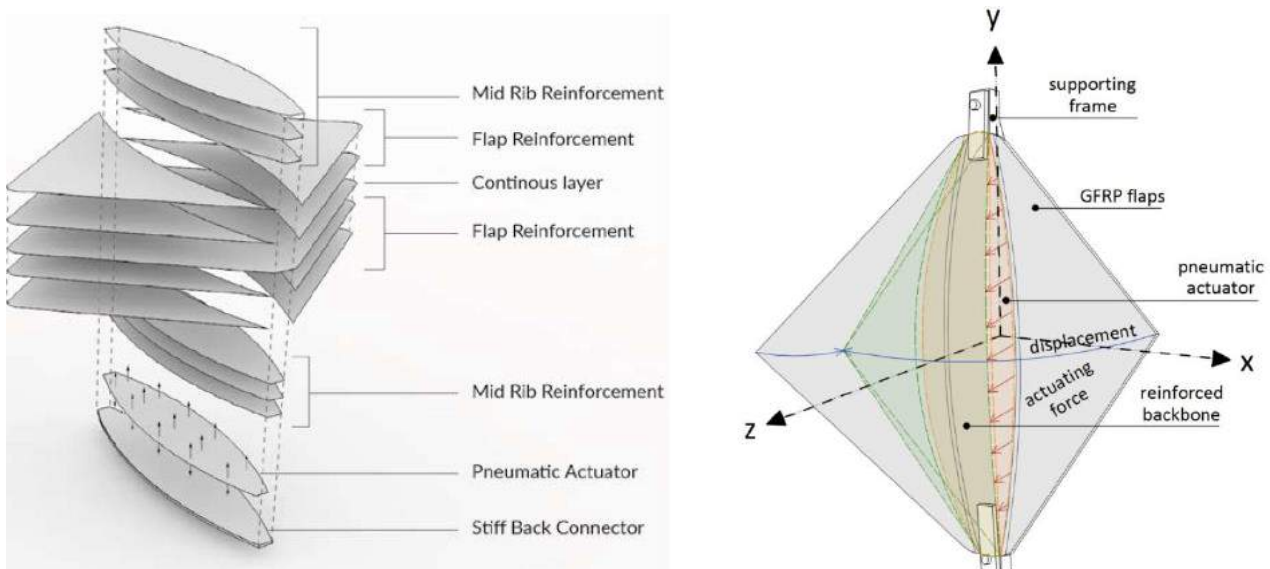
A series of kinematic and kinetic simulations with a rigid origami simulator and FEM respectively were conducted for the abstraction of the trapping mechanism and the translation into a bio-inspired mechanism (Schleicher et al. 2015). The simulations led to a better understanding of the underlying working principle and contributed to the design of a kinetic shading element. A fundamental part of the technical implementation of the trap mechanism was the definition of zones with different mechanical properties. The midrib and the flaps are much stiffer than the area of the curved living hinge yet allow elastic deformability. This led to the construction of a physical prototype in glass fibre reinforced polymers (GFRP), allowing a stiffness gradient in which the matrix takes up the load transmissions and the fibres absorb the forces (Knippers, Nickel, and Speck 2016).





**Figure 33:** *Left:* Flectofold Large Scale Demonstrator at the Baubionik Exhibition 2017 (Saffarian 2017). *Right:* The trap leaves of the waterwheel plant are closing when small prey trigger its sensory hairs (Schleicher et al. 2015).

As **Figure 34** depicts, the curved folding mechanism is made possible by tailoring the fibre orientation and shifting the layers. The component is locked onto a stiff supporting structure and the induced bending displacement of the backbone is made up for by movable hinges, permitting the vertical sliding of the component along the substructure (Körner et al. 2016). Actuation tests with cables, a pneumatic piston and a pneumatic cushion showed that the latter severely reduced the required actuation force (Körner et al. 2018). The lens-shaped pneumatic cushion, located between the component and the substructure exerts a distributed surface actuation on the backbone, making the flaps bend around the softer living hinges. The folding and unfolding movement of the Flectofold can be adjusted to user preferences, visual or thermal comfort by regulating the pressure of the actuator cushion (Körner et al. 2016).

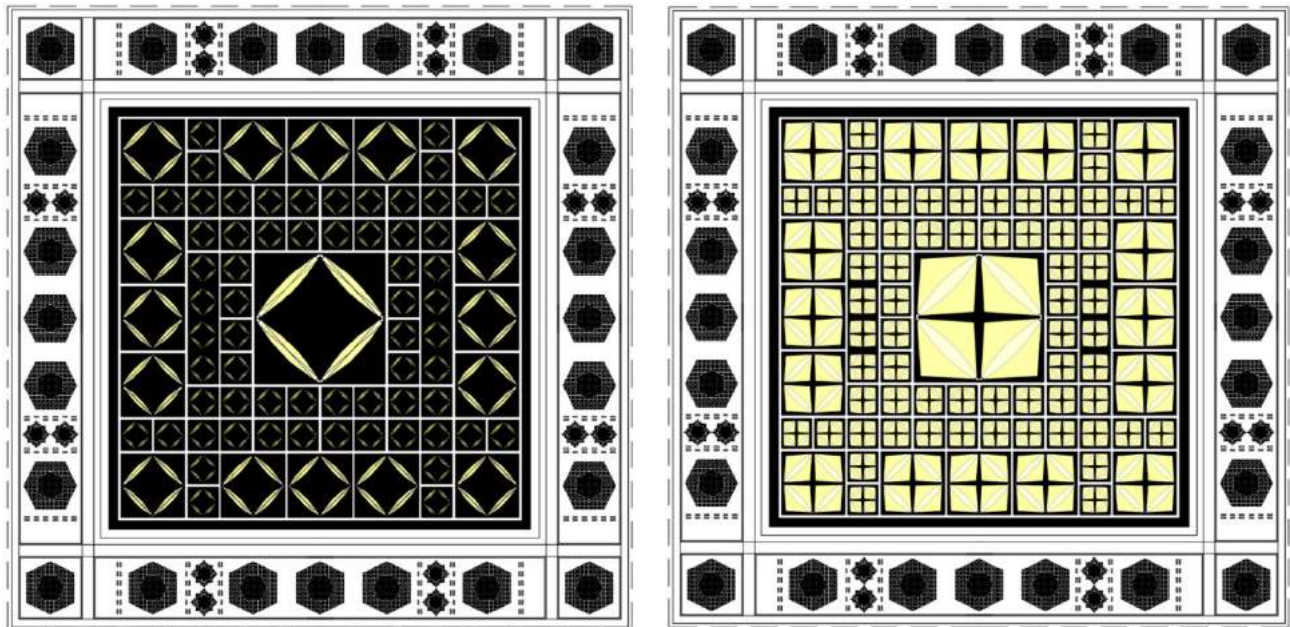


**Figure 34:** *Left:* Exploded composition scheme of the layered build-up of a Flectofold unit (Körner et al. 2016). *Right:* Operation scheme of the one Flectofold unit (the author 2018).

It is relatively easy to imagine four Flectofolds together to fit in a square component frame of the AWI, as illustrated in **Figure 35**. When assembled this way, the open configuration forms the same rotated square we find in one of the smaller components of the AWI. Moreover, the intermediate configuration is a 4-pointed



star, a shape that often returns in Islamic architecture. If this composition is repeated for all the components, we get an aperture area ratio domain that is supposedly much higher than that of the AWI. Furthermore, the absence of rigid connections in the compliant mechanism would probably be beneficial regarding maintenance costs and be less prone to failure. Then again, a 'Flectofold module' would require 324 actuators which may lead to high production costs.



**Figure 35:** Representation of the Flectofold components in open (left) and closed (right) configurations, inserted in a blank module of the AWI.

### 3.2.6 Discussion

To assess the five case studies, a preliminary evaluation is done considering the redesign parameters that were formulated in **Paragraph 3.1.7**. Concerning the biomimetic principles (**Table 2**), the Al Bahr Towers followed the least rigorous approach by simply drawing inspiration from the opening and closing behaviour of flowers in relation to changing temperatures. The Air Flower attempted to mimic this process by using smart materials whereas the HygroSkin, Flectofin® and Flectofold projects investigated the behaviour of nastic structures in plants at a biomechanical level and performed multiple phases of biomimetic abstraction. The two latter projects are successful results from the application of the biomimetic push-pull method discussed in **Paragraph 2.3.3.2**.

**Table 2:** Summary of the biomimetic principles.

	Biomimetic approach	Biological role model	Environmental stimulus	Responsive movement	Mechanical principle
<b>Al Bahr Towers</b>	Inspiration	Flowers	Temperature	Opening/closing	Not determined
<b>HygroSkin</b>	Bottom-up	<i>Pinophyta</i>	Humidity	Curling	Hygro-expansion
<b>Air Flower</b>	Top-down	<i>Crocus flavus</i>	Temperature	Bending	Differential expansion
<b>Flectofin®</b>	Push-pull	<i>Strelitzia reginae</i>	Mechanical force	Flapping	Lateral torsional buckling
<b>Flectofold</b>	Push-pull	<i>Aldrovanda vesiculosa</i>	Mechanical force	Snapping	Sequential bending

Regarding their application as a climate adaptive facade system, a classification (**Table 3**) was done respecting Loonen et al.'s method discussed in **Paragraph 2.2**. Although the HygroSkin and the Air Flower are designed for ventilation purposes, their intrinsic control type is interesting as the sensing and actuation are embedded in the material, bypassing the need for high-tech equipment. Moreover, their gradual adaptation of small elements at a rate of seconds makes them particularly suitable to envision a redesign for the AWI's modules. Another important design parameter was the ability to produce Arabic geometric patterns. As the Al Bahr Towers were designed as a modernized mashrabiya system, it scores the highest marks for this requirement. Nevertheless, the HygroSkin and Air Flower projects evoke similar patterns and when positioned correctly, the Flectofold components are able to display 4-pointed Islamic star patterns.

**Table 3:** Summary of the climate adaptive properties.

	Adaptive system	Modulation	Control type	Timescale	Adaptation scale
<b>Al Bahr Towers</b>	Shading	Thermal-optical	Extrinsic	Diurnal	Macro - large
<b>HygroSkin</b>	Ventilation	Thermal-air flow	Intrinsic	Seconds	Macro - small
<b>Air Flower</b>	Ventilation	Thermal-air flow	Intrinsic	Seconds	Macro - small
<b>Flectofin®</b>	Shading	Thermal-optical	Extrinsic	Minutes	Macro - large
<b>Flectofold</b>	Shading	Thermal-optical	Extrinsic	Minutes	Macro - large

In terms of energy performance, a prediction can be made based on the aperture area ratio which was calculated for the AWI' modules in **Paragraph 3.1.4**. As the Flectofin and Flectofold components produce the largest movement, their range of aperture area ratio between open and closed configurations is the highest (**Table 4**). To counteract the operational and mechanical complexity of the AWI's modules (**Paragraphs 3.1.1, 3.1.2, and 3.1.3**), the project with the least potential is the Al Bahr Towers, as it features a system similar in complexity based on conventional rigid-body mechanics. The use of compliant mechanisms in the HygroSkin, Flectofin® and Flectofold is based on soft mechanics in plant movements and seems very promising.

**Table 4:** Summary of the mechanical characteristics and energy performance predictions.

	Movement	DO F	Ap. area ratio range	Actuator	Materiality	Complexity
<b>Al Bahr Towers</b>	Origami-based folding	2	Medium	Electric motor	PTFE coated glass fibre	High
<b>HygroSkin</b>	Bending	1	Medium	Humidity variations	Hygroscopic wood	Very low
<b>Air Flower</b>	3D-rotation	1	Medium	Shape memory alloy	unknown	Medium
<b>Flectofin®</b>	Sideways flapping	2	High	Electric motor	GFRP	Low
<b>Flectofold</b>	Curved-line folding	2	High	Pneumatic cushion	GFRP	Low

## Chapter 4

# Exploration

*In this section, two mechanisms will be explored with regard to their potential to replace the diaphragms of the Arab World Institute. Through geometric representations and kinematic simulations, the new configurations are compared to the existing ones concerning aesthetics, complexity, and performance. Then, a visual documentation of the prototyping development process is presented and the occurring design obstacles are discussed.*

### 4.1 Thermo-bimetal curling

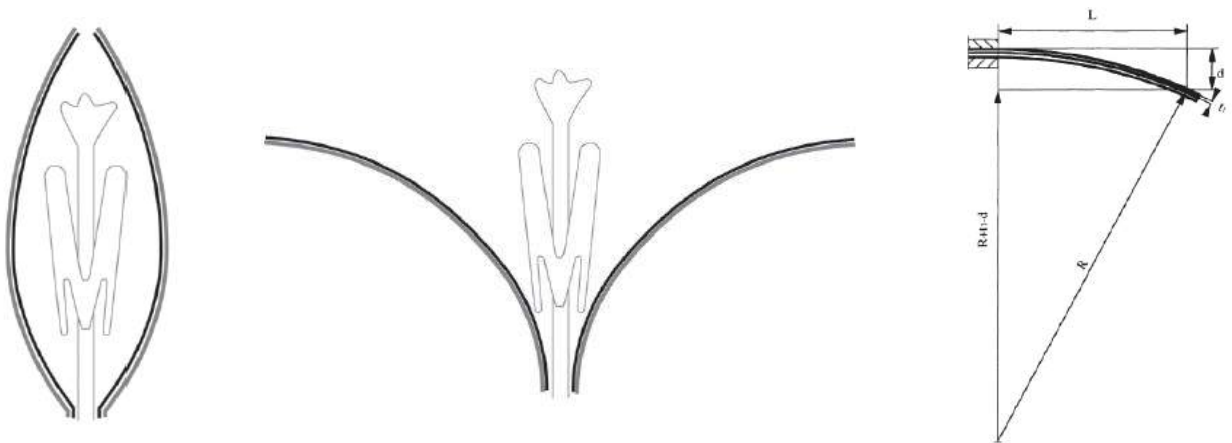
One of the most promising case studies that were studied in Chapter 3 was the HygroSkin project, analysed in **Paragraph 3.2.2**. Acting as a hygroscopic wooden composite adapting to humidity conditions, this climate adaptive system relies on the inherent properties of the material to adapt itself to its changing environment. It makes the need for sensors, processors, power supplies and actuators redundant, as the material itself serves as an all-inclusive system due to its innate characteristics. Moreover, the design freedom becomes nearly infinite as the wooden veneer sheets can take many shapes and the destined surface can be fully clad. As the complexity of the diaphragms in the Arab World Institute's modules caused its premature failure, the alternative of a no-tech strategy requiring minimal maintenance is interesting. Besides, the concept of intrinsic instead of extrinsic control for the AWI can be appealing as most of its occupied spaces are destined for public activities, meaning the building's occupants do not have any control on the system.

#### 4.1.1 State of the art

Since the wooden composite used in the HygroSkin project required a substantial amount of knowledge in material engineering and the hygroscopic behaviour is difficult to experiment with, another smart material will be explored: thermo-bimetal. Consisting of an active and a passive metal layer, the laminated sheet curls when subjected to temperature changes due to differential thermal expansion.

#### 4.1.1.1 History

Thermo-bimetals were discovered at the beginning of the Industrial Revolution and have had numerous applications ever since. Ranging from measurement and control systems in thermostats to electrical control elements in mechatronics, thermo-bimetals are commonly used to this day. Despite having established a prominent role in engineering fields, no applications in architecture had been recorded until very recently. Inspired by the temperature regulation of the human skin, Doris Kim Sung proposed to use thermo-bimetals to regulate the 'building skin', making it responsive and dynamic (Doris Kim Sung n.d.). Functioning as a ventilation system, it has the potential to evolve into a self-actuating facade that 'breathes' (D.K. Sung 2008). From another perspective, by approaching architecture as a four-dimensional entity, Foged and Pasold explored responsive environments in nature and studied the thermonastic behaviour of flower heads (Foged and Pasold 2010). Just like pinecone scales respond to varieties in humidity, some flower petals open and close with the rise and fall of temperature. This is due to the different growth-rates of an inner and an outer layer, reacting on a molecular level to obtain a curled shape on a macroscopic level. As depicted in **Figure 36**, an analogous phenomenon is found in the nature of bimetallic strips. An active element with a high and a passive element with a low thermal expansion rate causes an out-of-plane bending of the joint part at different temperatures, due to the perfect attachment of the layers (Foged and Pasold 2010).



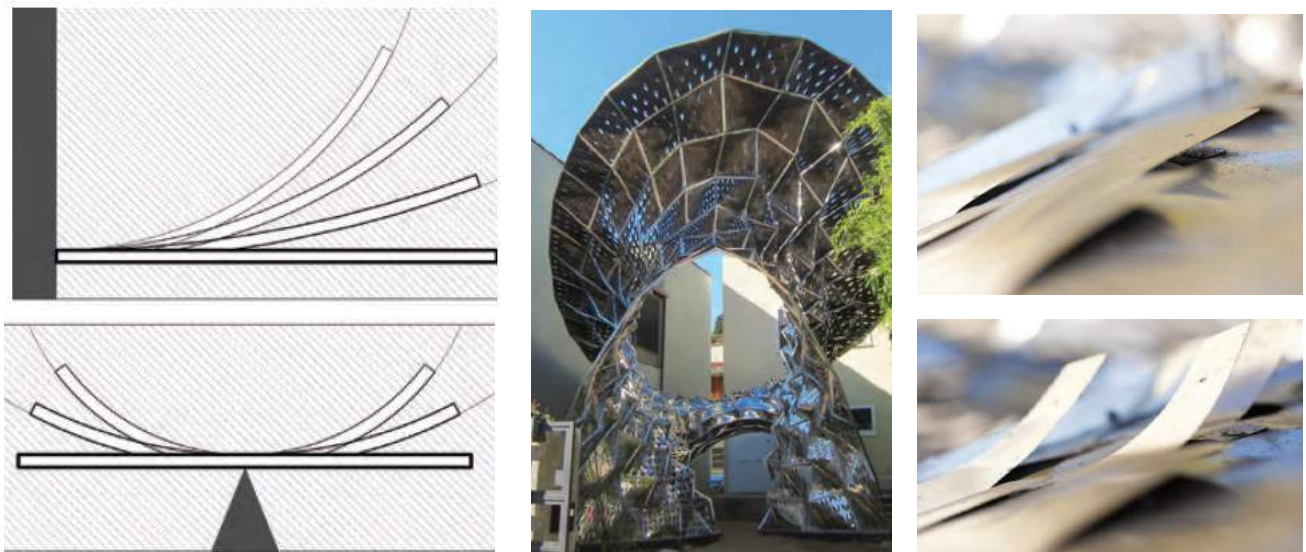
**Figure 36:** *Left:* Inward bending of flower caused by rapid growth of the outer petals. *Middle:* Outward bending due to the rapid growth of the inner petals. *Right:* Bending of a cantilevered thermo-bimetal strip at a raised temperature (adapted from Foged and Pasold 2010).

#### 4.1.1.2 Current developments

Where Foged and Pasold remained to the digital modelling level of an adaptive facade system based on thermo-bimetal responsiveness, D.K. Sung experimented also on the physical level. Her conclusions on the behaviour of this smart material are that its deflection depends on four properties: the shape and size of the piece, the clamping position, the material thickness and the surrounding air temperature. Large, elongated, cantilevered strips show higher deflections under higher temperatures. Additionally, by changing the properties of the two metals composing the bimetallic device, the behaviour can be altered to meet specific design requirements. The latter approach is however not recommended in the design of an adaptive facade system, as this would involve high production costs and long manufacturing processes. A more efficient

method is to choose a thermo-bimetal with suitable properties for the overall performance and then, by plain manipulations of the geometry, enhance or retard the behaviour to specific needs. Thanks to its isotropic crystalline structure, the raw material can be cut in any desired form to control the curl, twist, direction, deflection, and deformation. As shown in **Figure 37**, these findings were put to practice in 2011 in a brise-soleil pavilion called 'Bloom', located at the M&A Gallery in Los Angeles, California. Computational modelling tools were used to assign the ideal geometry to each of the bimetal pieces to achieve optimal performance regarding shading, lighting, and ventilation. Every strip reacts in a distinct way when exposed to solar radiation, accordingly to its desired performance on that specific location of the tessellated surface. This way, various regions of the canopy can be triggered to filter sunlight or exhaust trapped air.

In ongoing research projects called 'HexSphere' (2014) and 'Pivot Shading System' (2015), Sung considers the capability of the flexibility of bimetals to transform potential energy into kinetic energy. By connecting the parts in a pre-bent configuration, the tendency of the material to curl around the axis of least resistance causes it to flip into a new orientation. In other words, the surface undergoes a rotation when heated, able to block solar rays as its rotated configuration is almost perpendicular to its initial position. This means that in cooler conditions the pieces are parallel to the dominant light direction, allowing solar radiation to penetrate the building. Contrarily, the pieces twist perpendicularly to the solar rays when exposed to higher temperatures.



**Figure 37:** *Left:* More deformation occurs in the cantilevered thermo-bimetal than the centre-pinned due to more operable length. *Middle:* Street view of the Bloom Pavilion, containing over 9000 unique pieces of thermo-bimetal, each designated to a different performance benchmark. *Right:* A select fraction of the strips curl a pre-defined amount to shade or ventilate when exposed to solar radiation (adapted from D. Sung 2016).

#### 4.1.2 Redesign

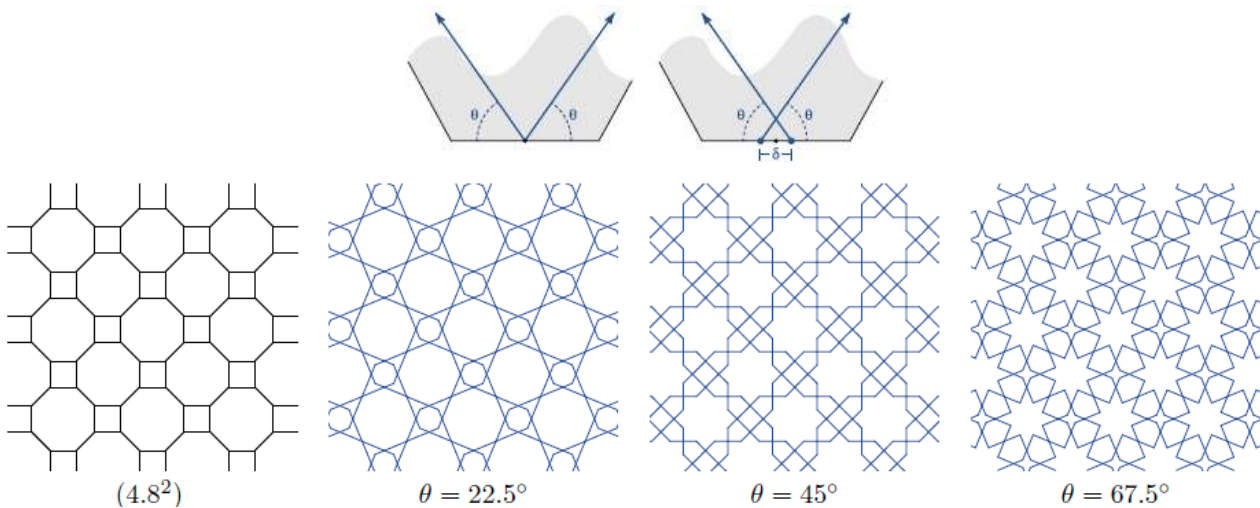
In **Paragraph 3.1.7** of Chapter 3, the design parameters considered for the redesign of the AWI's south facade modules were discussed. In general, the main objectives are to respect the references to traditional Arabic architecture in Jean Nouvel's design, to increase the performance of the module and to reduce the



mechanical complexity of the adaptive shading system. By making use a 'blank module', the (Figure 20) original hierarchical levels are conserved as well as the geometric perforations in the perimetry of the module. In the following sections, it will be studied how the Arabic star patterns can be enhanced, the range of the aperture area ratio can be expanded and the overall complexity of the system can be reduced by designing thermo-bimetal-based components.

#### 4.1.2.1 Arabic geometric patterns

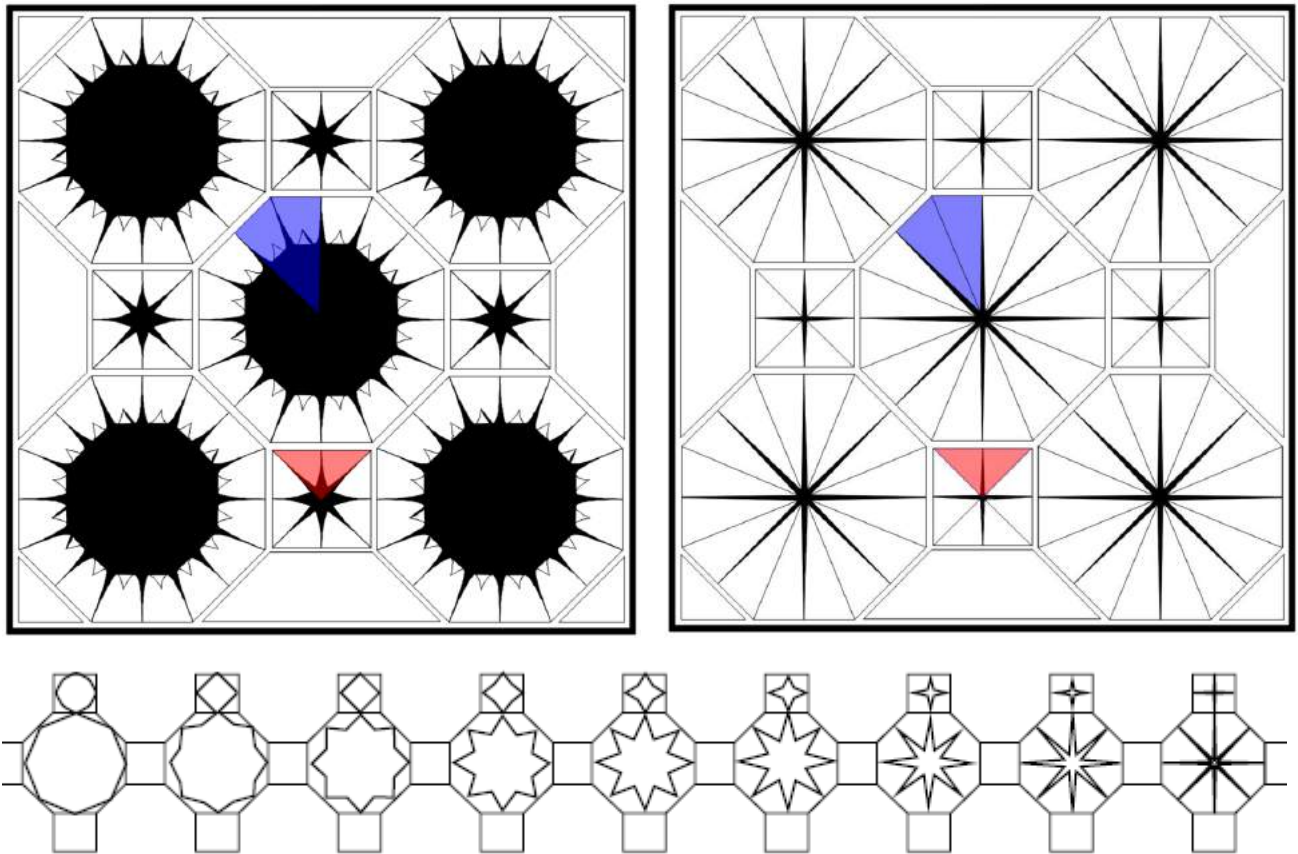
In the early twentieth century, an algorithmic method for developing Islamic star patterns was discovered by E.H. Hankin. The approach starts from a network of polygons in contact, also called a tessellation (Kaplan 2005). A tessellation can be described as an infinite repetition of one or more shapes in a two-dimensional plane, without allowing gaps or overlapping. The simplest way to do this is by tiling the surface with convex polygons. An additional feature of tessellations is that in every contact point of the polygons, the sum of the angles is  $360^\circ$  (Lee, Kim, and Jeon 2015). The classification of tessellations is done by considering one vertex and mark the number of sides of each polygon surrounding it by going around it clockwise or counter clockwise. For instance, a regular tessellation of triangles is called a '3.3.3.3.3.3 ( $3^6$ ) tessellation', as six equilateral triangles combined to form a polygon with a total internal angle of  $360^\circ$ . By combining squares with octagons, we get a 4.8.8 ( $4.8^2$ ) tessellation, as illustrated in Figure 38. Hankin's algorithm that turns a tiling into an Islamic pattern, is done by identifying the midpoints of each polygon side and associate a pair of rays to them. As the rays grow, they encounter those coming from other midpoints and form the typical star pattern recurring in Arabic architecture and design. By changing the contact angle  $\theta$ , the whole range of star pattern designs for the tessellation can be formed (Kaplan 2005).



**Figure 38:** Top: Two rays growing from the midpoint of a polygon's side. The ray origins can be separated by distance  $\delta$  to form overlapping star patterns. Bottom: Demonstration of Hankin's method, applied to a 4.8.8 tessellation (adapted from Kaplan 2005).

Applying this method to the redesign of the square-shaped components constituting the modules of the AWI, the infinite tessellations need to be framed. As the central and largest component of the module shows the highest hierarchical levels, it could be assigned a more complex Islamic star pattern such as the one originated from the 4.8.8 tessellation. Now, a square must be positioned inside the tessellation, trimming it

on the outside of the square's boundary. A compromising way of doing this is visualized in **Figure 39**, centrally positioning the most complex polygon and limiting the expansion of the tessellation to one propagation. In other words, it is the smallest representation of the tessellation without cutting through polygons. At this stage, the thermo-bimetal strips can be assigned a shape and a location on the component. Since it is the objective to form the Islamic star pattern, eight quadrangular pieces per octagon and four triangular pieces per square can compose the eight-pointed star and the four-pointed star respectively. However, following this approach the bimetal triangles would have a large base length compared to their height and the quadrangles would be clamped in three corners, both limiting their ability to curl. For this reason, the quadrangles and triangles are equally divided into two triangular pieces. By doing so, the 4-pointed and the 8-pointed stars are transformed into 8-pointed and 16-pointed stars respectively. However, due to the curling of the material, the geometric shapes lack the accentuation of the star pattern. Then again, as the star patterns in traditional Arabic architecture demonstrate only one static state, i.e. one value for the contact angle  $\theta$ , the kinetic system displays a larger, continuous range of intermediate positions.



**Figure 39:** *Top:* Possible intermediate (left) and closed (right) configurations of the central component of the AWI, substituted by a 4.8.8 tessellation with bimetal strips. The triangular (red) and quadrangular (blue) pieces are split in two for enhanced performance. *Bottom:* Discrete representation of the whole range of intermediate states in a 4.8.8 tessellation, for various contact angles  $\theta$ , the demonstrating the potential for dynamic elements in an adaptive facade system (adapted from Lee, Kim, and Jeon 2015).

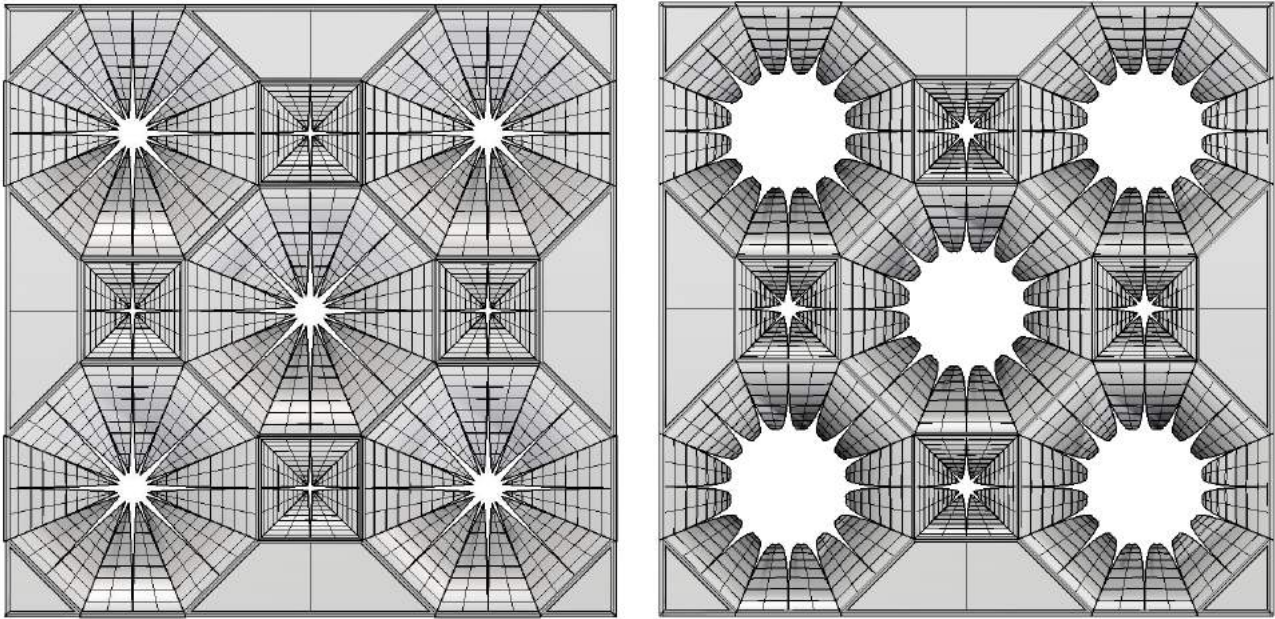
#### 4.1.2.2 Geometric simulations

To determine how and to what extent the thermo-bimetal pieces in the 4.8.8 component can curl, a simulation taking into account the deformation under the influence of temperature needs to be developed. A

parametric script in Grasshopper for Rhinoceros 5 was chosen to perform this kind of simulation, as it allows to visualize the entire process of deformation and makes it able to perform geometric calculations. In addition, the aesthetics of the movement can be evaluated and provide guidance in the preliminary design phase. The curvature of the thermo-bimetal can be calculated by the following formula:

$$R = \frac{t}{k(T - T_0)} ;$$

where  $R$  = radius of curvature [mm],  $t$  = thickness [mm],  $k$  = flexivity [ $1/^\circ\text{C}$ ],  $T$  = current temperature [ $^\circ\text{C}$ ] and  $T_0$  = activation temperature [ $^\circ\text{C}$ ] ('Thermostatic Bimetal – Kanthal' n.d.). By changing the current temperature  $T$ , the middle line of the triangular pieces running through their centre of gravity is assigned a new curvature  $R$ . The two free triangle edges move with it by an approximated helicoidal transformation. For a deeper comprehension of the parametric script, the reader can consult **Appendix C**. **Figure 40** illustrates the outcome of this approach, generating Islamic star pattern evocations, though much less at higher temperatures due to the curling of the bimetal sheets. The open configuration is estimated to be around  $45^\circ\text{C}$  in summer due to the greenhouse effect caused by the double glass layers inside which the modules reside.



**Figure 40:** Simulation of an intermediate state occurring at  $30^\circ\text{C}$  (left) and a fully opened configuration at  $45^\circ\text{C}$  (right). The inner edges of the bimetal strips show the surface subdivisions and thus the degree of accuracy of the geometric simulation.

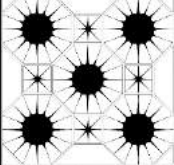
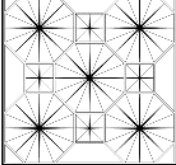
#### 4.1.2.3 Aperture area ratio

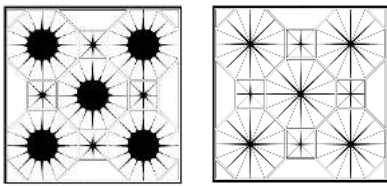
Since it is now approximately determined what the fully opened configuration might look like, a prediction on the performance of the redesign can be made. In **Paragraph 3.1.4**, it was explained how the aperture area ratio can give an idea of how much the facade can be shaded in hot temperatures and how much solar radiation can penetrate the building in cold temperatures. By substituting the central component of the AWI's south facade modules with a 4.8.8 tessellation component with thermo-bimetals, the calculations for the aperture area ratio in open and closed configurations can be made (**Table 5**). The aperture area ratio domain has decreased by 18% compared to the original central component with a circular diaphragm. The



value for the aperture area ratio with thermo-bimetals in closed configuration comprises the lower boundary of the original component by 5%, whereas the upper boundary (open configuration) is 22% lower. In other words, the lower boundary of 7% is lower than the 12% of the diaphragm and the upper boundary of 21% is also lower than the 44% of the diaphragm. This means the bimetal component would provide little more shade but allow way less daylight to enter the building, which is probably due to the density of the pattern.

**Table 5:** Results of the aperture area ratio for the central component of the thermo-bimetal-based redesign of the AWI.

Component	#	Configuration	Component area $A_c$ [cm <sup>2</sup> ]	Void area $A_v$ [cm <sup>2</sup> ]	Aperture area $A_a$ [cm <sup>2</sup> ]	Obstruction area $A_o$ [cm <sup>2</sup> ]	Aperture area ratio (%)
4.8.8 Tessellation	1	Open	3600.00	127.26	614.12	2858.62	21
		Closed			130.70	3469.30	7
						Range	14
Component dimensions: 60 x 60 cm							

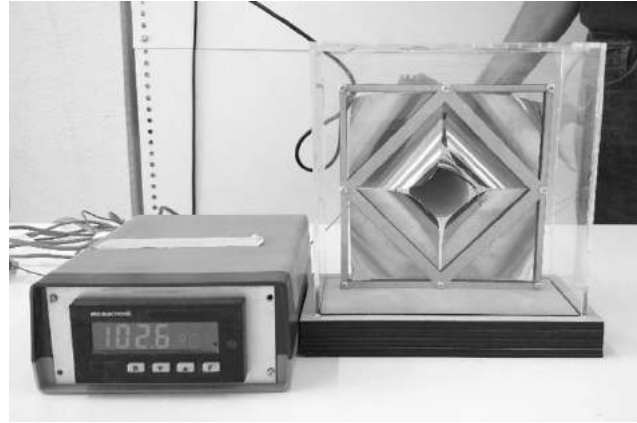
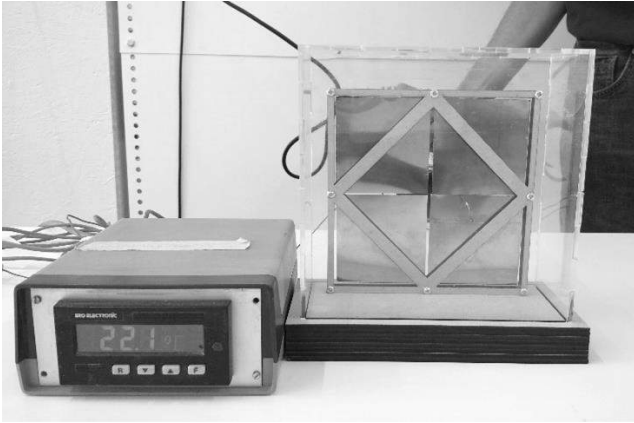


### 4.1.3 Prototyping

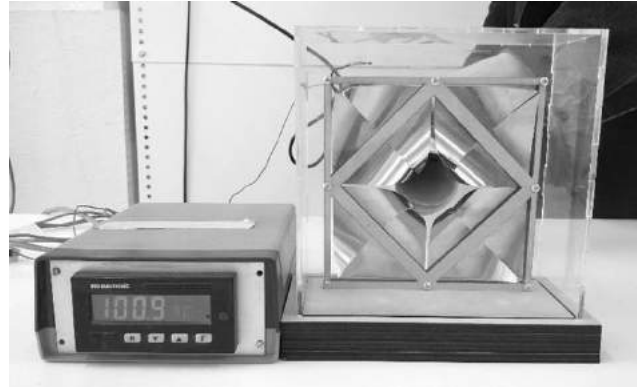
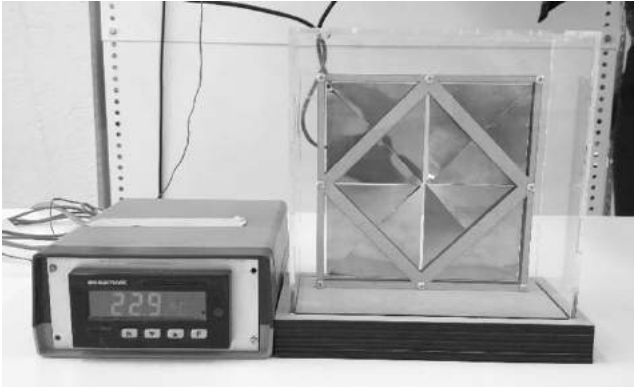
The next step is to test the simulations with physical models. This way, it can be checked whether the practical execution corresponds to the previously calculated aperture area ratios. However, due to the expensiveness and limited availability of samples of the acquired thermo-bimetal sheets, the prototyping development process is limited to a smaller component of the AWI, i.e. a component of 15 by 15 cm. The frame is composed by starting from a 4.4.4.4 tessellation and the bimetal sheets are positioned in such a way that the centre of the component generates a 4-pointed star shape. The density of the pattern is thus reduced compared to the redesign with a 4.8.8 tessellation, which may lead to better results. For an extended visualization of the deformations in relation to temperature changes, the reader is referred to **Appendix C**.

#### 4.1.3.1 In-the-plane positioning

The first experimentation consists in positioning the thermo-bimetal sheets inside the frame, parallel to the facade. The component is positioned inside an acrylic glass box in which a heat gun blows hot air to activate the bimetal sheets. A thermocouple inside the box is connected to a digital thermometer to measure the relationship between temperature and deformation. The latter property is however not measured numerically but remains a visual variable. In **Paragraph 4.1.2.1** it was mentioned that the triangular bimetal sheets should be cut in two for an expanded movement. To control this reasoning, both configurations are tested physically. As it appears that the difference between them is nearly invisible (**Figure 41** and **Figure 42**), the configuration with uncut elements is preferred over the cut ones for aesthetic reasons and a better evocation of the Islamic star pattern. Moreover, it is remarkable to which extent the temperature needs to be increased to induce a relatively small curling movement of the bimetal sheets. Furthermore, this configuration is contra-intuitively the reverse of what a shading device is intended to do. Rather than opening under increased temperature, the bimetal sheets should close to block solar radiation.



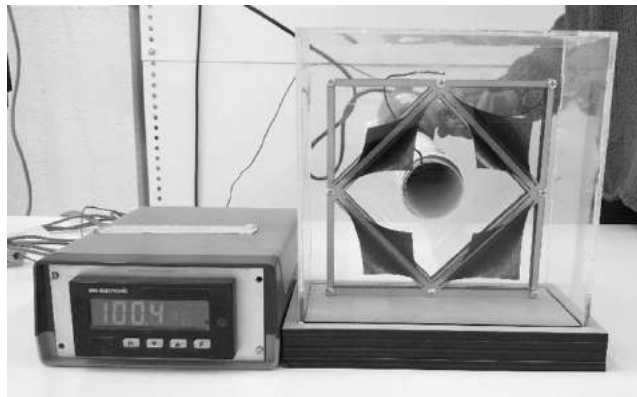
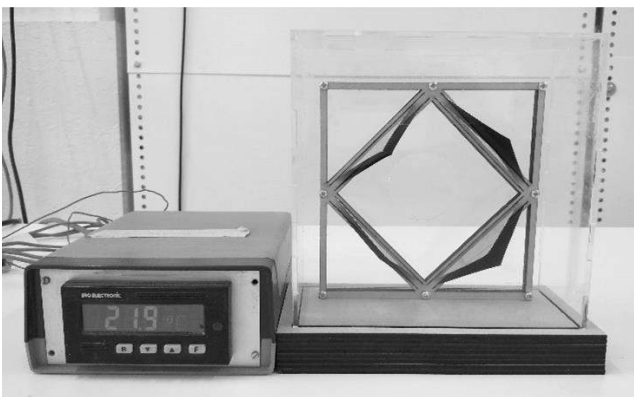
**Figure 41:** Closed (left) at room temperature and open (right) at  $\pm 100^\circ\text{C}$  configuration of the component with uncut bimetal sheets.



**Figure 42:** Closed (left) at room temperature and open (right) at  $\pm 100^\circ\text{C}$  configuration of the component with cut bimetal sheets.

#### 4.1.3.2 Out-of-plane positioning

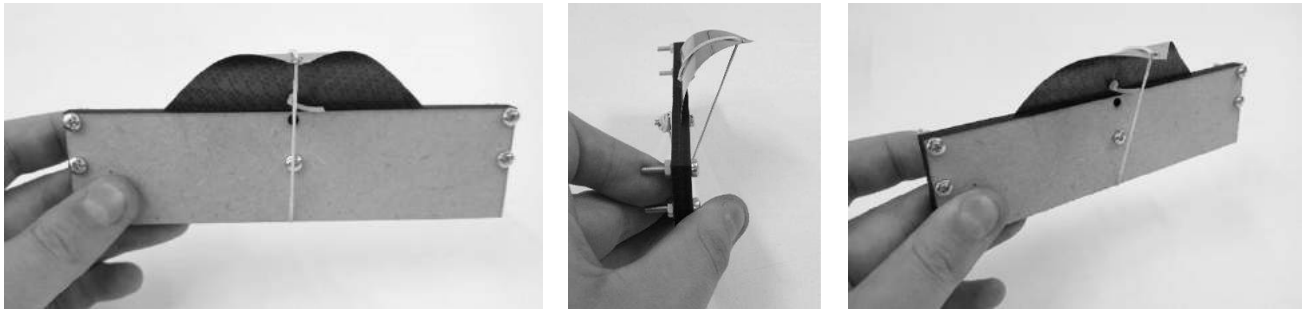
As explained in the previous paragraph, the component should be closing instead of opening when the temperature rises. Therefore, the inverse movement is generated by positioning the equally-dimensioned bimetal sheets perpendicular to the frame's plane. Although the bimetal sheets now move correctly (**Figure 43**), it is again produced to a limited extent under very high temperatures which would not take place in real-occurring situations. However, this configuration may be more effective if the sheets were dimensioned differently. By elongating the triangular pieces at the top corner, their altered proportions would result in a larger deformation. Due to the limited dimensions of the glass box, this experiment was not performed.



**Figure 43:** Open (left) at room temperature and closed (right) at  $\pm 100^\circ\text{C}$  configuration of the component with perpendicular sheets.

#### 4.1.3.3 Pre-bending with elastic cords

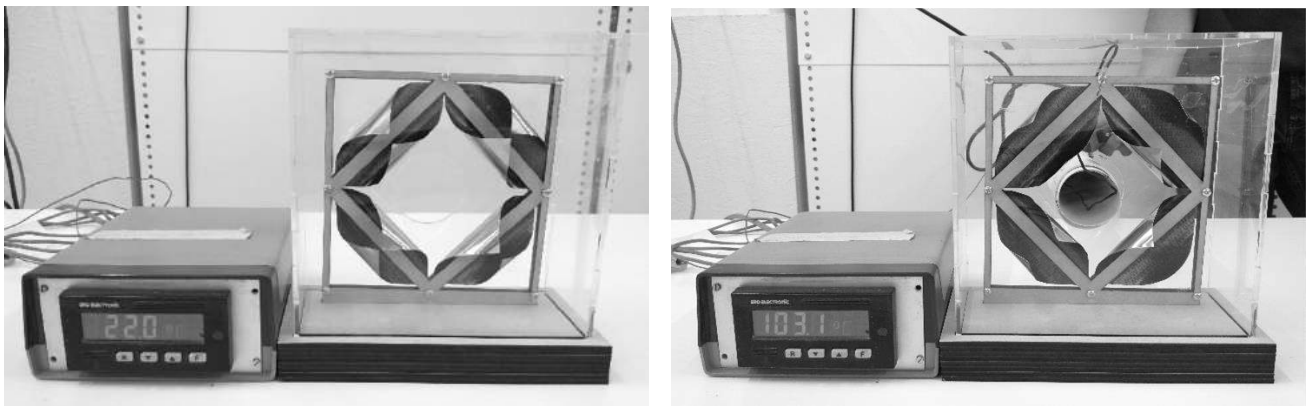
The two previous experiments show both extremes of the component's initial configurations, i.e. either too opened or too closed. To find an intermediate configuration, the bimetal pieces can be pre-bent by elastic cords. This allows for an initial inclined position that when heated, turns into a flat position to provide more shade. However, the tensional force required to pre-bend the sheets cannot be taken up by regular elastic cords and they require tensioning over a larger distance than the dimensions of the bimetal piece (**Figure 44**). These complications made it too difficult to test the entire component with tensioned bimetal pieces. Moreover, the movement becomes bi-stable due to the tensional threshold force of the elastic cord. Besides, the additional cords add to the overall complexity of the system, which thanks its beauty to its simplicity.



**Figure 44:** Illustrations of one triangular bimetal sheet that is pre-bent by an elastic cord.

#### 4.1.3.4 Pre-bending by plastic deformation

Another means to obtain an initial inclined position is by plastically deforming the bimetal sheets. By manually pre-bending them into a curled shape, a result similar to the method with elastic cords is achieved. However, the manual bending of the elements results in a less symmetric configuration and a staggered movement due to small differences in the plastic deformation of segments within one triangular piece. As expected, the movement is again limited when the component is subject to very high temperatures. Overall, it can be said that the exploration with thermo-bimetal sheets shows relatively poor results. Surprisingly, the physical development shows large differences with the expectations coming from the geometric simulations. This is probably due to the severe downsizing of the component used for the prototypes compared to the one used for the simulations, as larger and more elongated elements show larger deformations.



**Figure 45:** Open (left) at room temperature and closed (right) at  $\pm 100\text{ }^{\circ}\text{C}$  configuration of the component with pre-bent sheets.

## 4.2 Curved-line folding

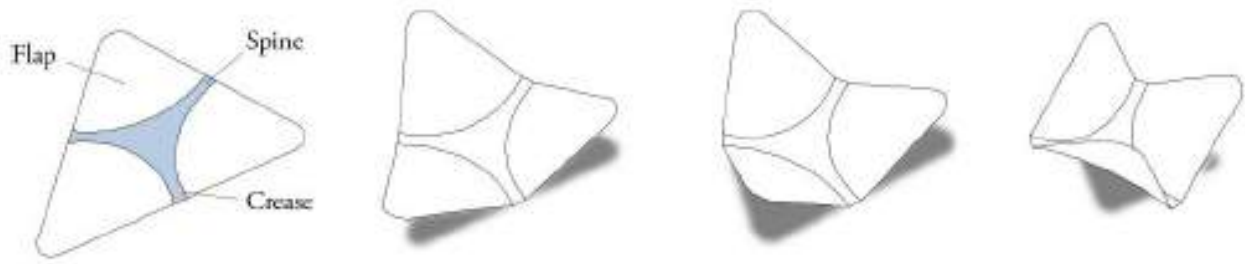
The concept of curved-line folding has proven to be successful in the Flectofold project, as mentioned in **Paragraph 3.2.5** of the previous chapter. It requires a small actuation force for the amplified movement of a large element. Furthermore, the shape of the element allows a variety of complex shapes when properly combined, whilst retaining a large range of aperture area ratio between its open and closed configuration. Parallel to its biomimetic discovery, this approach was also expanded using origami techniques. It was observed in a master thesis research that in terms of energy performance and indoor comfort, the application of curved-line folding systems for kinetic facades was found to be promising and able to compete with existing systems (Goetschalckx 2015). Concerning the materialization and actuation of elements with more than two creases, a Ph.D. research investigated the efficiency of several methods by means of kinetic simulations and prototypes (Vergauwen 2016). In this exploration, the aim is to find a way to activate the efficient mechanism of curved-line folding elements without the use of a complex motorizing system, like the Hygroskin project for instance (**Paragraph 3.2.2**) or like the previous exploration with thermo-bimetal sheets. Similar to flowers opening and closing, the curved-line folding elements should be able to fold and unfold by temperature changes in the environment. At the end of this chapter, two actuation methods will be presented: a controllable actuation using electrical current but without the use of motors; and a spontaneous actuation relying on ambient heat.

### 4.2.1 State of the art

Recent discoveries on curved-line folding techniques are briefly described below. It is remarkable to notice that two research groups independently developed a kinetic shading prototype following this approach, one using a biomimetic approach and the other applying an origami-based exploration.

#### 4.2.1.1 History

Discovered by students from the Bauhaus in the late 1920's, curved-line folding gradually found its way in art and architecture in addition to rigid-origami. The technique is based on folding paper into a three-dimensional form along curved creases, combining both bending and folding. Up until now, the method had only been used for architectural applications to create static structures. Recently, researchers got interested in the investigation of the transformation process as a whole for applications in kinetic architecture (Vergauwen 2016). The intermediate states of the curved-line folding process were discovered in nature as an abstracted plant movement found in *Aldrovanda vesiculosa*. The fast snapping motion of this aquatic plant was used as a biological role model for the prototyped kinetic shading device called Flectofold (Schleicher et al. 2015), which was analysed in **Paragraph 3.2.5**. Parallel to this discovery, researchers at the University of Brussels (VUB) expanded the range of curved-line folding elements from two creases (as in Flectofold) to three or four creases that generate a bending-active kinetic system (Vergauwen, De Temmerman, and Brancart 2014). **Figure 46** illustrates such a mechanism that will be investigated further in this chapter.



**Figure 46:** A curved-line folding element with three concave creases. The flaps fold upwards around the creases when the spine is bent (Vergauwen 2016).

#### 4.2.1.2 Materialization

In her Ph.D. research, Vergauwen studied the materialization and actuation of curved-line folding elements for their application as a pliable shading system. As such systems rely on elastic deformation without rupture, materials with high strength and low bending stiffness are required. Moreover, the compliant mechanism needs to be reversible and thus able to return to its initial state after actuation. Hence, the applied material should have a high resilience to absorb kinetic energy during the elastic deformation. By using Ashby's method for material selection, it was found that a group of thermoplastic elastomers corresponds to the three criteria explained above. It turns out polypropylene is a valuable candidate for several reasons. Firstly, it shows remarkable resistance to fatigue, which is important for the many cycles of folding/unfolding in its lifetime. Secondly, it is an affordable material that is suitable for laser cut technology. Thirdly, it is an ecological material since it is 100% recyclable. However, polypropylene is not a very strong material and it has a poor resistance to high temperatures and UV radiation. For the materialization of the curved crease, it was discovered that using traditional rotational joints causes the connection between the spine and the flaps to detach due to planarity in undesired areas. Instead, by locally reducing the thickness of the material, a zone with lower stiffness is created that acts like a continuous living hinge. Furthermore, the use of a living hinge reduces friction and wear problems and thus requires less maintenance (Vergauwen 2016).

Be that as it may, the Flectofold prototype was developed using a very different type of material. The material used in this project was a glass-fibre reinforced polymer (GFRP). This way, the structural parts can be customized by modifying the fibre direction and concentration in the matrix, allowing the stresses to be more evenly distributed. Adding multiple layers with different properties additionally facilitates the force flow (Körner et al. 2018).

#### 4.2.1.3 Actuation

As discussed in **Paragraph 3.2.5**, the actuation of the Flectofold prototype was found to act most efficiently using a continuous pneumatic actuator covering the backbone between the Flectofold and the frame (Körner et al. 2018). For an element with three concave creases, (Vergauwen 2016) investigated three types of actuation: the horizontal, vertical and combined actuation. The different types were studied with simulations and tested with small-scale prototypes (**Figure 47**).

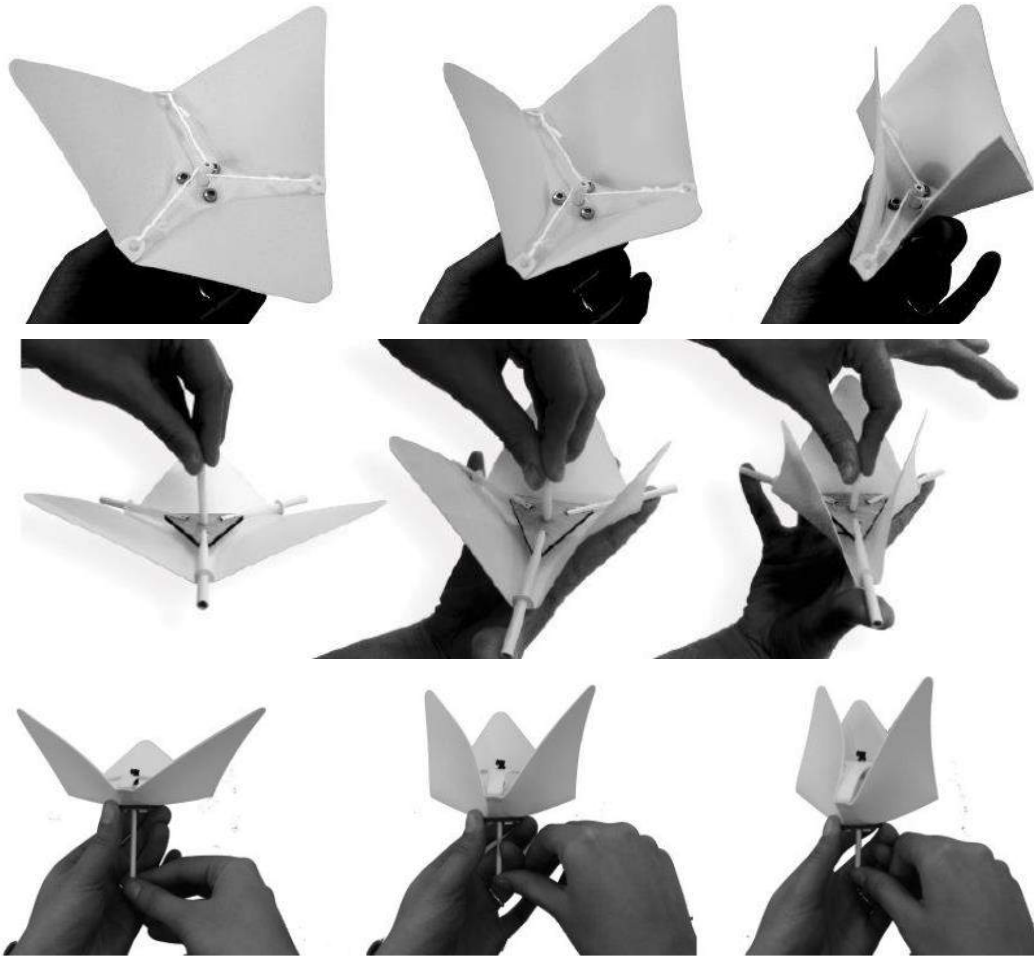
The horizontal actuation consists in pushing the boundary edges of the spine towards the centre of the element. As this would require three actuators per element that move the boundary segments over the exact same distance, it could lead to high production costs and asymmetric deformations of the flaps. An alternative solution was proposed to perform the horizontal actuation. This was done by wounding three cables around one central winch, pulling the spine edges towards the centre. Although this is a better method, it still requires a high actuation force and as the cables cannot take up compression forces, it is less suited when the structure has a low reversibility. The vertical actuation is done by pushing the centre of the spine downwards, making the flaps fold upwards. This was done by combining a central actuator bar with three sliders, allowing the horizontal displacement of the boundary spine edges. Unlike the horizontal actuation, this method also works for asymmetric crease patterns. Even though the actuation force and stresses in the creases are lowered using this technique, the integration of a sliding system increases the complexity and thus the costs and maintenance of the kinetic shading device. However, an innovative actuation technique using an additional spine layer was developed to perform the combined actuation type. Using a second spine layer with the same contour and joined at the spine edges, one linear actuator can be applied to increase the distance between those two layers. As shown in **Figure 47**, the central bar pushes the layers away from each other, tensioning the spine's boundary segments and guiding the elastic deformation of the spine optimally. This actuation method drastically reduces the required actuation force and makes it an elegant solution, eliminating the need for a secondary structure and demanding just one linear actuator. It is this actuation type that was successfully prototyped at a medium scale (Vergauwen 2016).

### 4.2.2 Redesign

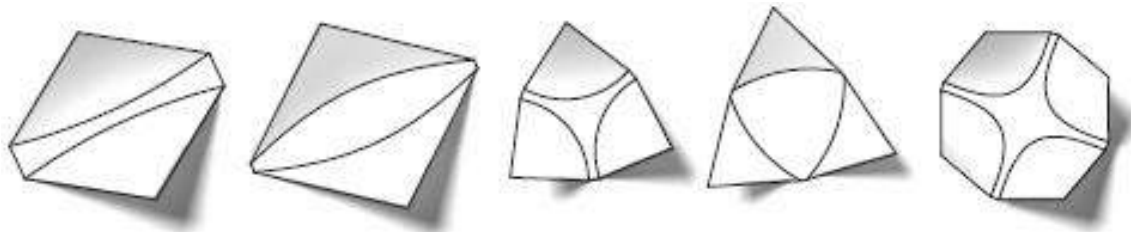
Bearing in mind the design parameters that were discussed in **Paragraph 3.1.7** of Chapter 3, a similar redesign process as in **Paragraph 4.1.2** of this chapter can be elaborated with curved-line folding elements. The starting point is a blank module of the south facade of the Arab World Institute (**Figure 20**), in which combinations of elements ought to form traditional Arabic patterns whilst retaining a large range of aperture area ratio between open and closed configurations. Siemen Goetschalckx (Goetschalckx 2015) compared several curved-line folding elements (**Figure 48**) with regard to energy performance and indoor comfort. He concluded that for elements with more than two creases, concave creases are preferred over convex creases as it reduces the permanently covered area of the facade. Also, compositions of elements with more creases are more efficient due to more scattered or reflection of sunlight. However, in this design this is less important as the scale of the components is relatively small.

#### 4.2.2.1 Arabic geometric patterns

Considering Hankin's method for the generation of Arabic geometric patterns, which was explained in **Paragraph 4.1.2** of this chapter, a new composition for the AWI's south facade can be proposed. A method for framing Euclidean tessellations into the square components is visualized in **Table 6** and described hereunder in 10 steps:



**Figure 47:** *Top:* Horizontal actuation using a winch and three cables. *Middle:* Vertical actuation using a central actuator bar and three sliding bars. *Bottom:* Combined actuation using a central actuator bar and a double layer (adapted from Vergauwen 2016).



**Figure 48:** From left to right: two concave creases, two convex creases, three concave creases, three convex creases, four concave creases (Goetschalckx 2015).

- 1) A Euclidean tessellation able to produce Arabic geometric patterns is chosen.
- 2) The most complex polygon is centralized and the midlines for all polygon sides are drawn.
- 3) The diameter of central polygon's circumcircle is equal to the square component's side length.
- 4) In between the tessellation and the midlines, a curved-line folding element is imagined.
- 5) The curved-line folding element is repeated to fill the central polygon.
- 6) The creases are drawn to form a joined circle in open configuration.
- 7) If necessary, the drawing is rescaled to fit inside the square component.
- 8) The finished component is evaluated and assigned to one of the three component sizes.
- 9) The frame to which the elements are attached is drawn.
- 10) When the elements open, the generated Arabic geometric pattern is demonstrated.

There are a few remarks to be made on this method. Firstly, the method does not work for all tessellations. Preliminary, intuitive tests were done before choosing the tessellations with the greatest potential for substituting the components of the AWI. Secondly, the evaluation in step 8 was done by reasoning that for aesthetic reasons, the most complex Arabic pattern should be assigned to the component with the highest level of hierarchy in the module. Moreover, the dimensions of the elements should not become too small, therefore a component with a larger number of elements should correspond to a component at a larger scale. Thirdly, a pleasing aspect to notice is that the frame to which the elements can be attached (step 9) coincides with the initial tessellation that was chosen. Finally, to respect the geometric complexity of the existing module, it must be noted that there are three different types of the smaller diaphragms. Hence, two more types of small components must be designed. By slightly adapting the method described above, two additional designs evoking Arabic patterns were found: one element with four concave creases and four elements with two convex creases. In open configuration, the first one resembles a 4-pointed star and the second a cross which occurs in Arabic tiling as well. The three smaller component designs were positioned in the blank module as follows: the element with four creases gets the most number of components as it requires only one actuator per component; the element with two creases forming a 4-pointed star is positioned around the central component and the element with two creases forming a cross is awarded the least number of components as it has the least strong reference to Arabic architecture.

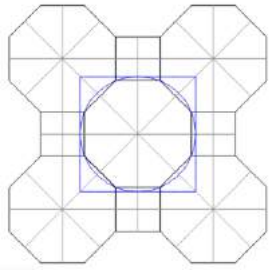
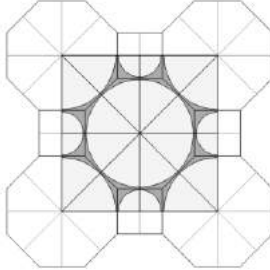
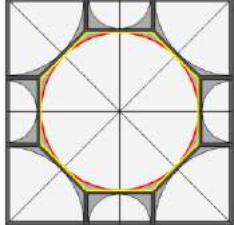
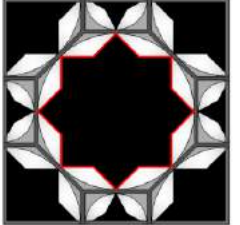
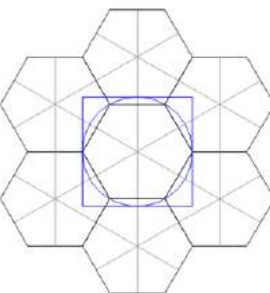
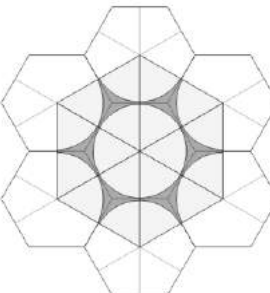
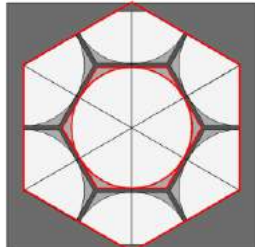
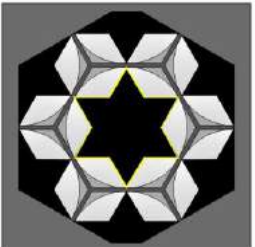
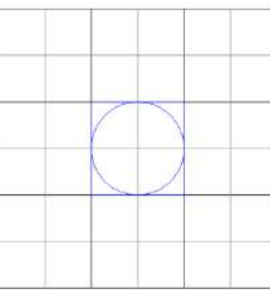
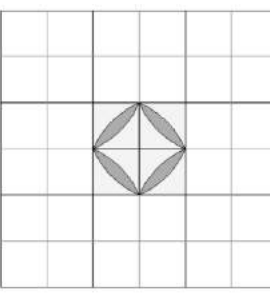
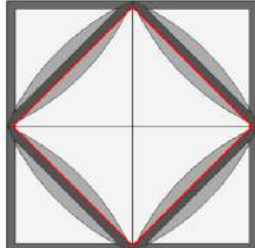

In **Figure 49**, the newly designed components are positioned accordingly, clearly evoking the traditional mashrabiya pattern like Jean Nouvel intended. Additionally, the module of the AWI contained eight smaller elements without diaphragms but instead a piece of stainless steel to hide the two pistons that actuate the system. In this design, those are not required so the whole module can be filled with components containing curved-line folding elements. Another important remark to be made is that the original design produced a series of static Islamic star patterns, whereas the redesign with kinetic curved-line folding elements is able to produce a whole range of intermediate states of the same and supplementary patterns originating from several tessellations.

### 4.2.2.2 Aperture area ratio

Just as in **Paragraph 4.1.2.3** of the thermo-bimetal exploration, the aperture area ratio for the curved-line folding components are calculated and given in **Table 7**. Unlike the components of the AWI, the range between the aperture area ratio in the open and closed configuration does not necessarily increase with higher component dimensions. As the 6.6.6 tessellation component required an additional hexagonal framing, it has a lower aperture area ratio range than the 4.4.4.4 tessellation components. The total domain for the module is now 47%, which means it almost quadrupled the original range of the AWI. Additionally, the total domain of the AWI fits inside that of the curved-line folding based redesign. This means the redesign respects the aperture area ratio domain boundaries of the IMA and extends it on both sides. Hence, as explained in **Paragraph 3.1.4**, the energy performance of the redesign with curved-line folding elements is expected to be more beneficial than that of the original design.



**Table 6:** Demonstration of the method for framing tessellations with curved-line folding elements. The steps to be taken were explained earlier in this section and are included in the titles. The two right columns are showing the rear view of the component. The red indicates geometric shapes recurring in the AWI, the yellow depicts new Arabic references.

Tessellation (1-3)	Curved-line folding (4-7)	Square component (8-9)	Arabic pattern (10)
4.8.8	3 asymmetric concave creases (8x)	60 x 60 cm	8-pointed star
			
6.6.6	3 concave creases (6x)	30 x 30 cm	6-pointed star
			
4.4.4.4	2 convex creases (4x)	15 x 15 cm	4-pointed star
			

#### 4.2.2.3 Kinematic simulations

To visualize the kinetic facade system dynamically, it was decided to model it in a digital environment. By changing parameters and visualizing the consequential effect, the structural behaviour of the kinetic system can be studied to materialize and prototype it afterwards in an efficient manner (Vergauwen 2016). Additionally, it provides a preliminary design to review the aesthetics of the movement, as well as the composition of the components in the module. However, there is no numerical outcome from this process, for such results are drawn from kinematic and kinetic simulations done with Finite Element Analysis (FEA) software. As the curved-line folding elements remain relatively small in this design, it is preferred to experimentally determine certain properties, which will be done in the next section.

During her Ph.D., Vergauwen investigated software for the geometric modelling of pliable systems. Tomohiro Tachi's Freeform Origami © tool seemed convenient during the phase of exploration, as it was able to rapidly perform the folding action of a certain pattern. However, it appeared to be difficult to measure the

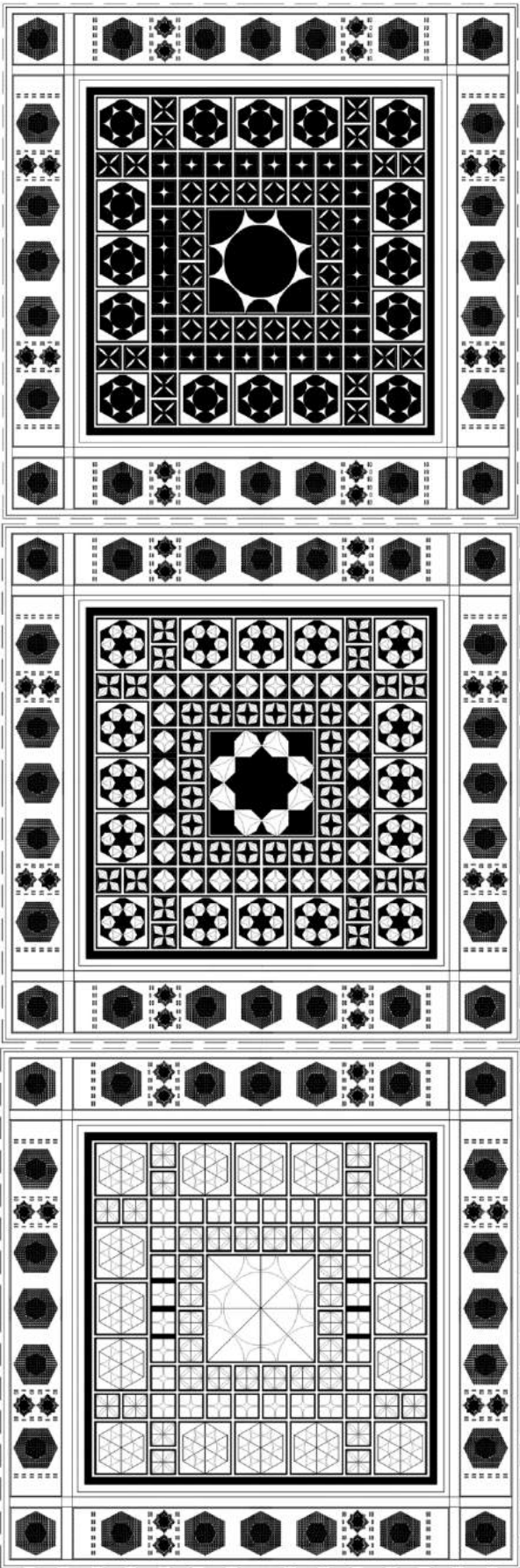

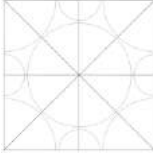

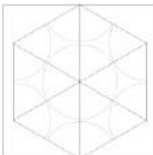

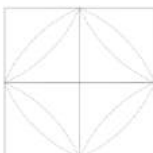
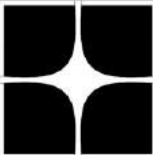
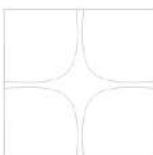
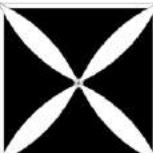
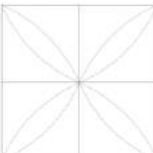
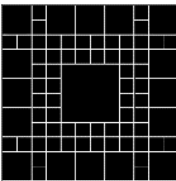

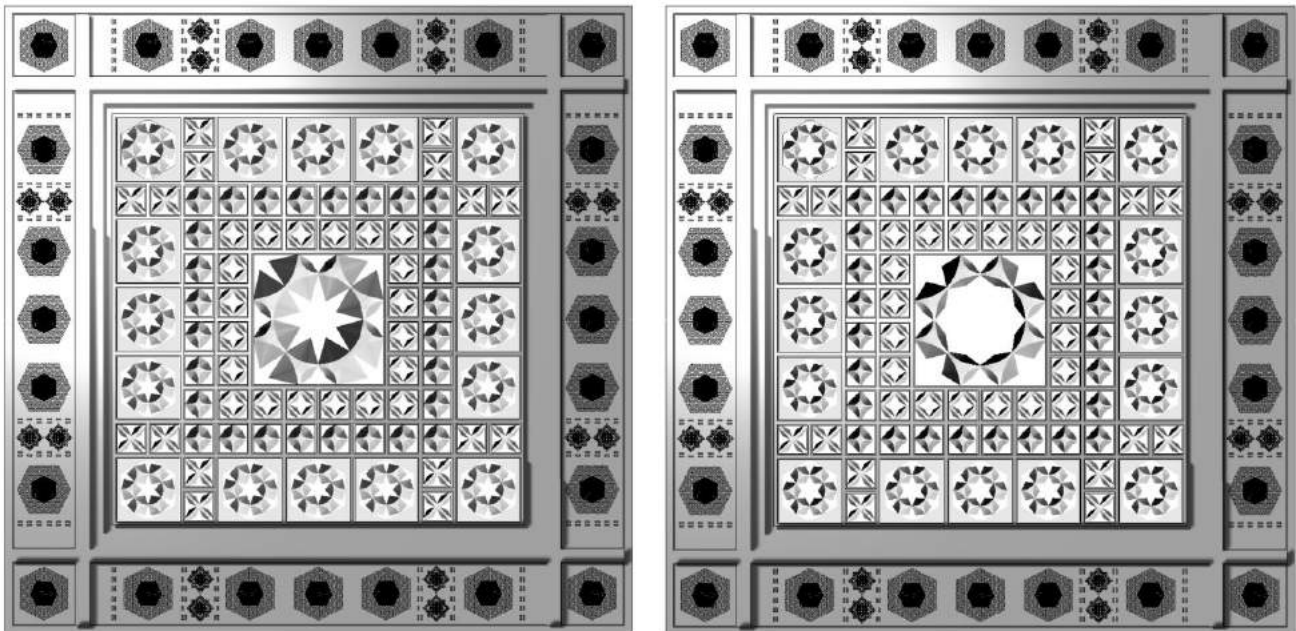


Figure 49: Open (top), intermediate (middle) and closed (bottom) configuration of the redesign of the AWI’s south facade with curved-line folding elements.

**Table 7:** Calculation of the aperture area ratio for one module of the curved-line folding based redesign of the AWI.

Component	#	Configuration	Component area $A_c$ [cm <sup>2</sup> ]	Void area $A_v$ [cm <sup>2</sup> ]	Aperture area $A_a$ [cm <sup>2</sup> ]	Obstruction area $A_o$ [cm <sup>2</sup> ]	Aperture area ratio (%)
4.8.8 Tessellation	1	Open	3600.00	127.26	3023.59	449.15	88
		Closed		0.00	3600.00	0.04	4
						Range	84
Component dimensions: 60 x 60 cm							
6.6.6 Tessellation	16	Open	900.00	61.00	499.03	339.97	62
		Closed		0.00	839.00	0.07	7
						Range	55
Component dimensions: 30 x 30 cm							
4.4.4.4 Tessellation I	20	Open	225.00	28.30	141.73	54.97	76
		Closed		0.00	196.70	0.13	13
						Range	63
Component dimensions: 15 x 15 cm							
4.4.4.4 Tessellation II	28	Open	225.00	28.30	170.03	26.67	88
		Closed		0.00	196.70	0.13	13
						Range	75
Component dimensions: 15 x 15 cm							
4.4.4.4 Tessellation III	16	Open	225.00	28.30	140.38	56.32	75
		Closed			0.00	196.70	13
						Range	62
Component dimensions: 15 x 15 cm							
Framework	1	Invariable	2800.00	132.31	0.00	2667.69	
							
Module dimensions: 200 x 200 cm							
Module	1	Invariable	44100.00	3071.97	35344.08	5683.95	
							
Module dimensions: 200 x 200 cm							
Total		Open		6118.70	20849.45	16987.77	61
		Closed			0.00	37964.48	14
						Range	47

amount of folding and therefore to compare various patterns. Robofold's Kingkong plugin for Grasshopper and Rhinoceros 5 functioned very well for uncomplicated patterns, but due to the inaccessible script used for the folding simulation, the plugin does not work for more complex patterns. Still, a recently developed component for the Kangaroo plugin for Grasshopper called Origami, by Daniel Piker, proved to be the most promising tool for geometric simulations of pliable systems. It allows the user to define a mesh with mountain and valley folds as the input and retrieve a new mesh along with a list of forces as the output, which can then be used again as an input for the Kangaroo Live Physics component to simulate the folding process. The only drawback of this tool is that the relatively slow form-finding process can become very heavy for a large number of elements to be simulated simultaneously (Vergauwen 2016). In **Figure 50**, the module of the AWI is modelled in Rhinoceros 5 and the curved-line folding elements are simulated in the Kangaroo plugin for Grasshopper. By activating one button, all the component's elements can fold at once. For images of the Grasshopper script used for this simulation, the reader is referred to **Appendix D**.



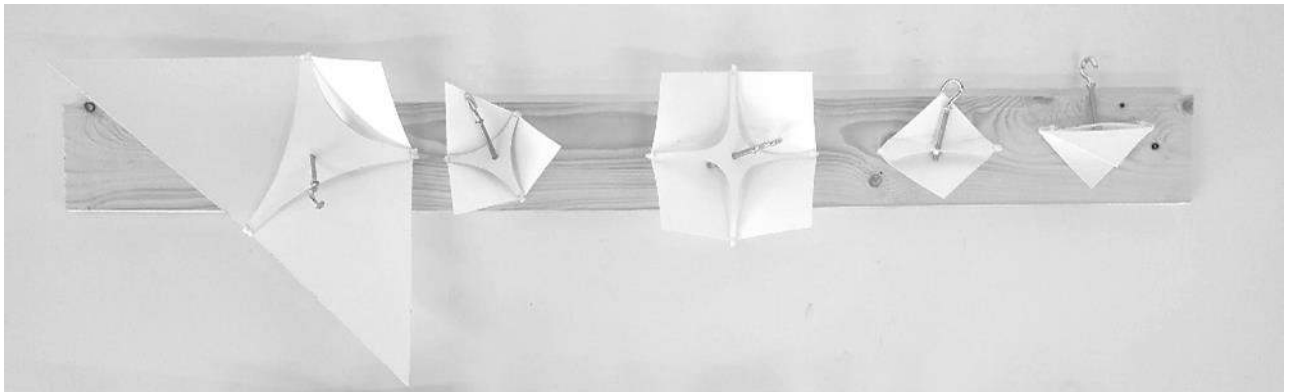
**Figure 50:** Simulation of two intermediate configurations of the redesign of the AWI's south facade with curved-line folding elements.

### 4.2.3 Prototyping

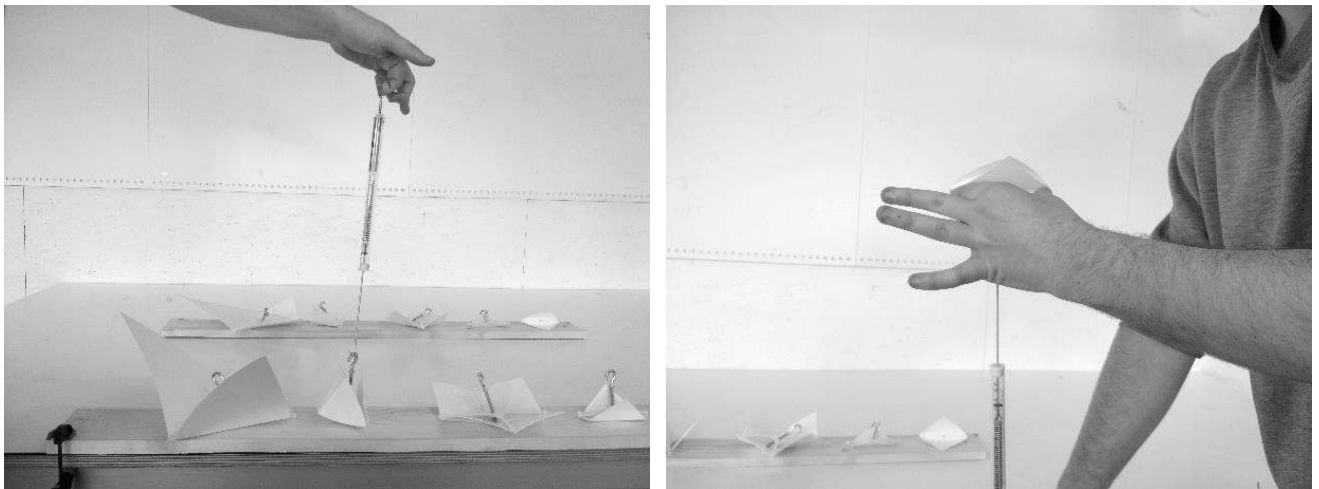
In this section, just as in **Paragraph 4.1.3** of the thermo-bimetal exploration, the curved-line folding based experimentations are described. First, it is explored how the elements can be pre-folded, that is, how they are kept in their folded position or open configuration 'at rest'. Then, a study follows on how the pre-folded elements can be actuated by a Nitinol wire when the temperature rises, turning the elements to their unfolded position or open configuration. As it turned out to be the most elegant and effective way to actuate curved-line folding elements, the technique with the double spine layer will be used in this exploration. The goal is to find a way to unfold the curved-line folding element when there is a need for shading. It is, in fact, the reverse actuation of the Flectofold and the prototype developed by Vergauwen.

#### 4.2.3.1 Folding force measurement

To determine what action is required to keep the elements in their folded position at rest, an experiment measuring the force needed to pull the upper spine until the element is in its closed configuration was set up. **Figure 51** illustrates the set-up for two series of experiments to test how much difference in pulling force there is, relative to the thickness. The elements are screwed into the wooden plank, the double spine is attached to the element with self-locking nylon winding strips and a hook and nut provide the possibility to measure the pulling force with a dynamometer, as is shown in **Figure 52**. The distance between the centres of the spines is also measured, and the results are summarized in **Table 8**.



**Figure 51:** Folding force measurement set-up of the five curved-line folding elements with a thickness of 0,5 mm. The same set-up was made for elements with a thickness of 0,8 mm.








**Figure 52:** Measurements of the folding force  $F_f$  of a 3-crease 6.6.6 element (left) and a 2-crease convex 4.4.4.4 element (right) using an analogue dynamometer.

A first conclusion from this table is the high difference in required folding force between the two thicknesses. The elements with a thickness of 0,8 mm are more rigid and thus more resistant to external disturbances and show a smoother folding-unfolding movement. However, these advantages do not cope with the high differences in folding force. Moreover, the elements are protected by a double glass pane on both sides, so mechanical disturbances should be minimal. Yet, the 3-crease 4.8.8 element shows a very low difference in folding force between the two thicknesses. For elements of a larger scale, it can thus be concluded that choosing for a higher thickness is valid. A third noticeable aspect is the length between the

centres of the spines, which shows a very high value for the 4-crease 4.4.4.4 element that could be due to the high curvature of its creases. Finally, the 2-crease concave 4.4.4.4 element will be chosen over its convex brother, as it requires very high pulling forces and is not able to be attached to the frame the same way as the other elements. For the following experimentations, the 6.6.6 element with three concave creases and a thickness of 0,5 mm will be used for its symmetry and relatively low values of both  $F_f$  and  $L_i$ .

**Table 8:** Experimentally determined values of the folding force  $F_f$  and the interlayer distance  $L_i$  for two thicknesses  $t$ .

			4.4.4.4 Elements			6.6.6 Elements	4.8.8 Elements
			2-creases convex	2-creases concave	4-creases concave	3-creases concave	3-creases concave asymmetric
							
$t$ [mm]	0,5	$F_f$ [N]	12	5	9	8	6
	0,8		70	9	25	20	8
	$L_i$ [mm]		23	42	81	28	41

#### 4.2.3.2 Pre-folding with elastic cord

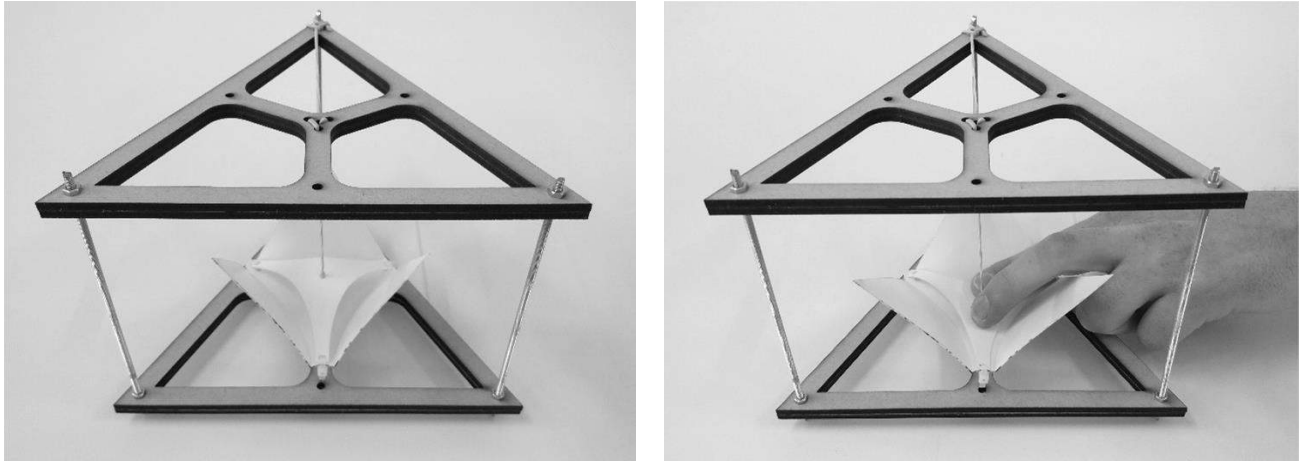
As the curved-line folding element needs to be closed 'at rest', a force equal to  $F_f$  is needed to keep the spine layers away from each other at distance  $L_i$ . One way to do this is to pull with an elastic cord with force  $F_f$  from the outside of the element in the centre of the spine until the element is in a folded position. However, the other end of the cord needs to be attached to another point in the extension of the pulling force. This can be done by adding an additional frame with an offset distance at least equal to the height of the element in the folded position (**Figure 53**). However, a regular elastic cord is not able to take up the tensional force to pre-fold the element completely. Moreover, when a vertical point load is applied on the upper spine, the unfolding movement is very limited as the most of the load is transmitted to an additional tensioning of the elastic cord. Besides, the elastic cord loses its tensile strength over time due to creep deformation.

#### 4.2.3.3 Pre-folding with pressure spring

Another approach is to push instead of pulling the layers away from each other to keep the element in its folded position, which can be done with a pressure spring. However, a traditional cylindrical pressure spring would be subjected to buckling due to the pressure of the spines. Besides, such a type of spring cannot be fully compressed, as the spring windings get stacked to a certain height. Then again, a conical pressure spring can solve both problems: its conical shape prevents the buckling effect and allows the spring to be compressed to a thickness of one spring winding. To find the conical pressure spring with the correct properties, a simple calculation based on Hooke's law, illustrated in **Figure 54**, was performed. When the spring is inserted in between the layers, these exert a force equal to the folding force  $F_f$  because the element wants to return to its initial flat state. The expression for the initial spring length  $L_0$  is thus:

$$L_0 = L_1 + L_f \text{ with } L_1 = L_i$$



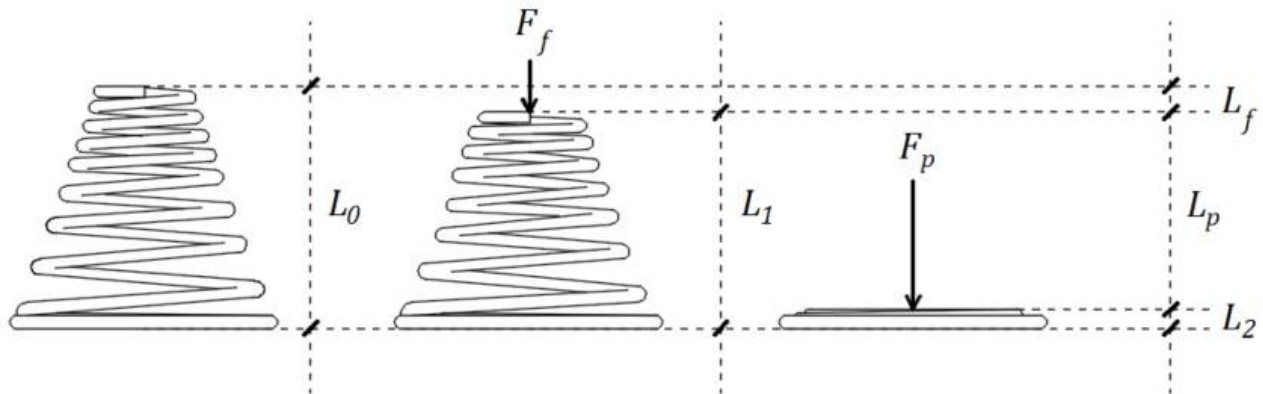


**Figure 53:** Small difference in folding position between the element in its folded position (left) and unfolded position (right).

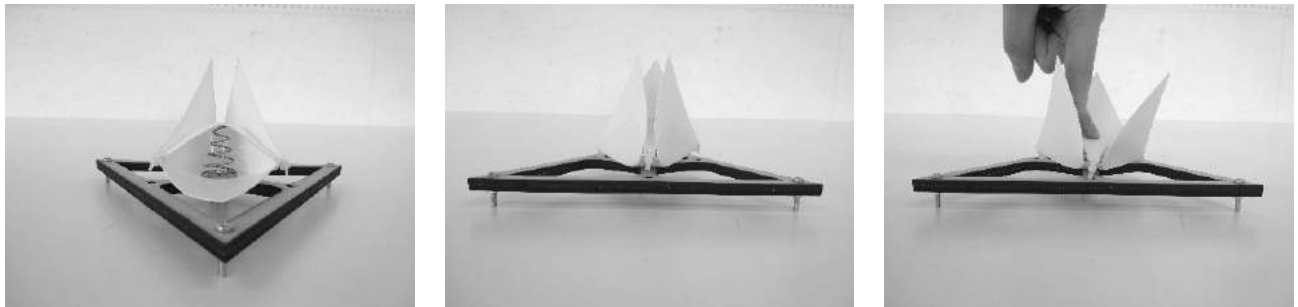
For a spring constant  $k$ , we know from Hooke's law:

$$F = kL \text{ and thus } L_f = \frac{F_f}{k} \text{ so } L_0 = L_i + \frac{F_f}{k}$$

The value for the spring constant  $k$  should not be chosen too high, for the actuation force  $F_p$  to unfold the element should be kept as low as possible. Nonetheless, the law of Hooke for springs is linear, but in practice, the force  $F_p$  grows exponentially with the compression length  $L_p$ . As demonstrated in **Figure 55**, the pre-folding with a pressure spring keeps the element folded, but it is quite hard to fully compress it again to unfold the element. Additionally, it is rather tricky to keep the spring symmetrically in between the layers, which eventually causes the element to unfold asymmetrically. However, a significant improvement has been done compared to the pre-folding with an elastic cord.



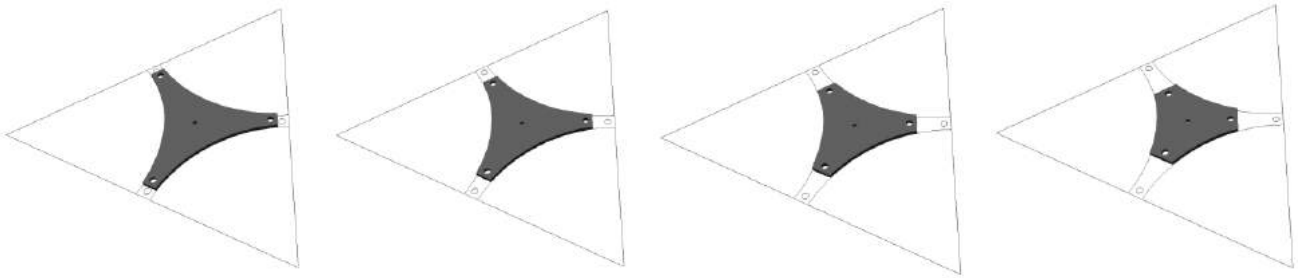
**Figure 54:** Scheme of the forces operating on the conical pressure spring. The folding force  $F_f$  will cause the spring to compress to from length  $L_0$  to length  $L_1$ . A vertical point load  $F_p$  compresses the spring to length  $L_2$ .



**Figure 55:** Left: Visualization of the conical spring. Middle: Element in folded position. Right: Unfolding under a vertical point load.

#### 4.2.3.4 Pre-folding with elastic spine

As the approaches discussed in the two previous paragraphs implied the use of an additional part of the mechanism, the possibility of pre-folding the element without adding complexity to the system will be explored. This can be done by changing the properties of the double layer. In a first instance, the additional spine should have shorter boundary segments to pull the curved-line folding element into its folded position (**Figure 56**). However, it should be able to return to its initial unfolded state after applying a vertical force in the centre of the spine. Therefore, the material of this added spine should be elastic, yet strong enough to keep the element in its folded position at rest. Multiple efforts have been done to 3D-print with flexible and elastic filaments such as nylon and plasticized copolyamide thermoplastic elastomer (PCTPE), with very poor results (**Appendix D**). Although the reasoning behind this method may seem to be correct, a possible outcome might be that the elastic spine will not make the element unfold when subjected to a vertical point load. A scenario similar to the one of Paragraph might occur if the point load is only partially transmitted to the boundary segments of the element.



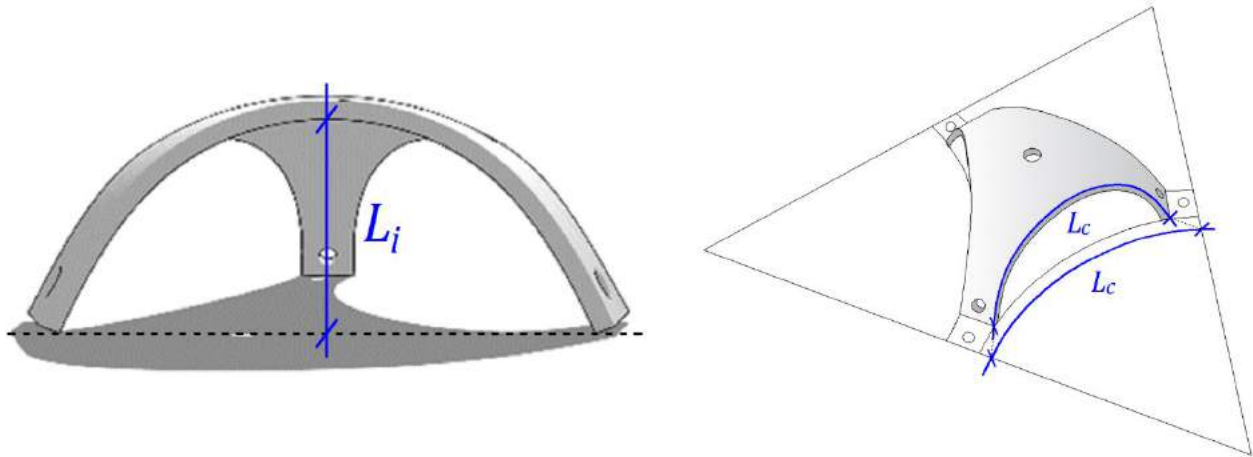
**Figure 56:** Variations of the elastic spine's dimensions by shorter boundary segments. From left to right: 5, 10, 15 and 20 mm indent.

#### 4.2.3.5 Pre-folding with pre-bent spine

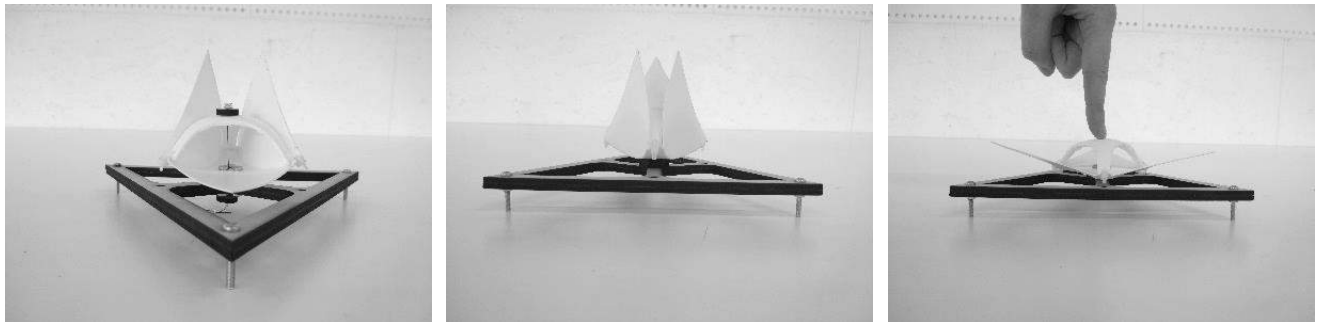
Another means to pre-fold the element is to create a pre-bent spine that acts like a pressure spring. For this method, the added spine should be lifted in its centre by a distance at least equal to  $L_i$ . In other words, the curvature of the pre-bent spine should be at least that of the polypropylene spine that was pre-folded by the conical pressure spring as explained in **Paragraph 4.2.3.3**. Like the spring, the pre-bent spine should retake its initial shape at all times after the application of a vertical point load in the centre. The length of the creases, i.e. the curved boundaries of the spine, should have the same length as the creases of the element in its flat state, as the spine should be able to obtain this flat position when actuated and have the same contour as the spine of the curved-line folding element. **Figure 57** visualizes these conditions in a comprehensive way. Calculating the exact shape needed to pre-fold the element sufficiently is quite hard, as it depends on the thickness, the height and the curvature. Therefore, a parametric model was developed in order to perform a trial-and-error process with 3D printing. For consulting the Grasshopper script used for these adaptations, the reader is referred to **Appendix D**. A Ultimaker<sup>2</sup> printer was used for this phase, printing with polylactic acid (PLA) filament. This 100% biodegradable plastic is commonly used for 3D printing as it is accurate and relatively easy to print with. The drawback is that it is brittle, but for the scale of this application, it should be rigid yet flexible enough. After a long series of tests, it turns out that the best performing model has a



height of 22 mm and a thickness of 2 mm. As shown in **Figure 58**, the element unfolds smoothly and symmetrically when applying a vertical point load, lower than in the case of the conical pressure spring. Moreover, the pre-bent spine does not need to be fully compressed to unfold the element. This may be due to the boundary segments of the spine exerting an almost vertical force on the boundary segments of the boundary segments of the polypropylene elements, making the flaps open up more easily.



**Figure 57:** *Left:* Front view of the pre-bent layer where the height should at least be equal to the interlayer height  $L_i$ . *Right:* Visualization of the crease length  $L_c$  of the pre-bent spine and the flat element.



**Figure 58:** *Left:* Visualization of the pre-bent spine. *Middle:* Element in folded position. *Right:* Unfolding under a vertical point load.

#### 4.2.3.6 Actuation with electrical current

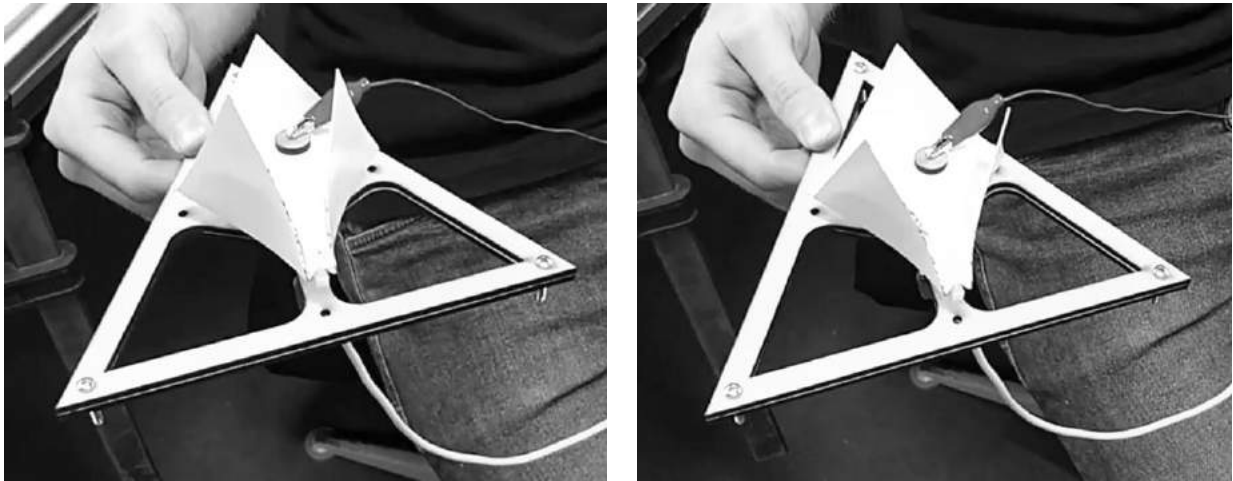
The most promising technique to pre-fold the curved-line folding element was by using a 3D printed pre-bent spine in PLA. It allows the element to be in its folded position at rest and requires a small vertical point load in the centre of the spine to unfold the element. Now, the objective is to investigate how the element can be actuated. This can either be done by applying a vertical point load like in the previous tests, or by pulling the two layers towards each other. Inspiration was drawn from the Air Flower designed by Lift Architects which was discussed in **Paragraph 3.2.3**. Fascinated by the blooming mechanism of the yellow crocus, they developed a ventilation system able to open and close without the use of motors or other bulky actuating systems. Although the flower blooms due to the intrinsic properties of its flower petals, i.e. differential expansion of cell layers under the influence of temperature difference, the actuation system developed by Lift Architects is using a similar stimulus to activate the device. Solar radiation as a heat source warms up a shape memory alloy (SMA) wire that contracts about 8% of its length and induces a rotation of the panels around hinge tubes, opening up the component like a blooming flower.

In this adaptive shading system, the Nitinol wire can function as a linear actuator to pull the pre-bent spine towards the curved-line folding element, generating a flower-like blooming effect. The SMA wire works best when electrically powered, generating a heat source due to the resistivity of the wire. When the electrical current is removed, the wire cools down and due to the relaxation effect, the element takes back its initial folded position. Using this approach, the components of the adaptive facade can be controlled in a way that building occupants can choose whether the shading elements are in an open or closed configuration. For the first test, a Flexinol® wire with a length of  $\pm 5$  cm and a diameter of  $375 \mu\text{m}$  was used. This SMA wire has an activation temperature of  $70^\circ\text{C}$ , a pulling force of about  $2250 \text{ g}$  ( $\pm 22 \text{ N}$ ) and contracts about 3-5% of its length. It has a resistance of  $8.3 \Omega/\text{m}$  and the recommended current to be applied is  $2250 \text{ mA}$ . To know the voltage to be used, we can apply Ohm's law:

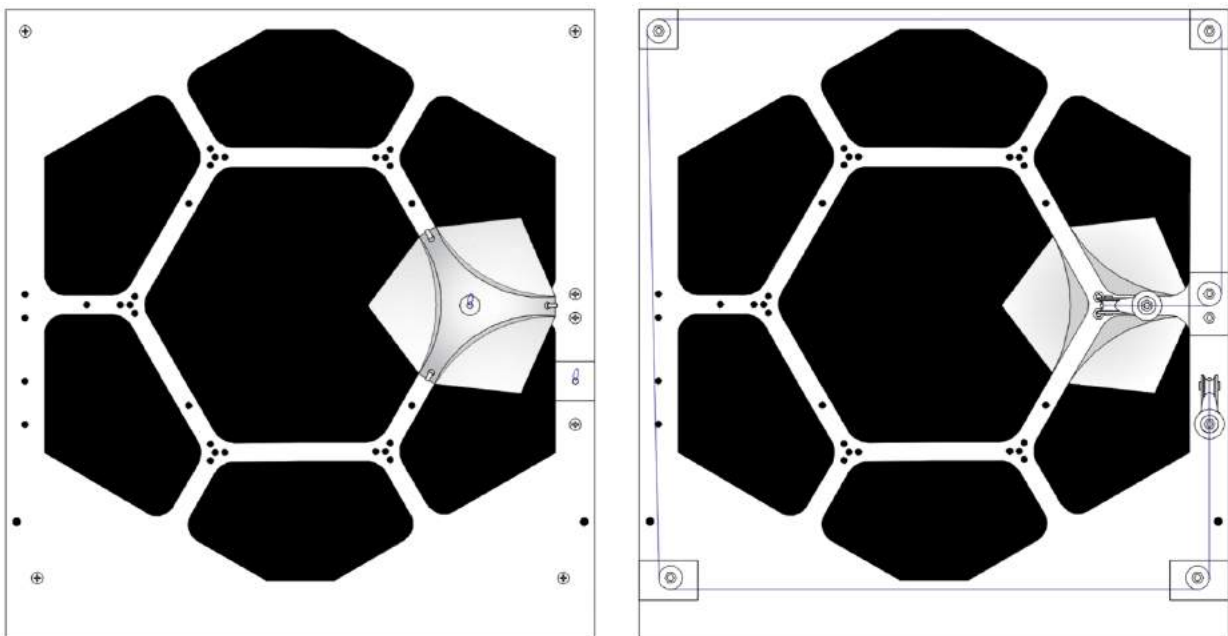
$$I = \frac{V}{R} \text{ so } V = 2,250 \text{ A} \times 8,3 \frac{\Omega}{\text{m}} \times 0,05 \text{ m} = 0,93 \text{ V}$$

**Figure 59** demonstrates the first actuation test with the electrical current applied to the Flexinol® wire of an element in a triangular frame. The ends of the wire are bent in a U-shape and held tightly by means of a crimping bead to avoid the sliding of the wire through its connections. The small piece of wood in between the spine and the crimping beads serves as an insulator to prevent the PLA from melting as the wire heats up. As can be seen, the unfolding movement is very limited. Naturally, this is due to the contraction of the wire over a small length: only 1,5 to 2,5 mm for a wire of 5 cm long. To extend the motion, a longer wire is needed. However, winding the wire up around a spool does not work as the friction becomes too high, limiting the active length of the wire to contract. Therefore, a system with pulleys around which the wire can slide freely needs to be developed.

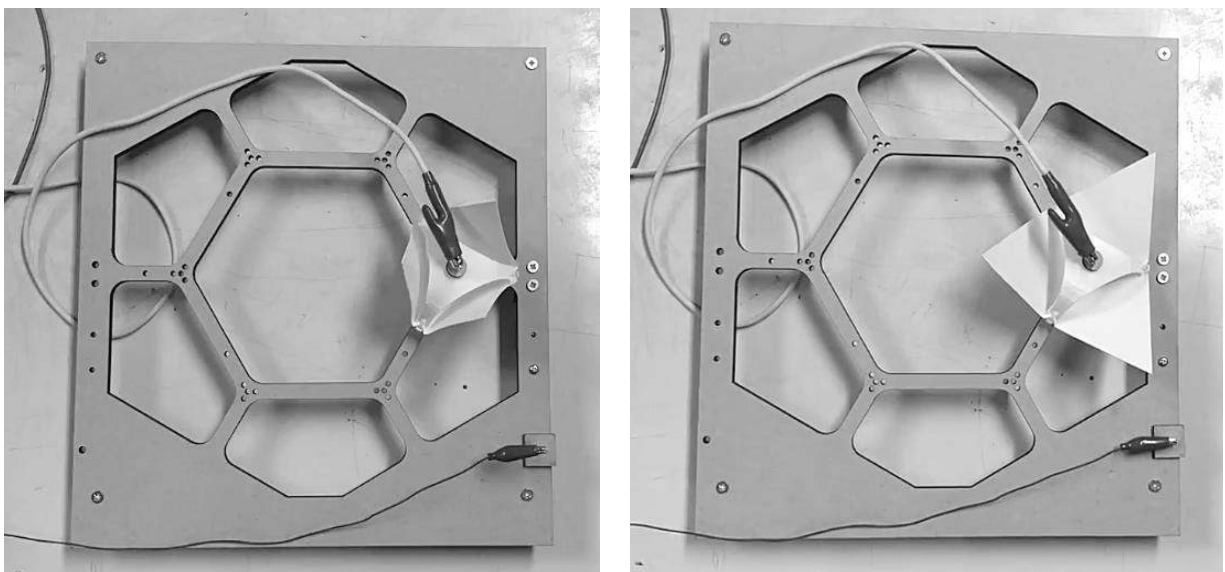
In order to allow the SMA wire to contract over a longer active length, the curved-line folded is tested within the 6.6.6 component frame. As illustrated in **Figure 60**, the actuator wire is now directed around the boundaries of the frame. It is connected on top of the pre-bent layer, vertically directed to the first pulley, turned horizontally to the back, lead around the four corners of the frame and finally connected to the front again. This way, the friction of the wire is minimized and it can contract on its whole length. **Figure 61** demonstrates the actuation with an electrical current applied to the ends of the SMA wire, using the values that were given previously in this paragraph. The element unfolds somewhat asymmetrically, which may either be due to the connections of the pre-bent spine to the boundary segments, or to the slightly eccentric position of the insulator piece on top of the spine. The element opens up in about 10 seconds when the electric power is applied, but the reverse movement takes much longer (around two to three minutes). This can be due to the heated wire that takes a long time to cool down because of a rather high heat capacity. Furthermore, the element did not return to its folded state as much as before the applied current. An explanation for this might be that the strength of the pulling force of the wire was too high and it plastically deformed the pre-bent spine, weakening its spring effect. Then again, the prototype is a successful proof-of-concept for the actuation of one curved-line folding element in a 6.6.6 tessellation frame by means of electrical current through an SMA wire.



**Figure 59:** Closed (left) and open (right) element when applying an electrical current to the Nitinol wire.



**Figure 60:** Front (left) and rear (right) view of a 6.6.6 component frame for the actuation of one curved-line folding element. The SMA wire (blue) is guided around a series of pulleys to minimize friction. The empty holes in the frame indicate the location of the other elements and the extended actuation system for six elements.



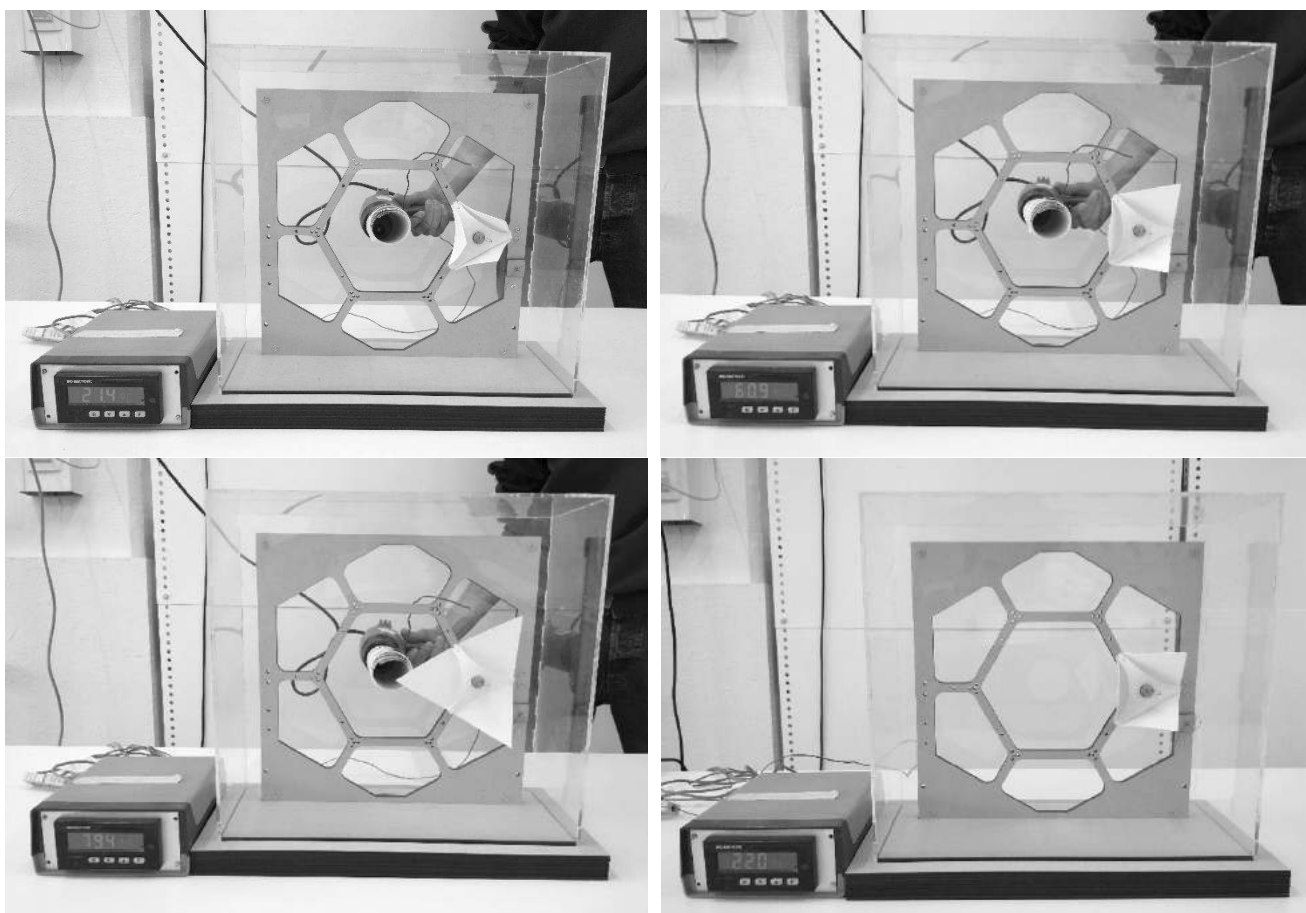
**Figure 61:** Closed (left) and open (right) element in a 6.6.6 component when applying an electrical current to the Nitinol wire.

### 4.2.3.7 Actuation with ambient heat

As most of the spaces inside the Arab World Institute are public, the building's occupants cannot change the indoor comfort conditions, unlike office spaces. Moreover, the fully computer-conducted operation of the south facade provided no user control. Therefore, it is interesting to consider the possibility of having a fully automated adaptive facade, independent of complex operating systems depending on computational control. The idea is to create an adaptive shading system, solely relying on the heat of solar radiation to operate. This concept is comparable to the HygroSkin project discussed in **Paragraph 3.2.2** or the Bloom Pavilion examined in **Paragraph 4.1.1**. However, in those projects, the intrinsic control is made possible by the inherent properties of the material. In this project, the intrinsic control is still done externally yet in a low-tech design.

The activation temperature of the Flexinol® wire is 70 °C, which means the heat of the sun is not sufficient to make the elements open up at the desired temperature. The greenhouse effect of the double facade contributes to a higher ambient temperature inside the glass panes, but for the climate in Paris, this is not effective enough. However, it is known that SMA's can be tailored to obtain the right transition temperature for the appropriate environmental zone. By changing the atomic weight by less than one percent of one of the elements that compose the alloy or by introducing impurities such as iron or oxygen, the activation temperatures can be modified up to 100 °C difference ( 'Air Flower' n.d.). This means that if the mechanism is proven to work for this wire, it can theoretically be used in any climate zone where adaptive shading devices are necessary.

In the next experiment, the 6.6.6 component frame with one curved-line folding element is placed inside an acrylic glass box. This is done to simulate the double facade of the AWI, as well as to attempt to heat up the entire wire to its activation temperature at once. A hole in the back is foreseen to fit a tube in which a heat gun can blow hot air. A thermocouple connected to a thermometer indicates the changes in temperature inside the box. As demonstrated in **Figure 62**, the curved-line folding element is unfolding at around 60 °C and is completely unfolded at around 70 °C. However, this process occurred relatively slowly as it took about an entire minute to heat up the box. When opening the box afterwards, the air inside did not seem to be so warm, but the acrylic glass itself was very hot and started deforming locally. This is probably due to the fact that the heat gun blows hot air in one direction, not allowing the heat to gradually heat up the box, but instead getting dissipated out of the glass panes. Furthermore, at around 70 °C the flaps are opened too extensively and enter into a bi-stable position from which they cannot return. When manually returning the flaps to their pre-folded position, it is visible that the pre-folding is not as strong as before the actuation. This may be due to the plastic deformation of the pre-bent spine caused by the high pulling force of the Nitinol wire. In addition, the polypropylene sheets felt weakened due to the high temperatures, which could contribute to the reduced refolding effect. Nevertheless, the prototype has proven to work for the actuation of one curved-line folding element by means of an ambient heat source.



**Figure 62:** *Top:* Closed (left) at room temperature and intermediate (right) at  $\pm 60$  °C configuration of one element actuated by ambient heat. *Bottom:* Open (left) at  $\pm 70$  °C and closed (right) configuration at room temperature. The element is visibly less pre-folded after one actuation by ambient heat.



## Chapter 5

# Results and discussion

*In the previous chapter, brief discussions and evaluations of the results were made by analysing and documenting design complications and obstacles. This chapter provides a reflection of the redesign and prototyping phases with regard to the redesign parameters that were formulated in Chapter 3. A verification of the prototype is done in relation to the redesign models and a validation of both the prototype and the redesign is done with regard to the redesign parameters.*

### 5.1 Verification

A verification of the prototypes can be done by answering the following question: *Are we building the system the right way?* Or more specifically, by asking: *Does the prototype fulfil the requirements of the redesign?* First, it must be noted that the prototypes represent only a limited selection of the whole redesigned module. For instance, the prototypes for the thermo-bimetal curling exploration were applied to one of the smaller components of the module, whereas the prototypes for the curved-line folding exploration focused only on the medium-sized components. Second, the material availability and expensiveness of the thermo-bimetal samples led to a different choice of the component to be used for the prototype and the component selected for the redesign. Besides, the thermo-bimetal exploration regarded the redesign of only the central component, whereas the curved-line folding exploration considered the entire module.

Concerning the prototypes for the thermo-bimetal curling component, four methods were explored: in-the-plane and out-of-plane positioning, pre-bending with elastic cords and by plastic deformation. The in-the-plane positioned bimetal sheets produce in fact the reverse motion of what they are intended to do, i.e. they open up instead of closing down under higher temperatures, which is not the objective of adaptive shading systems. This was a contra-intuitive mistake that led to the development of three solutions that had not yet been explored. The first solution was the out-of-plane positioning perpendicular to the frame, causing the bimetal sheets to bend inwards when subjected to higher temperatures. This method succeeded in



making the system moving in the right direction at the requested conditions but failed as a strategy to provide enough shade. As the perpendicular positioning reverses the boundaries of the aperture area ratio, it does not close sufficiently under increased temperature. Moreover, the evocation of the Islamic star pattern was relatively poor in this configuration, as the intermediate positions do not reveal a clear geometric shape. A second solution was to provide an initial inclination of the bimetal strips by pre-bending them using elastic cords. On one hand, this approach provides an improvement with regard to the previous methods but on the other hand, it increases the complexity of the system by adding an additional element. The strength of the cords was not sufficient to pre-bend the bimetal sheets and the relaxation of the elastic cords over time will probably cause the system to fail in an early state. Moreover, due to accumulating stresses in the bimetal versus the tension in the elastic cord, it flips into a bi-stable state instead of gradually curling into position. The third solution consisted in eliminating the need for elastic cords by plastically deforming the bimetal strips in order to obtain the initial pre-bent shape. However, as the plastic deformation was done manually, it generated a sequential, staggering movement of individual parts of the sheets. Overall, the thermo-bimetal curling did not satisfy the requirements adequately for the redesign and further exploration was put aside to make time for the investigation of the potential of curved-line folding.

Regarding the prototypes constructed for the curved-line folding component, the mistake in the reasoning of the first method of the thermo-bimetal curling was avoided by deducing that the elements had to be in a pre-folded position 'at rest'. To obtain this condition, four approaches were explored: pre-folding with an elastic cord, with a pressure spring, with an elastic spine, and with a pre-bent spine. The use of an elastic cord required an additional frame and as mentioned for the previous exploration, the relaxation of the elastic cord over time will reduce its tensional strength. Implementation of a pressure spring between the two spines provided a stable pre-folded position but the unfolding movement was asymmetric due to the eccentric position of the spring. Moreover, a high point load was required for an average unfolding movement. A third method consisted in using an elastic spine with downscaled dimensions to keep it folded at rest and to allow a stretching of the spine when the element unfolds. However, this method was not executed due to poor 3D-printing results with elastic filaments. The fourth approach consisted in using a 3D-printed, pre-bent spine that takes over the role of a pressure spring and thus reduces the mechanical complexity. Additionally, it reduced the amount of force required to unfold the element and negated the eccentric effect of the pressure spring.

The latter pre-folding system was selected for the following actuation methods: actuation with electrical current and actuation with ambient heat. As the Flexinol® wire contracts over 3 to 5 % of its length, a long piece of wire was needed to actuate one curved-line folding element in a 6.6.6 tessellation frame. To avoid friction and maintain the active part of the wire distributed over its total length, a pulley system was conceived to guide the wire around the edges of the frame. By heating the wire with an electrical current, a smooth yet slightly asymmetric unfolding movement was obtained, reaching to about 80 % of a totally unfolded state. However, the reverse movement took a longer time for the wire cools down slowly due to a

relatively high heat capacity. In the actuation using an ambient heat source, it last about an entire minute to activate the element due to the stagnant build-up of heat inside the acrylic glass box. This was mainly due to the heat gun blowing in one direction, locally deforming the acrylic glass and causing a fast dissipation of heat to the outside of the box and. Moreover, in both approaches, the high pulling force of the Nitinol wire caused the pre-bent spine to plastically deform, resulting in a reduction of its spring-effect and thus a diminished reversibility of the system. Furthermore, some of the flaps flipped into a bi-stable position due to excessive pulling of the wire, additionally limiting the reversibility.

In general, it can be concluded that the curved-line folding prototype corresponds to more requirements of its respective redesign than the thermo-bimetal prototype, even though both methods demonstrate a successful proof of concept. Regarding the thermo-bimetals, the extent of the movement is a key working point whereas, for the curved-line folding elements, the asymmetry as well as the reversibility can be optimized. For both approaches using actuation with ambient heat, the adaptation at the adequate temperature is a remaining challenge. However, the real-occurring situation when relying on solar radiation as a heat source will probably be more efficient due to a uniform heat distribution inside the glass panes.

## 5.2 Validation

In order to validate the redesigned modules, an answer is needed to the following question: *Are we building the right system?* Or, more specifically: *Do the redesign and its proof of concept fulfil the requirements of the redesign parameters?* Providing a response to these questions takes us back to the list of design parameters that were formulated in Chapter 3 and are repeated again hereunder:

- 1) *The redesign must recognize the aesthetic values of the AWI and incorporate a collection of references to Arabic architecture by means of introducing geometric patterns such as polygons and Islamic star patterns. The hierarchy of the mashrabiya module is respected and the new components must retrofit their original sizes and diversities.*
- 2) *The domain of the aperture area ratio must be expanded through an increase in the range of obstruction of sunlight by the kinetic shading elements between open and closed configurations.*
- 3) *The adaptive shading device must present a simplified alternative regarding its mechanism, control system and operability by mimicking a biological responsive system and thus obtain a biomimetic product with reduced technical complexity.*

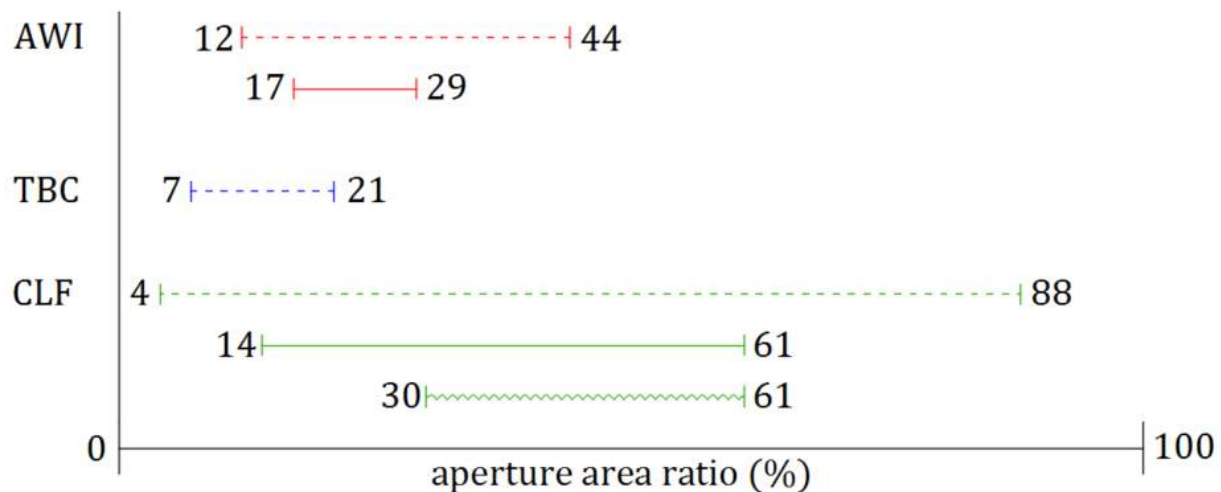
To answer the first rule, the redesign needs to reflect enough aesthetic values of the original design by means of the implementation of traditional Arabic geometric patterns. As regards the redesign using thermo-bimetals, only one component was studied with a 4.8.8 tessellation and it turned out the curling of the bimetal sheets does not accentuate the Islamic star patterns in a satisfying manner. Yet, the frame in which

the bimetal strips are positioned depict the polygons of the tessellation, i.e. octagons and squares. In contrast, the redesign using curved-line folding elements succeeded in reproducing all of the polygons and Islamic star patterns from the original design. Moreover, two additional Islamic star patterns and a supplementary polygon were introduced, generating a redesigned module able to enhance the evocation of the traditional mashrabiya window even more than the original design. Furthermore, due to the kinetic nature of the curved-line folding elements, it was discovered that in a front view projection the elements can produce the whole range of Islamic star patterns for a certain tessellation, rather than a discrete number of pattern representations found in the diaphragms of the AWI.

Concerning the general aesthetic recognition, it can be argued that the materiality of the original diaphragms is more uniform with the totality of the module than the curved-line folding elements. The aesthetics of the heavy, stainless-steel mechanism is harmoniously integrated into the totality of the monumental facade. Due to their colour, gloss and reflectivity, the thermo-bimetals are partially able to evoke the original building envelope. However, the flimsy sheets are not able to emulate the solid shutters of the AWI. Withal, the curved-line folding elements do not possess any material characteristics similar to the diaphragms. Then again, both investigated techniques are extremely lightweight and may thus facilitate transportation and implementation in the facade.

The second redesign parameter regards the aperture area ratio as a predictive factor for the energy performance of the module. As only one component was considered for the redesign with thermo-bimetals, it is not representative for the entire module. Yet, the domain of the aperture area ratio showed a decrease of 18 % compared to the same component of the original design. This was probably due to the excessive density of the 4.8.8 tessellation, not allowing the short bimetal sheets to curl extensively. The redesign with curved-line folding elements demonstrated an impressive increase of 35 % of the aperture area ratio domain, calculated for the entire module. Moreover, the original design's upper and lower boundaries of the aperture area ratio in open and closed configurations respectively is comprised within the nearly quadrupled domain for the curved-line folding redesign. However, the practical execution did not generate the same results as were predicted during the redesign. On one hand, the element cannot be completely opened because it turns into a bi-stable position from which it cannot return. On the other hand, after actuation, the element shows a less folded position than initially. A raw assumption is that the domain of the aperture area ratio is reduced by one third, which still doubles the original domain for the curved-line folding elements.

To get a better understanding of the reasoning above, a comparison of the domains of the aperture area ratio for each of the projects is visualized in **Figure 63**. Generally, it can be concluded that the prediction of the energy performance is most beneficial for the redesign with curved-line folding elements. However, this prediction was done by calculating the range of frontal obstructed sunlight in open and closed configurations. As this method considers only one fictive position of the sun, it is not considered to be a very rigorous approach and the conclusions must be interpreted carefully.



**Figure 63:** Visual representation of the aperture area ratio for the Arab World Institute (AWI), the thermo-bimetal curling (TBC) and the curved-line folding (CLF) design. The left (lower) boundaries show the values for the closed configurations while the right (upper) boundaries show the values for the open configurations. The dashed line corresponds to the central component, the filled line to the entire module and the zigzagged line is an assumption on the prototype.

As to the third criterion for the redesign, a biomimetic solution with reduced mechanical complexity should be presented to replace the existing diaphragms. As the two explored methods work independently from sensors, processors and motorizing systems, they can be considered to have diminished the overall complexity and operability of the system significantly. However, the main drawback of an all-inclusive mechanism like the thermo-bimetals is that it is not controllable. This could be accomplished by heating up the air in between the glass panes, but that would be a contra-productive approach to reduce cooling loads. Direct solar radiation on the bimetal sheets will acquire the effect more rapidly without the ambient air temperature being increased excessively. The advantage of the curved-line folding elements is that the smart Nitinol wire can be activated by electrical current or by ambient heat. This means that both an intrinsic control by solar radiation and extrinsic control by means of electrical power are possible. The intrinsic control can be obtained by tailoring the material properties of the Nitinol wire to the corresponding climate conditions, whereas the extrinsic control can be achieved by integrating solar cells in the components and connecting them to a control unit.

Another important asset regarding control and operation is that both techniques respond to very local variations of changing weather conditions and thus reveal a map of changing apertures and light levels across the vast rectangular facade. Moreover, this benefit applies to the aesthetics and the energy performance as well, as it corresponds to the way the south facade modules of the AWI were intended to function. Regarding the mechanism itself, it can be said that the mechanical complexity of both approaches has been significantly reduced compared to the diaphragms of the original design. The classical engineering view of rigid-body mechanics using technical hinges and rigid members may be inferior to the compliant mechanisms observed in plant movements, exploiting elastic deformations of flexible members around living hinges. The approach using thermo-bimetals is by far the simplest mechanism, as all its technology is embedded in the material properties. Even though the actuation of curved-line folding elements with smart materials is more complex than for thermo-bimetals, it still remains far less complicated than the diaphragms of the AWI.

In general, it can be concluded that the redesign using curved-line folding elements activated by smart materials show great potential for the redesign of the south facade modules of the AWI. By corresponding to more redesign parameters at the scale of the redesigned model and its proof of concept, this method has proven to be more valuable than the implementation of thermo-bimetals. Moreover, it has combined two existing techniques into an innovative biomimetic solution, whilst respecting the original design and even enhancing its architectural concept.

## Chapter 6

# Conclusions

*In Chapter 4, the redesign and prototyping of the adaptive shading system AWI's south facade were elaborated for two techniques: thermo-bimetal curling and curved-line folding. In Chapter 5, these were verified and validated regarding the redesigned model and redesign parameters respectively. In this chapter, a general overview of the research phases and a comprehensive review of the two techniques are given. As a result of the inapplicable biomimetic research approaches and transfer methods that were discussed in Chapter 2, a new R&D methodology is proposed for the retrofitting of existing climate adaptive facades. The master thesis is completed by discussing future research subjects that can provide further insight into the conception of climate adaptive facade systems using a biomimetic approach.*

### 6.1 General overview

In Chapter 1, the master thesis was introduced by stating that the growing awareness of global overpopulation and climate change has significantly increased the demand for sustainable project developments. Since the building sector accounts for almost half of the total energy consumption and the building envelope is mainly responsible for the energy metabolism of an edifice, climate adaptive facade technology is steadily gaining ground in research and development projects. As it is able to act as an energy modulator by responding to changing environmental conditions and thereby reduce the energy demands in order to maintain indoor comfort, it is likely to become a contributing factor to obtain future energy targets. More specifically, the implementation of adaptive shading systems may be the most important solar strategy as preventing heat gains is one of the most energy-consuming necessities for many climates. Therefore, the south facade of the Arab World Institute in Paris was selected as the main case study for this thesis as it incorporates an adaptive shading system that was abandoned soon due to multiple failures and high maintenance costs. Moreover, its rotating diaphragms regulating daylight and thermal gains were biologically inspired by the contraction and relaxation of the human eye iris. Since nature provides an endless resource of intelligent systems through millions of years of evolution, the aim was to search for an alternative

biomimetic solution by investigating climate responsive organisms using efficient mechanisms with reduced complexity.

Chapter 2 tackled three subjects to provide a better description of this thesis' case study: an architectural review on the AWI itself, and in particular its south facade; current research on the classification of climate adaptive facades and adaptive shading systems; and the latest theories on biomimetic research methods for architectural developments. In Chapter 3, the south facade of the AWI was analysed more thoroughly, especially regarding its premature deficiency. Considering the aim of redesigning the south facade modules by respecting the architectural concept of the building, the aesthetics and references to Arabic architecture were examined likewise. The analysis of the south facade on several facets was boiled down to a set of design parameters to be considered for the redesign. However, as the biomimetic research methods reviewed in Chapter 2 required an interdisciplinary approach with a considerable amount of expertise in biology and biomechanics, another methodology was conceived. By investigation of five relevant case studies integrating biomimetic adaptive facade systems, inspiration was drawn for the exploration and elaboration of two bio-inspired concepts: thermo-bimetal curling and curved-line folding. While thermo-bimetal curling was inspired by the hygroscopic responsiveness of *Pinophyta* in the HygroSkin project, the actuation using smart materials in the Air Flower and the snap-trapping motion of *Aldrovanda vesiculosa* in the Flectofold system provided the stimulus for the curved-line folding exploration.

In Chapter 4, these techniques were introduced by scanning literature on the latest developments regarding their physical behaviour such as material capacities and limitations, and actuation methods. This knowledge provided a reliable basis for the redesign phase, which consisted in reconfiguring the modules of the south facade of the AWI by respecting the implementation of Arabic geometric patterns, via predictions of energy performance and by means of preliminary testing through geometric and kinematic simulations. Subsequently, various methods were developed to prove the redesigned concept in a prototyped state and the multiple obstacles arising in this phase were interpreted and documented. Finally, the redesigns and prototypes were verified and validated in Chapter 5 with reference to the redesign parameters that were formulated in Chapter 3.

## 6.2 Review on two explorations

The two bio-inspired techniques that were explored in Chapter 4 have been extensively discussed in the previous chapter, regarding their ability to be verified and validated with respect to the requirements for the redesign. In this paragraph, their potential to substitute the original modules of the AWI is reviewed as an outcome of the precedent chapters and their value as innovative bio-inspired kinetic shading devices is assessed.

Concerning the methodology that was used to produce the two biomimetic products, there has not been made use of an existing rigorous biomimetic strategy. Instead of following the biomimetic top-down process



in a restrained way, inspiration was drawn from relevant case studies and existing techniques were combined into a new concept that is biologically inspired. Although both devices show flaws in their practical execution, they have been prototyped successfully using different methods of actuation. The thermo-bimetal component's most important feature is its mechanical simplicity and automated operability, but it lacks a sufficient range of aperture. For the curved-line folding component, the symmetry and reversibility of the movement are remaining challenges that require optimization. The documentation of the encountered obstacles in the prototyping process can help further research to improve the system and to avoid repeating errors in the design procedure. Still, both explorations already passed through many verifications and validation rules which were discussed in Chapter 5.

By investigation of the south facade of the AWI from an architectural as well as an engineering perspective, the list of parameters for the redesign included technical as well as aesthetic requirements. The redesign with curved-line folding elements mainly succeeded in both fields, leaving some remarks for speculation. Moreover, it was discovered that by the implementation of kinetic elements in adaptive facades, the typically static Islamic star patterns found in traditional Arabic architecture can make room for dynamic star patterns that contain the whole range of intermediate states. This could potentially introduce a new period in Arabic architecture, lifting the traditional mashrabiya window to a higher level by implementation of kinetic shading devices portraying a map of varying Arabic geometric patterns across the building envelope.

In general, the exploration of the curved-line folding elements actuated by smart materials shows the greatest potential as a bio-inspired kinetic shading device. The combination of two existing techniques – curved-line folding and actuation by smart materials – led to the conception of an innovative biomimetic adaptive shading system able to produce an array of Arabic geometric patterns. Another important asset is its ability to be intrinsically controlled by solar radiation through customization of the properties of the smart material to the climatic context of the building, and extrinsically controlled by applying an electrical current which could be powered by solar cells embedded in the facade. Furthermore, the materials used for the curved-line folding elements, i.e. the polypropylene sheets and the polylactic acid (PLA) pre-bent spine, are both 100 % recyclable.

However, it must be said that in terms of energy performance, the placement of the kinetic shading device inside the glass panes is not an optimal solution to reduce cooling loads as there is more heat absorption by the materials and little reflection to the outside. Then again, this positioning was preserved to respect the original configuration of the south facade of the AWI and in order to be able to retrofit the new components inside the existing framework of the modules. Besides, the fragile curved-line folding elements, as well as the flimsy thermo-bimetal sheets, would not be able to endure harsh environmental conditions such as wind gusts, snowfall, and rainstorms. In addition, the lightweight, white-coloured polypropylene curved-line folding elements would absorb way less heat than the heavy stainless-steel diaphragms, reducing this problem to a minimum.

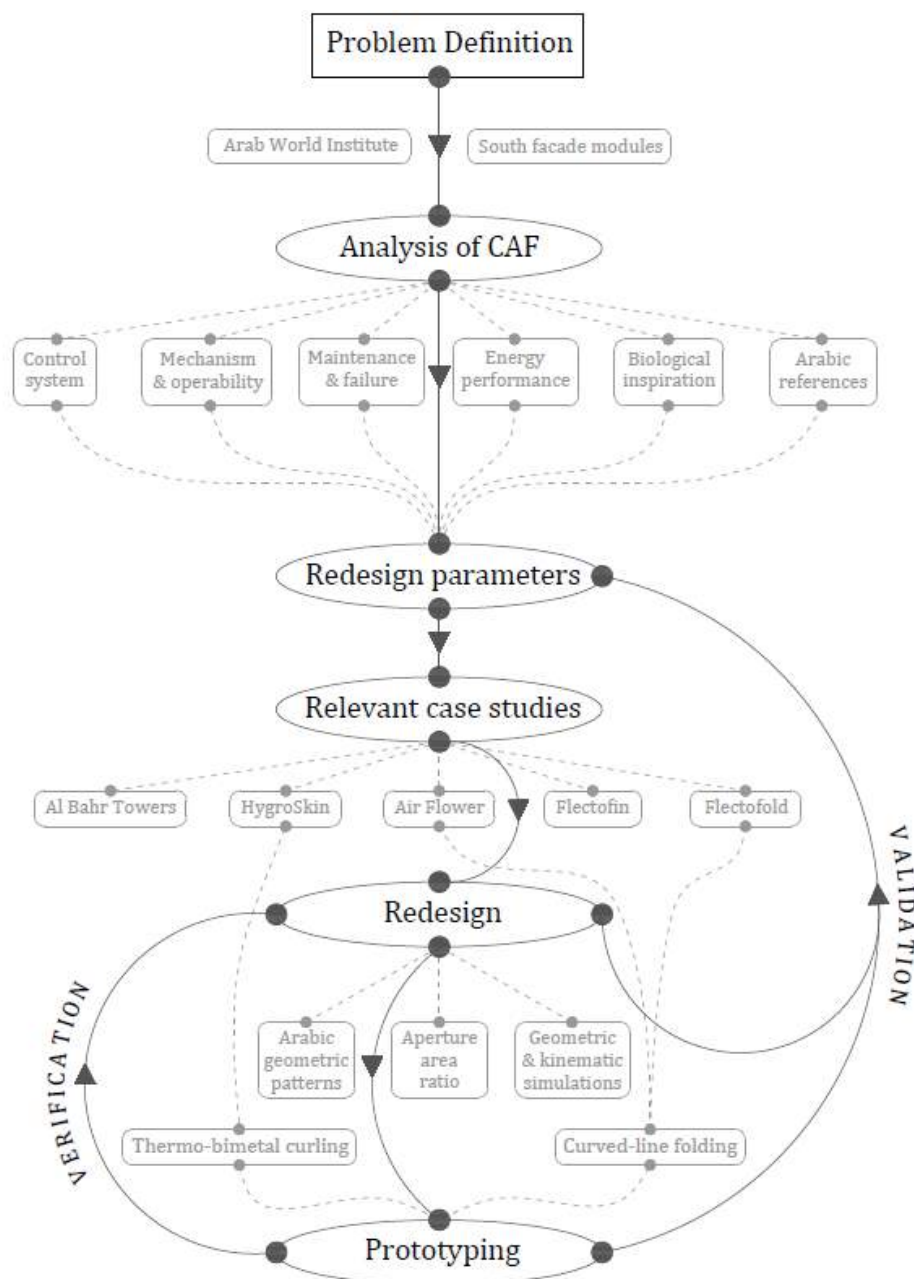
## 6.3 Proposal for a retrofitting methodology

The Arab World Institute was selected as the principal case study for this thesis and the main objective was to find a biomimetic solution to the early failure of the kinetic shading mechanism of the south facade. One of the main reasons behind its ceased functioning was the high mechanical complexity and maintenance intensity of the diaphragm components. Biomimetic research has unveiled a possible paradigm shift in mechanical engineering by considering the potential of compliant mechanisms in plant movements. The soft mechanics in nastic structures use elastic deformation of flexible components around living hinges, making the implementation of technical hinges connecting rigid members in conventional rigid-body mechanics become obsolete. Moreover, recent biomimetic discoveries in the plant kingdom have demonstrated the potential of smart materials, bypassing the need for complex high-tech equipment such as sensors, processors, actuators and control systems. In this thesis, these types of bio-inspired devices have proved to be valuable substitutions for the defective diaphragms of the AWI, as they significantly reduce the mechanical complexity and operability of the system.

Since the construction of the AWI in 1981, many projects incorporating climate adaptive facades have been realized. As the vast majority of these buildings integrate kinetic devices using classical engineering methods, the chances are high they will undergo failure scenarios similar to the south facade modules of the AWI. Parallel to this tendency, an increasing interest for the implementation of biomimetic kinetic devices in climate adaptive facades will result in the growth of reference projects which can be used as inspiration sources and for optimization purposes in architectural developments. Additionally, most biomimetic research methods require a multidisciplinary approach between biologists, physicists, chemists and engineers and may take a long time to develop new biomimetic products. Furthermore, there is no guarantee whatsoever these methodologies bear in mind the architectural concept of a building and consider the aesthetics of the facade. During this thesis research, the approach of studying the south facade of the AWI from both an architectural as well as an engineering point of view has stimulated the development of a research and development methodology for architectural design projects. Rather than demolishing buildings to make room for mainstream, so-called 'sustainable' projects built from scratch, the idea is to preserve a building's historical and cultural content and to restore its value with a bio-inspired, energy-efficient adaptive facade respecting the architectural context. Therefore, a first step towards the redesigning and retrofitting of deficient climate adaptive facade systems in existing buildings is proposed.

To elucidate the argumentation and reasoning above, the proposal of a retrofitting methodology for climate adaptive facades is illustrated in **Figure 64**. In this thesis, the methodology was not always applied in a precise and chronological way, but the following description demonstrates an updated version with additional recommendations. The method starts by identifying the problem, which is generally the deficiency or poor performance of an existing climate adaptive facade. Then, the facade is analysed considering the mechanism, control and operability from an engineering point of view and the building's concept, historical context and

aesthetics from an architectural perspective. The energy performance can be studied by environmental simulations and by regarding thermal and visual comfort. Next, the analysis is boiled down to a list of parameters that need to be considered for the redesign and serve as a set of validation rules. The following phase is to consider similar architectural projects, analyse them, compare them to the selected project and to draw inspiration from them. In the redesign stage, the accumulated knowledge from the case studies is used to envision a new concept with respect to the redesign parameters. The preliminary design can be tested through parametric, geometric, kinematic and kinetic simulations and by performing calculations on energy performance and indoor comfort. Once the redesign is approved, a proof of concept of the bio-inspired device is done by means of prototyping. Finally, if the prototype is successful, it is verified regarding the redesigned models and simulations and validated according to the redesign parameters.



**Figure 64:** Diagram of the retrofitting methodology proposal representing the steps to be taken for retrofitting a climate adaptive facade (CAF). The grey parts depict the specific case for this thesis, while the black parts reveal the general methodology.

## 6.4 Future Research

The research carried out in this thesis tackled many subject matters at once, yet an attempt was done to handle each of them with care. Although complete research is an oxymoron, this research topic could reach completion by the in-depth analysis and extended development of several parts. The analysis of the south facade modules of the AWI was executed with a surprisingly limited source of literature and a visit to the building itself in 2016. As it was impossible to obtain detailed documents on the facade by the project's architectural or engineering team, future research could provide an expanded review of the facade leaving no substances undisclosed. Moreover, the study on relevant case studies could – apart from being extended to a higher number of cases – be expanded to other types of projects like speculative concepts or be broadened to adaptive facade designs without a biomimetic approach to gain further insight in their conception and development. Furthermore, the redesign parameters are subjective and based on academic design experience in relation to what seemed to be answering the most important design problems whilst respecting the original design, leaving a great deal of design freedom. Another approach could have been applied by investigating exactly what the technical problem was and by simply 'fixing' it with a redesigned model implementing the same diaphragms with a slightly different mechanism and operability. Then again, this approach would merely consider the engineering facet and additionally, one might even argue that architecture is not only a matter of ticking requirements.

Concerning the redesign and prototyping parts, the thermo-bimetal exploration was relatively quickly put aside to make time for an elaborated research on curved-line folding elements. Future research can treat this part to an analogous extent, or even develop a new method by combining thermo-bimetal curling with another technique acquired from the examination of the relevant case studies. Additionally, the predictions on the energy performance of the redesign remained very basic. Future research could perform simulations for the redesign regarding energy performance, visual and thermal comfort. Besides, kinetic simulations using FEA engineering software may facilitate the understanding of the system and optimize it thusly. Regarding the curved-line folding exploration, only one redesigned component was selected for the prototyping process. The four other components types could be actuated similarly as their folding forces have already been experimentally determined. As previously mentioned, the symmetry and reversibility of the movement are remaining challenges, as well as the equal heat distribution inside the acrylic glass box. Moreover, as the prototype was tested to activate only one element in a 6.6.6 tessellation component, the actuation of six elements remains unexplored. Although this may be realized by connecting one Nitinol wire to six other wires without shape memory features, it would distribute the contraction force of the wire and result in a reduced motion of the elements. Furthermore, the elements can undergo fatigue and creep tests and the technical joints can be optimized using more advanced technologies.

Finally, the retrofitting methodology that was proposed in the previous paragraph is in a very early phase. It may possibly be rejected by refutation from future research but it might as well be adapted or improved.

As the majority of buildings are of orthogonal nature with vertical facades, it should be relatively easy to retrofit them with a double facade with adaptive features, attaching itself to the existing structure. Buildings that would normally be demolished could instead be retrofitted with bio-inspired kinetic facades using little actuation energy to save high amounts of energy from active HVAC devices. This would probably result in a more sustainable approach than the classical build-scrap-rebuild routine. Besides, the modules of the AWI's south facade were designed to regulate daylight and thermal comfort. Multifunctional biomimetic devices, tackling more than two physical entities at the same time, are still to be explored.

As a last remark, the examination of nature as a concept generator for efficient design appears to be a promising research field. Through millions of years of evolution by natural selection, biological systems have been optimized by the governing laws of nature. By exploring the minimum balance between energy and material use, it produced an infinite resource of beautiful and fascinating structures relying on elementary principles. Then again, this thesis has triggered the realization that the challenge in biomimicry resides in the intelligent abstraction of nature's wonders to answer specific human needs. The function of an organism can vary widely from the context of its biomimetic application and the elegance consists in unveiling its useful essence, as "*simplicity is the ultimate sophistication*", to quote Leonardo da Vinci.



## Bibliography

- ‘AD Classics: Institut Du Monde Arabe / Enrique Jan + Jean Nouvel + Architecture-Studio’. 2011. ArchDaily. 2 October 2011. <http://www.archdaily.com/162101/ad-classics-institut-du-monde-arabe-jean-nouvel/>.
- Aðalheiðr. 2011. *Apertured Windows at L’institute Du Monde Arabe - Paris*. Photo. <https://www.flickr.com/photos/kon-a-n/6314570538/>.
- ‘Adaptive Facade Network – Europe – COST Action TU1403’. n.d. Accessed 2 September 2017. [http://tu1403.eu/?page\\_id=209](http://tu1403.eu/?page_id=209).
- Adriaenssens, Sigrid, Landolf Rhode-Barbarigos, Axel Kilian, Olivier Baverel, Victor Charpentier, Matthew Horner, and Denisa Buzatu. 2014. ‘Dialectic Form Finding of Passive and Adaptive Shading Enclosures’. *Energies* 7 (8): 5201–20. <https://doi.org/10.3390/en7085201>.
- Aelenei, Daniel, Laura Aelenei, and Catarina Pacheco Vieira. 2016. ‘Adaptive Façade: Concept, Applications, Research Questions’. *Energy Procedia*, Proceedings of the 4th International Conference on Solar Heating and Cooling for Buildings and Industry (SHC 2015), 91 (June): 269–75. <https://doi.org/10.1016/j.egypro.2016.06.218>.
- ‘Air Flower’. n.d. LIFT Architects. Accessed 20 April 2018. <http://www.liftarchitects.com/air-flower/>.
- ‘Air Flow(Er) - Thermally Active Architectural Skin’. n.d. Vimeo. Accessed 28 May 2018. <https://vimeo.com/74264389>.
- ‘Al Bahar Towers - Data, Photos & Plans - WikiArquitectura’. n.d. Accessed 21 May 2018. <https://en.wikiarquitectura.com/building/al-bahar-towers/>.
- ‘Al Bahr Towers | Aedas - Arch20.Com’. n.d. Accessed 21 May 2018. <https://www.arch20.com/al-bahr-towers-aedas/>.
- Al Dakheel, Joud, and Kheira Tabet Aoul. 2017. ‘Building Applications, Opportunities and Challenges of Active Shading Systems: A State-of-the-Art Review’. *Energies* 10 (10): 1672. <https://doi.org/10.3390/en10101672>.



- ally\_quemere. 2007. *The Diaphragm of Camera like the Iris of the Eye Changes the Size of the Opening to Admit Light*. Photo. <https://www.flickr.com/photos/13827586@N03/2397384383/>.
- Almusaed, Amjad. 2010. *Biophilic and Bioclimatic Architecture: Analytical Therapy for the Next Generation of Passive Sustainable Architecture*. Springer Science & Business Media.
- Al-Obaidi, Karam M., Muhammad Azzam Ismail, Hazreena Hussein, and Abdul Malik Abdul Rahman. 2017. 'Biomimetic Building Skins: An Adaptive Approach'. *Renewable and Sustainable Energy Reviews* 79 (November): 1472–91. <https://doi.org/10.1016/j.rser.2017.05.028>.
- Alotaibi, Fahad. 2015. 'The Role of Kinetic Envelopes to Improve Energy Performance in Buildings'. *Journal of Architectural Engineering Technology* 4 (3): 1–5. <https://doi.org/10.4172/2168-9717.1000149>.
- 'Arab World Institute (AWI)'. n.d. Ateliers Jean Nouvel. Accessed 10 May 2018. <http://www.jeannouvel.com/en/projects/institut-du-monde-arabe-ima/>.
- 'Architecture'. 2016. Institut Du Monde Arabe. 16 June 2016. <https://www.imarabe.org/en/architecture>.
- 'ARCHITECTURE STUDIO - Arab World Institute'. n.d. Accessed 30 August 2017. [http://www.architecture-studio.fr/en/projects/pastb1/arab\\_world\\_institute.html](http://www.architecture-studio.fr/en/projects/pastb1/arab_world_institute.html).
- Attia, S. 2017. 'Evaluation of Adaptive Facades: The Case Study of Al Bahr Towers in the UAE'. *QScience Connect, Shaping Qatar's Sustainable Built Environment*, 2.
- Badarnah, L., and U. Knaack. 2008. 'Organizational Features in Leaves for Application in Shading Systems for Building Envelopes'. In *Design and Nature Iv: Comparing Design in Nature with Science and Engineering*, edited by C. A. Brebbia, 114:87–96. Southampton: Wit Press.
- Badarnah, Lidia, and Usama Kadri. 2015. 'A Methodology for the Generation of Biomimetic Design Concepts'. *Architectural Science Review* 58 (2): 120–33. <https://doi.org/10.1080/00038628.2014.922458>.
- Bar-Cohen, Yoseph. 2005. *Biomimetics: Biologically Inspired Technologies*. 1 edition. Boca Raton, FL: CRC Press.
- Barozzi, M., J. Lienhard, A. Zanelli, and C. Monticelli. 2016. 'The Sustainability of Adaptive Envelopes: Developments of Kinetic Architecture'. *Procedia Engineering*, Procedia Engineering, 155 (International Symposium on Novel Structural Skins-Improving Sustainability and Efficiency through New Structural Textile Materials and Designs): 275–84.
- Boissiere, Olivier. 1997. *Jean Nouvel*. Trilingual Ed edition. Paris: Terrail.
- Casamonti, Marco. 2009. *Jean Nouvel*. Edited by Giovanni Leoni. Milan: Motta.
- Chaslin, François. 2008. *Jean Nouvel critiques*. Gollion: Infolio.
- Croquis, El. 1994. *El Croquis No. 65/66 Jean Nouvel 1987-1994*. First Edition edition. El Croquis.
- 'Datasheets'. n.d. Accessed 29 May 2018. <https://www.auerhammer.com/en/downloads/datasheets.html>.

- Decker, Martina, and Andrzej Zarzycki. 2014. 'Designing Resilient Buildings with Emergent Materials'. *Material* 2. [https://www.academia.edu/10331705/Designing\\_Resilient\\_Buildings\\_with\\_Emergent\\_Materials](https://www.academia.edu/10331705/Designing_Resilient_Buildings_with_Emergent_Materials).
- Dubois, S., and M. de Bouw. 2015. 'Experience-Based Guidelines for Architectural Industrialized Multifunctional Envelope Systems (AIM-ES)'. *Advanced Building Skins*. [https://www.academia.edu/21361209/Experience-based\\_guidelines\\_for\\_Architectural\\_Industrialized\\_Multifunctional\\_Envelope\\_Systems\\_AIM-ES\\_](https://www.academia.edu/21361209/Experience-based_guidelines_for_Architectural_Industrialized_Multifunctional_Envelope_Systems_AIM-ES_).
- 'DYNALLOY, Inc. Makers of Dynamic Alloys'. n.d. Accessed 29 May 2018. [http://www.dynalloy.com/tech\\_data\\_wire.php](http://www.dynalloy.com/tech_data_wire.php).
- 'Équerre d'argent 1987 / Jean Nouvel Architecture Studio – Institut du monde arabe – Paris V'. n.d. AMC Archi. Accessed 28 May 2018. <https://www.amc-archi.com/photos/equerre-d-argent-1987-jean-nouvel-architecture-studio-institut-du-monde-arabe-paris-v,2919/ima-coupe-transversale.3>.
- 'Featured Design - SlideShare'. n.d. Wwww.Slideshare.Net. Accessed 28 May 2018. <https://www.slideshare.net/category/design>.
- Fiorito, Francesco, Michele Sauchelli, Diego Arroyo, Marco Pesenti, Marco Imperadori, Gabriele Masera, and Gianluca Ranzi. 2016. 'Shape Morphing Solar Shadings: A Review'. *Renewable and Sustainable Energy Reviews* 55 (March): 863–84. <https://doi.org/10.1016/j.rser.2015.10.086>.
- Foged, Isak Worre, and Anke Pasold. 2010. 'Performative Responsive Architecture Powered by Climate'. *ACADIA 2010 Life In:Formation: On Responsive Information and Variations in Architecture*. [http://vbn.aau.dk/en/publications/performative-responsive-architecture-powered-by-climate\(b6040f06-deca-419d-a527-e638066b351c\)/export.html](http://vbn.aau.dk/en/publications/performative-responsive-architecture-powered-by-climate(b6040f06-deca-419d-a527-e638066b351c)/export.html).
- Goetschalckx, S. 2015. *Climate Adaptive Facades: Analysis of Curved Line Folding Systems with Regards to Visual Comfort, Thermal Comfort and Energy Performance*. Vol. Master Thesis.
- Goulet, Patrice. 1994. *Jean Nouvel*. Paris: Editions du Regard.
- Han, Zhiwu, Zhengzhi Mu, Wei Yin, Wen Li, Shichao Niu, Junqiu Zhang, and Luquan Ren. 2016. 'Biomimetic Multifunctional Surfaces Inspired from Animals'. *Advances in Colloid and Interface Science* 234 (August): 27–50. <https://doi.org/10.1016/j.cis.2016.03.004>.
- Hensel, Michael, and Achim Menges. 2008. 'Designing Morpho-Ecologies: Versatility and Vicissitude of Heterogeneous Space'. *Architectural Design* 78 (2): 102–11. <https://doi.org/10.1002/ad.648>.
- Heylighen, Ann, and Genevieve Martin. 2004. 'That Elusive Concept of Concept in Architecture'. In *Design Computing and Cognition '04*, 57–76. Springer, Dordrecht. [https://doi.org/10.1007/978-1-4020-2393-4\\_4](https://doi.org/10.1007/978-1-4020-2393-4_4).

- Hoberman, Chuck. 1994. 'Projects 45: Chuck Hoberman: The Museum of Modern Art, New York'. *The Museum of Modern Art*, 1–8.
- Holstov, Artem, Ben Bridgens, and Graham Farmer. 2015. 'Hygromorphic Materials for Sustainable Responsive Architecture'. *Construction and Building Materials* 98 (November): 570–82. <https://doi.org/10.1016/j.conbuildmat.2015.08.136>.
- Holstov, Artem, Graham Farmer, and Ben Bridgens. 2017. 'Sustainable Materialisation of Responsive Architecture'. *Sustainability* 9 (3): 435. <https://doi.org/10.3390/su9030435>.
- 'Institut Du Monde Arabe | B&W Drawing, Site Plan'. n.d. Archnet. Accessed 2 September 2017. [http://archnet.org/sites/637/media\\_contents/10042](http://archnet.org/sites/637/media_contents/10042).
- 'Institut Du Monde Arabe - Data, Photos & Plans'. n.d. WikiArquitectura. Accessed 28 May 2018. <https://fr.wikiarquitectura.com/bâtiment/institut-du-monde-arabe/>.
- Kaplan, C.S. 2005. 'Islamic Star Patterns from Polygons in Contact'. *Proceedings of Graphics Interface 2005*, 177–85.
- Karanouh, A., and E. Kerber. 2015. 'Innovations in Dynamic Architecture: The Al-Bahr Towers Design and Delivery of Complex Facades'. *Journal of Facade Design and Engineering* 3: 185–221.
- Khan, Ahmed Zaib, Han Vandevyvere, and Karen Allacker. 2013. 'Design for the Ecological Age: Rethinking the Role of Sustainability in Architectural Education'. *Journal of Architectural Education* 67 (2): 175–85. <https://doi.org/10.1080/10464883.2013.817155>.
- Knippers, Jan, Klaus G. Nickel, and Thomas Speck (eds.). 2016. *Biomimetic Research for Architecture and Building Construction: Biological Design and Integrative Structures*. 1st ed. Biologically-Inspired Systems 8. Springer International Publishing. <http://gen.lib.rus.ec/book/index.php?md5=e1e8642c3a747b6a0f45ad9b5c5c96da>.
- Knippers, Jan, and Thomas Speck. 2012. 'Design and Construction Principles in Nature and Architecture'. *Bioinspiration & Biomimetics* 7 (1): 015002. <https://doi.org/10.1088/1748-3182/7/1/015002>.
- Konstantoglou, Maria, and Aris Tsangrassoulis. 2016. 'Dynamic Operation of Daylighting and Shading Systems: A Literature Review'. *Renewable and Sustainable Energy Reviews* 60 (July): 268–83. <https://doi.org/10.1016/j.rser.2015.12.246>.
- Körner, A., L. Born, A. Mader, R. Sachse, S. Saffarian, A. S. Westermeier, S. Poppinga, et al. 2018. 'Flectofold-a Biomimetic Compliant Shading Device for Complex Free Form Facades'. *Smart Materials and Structures* 27 (1): 017001. <https://doi.org/10.1088/1361-665X/aa9c2f>.
- Körner, A., A. Mader, S. Saffarian, and J. Knippers. 2016. 'Bio-Inspired Kinetic Curved-Line Folding for Architectural Applications'. *ACADIA 2016 Proceedings of the 36th Annual Conference of the Association for Computer Aided Design in Architecture*: 270–79.

- Lechner, Norbert. 2014. *Heating, Cooling, Lighting: Sustainable Design Methods for Architects*. John Wiley & Sons.
- Lee, JY, SW Kim, and YC Jeon. 2015. 'Study of the Control of Geometric Pattern Using Digital Algorithm (with Focus on Analysis and Application of the Islamic Star Pattern)' . *Advances in Materials Science and Engineering* 2015: 14.
- Lienhard, J., S. Poppinga, S. Schleicher, T. Speck, and J. Knippers. 2010. 'Elastic Architecture: Nature Inspired Pliable Structures' . In , 469–77. <https://doi.org/10.2495/DN100421>.
- Lienhard, J., S. Schleicher, S. Poppinga, T. Masselter, M. Milwich, T. Speck, and J. Knippers. 2011. 'Flectofin: A Hingeless Flapping Mechanism Inspired by Nature' . *Bioinspiration & Biomimetics* 6 (4): 045001. <https://doi.org/10.1088/1748-3182/6/4/045001>.
- Loonen, R. C. G. M., J. M. Rico-Martinez, F. Favoino, L. Aelenei, M. Brzezicki, C. Ménézo, and G. La Ferla. 2015. 'Design for Façade Adaptability – Towards a Unified and Systematic Characterization' . In *Proceedings of the 10th Energy Forum - Advanced Building Skins*, 1274–84.
- Loonen, R. C. G. M., M. Trčka, D. Cóstola, and J. L. M. Hensen. 2013. 'Climate Adaptive Building Shells: State-of-the-Art and Future Challenges' . *Renewable and Sustainable Energy Reviews* 25 (September): 483–93. <https://doi.org/10.1016/j.rser.2013.04.016>.
- Loonen, R. C. G. M., M. Trčka, and J. L. M. Hensen. 2011. 'Exploring the Potential of Climate Adaptive Building Shells' . *Proceedings of Building Simulation 2011: 12th Conference of International Building Performance Simulation Association*, 2148–55.
- Meagher, Mark. 2015. 'Designing for Change: The Poetic Potential of Responsive Architecture' . *Frontiers of Architectural Research* 4 (2): 159–65. <https://doi.org/10.1016/j.foar.2015.03.002>.
- Moloney, Jules. 2011. *Designing Kinetics for Architectural Facades: State Change*. Taylor & Francis.
- Morgan, Conway Lloyd. 1998. *Jean Nouvel: The Elements of Architecture*. New York: Universe.
- 'Moucharabiehs de l' Institut Du Monde Arabe à Paris - Light ZOOM Lumière - Le Portail de La Lumière et de l' Éclairage' . n.d. Accessed 10 April 2018. <https://www.lightzoomlumiere.fr/realisation/moucharabiehs-institut-du-monde-arabe-paris/>.
- Pawlyn, Michael. 2011. *Biomimicry in Architecture*. Riba Publishing.
- Reichert, Steffen, Achim Menges, and David Correa. 2015. 'Meteorosensitive Architecture: Biomimetic Building Skins Based on Materially Embedded and Hygroscopically Enabled Responsiveness' . *Computer-Aided Design, Material Ecology*, 60 (March): 50–69. <https://doi.org/10.1016/j.cad.2014.02.010>.
- Roger, A. 2014. *Bending Activated Transformable Facade and Roof Elements*. Vol. Master Thesis.

- ‘SamanSaffarian ESR12 InnoChain / FlectoFold Large Scale Demonstrator / BauBionik Exhibition / Schloss Rosenstein / Stuttgart’. n.d. Vimeo. Accessed 15 April 2018. <https://vimeo.com/238750966>.
- Schleicher, Simon. 2015. *Bio-Inspired Compliant Mechanisms for Architectural Design : Transferring Bending and Folding Principles of Plant Leaves to Flexible Kinetic Structures*. <http://dx.doi.org/10.18419/opus-123>.
- Schleicher, Simon, Julian Lienhard, Simon Poppinga, Thomas Speck, and Jan Knippers. 2015. ‘A Methodology for Transferring Principles of Plant Movements to Elastic Systems in Architecture’. *Computer-Aided Design, Material Ecology*, 60 (March): 105–17. <https://doi.org/10.1016/j.cad.2014.01.005>.
- Schmitt, O.H. 1969. ‘Some Interesting Useful Biomimetic Transforms’. *Proceedings of the Third International Biophysics Congress*, 297.
- Sharaidin, M. 2014. ‘Kinetic Facades: Towards Design for Environmental Performance’. <https://researchbank.rmit.edu.au/view/rmit:161145>.
- Speck, T., and O. Speck. 2008. ‘Process Sequences in Biomimetic Research’. *Brebbia CA (Ed) Design and Nature IV*, 3–11.
- Sung, D.K. 2008. ‘Skin Deep: Breathing Life into the Layer between Man and Nature’. *AIA Report on University Research 3*: 23.
- Sung, Doris. 2016. ‘Smart Geometries for Smart Materials: Taming Thermobimetals to Behave’. *Journal of Architectural Education* 70 (1): 96–106. <https://doi.org/10.1080/10464883.2016.1122479>.
- Sung, Doris Kim. n.d. *Metal That Breathes*. Accessed 2 May 2018. [https://www.ted.com/talks/doris\\_kim\\_sung\\_metal\\_that\\_breathes](https://www.ted.com/talks/doris_kim_sung_metal_that_breathes).
- ‘Thermostatic Bimetal – Kanthal’. n.d. Accessed 24 May 2018. <https://www.kanthal.com/en/products/download-documentation/materials-in-wire-and-strip-form/thermostatic-bimetal/>.
- Tonka, Hubert. 1990. *Une Architecture De Jean Nouvel, Gilbert Lezenes, Pierre Soria, Architecture Studio - Institut Du Monde Arabe*. Paris: Editions Du Demi Cercle.
- Tonka, Hubert, and Georges Fessy. 1988. *Institut Du Monde Arabe, Un Architecture De Jean Nouvel, Gilbert Lezenes, Pierre Soria, Architecture Studio, Georges Fessy Photography*. Champ Vallon.
- Vergauwen, A. 2016. *Curved-Line Folding: Exploring, Understanding and Designing Pliable Structures for Kinetic Architecture*. Vol. Doctoral Thesis. Vrije Universiteit Brussel.
- Vergauwen, A., N. De Temmerman, and S. Brancart. 2014. ‘The Design And Physical Modelling Of Deployable Structures Based On Curved-Line Folding’. *Mobile and Rapidly Assembled Structures IV*, 145–55.

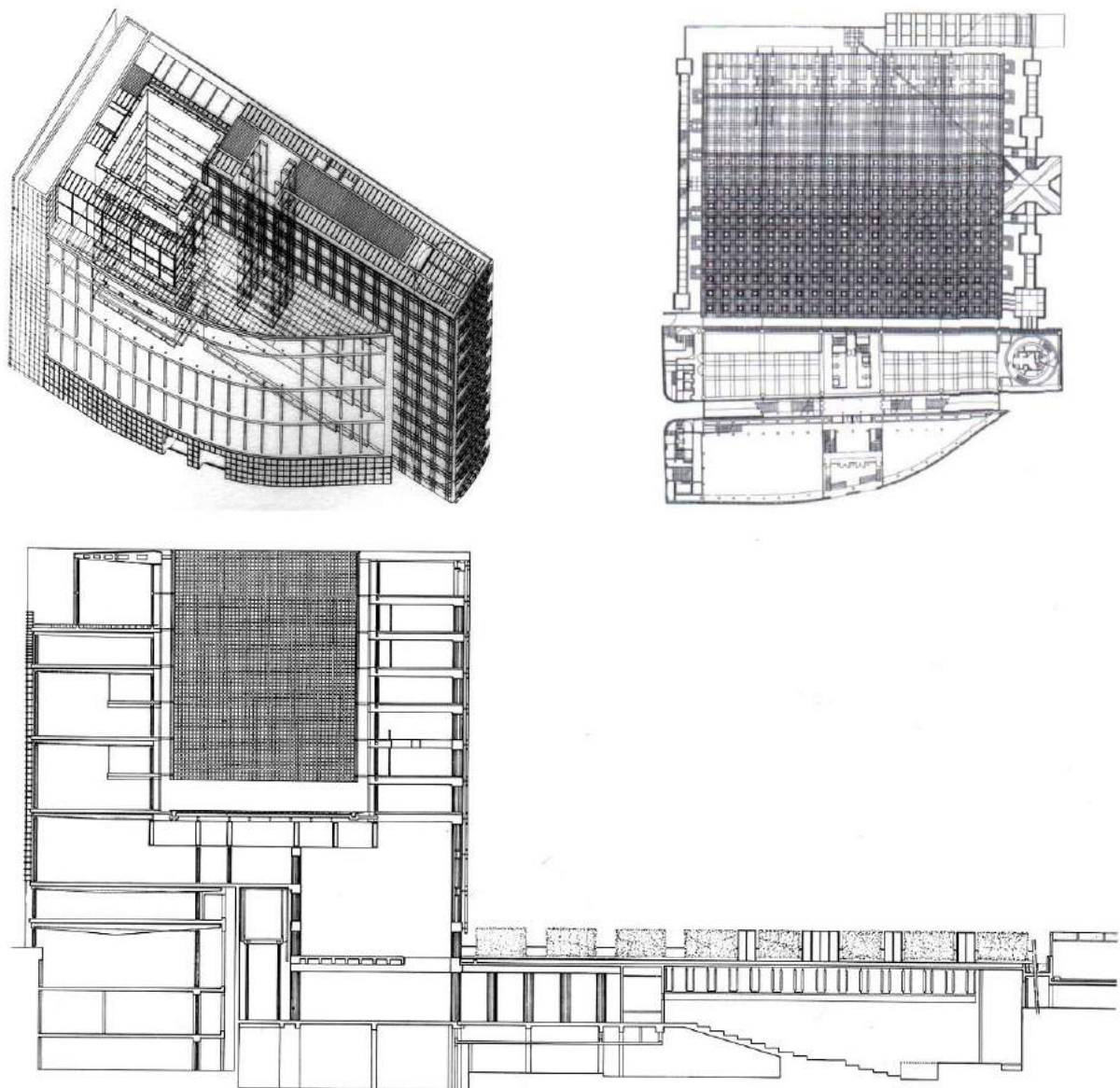
- Vincent, Julian F. V., Olga A. Bogatyreva, Nikolaj R. Bogatyrev, Adrian Bowyer, and Anja-Karina Pahl. 2006. 'Biomimetics: Its Practice and Theory'. *Journal of The Royal Society Interface* 3 (9): 471–82. <https://doi.org/10.1098/rsif.2006.0127>.
- Wang, J., L. Beltran, and J. Kim, eds. 2012. *From Static to Kinetic: A Review of Acclimated Kinetic Building Envelopes*. PROCEEDINGS OF THE SOLAR CONFERENCE. Boulder, Colorado: American Solar Energy Society.
- You, Z., and S. Pellegrino. 1997. 'Foldable Bar Structures'. *International Journal of Solids and Structures* 34 (15): 1825–47. [https://doi.org/10.1016/S0020-7683\(96\)00125-4](https://doi.org/10.1016/S0020-7683(96)00125-4).





## Appendix

## A Arab World Institute



**Figure A - 1:** *Top-left:* Axonometric drawing. *Top-right:* Plan of the first floor ( 'Institut Du Monde Arabe - Data, Photos & Plans' n.d.). *Bottom:* North-south section ( 'Équerre d' argent 1987 / Jean Nouvel Architecture Studio – Institut du monde arabe – Paris V' n.d.).

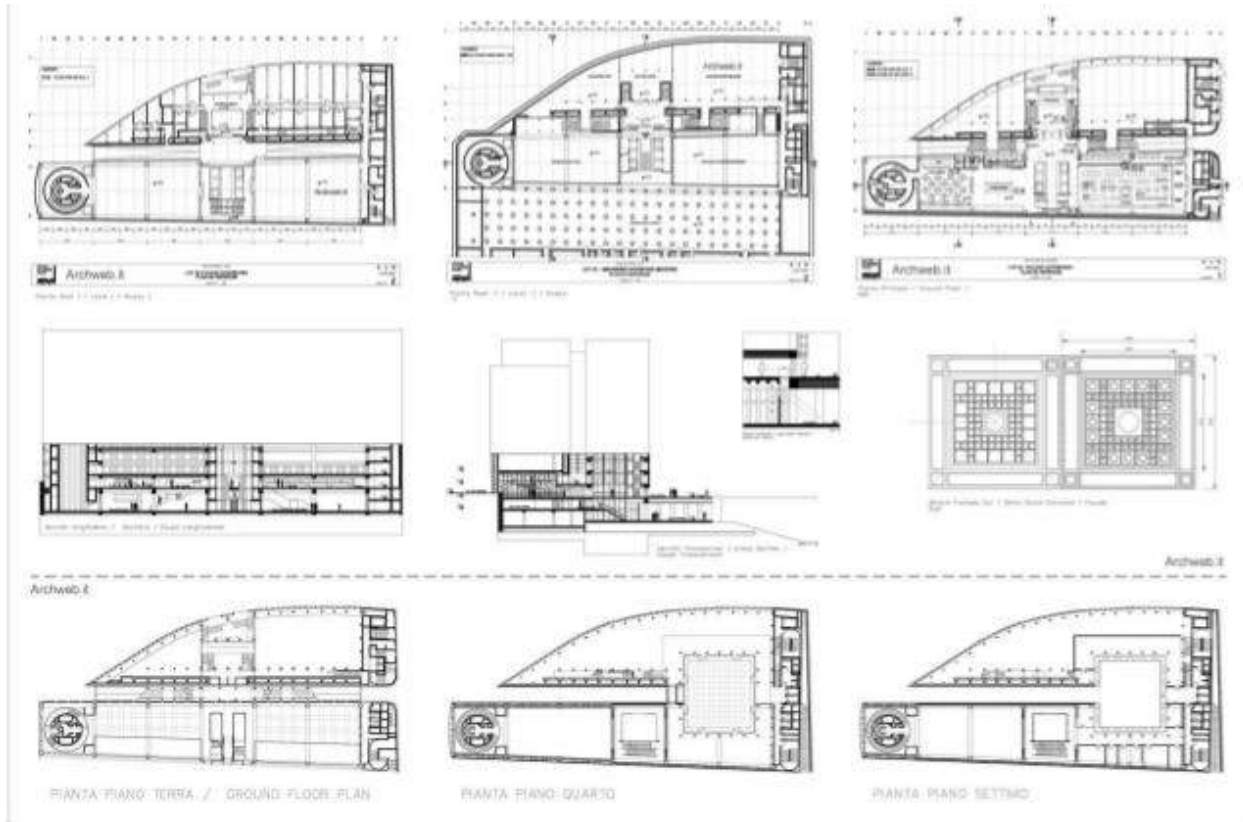


Figure A - 2: Summary of plans and sections ( 'Featured Design - SlideShare' n.d.).

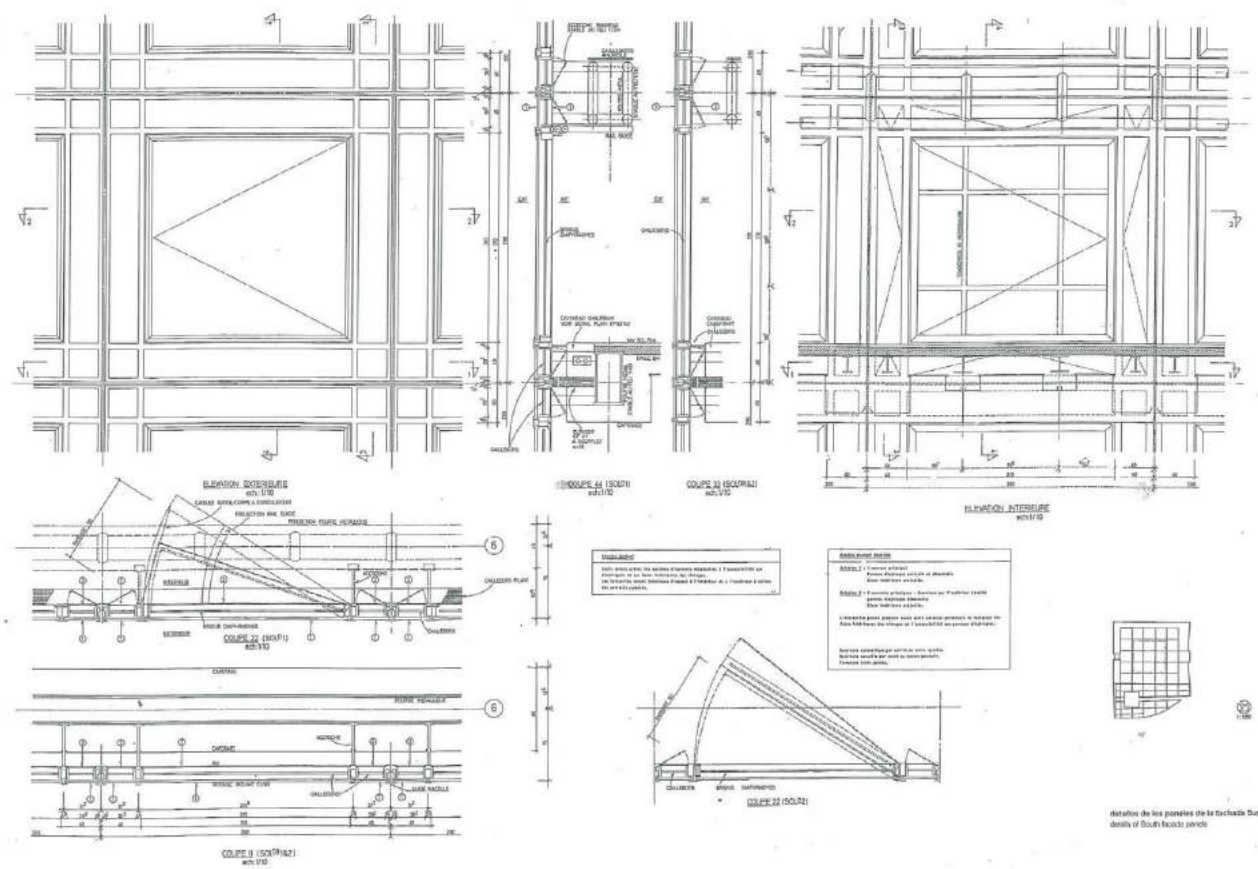


Figure A - 3: Constuction details of the mashrabiya modules of the south facade (Croquis 1994).

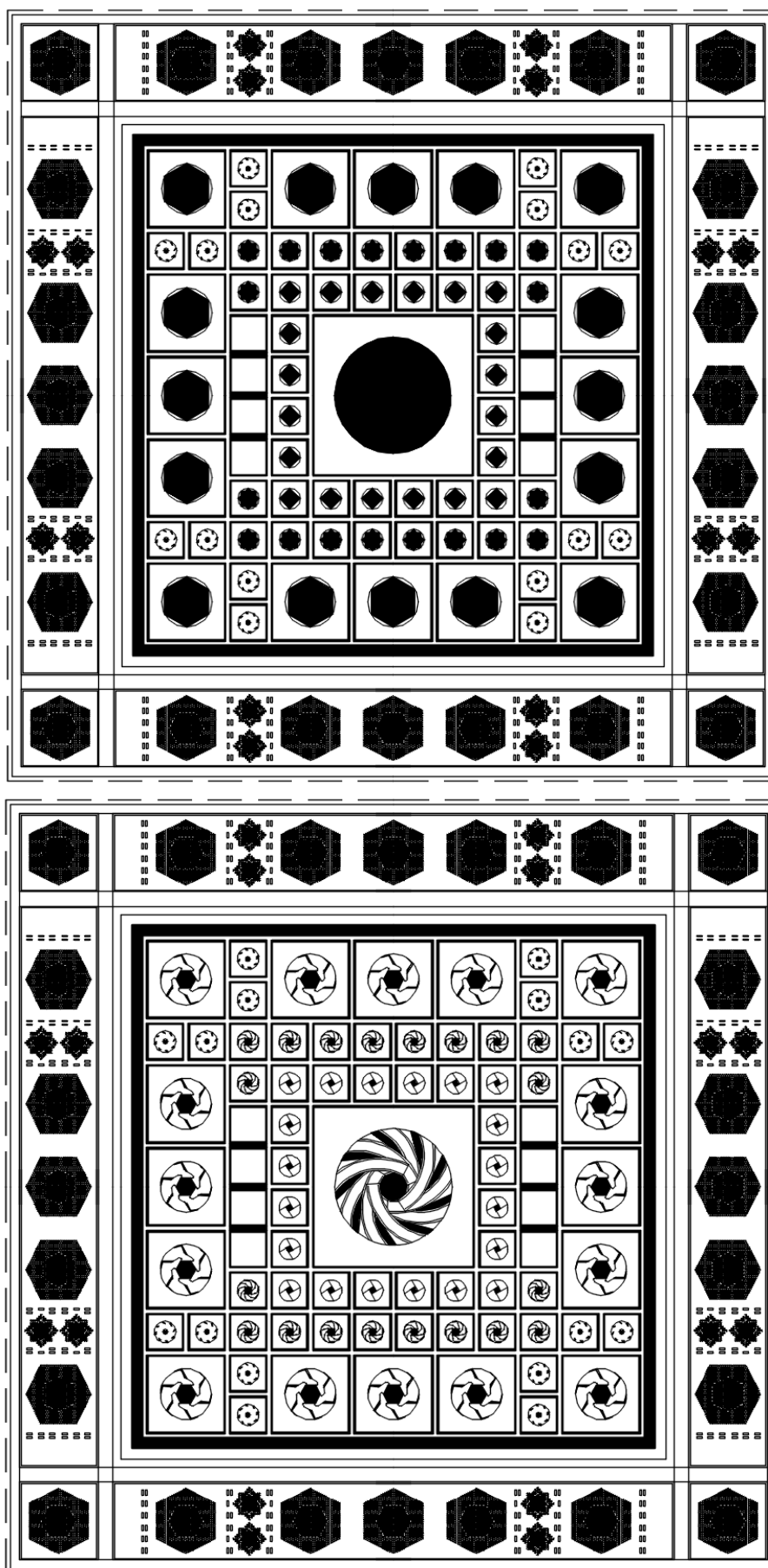


Figure A - 4: Open (top) and closed (bottom) configurations of one module of the Arab World Institute (the author 2017).

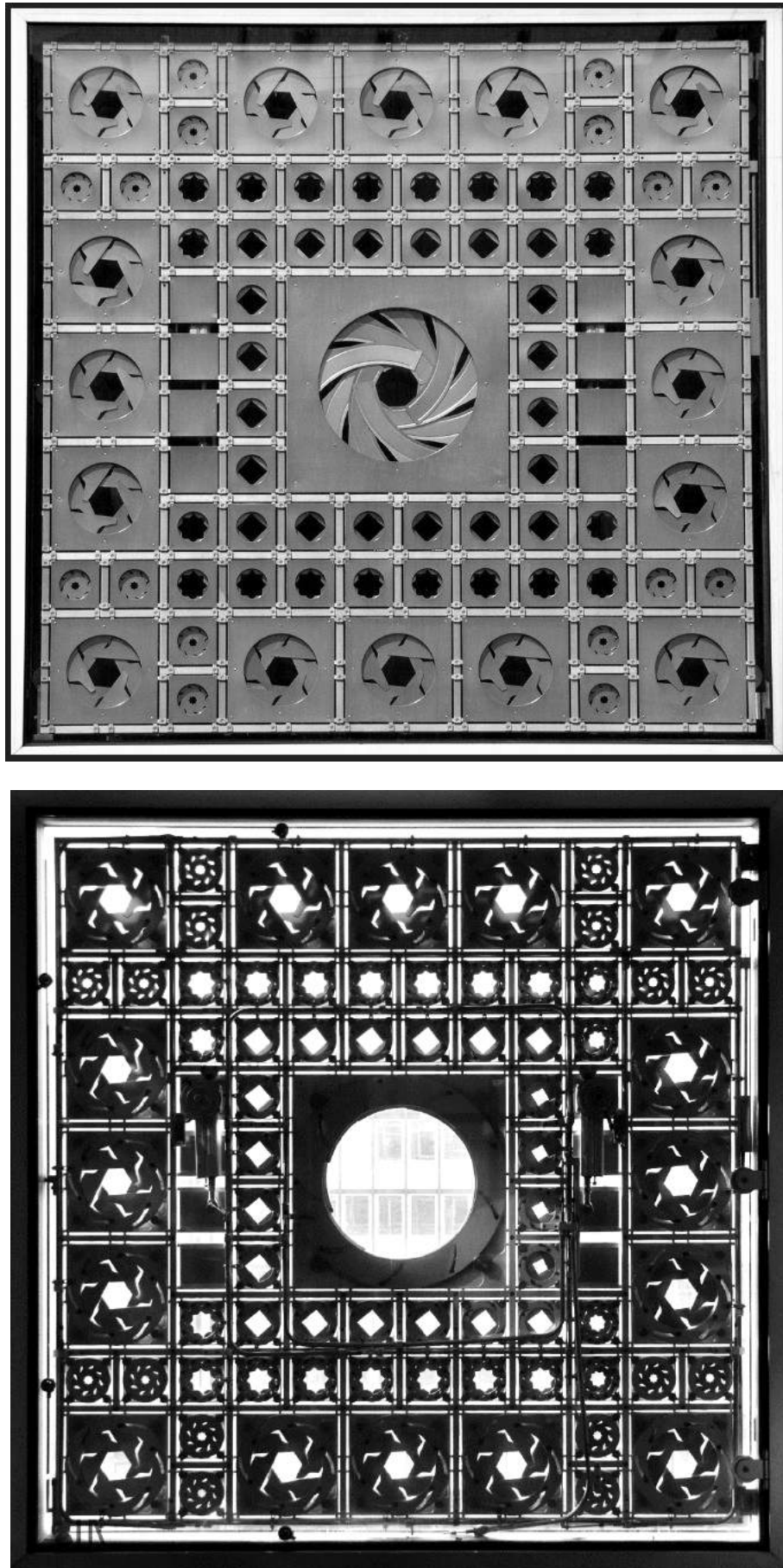
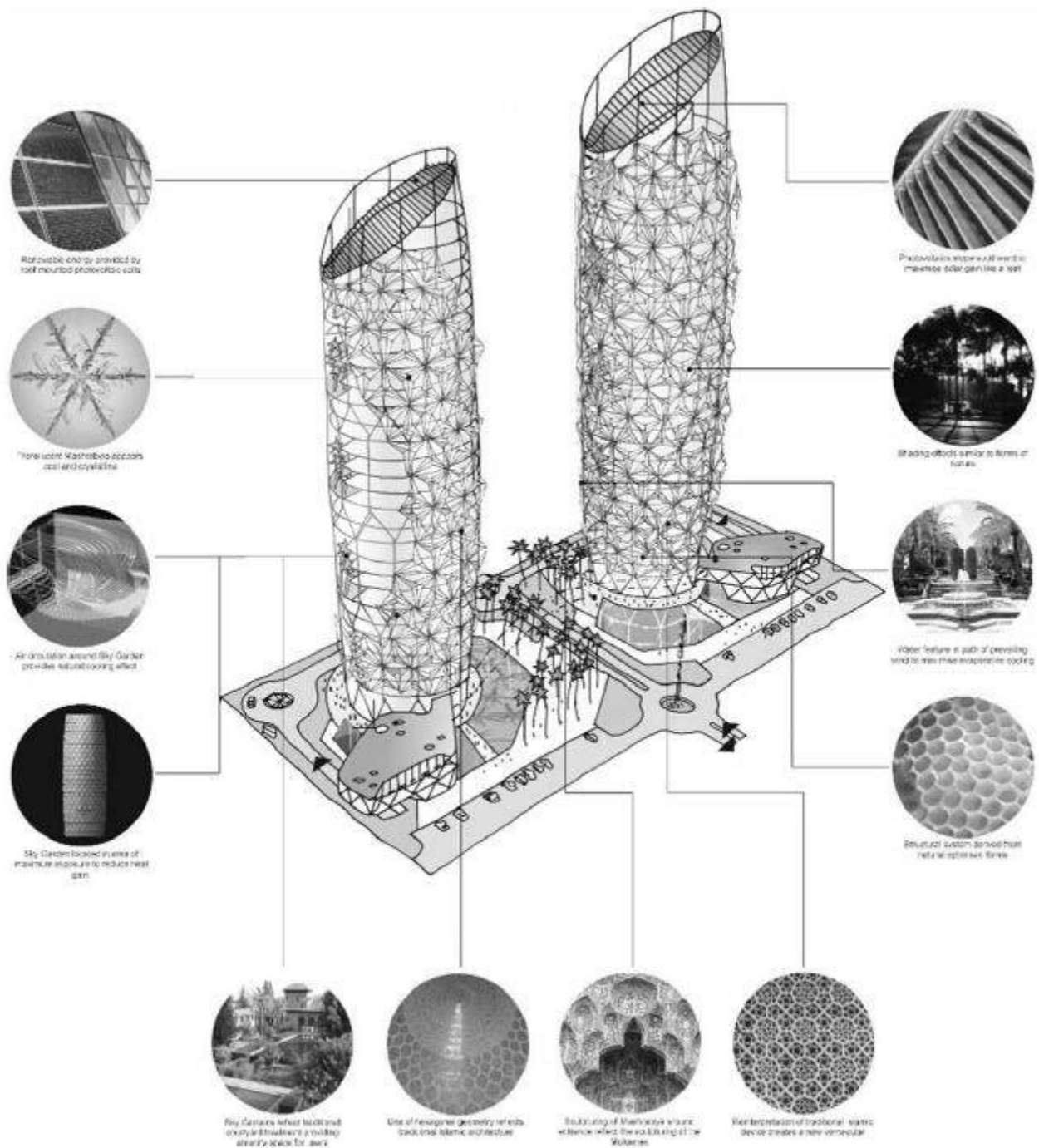


Figure A - 5: View of one module from the outside (top) and inside (bottom) of the building (Aðalheiðr 2011).

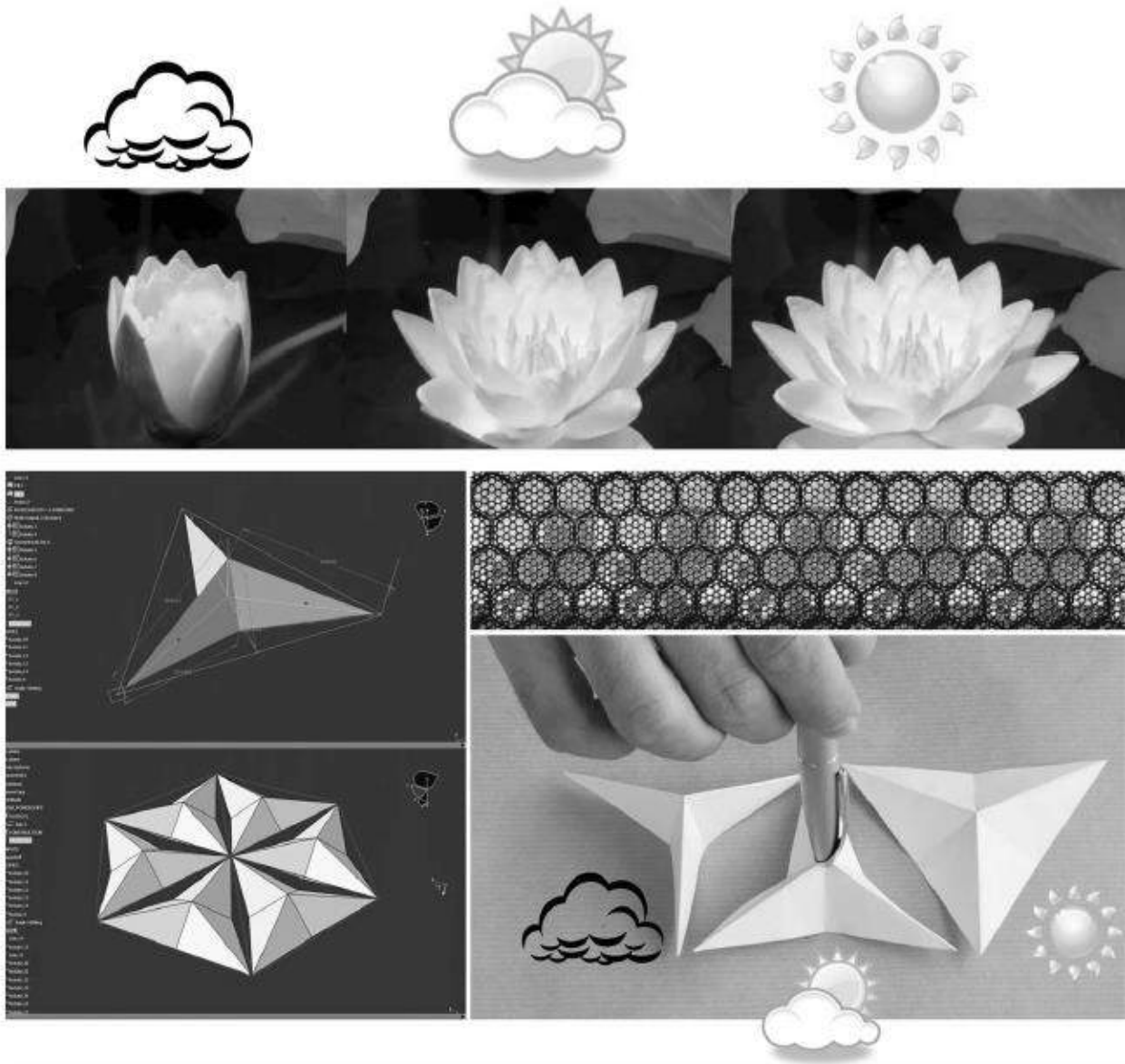


## B Relevant case studies

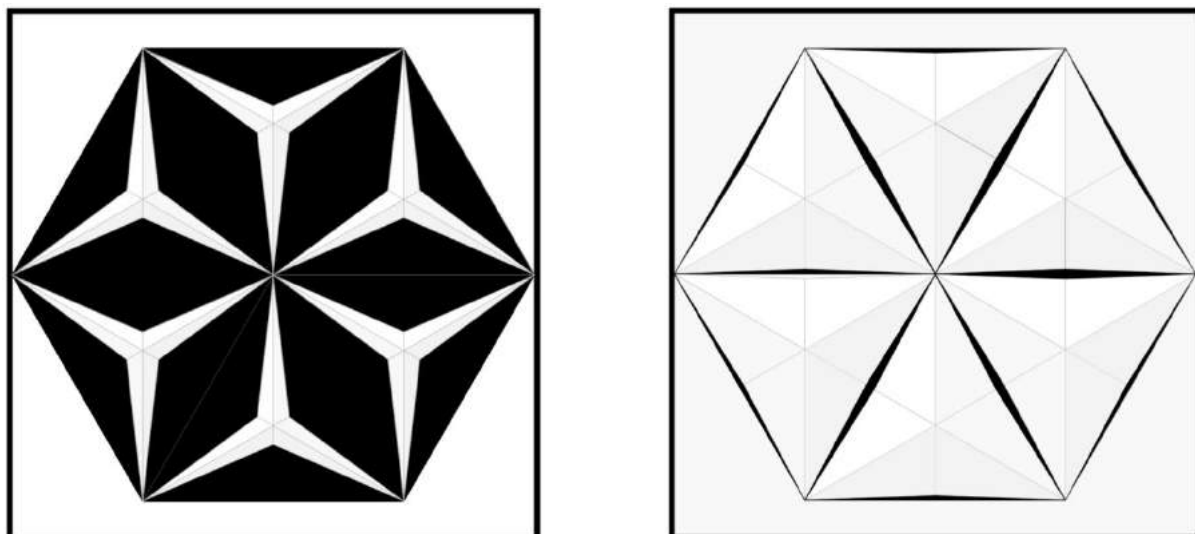
### Al Bahr Towers



**Figure B - 1:** Conceptual diagram of the Al Bahr Towers illustrating the various inspiration sources from biological systems and traditional Arabic architecture (Karanouh and Kerber 2015).

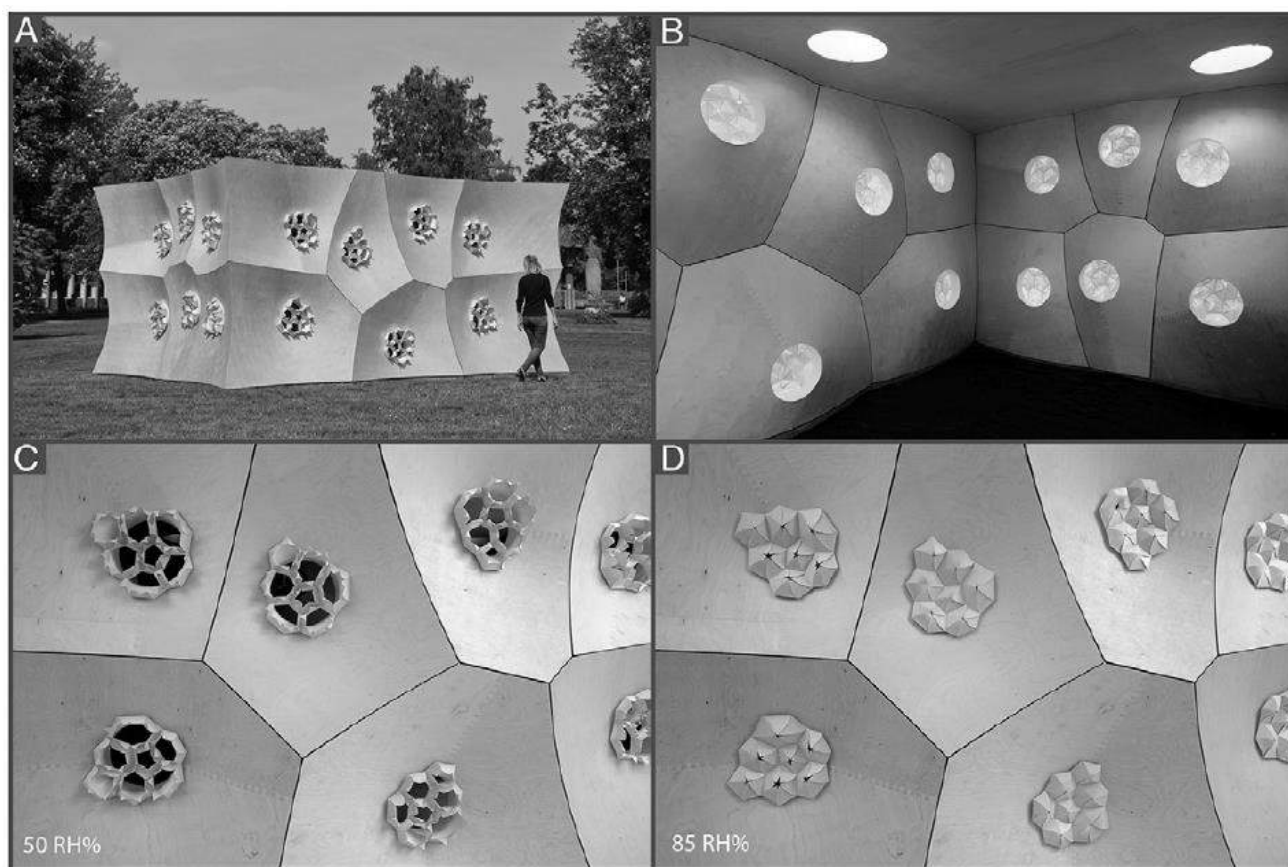


**Figure B - 2:** Dynamic origami shading device inspired from the traditional mashrabiya window and the opening and closing sequences of blooming flowers(Karanouh and Kerber 2015).

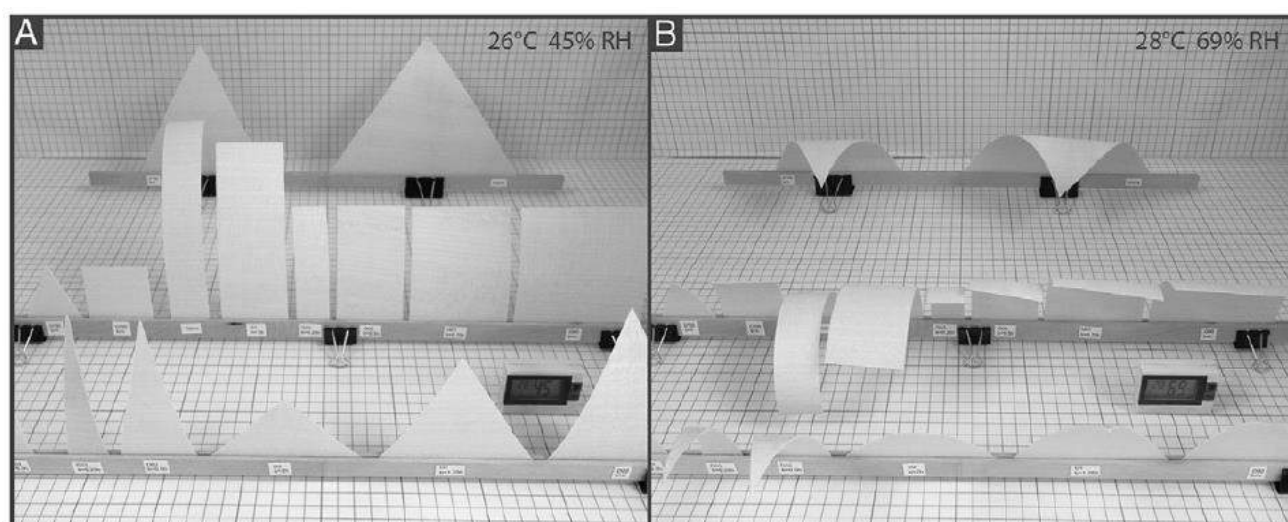


**Figure B - 3:** Six triangular units inserted in an AWI component in open (left) and closed (right) configurations (the author 2018).

## HygroSkin



**Figure B - 4:** Visualization of the HygroSkin Pavilion from outside and inside (top) and the opening and closing of the hygroscopic wooden veneer sheets under influence of relative humidity changes (Reichert, Menges, and Correa 2015).



**Figure B - 5:** Demonstration of the shape-dependency of hygroscopic elements in relation to deformation under relative humidity changes. Generally, the curling is the largest for long and narrow strips (Reichert, Menges, and Correa 2015).



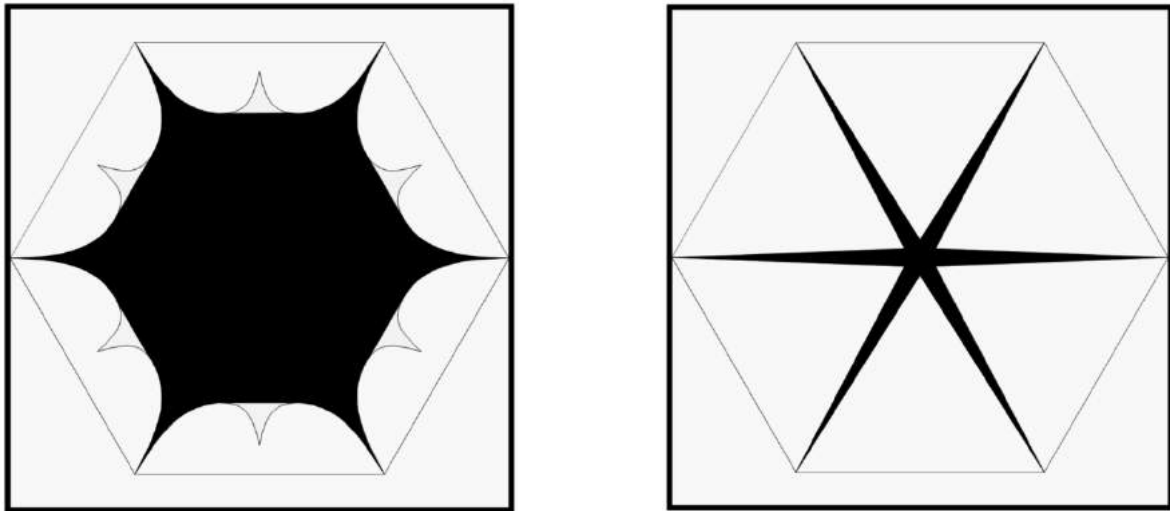


Figure B – 6: Six triangular sheets inserted in an AWI component in open (left) and closed (right) configurations (the author 2018).

## Air Flower

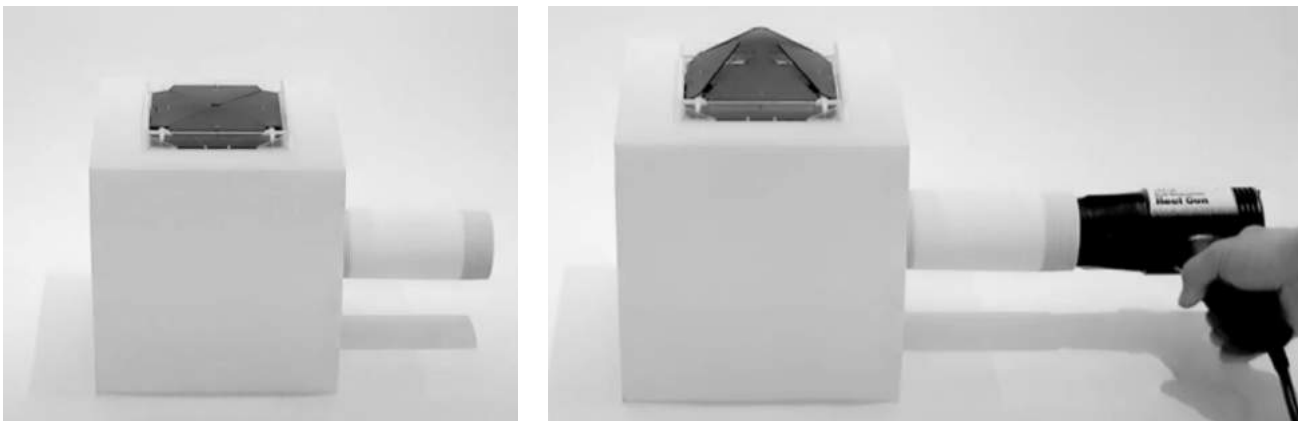


Figure B – 7: Opening of the Air Flower by contraction of an SMA wire through application of a heat source ( ‘Air Flow(Er) - Thermally Active Architectural Skin’ n.d.). The contraction overcomes the tension of the elastic cords, making the panels rotate around tubes.

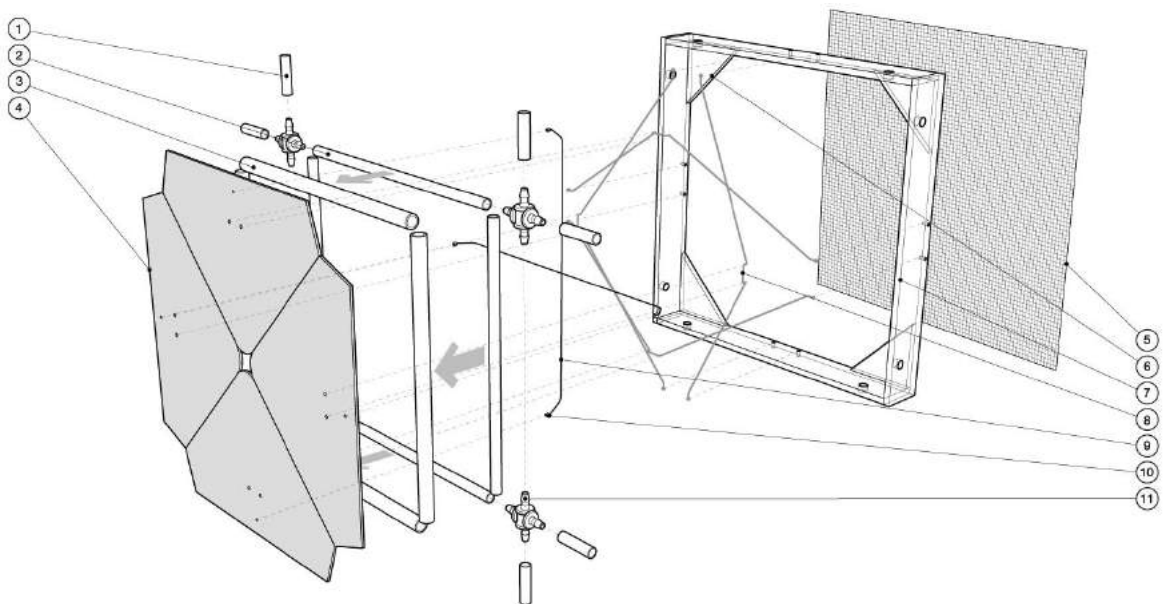


Figure B – 8: Exploded axonometry of the prototype’s assembly; 8 are the elastic cords and 9 is the SMA wire ( ‘Air Flower’ n.d.).

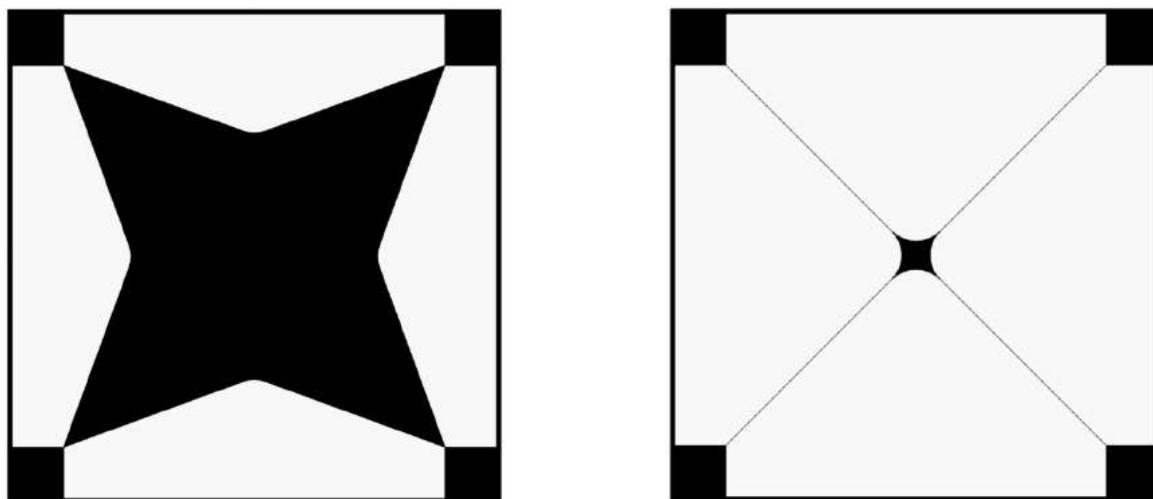


Figure B - 9: Air Flower unit inserted in an AWI component in open (left) and closed (right) configurations (the author 2018).

## Flectofin

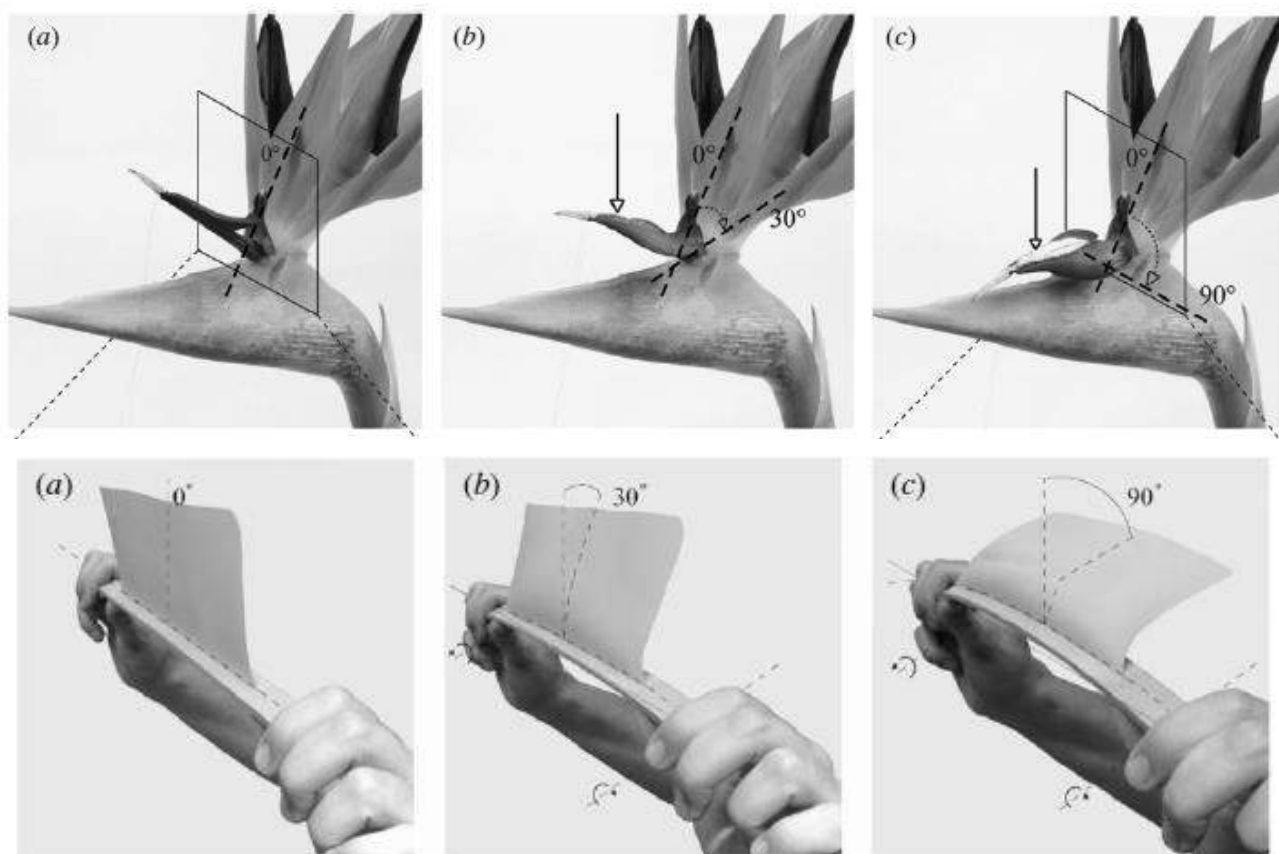


Figure B - 10: Top: Non-autonomous movement of the pollination mechanism in *Strelitzia reginae*. Bottom: Abstracted working principle by means of a simple physical model. The bending of the backbone causes lateral torsional buckling in the attached fin and results in a sideways deflection of 90° (Lienhard et al. 2011).

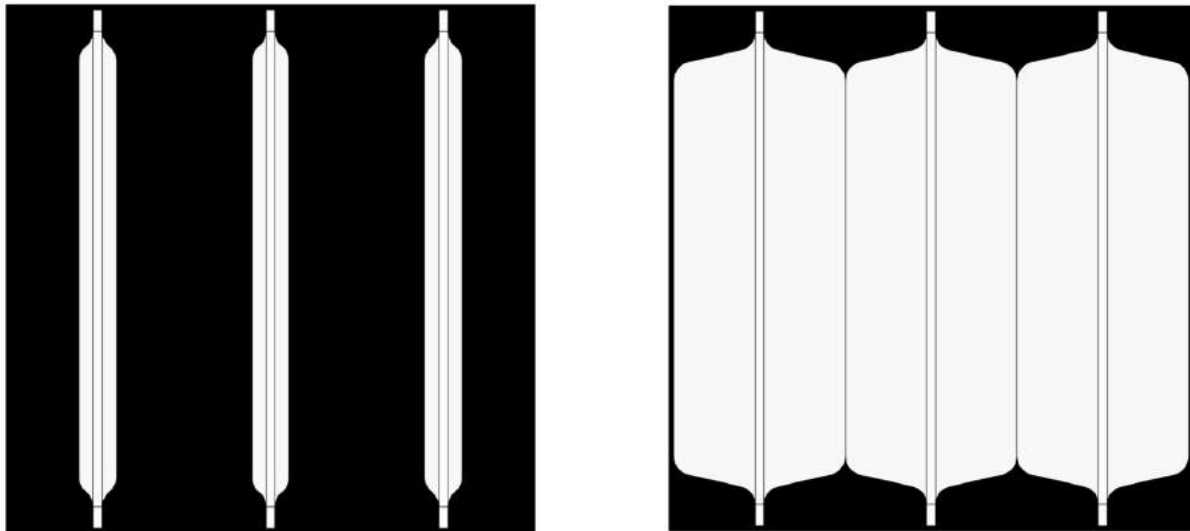


Figure B - 11: Three Flectofin<sup>®</sup> units inserted in an AWI component in open (left) and closed (right) configurations (the author 2018).

## Flectofold

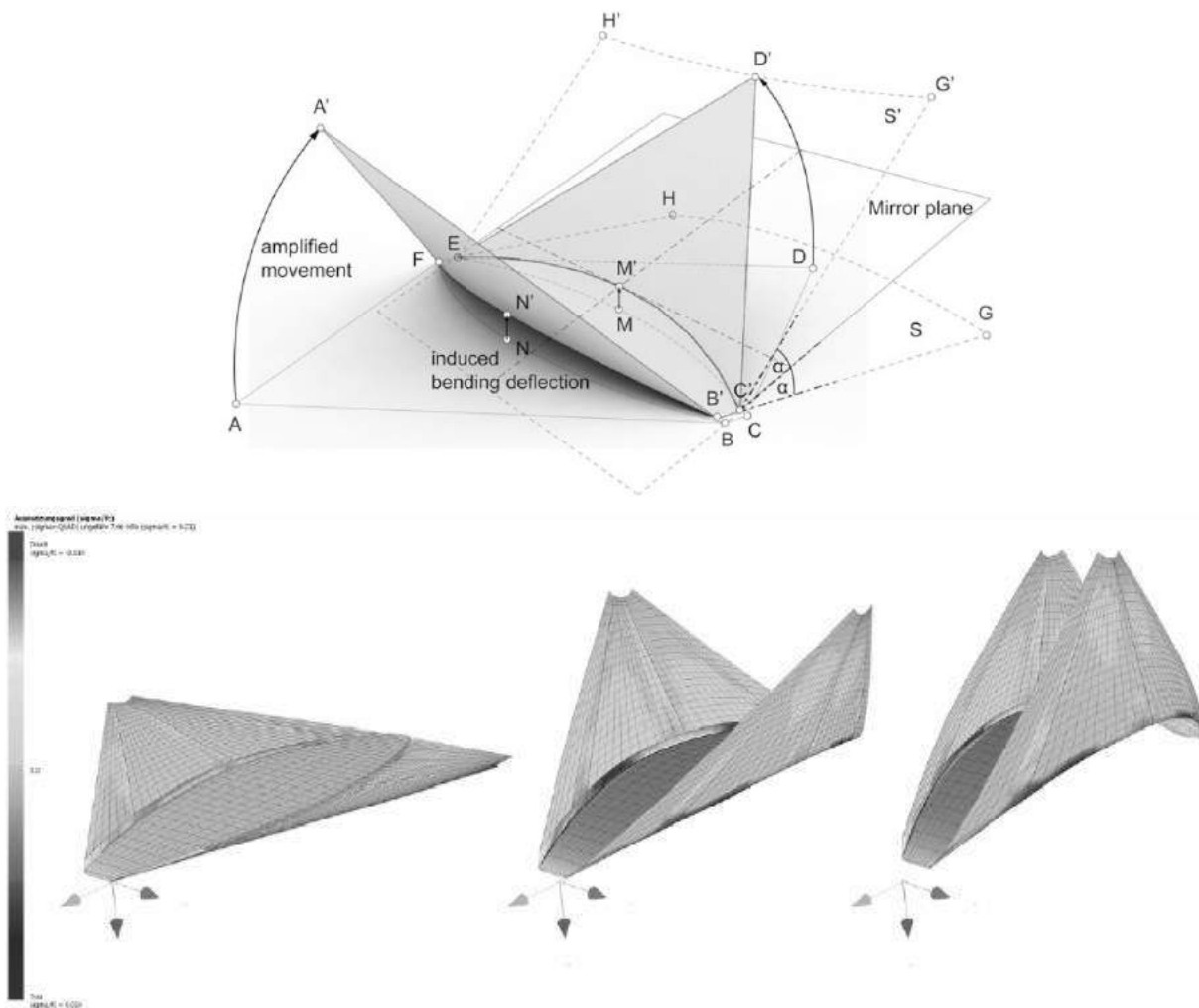
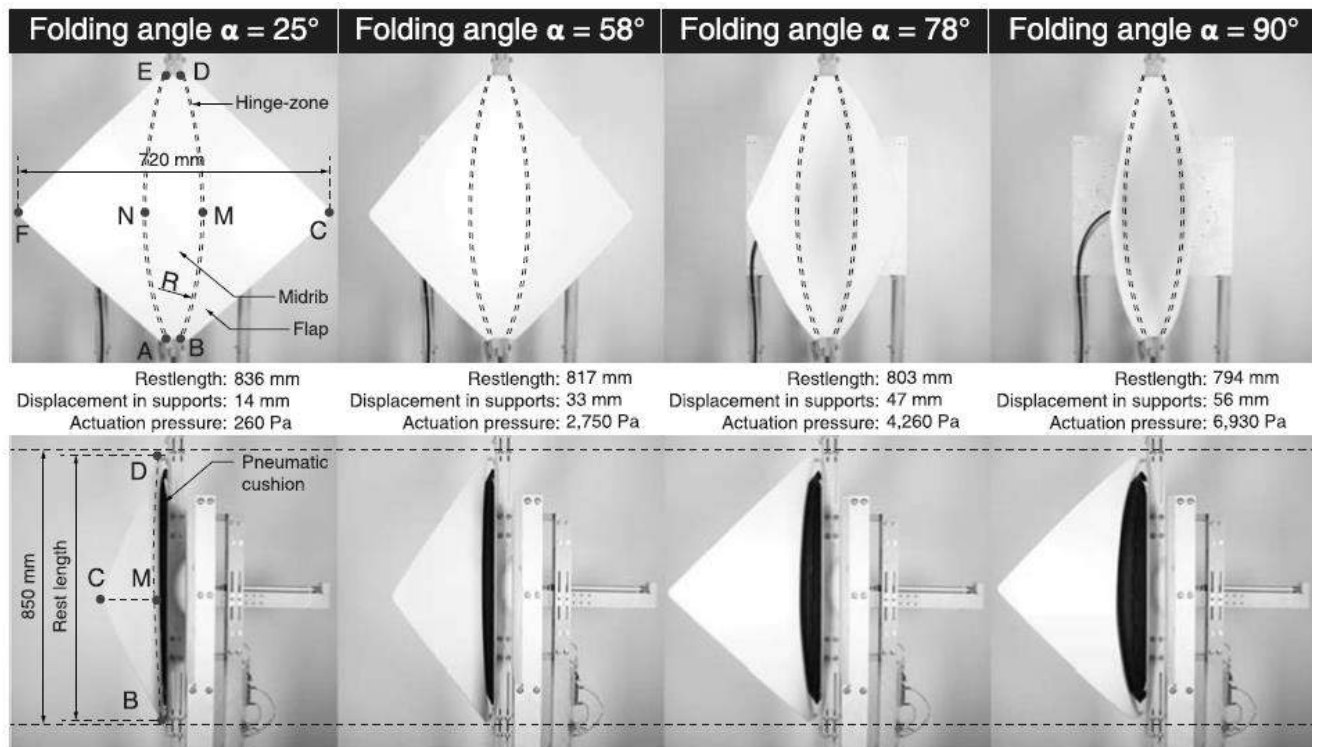
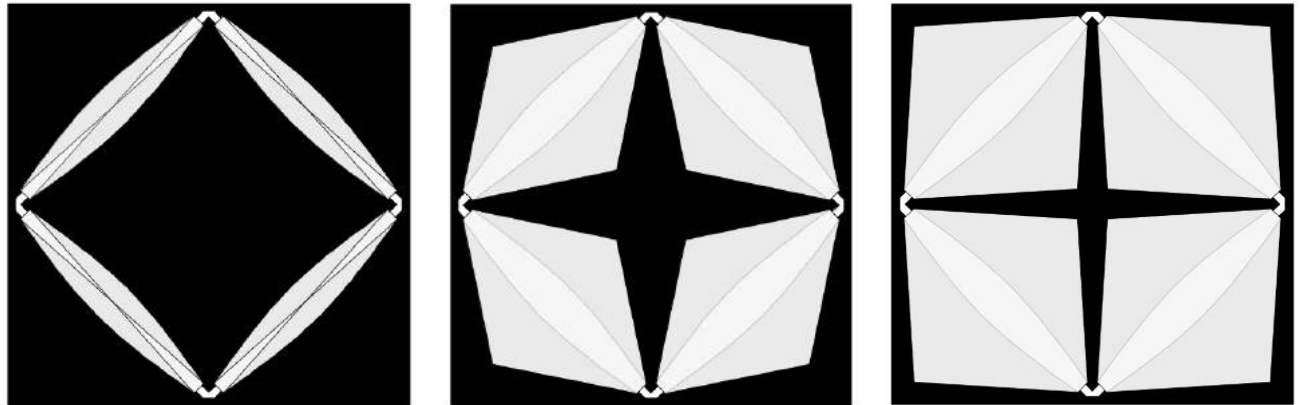


Figure B - 12: *Top*: Kinematic model of the abstracted folding mechanism using a rigid origami simulator (Körner et al. 2016). *Bottom*: Kinetic model of the abstracted folding mechanism using finite element modelling (FEM) (Schleicher et al. 2015).



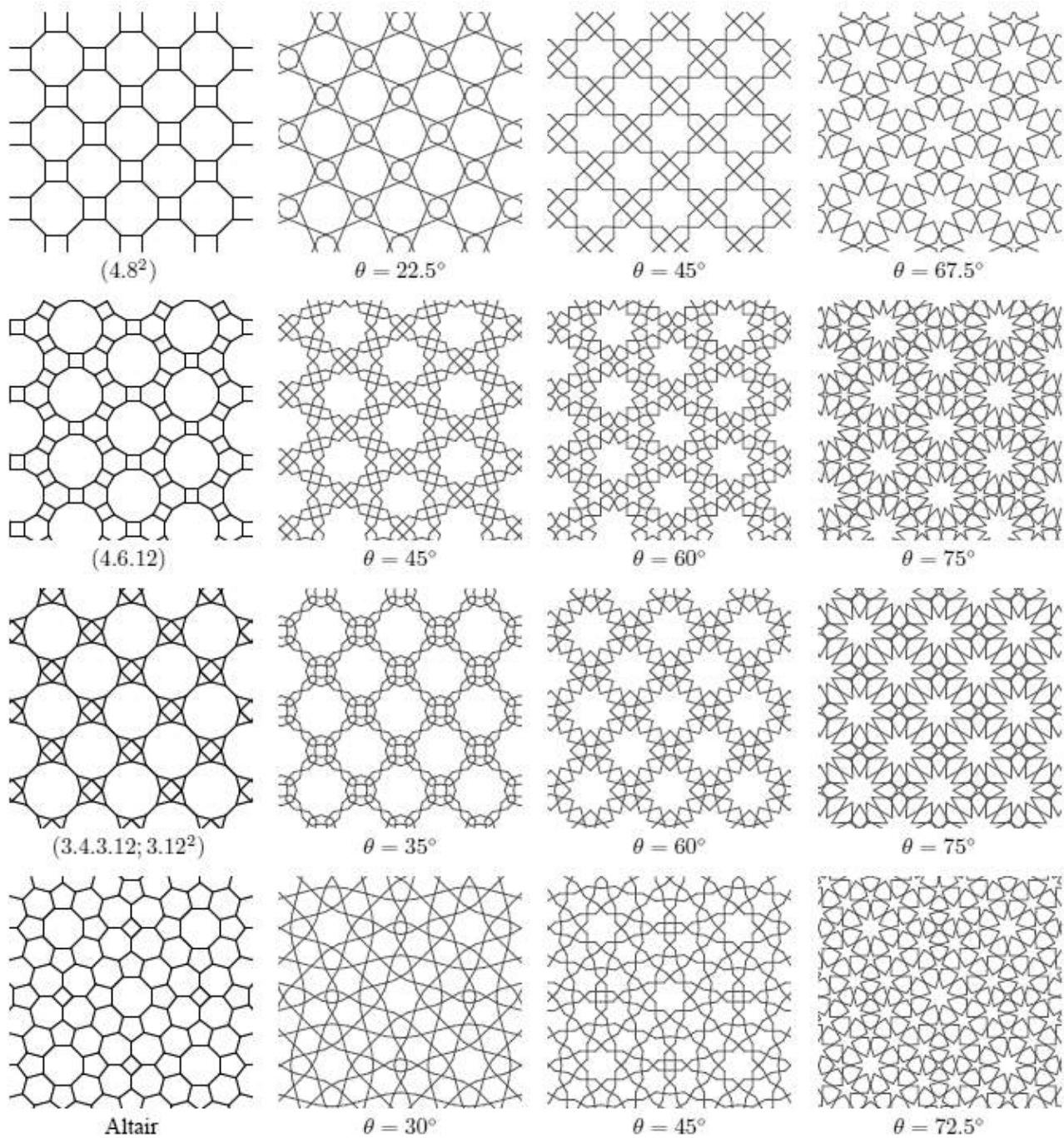
**Figure B - 13:** Actuation of the Flectofold prototype by a pneumatic cushion between the midrib and the backbone (Körner et al. 2018).



**Figure B - 14:** Open (left), intermediate (middle) and closed (right) configurations of one square framed component consisting of four Flectofolds. The intermediate state clearly accentuates a 4-pointed Islamic star pattern (the author 2018)

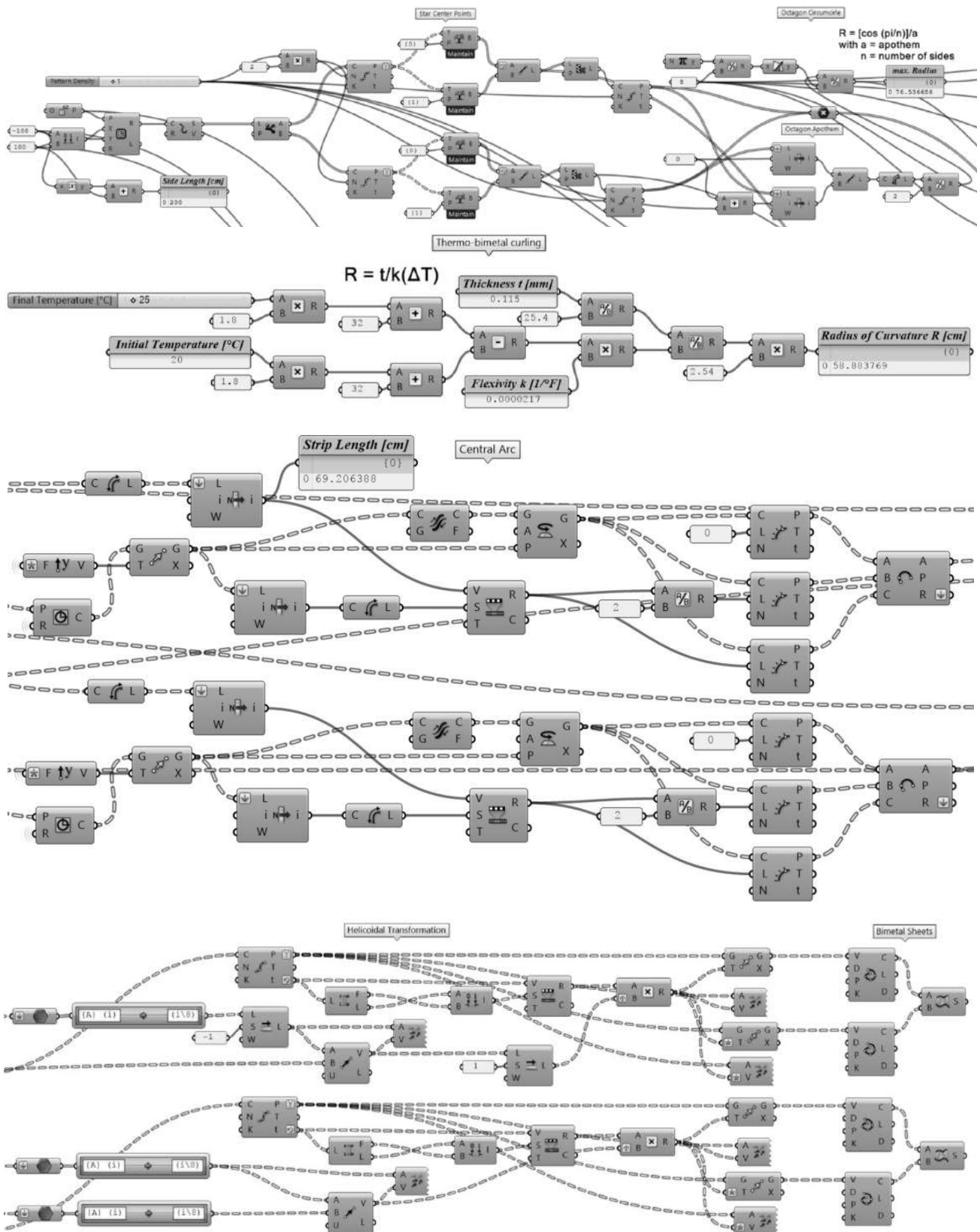
## C Thermo-bimetal curling

### Redesign – Arabic geometric patterns



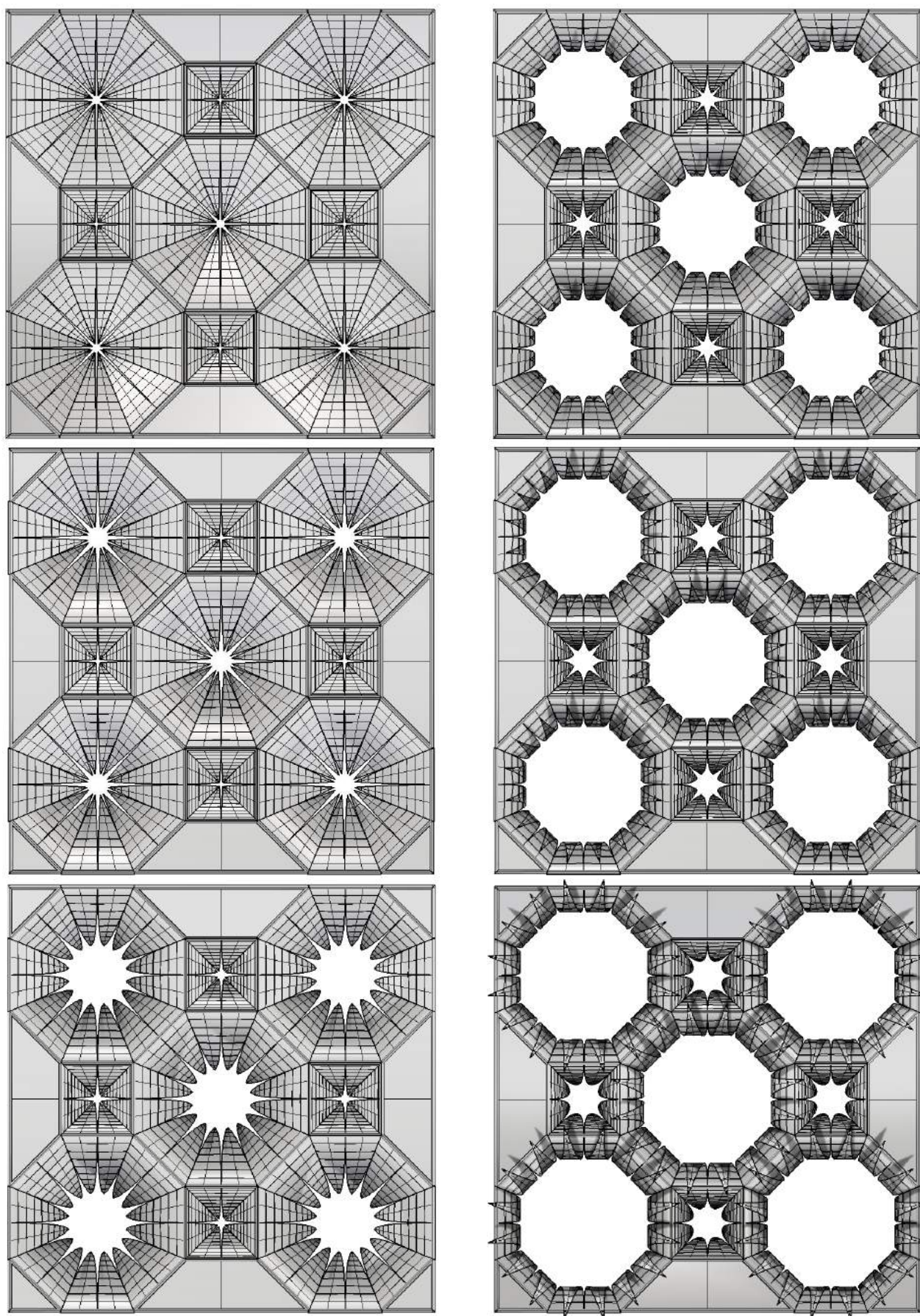
**Figure C – 1:** Star patterns originating from different tessellations by implementation of Hankin's method for polygons in contact. Each row represents a tessellation that is transformed into an Islamic star pattern by changing the contact angle  $\theta$ . The larger the contact angle, the more the stars are accentuated (Kaplan 2005).

## Redesign – Geometric simulations



**Figure C - 2:** Selection of the Grasshopper script for the parametric geometric simulation of thermo-bimetal curling for a 4.8.8 tessellation frame. From top to bottom: 1) Drawing of the tessellation (octagon part). 2) Calculation of the radius of curvature. 3) Definition for the central arc running through the middle of the triangular bimetal sheets. 4) Approximation of the movement for the triangle edges by a helicoidal transformation. The definition for the squares is similar as for the octagons.

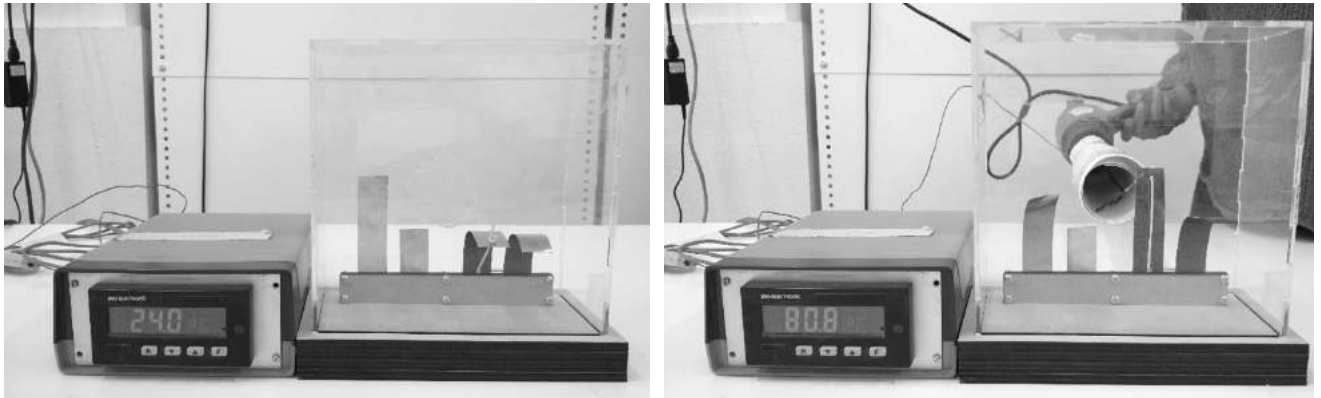




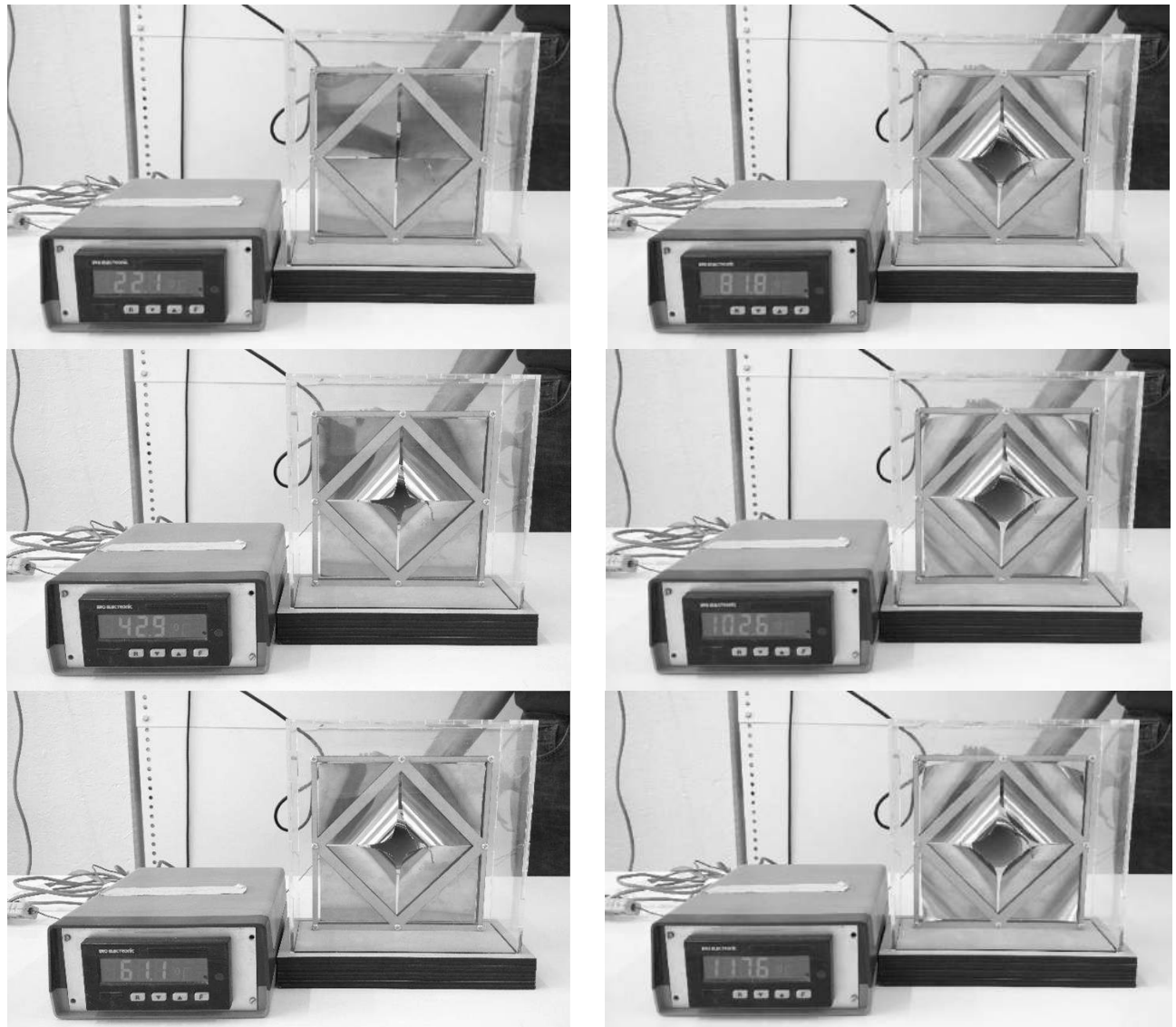
**Figure C - 3:** Geometric simulation of the thermo-bimetal curling in a square 4.8.8 tessellation frame of 60 by 60 cm (central component of the AWI). Motion sequence starting at 20 °C (top-left) and ends at 70 °C (bottom-right) with an interval of 10 °C.



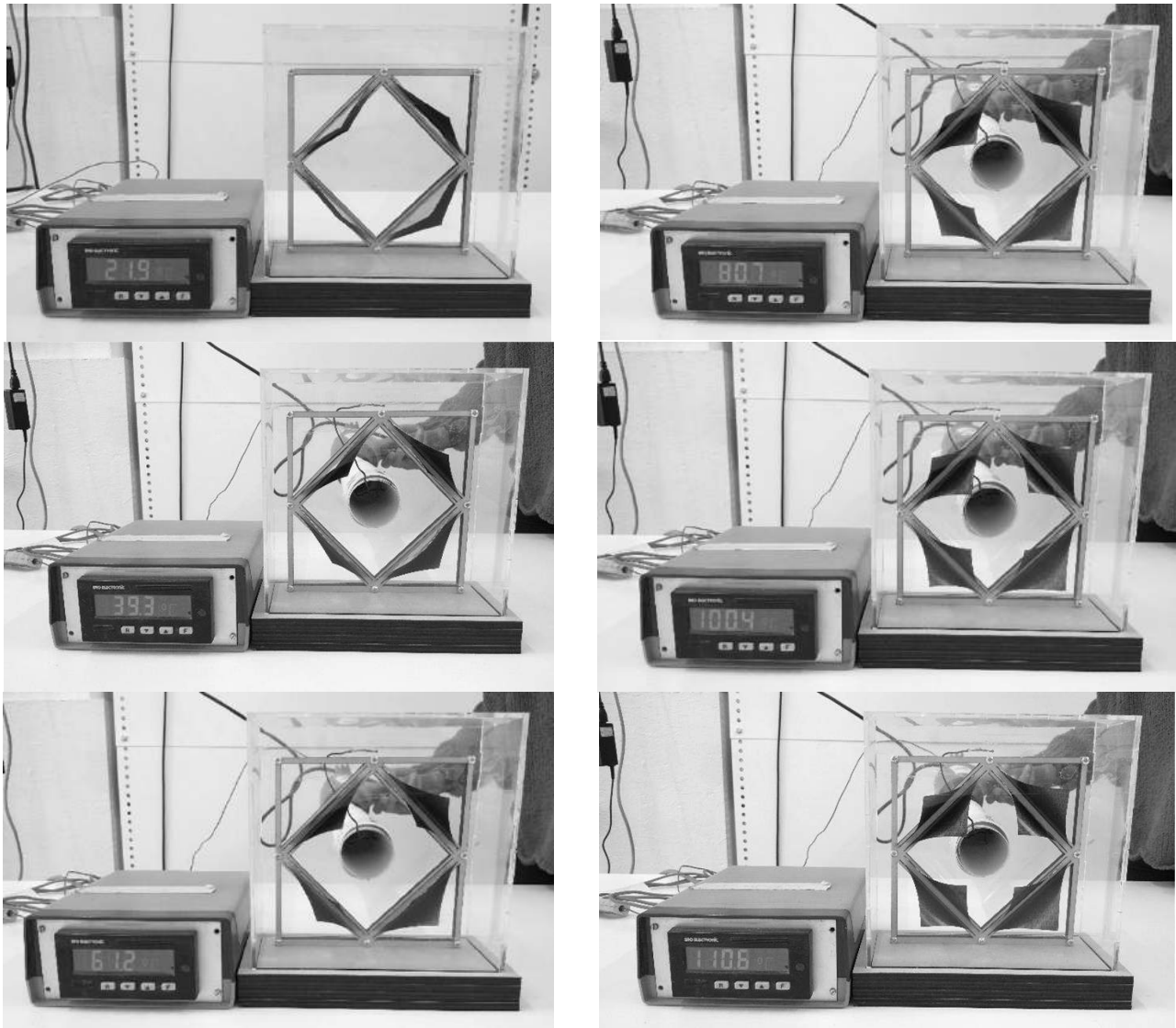
## Prototyping



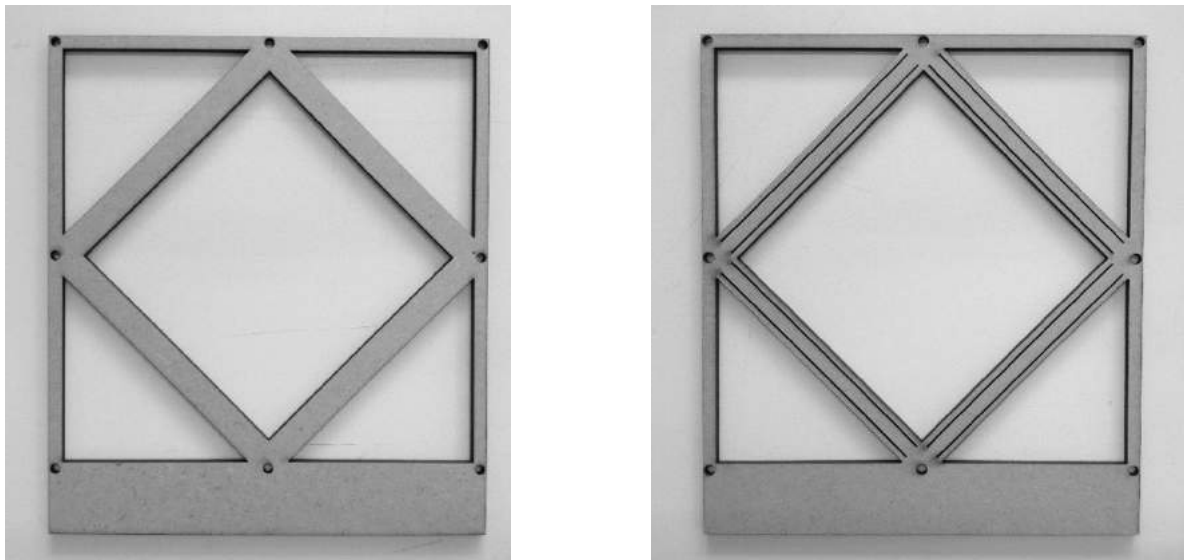
**Figure C - 4:** Comparison of four thermo-bimetal strips from room temperature (left) to  $\pm 80$  °C (right). From left to right: 1) Strip proportions 1:5. 2) Strip with proportions 1:5/2. 3) Pre-bent strip with elastic cord flipping into a bi-stable position at  $\pm 80$  °C. 4) Pre-bent strip by plastic deformation.



**Figure C - 5:** Motion sequence of the in-the-plane positioning of bimetal sheets in a 4.4.4.4 tessellation component of 15 by 15 cm. The experiment starts at room temperature and ends at  $\pm 120$  °C.



**Figure C - 6:** Motion sequence of the out-of-plane positioning of bimetal sheets in a 4.4.4.4 tessellation component of 15 by 15 cm. The experiment starts at room temperature and ends at  $\pm 110^{\circ}\text{C}$ .



**Figure C - 7:** Wooden frames used for the prototypes. *Left:* In-the-plane positioning. This one was also used for the tests with pre-bent sheets by plastic deformation. *Right:* Out-of-plane positioning.

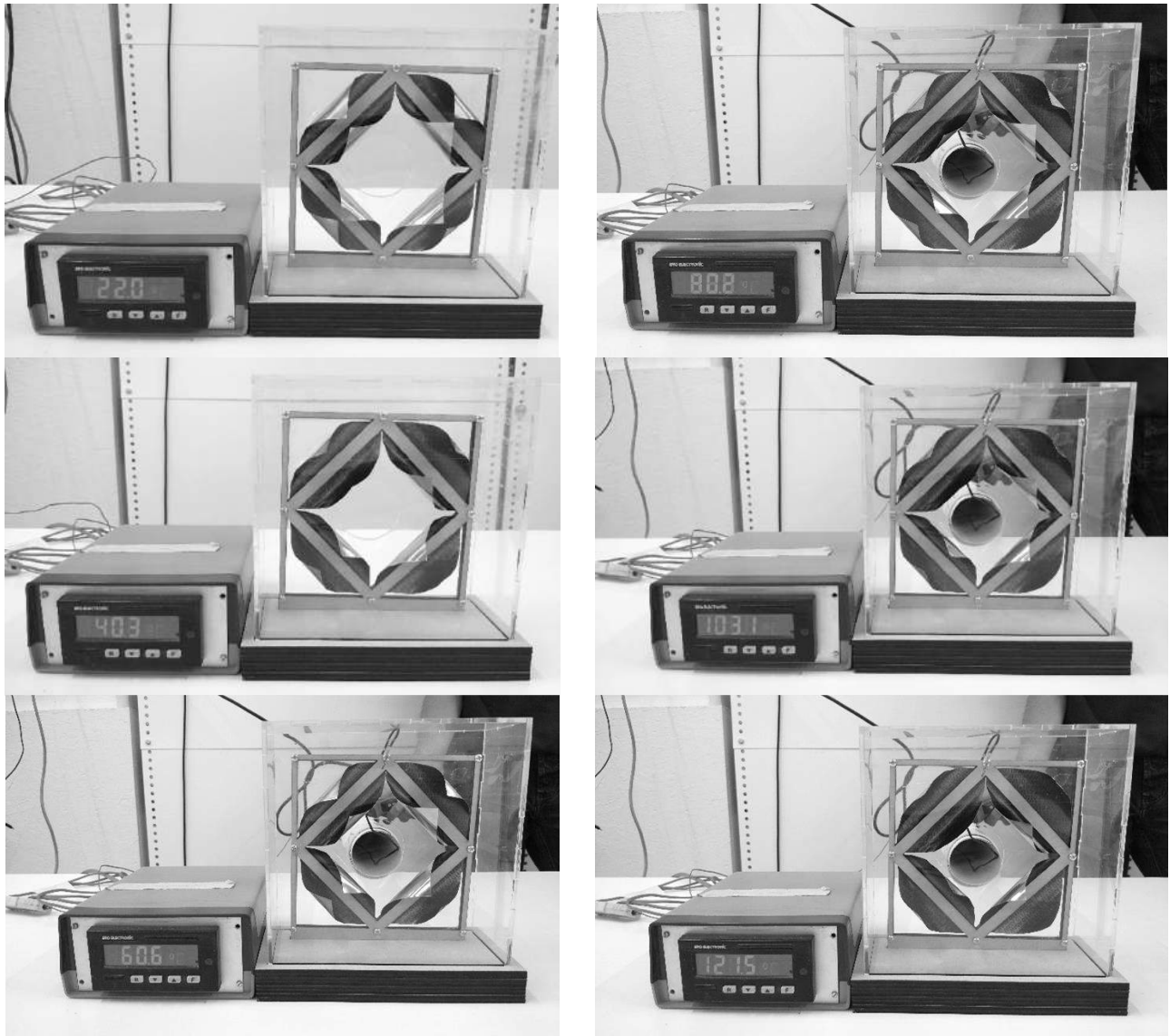


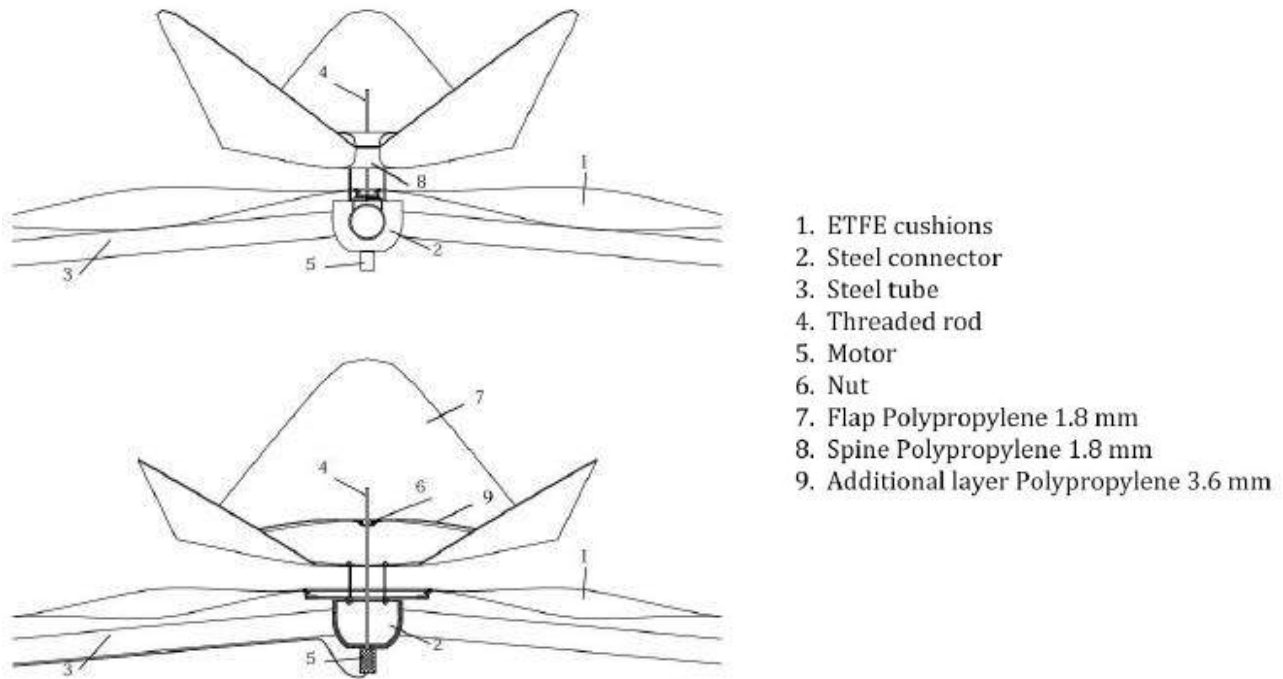
Figure C - 8: Motion sequence of bimetal sheets pre-bent by plastic deformation in a 4.4.4.4 tessellation component of 15 by 15 cm. The experiment starts at room temperature and ends at  $\pm 120^\circ\text{C}$ .

NUMBER	TYPE	SPEC. THERMAL CURVATURE 20-130°C	SPECIFIC DEFLECTION 20-100°C	ELECTRICAL RESISTIVITY AT 20°C	LINEARITY RANGE	MAX. OPERATING TEMPERATURE
		$10^{-6}/\text{K}$	$10^{-6}/\text{K}$	$\mu\Omega/\text{m}$	$^\circ\text{C}$	$^\circ\text{C}$
1	TB 230/110	$43.0 \pm 5\%$	23.0	$1.08 \pm 5\%$	+20 up to 230	350
2	TB 210/10	$39.0 \pm 5\%$	20.8	$0.10 \pm 7\%$	-20 up to 200	350
3	TB 208/110	$39.0 \pm 5\%$	20.8	$1.10 \pm 5\%$	-20 up to 200	350
4	TB 200/108	$37.5 \pm 5\%$	20.0	$1.08 \pm 5\%$	-20 up to 200	350
5	TB 200/80	$38.9 \pm 5\%$	20.8	$0.82 \pm 5\%$	-20 up to 200	350
6	TB 200/60	$38.8 \pm 5\%$	20.6	$0.58 \pm 5\%$	-20 up to 200	350
7	TB 200/40	$38.5 \pm 5\%$	20.5	$0.40 \pm 5\%$	-20 up to 200	350
8	TB 200/30	$38.6 \pm 5\%$	20.3	$0.30 \pm 7\%$	-20 up to 200	350
9	TB 200/20	$38.5 \pm 5\%$	20.2	$0.21 \pm 7\%$	-20 up to 200	350
10	TB 200/17	$38.4 \pm 5\%$	20.1	$0.166 \pm 7\%$	-20 up to 200	350

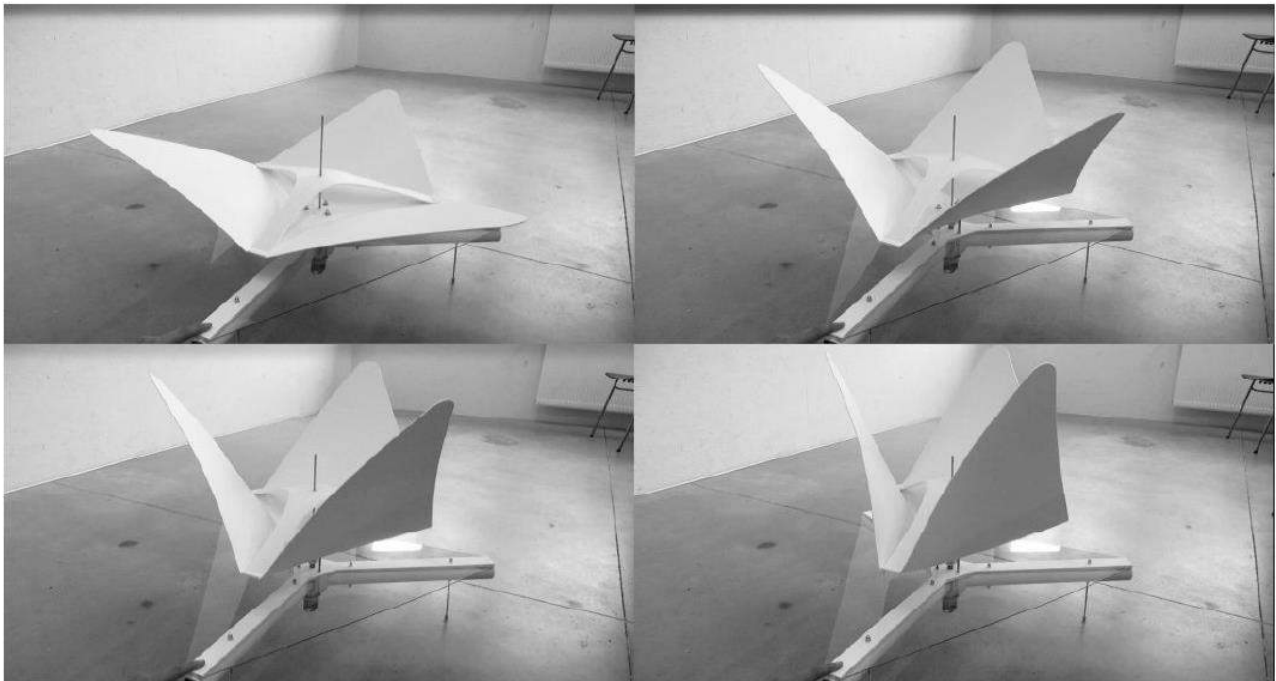
Figure C - 9: Datasheet of the thermostatic bimetal purchased from Auerhammer Metallwerk GmbH (‘Datasheets’ n.d.). The one used for the prototypes is highlighted and has one of the highest specific thermal curvatures available on the market.

## D Curved-line folding

### State of the art

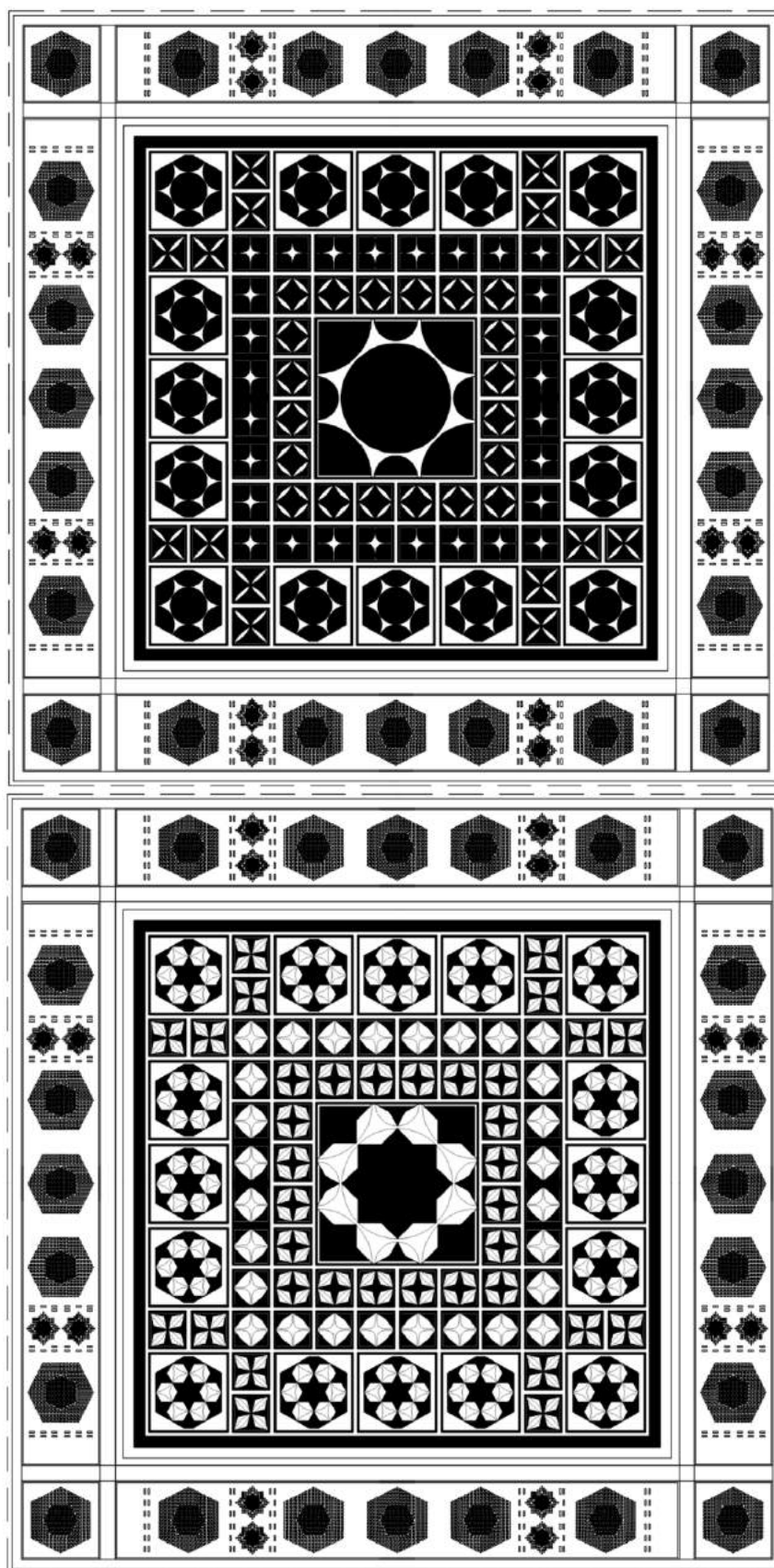


**Figure D - 1:** Section of the adaptive shading system developed by (Roger 2014) and adapted by (Vergauwen 2016). When the motor is activated, the threaded rod is either pushed upwards or pulled downwards. By connection of the additional spine to the threaded rod by means of a nut, the element performs a folding and unfolding movement.



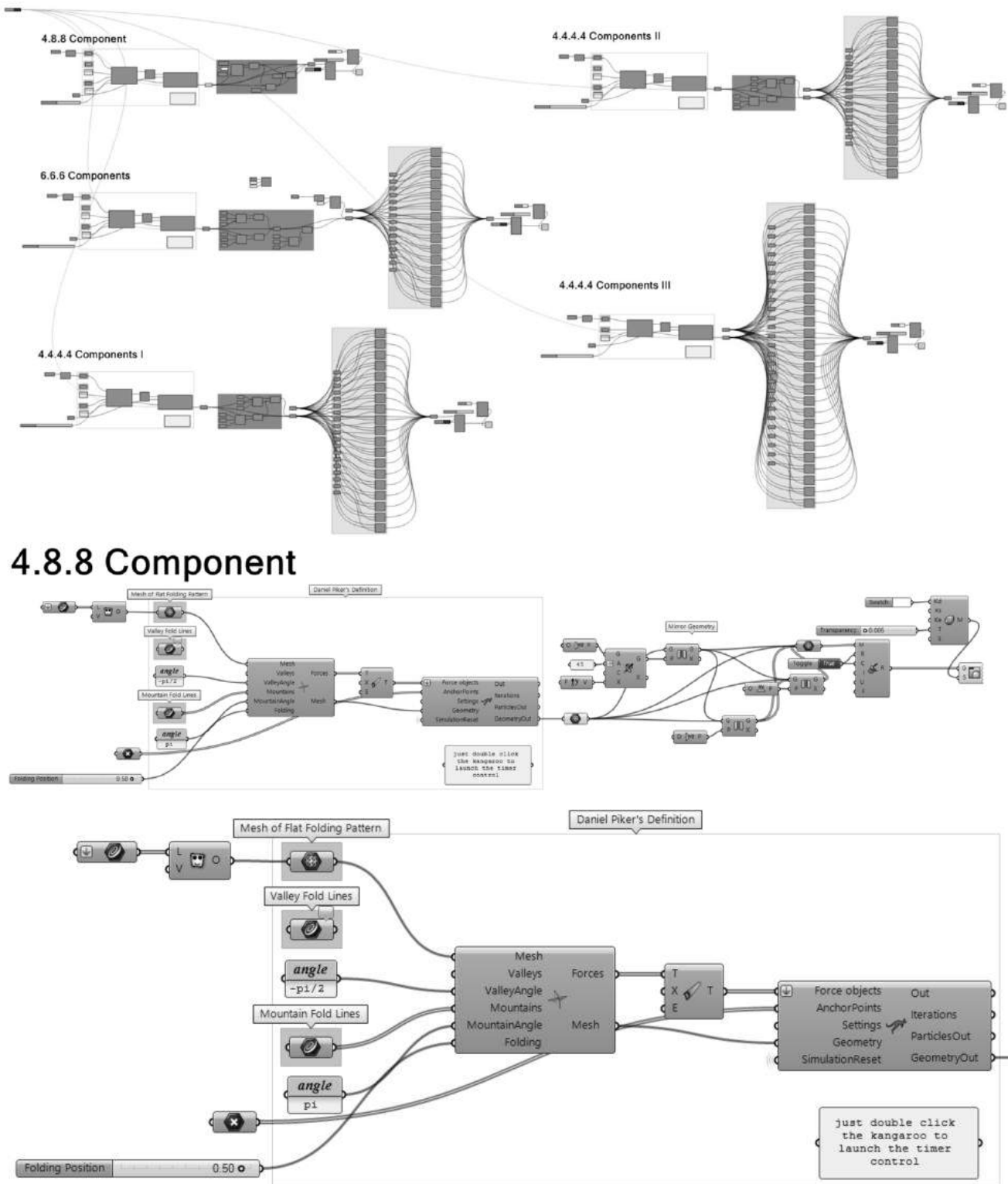
**Figure D - 2:** Motion sequence of the medium-scale prototype developed by (Vergauwen 2016). The side length of the triangular curved-line folding element with 3 concave creases is 0,89 m and the spine width at the boundaries is 0,03 m.

## Redesign – Arabic geometric patterns



**Figure D - 3:** Representation a redesigned module of the AWI with curved-line folding elements in open (top) and intermediate (bottom) configurations, showing more polygons and Islamic star patterns than in the original design with diaphragms.

## Redesign – Kinematic simulations



**Figure D - 4:** From top to bottom: 1) Global view of the Grasshopper script for the kinematic simulation of the entire redesigned module of the AWI with curved-line folding elements. By clicking one Boolean toggle unit, all the elements in the module can be activated at once. The long vertical series of units are needed to copy the components to all the corresponding locations within the module. 2) Script for the simulation of the central component. 3) Daniel Piker's definition for the kinematic simulation of origami elements. The folding pattern mesh is modelled in Rhinoceros and goes to the input of an Origami cluster unit along with the defined mountain folds and folding angles. The output is a set of forces and a new mesh, which serve as the input for the Kangaroo Live Physics unit to simulate the folding process.



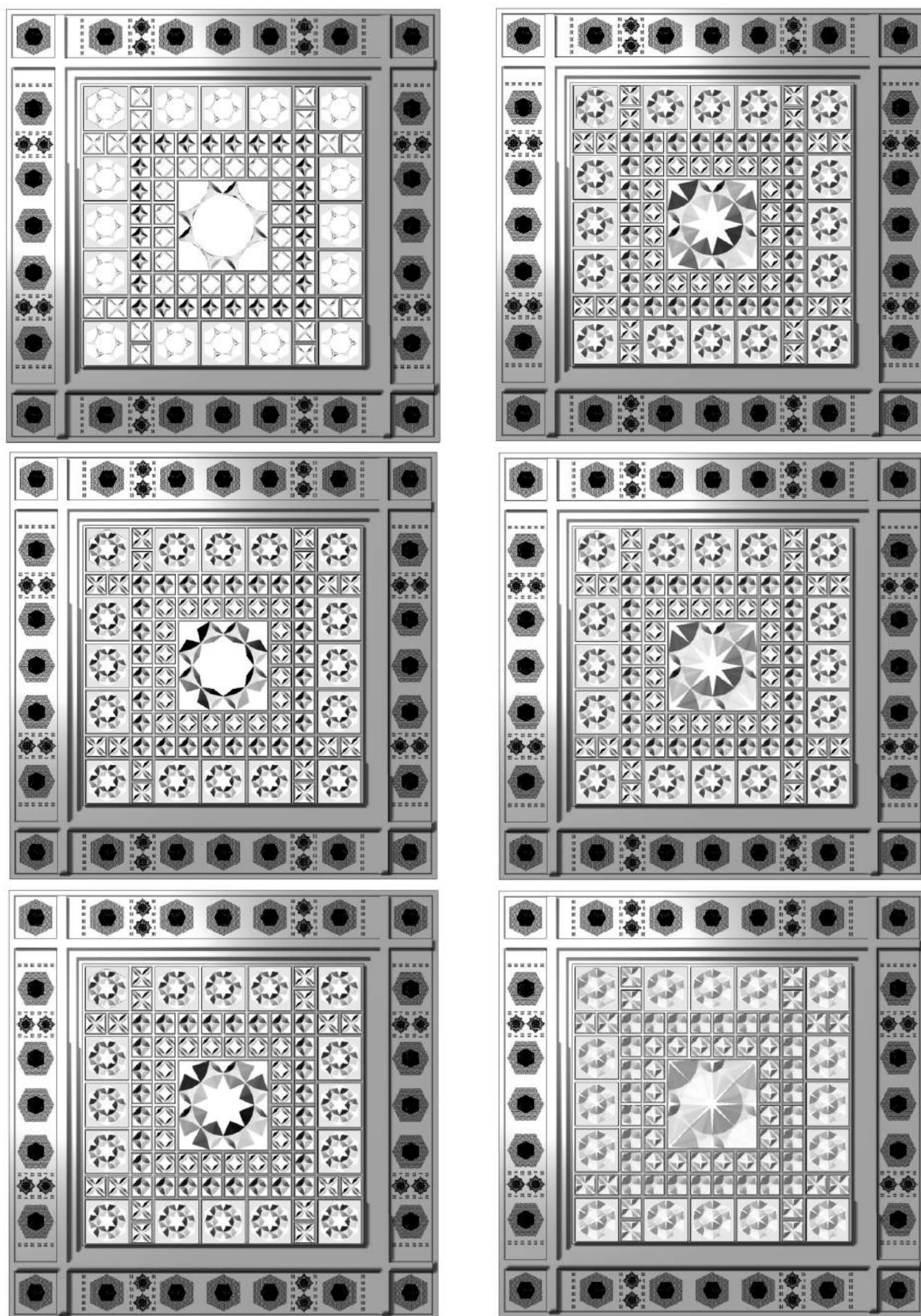


Figure D - 5: Motion sequence of the redesigned module with curved-line folding elements. The unfolding movement starts in the open configuration (top-left) and ends in the closed configuration (bottom-right) of the module.



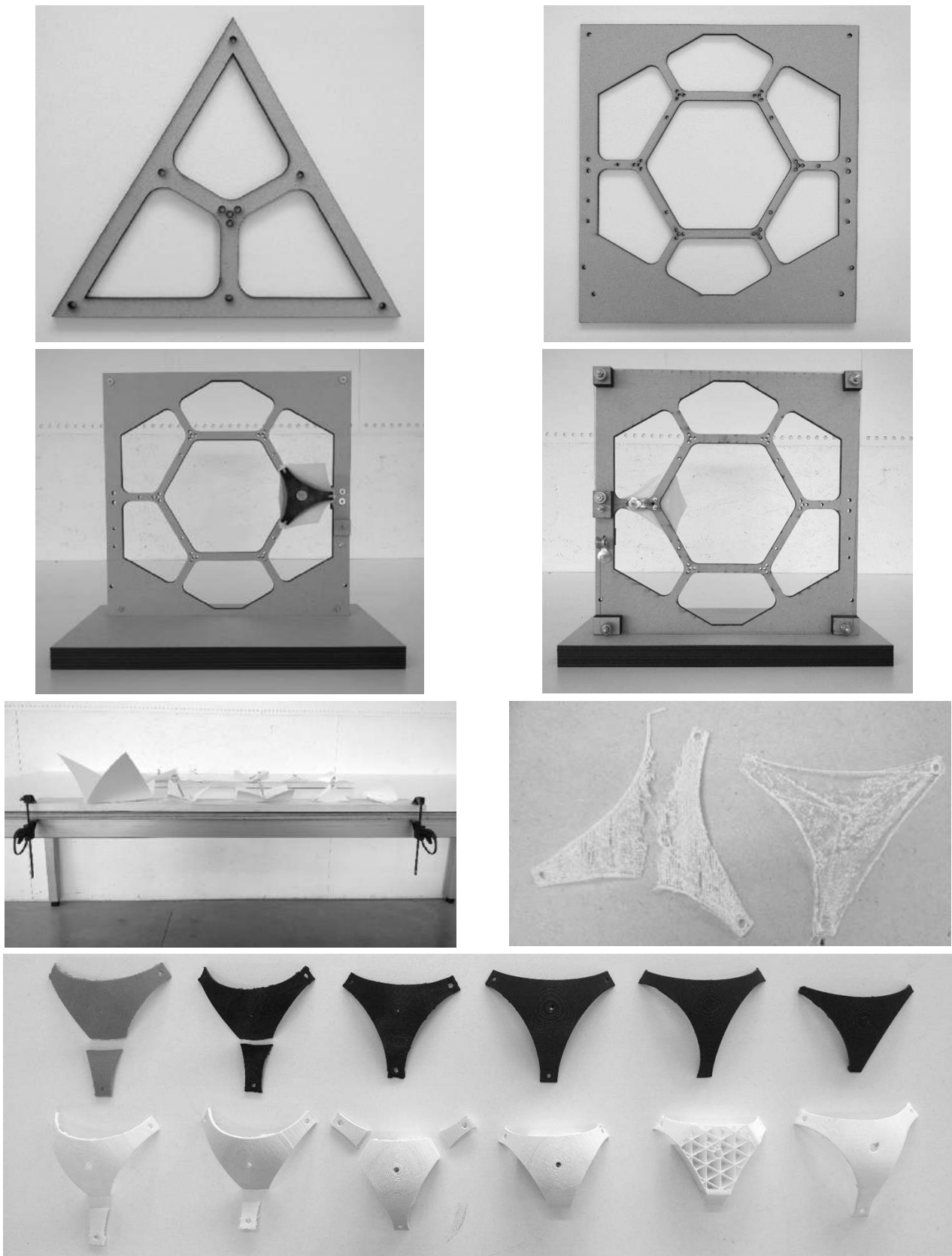
## Prototyping

1. Density	0.235 lb/in <sup>3</sup> (6.45 g/cm <sup>3</sup> )
2. Specific Heat	0.20 BTU/lb * °F (0.2 cal/g * °C)
3. Melting Point	2370 °F (1300 °C)
4. Latent Heat of Transformation	10.4 BTU/lb (5.78 cal/g)
5. Thermal Conductivity	10.4 BTU/hr * ft * °F (0.18 W/cm * °C)
6. Thermal Expansion Coefficient	
Martensite	3.67x10 <sup>-6</sup> /°F (6.6x10 <sup>-6</sup> /°C)
Austenite	6.11x10 <sup>-6</sup> /°F (11.0x 10 <sup>-6</sup> /°C)
7. Poisson Ratio	0.33
8. Electrical Resistivity (approx.)	
Martensite:	32 micro-ohms * in (80 micro-ohms * cm)
Austenite:	39 micro-ohms * in (100 micro-ohms * cm)

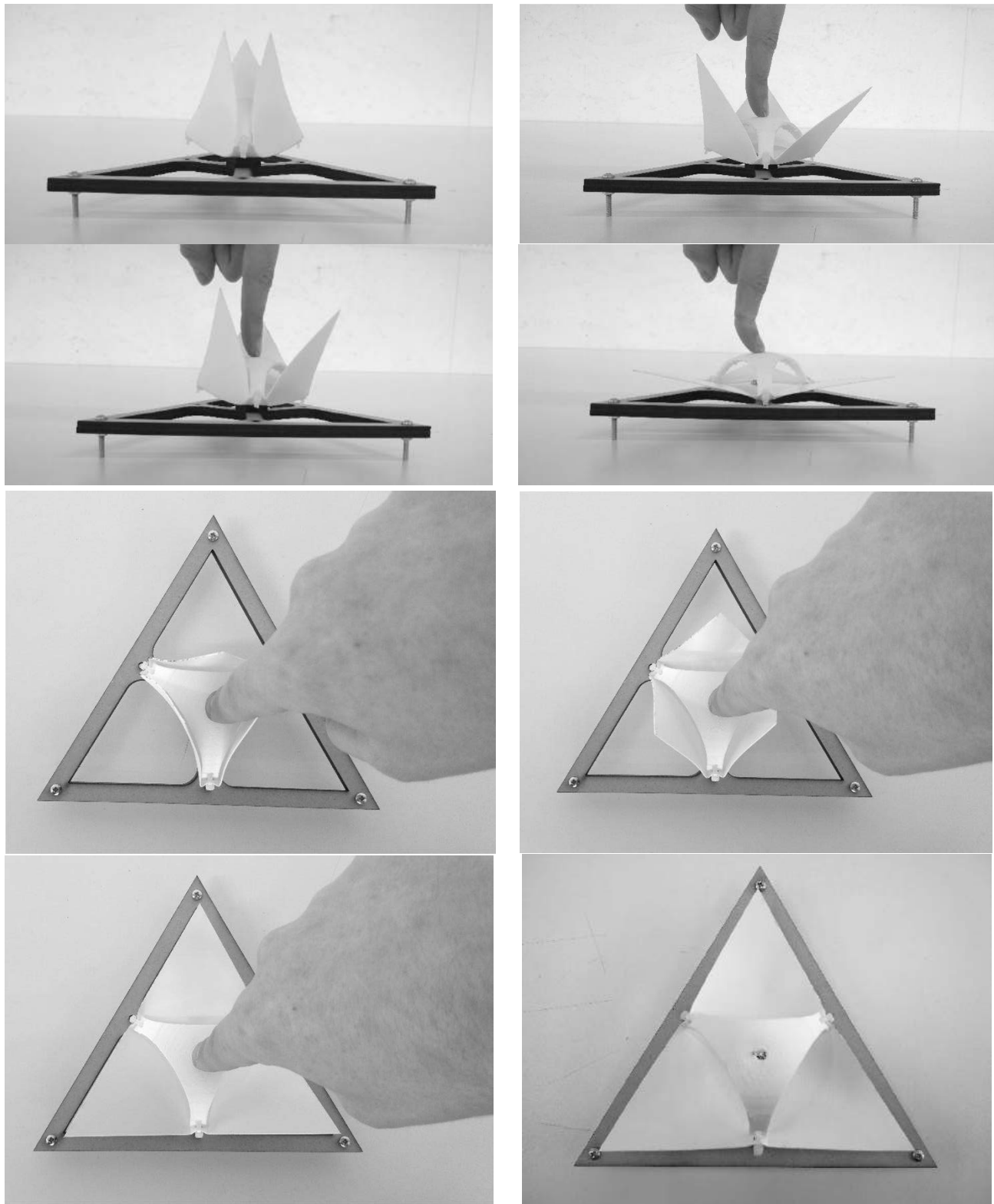
Diameter Size inches (mm)	Resistance ohms/inch (ohms/meter)	Pull Force* pounds (grams)	Cooling Deformation Force* pounds (grams)	Approximate** Current for 1 Second Contraction (mA)	Cooling Time 158°F, 70°C "LT" Wire *** (seconds)	Cooling Time 194°F, 90°C "HT" Wire *** (seconds)
0.001 (0.025)	36.2 (1425)	0.02 (8.9)	0.008 (3.6)	45	0.18	0.15
0.0015 (0.038)	22.6 (890)	0.04 (20)	0.016 (8)	55	0.24	0.20
0.002 (0.050)	12.7 (500)	0.08 (36)	0.032 (14)	85	0.4	0.3
0.003 (0.076)	5.9 (232)	0.18 (80)	0.07 (32)	150	0.8	0.7
0.004 (0.10)	3.2 (126)	0.31 (143)	0.12 (57)	200	1.1	0.9
0.005 (0.13)	1.9 (75)	0.49 (223)	0.20 (89)	320	1.6	1.4
0.006 (0.15)	1.4 (55)	0.71 (321)	0.28 (128)	410	2.0	1.7
0.008 (0.20)	0.74 (29)	1.26 (570)	0.50 (228)	660	3.2	2.7
0.010 (0.25)	0.47 (18.5)	1.96 (891)	0.78 (356)	1050	5.4	4.5
0.012 (0.31)	0.31 (12.2)	2.83 (1280)	1.13 (512)	1500	8.1	6.8
0.015 (0.38)	0.21 (8.3)	4.42 (2004)	1.77 (802)	2250	10.5	8.8
0.020 (0.51)	0.11 (4.3)	7.85 (3560)	3.14 (1424)	4000	16.8	14.0

	Approx. Stroke	0.003" Wire (0.076 mm)	0.006" Wire (0.15 mm)	0.010" Wire (0.25 mm)
Normal Bias Spring	3%	0.18 lb (80 g)	0.73 lb (330 g)	2.05 lb (930 g)
Dead Weight Bias	4%	0.18 lb (80 g)	0.73 lb (330 g)	2.05 lb (930 g)
Leaf Spring Bias	7%	0.18 lb (80 g)	0.73 lb (330 g)	2.05 lb (930 g)
Right Angle Pull	14%	0.04 lb (20 g)	0.18 lb (83 g)	0.51 lb (232 g)
Simple Lever (6:1 ex)	30%	0.024 lb (11 g)	0.10 lb (47 g)	0.29 lb (133 g)
Adjusting Curvature	110%	0.006 lb (3 g)	0.026 lb (12 g)	0.075 lb (34 g)
Clam Shell	100%	0.007 lb (3.2 g)	0.028 lb (13 g)	0.082 lb (37 g)

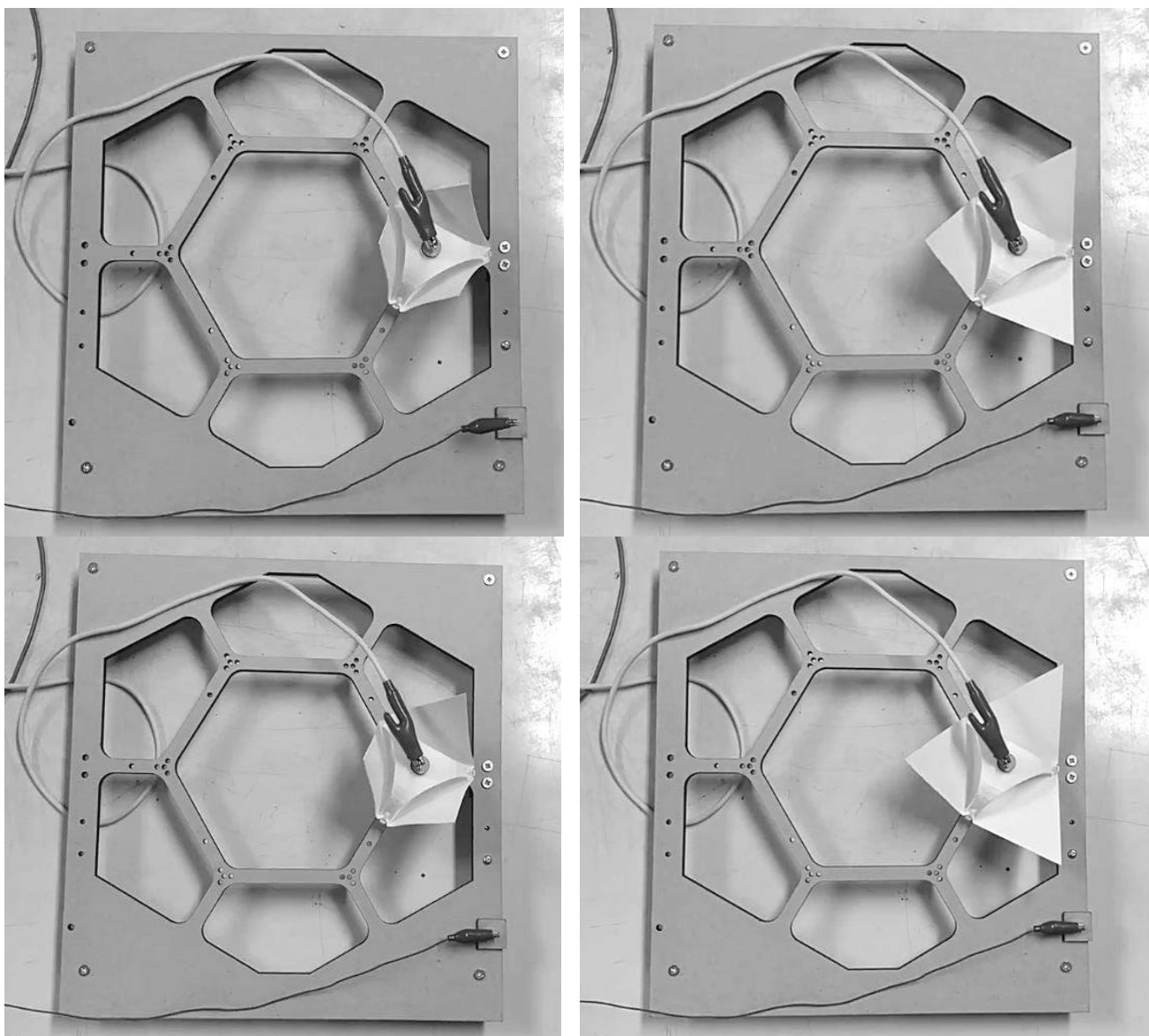
**Figure D – 6:** Datasheets for the Flexinol® actuator wire purchased from Dynalloy Inc. (‘DYNALLOY, Inc. Makers of Dynamic Alloys’ n.d.). From top to bottom: 1) Summary of the physical properties. 2) Electrical guidelines. The wire used for the prototypes is highlighted. 3) Stroke and available forces for some basic structures. The structure used in the prototypes is highlighted.



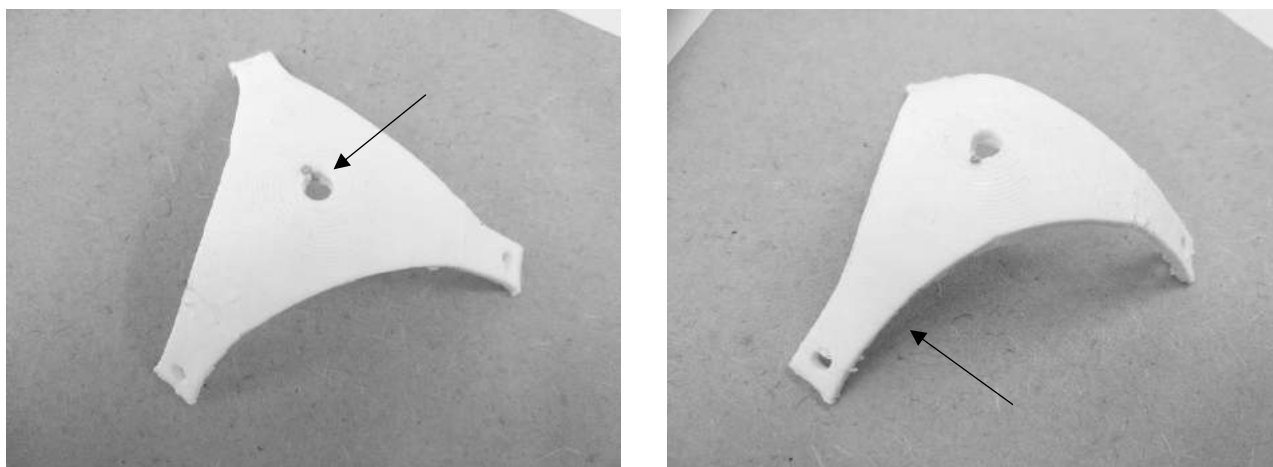
**Figure D - 7:** From top to bottom: 1) Wooden frame used for the pre-folding methods (left) and for the actuation methods with the Nitinol wire (right). The corners are round off to reduce stresses when the curved-line folding element is pushed to unfold. 2) Front (left) and rear (right) view of the 6.6.6 component frame with one curved-line folding element actuated by a Nitinol wire of  $\pm 1$  m long. 3) Experimental set-up for the folding force measurements (left) and poor printing results for the elastic spine with nylon and plasticized copolyamide thermoplastic elastomer (PCTPE) filaments (right). 4) Evolution process for the pre-bent spine with polylactic acid (PLA) filament. A compromise between thickness and curvature was required to obtain a sufficiently strong spine that would not break when actuated by the Nitinol actuator wire.



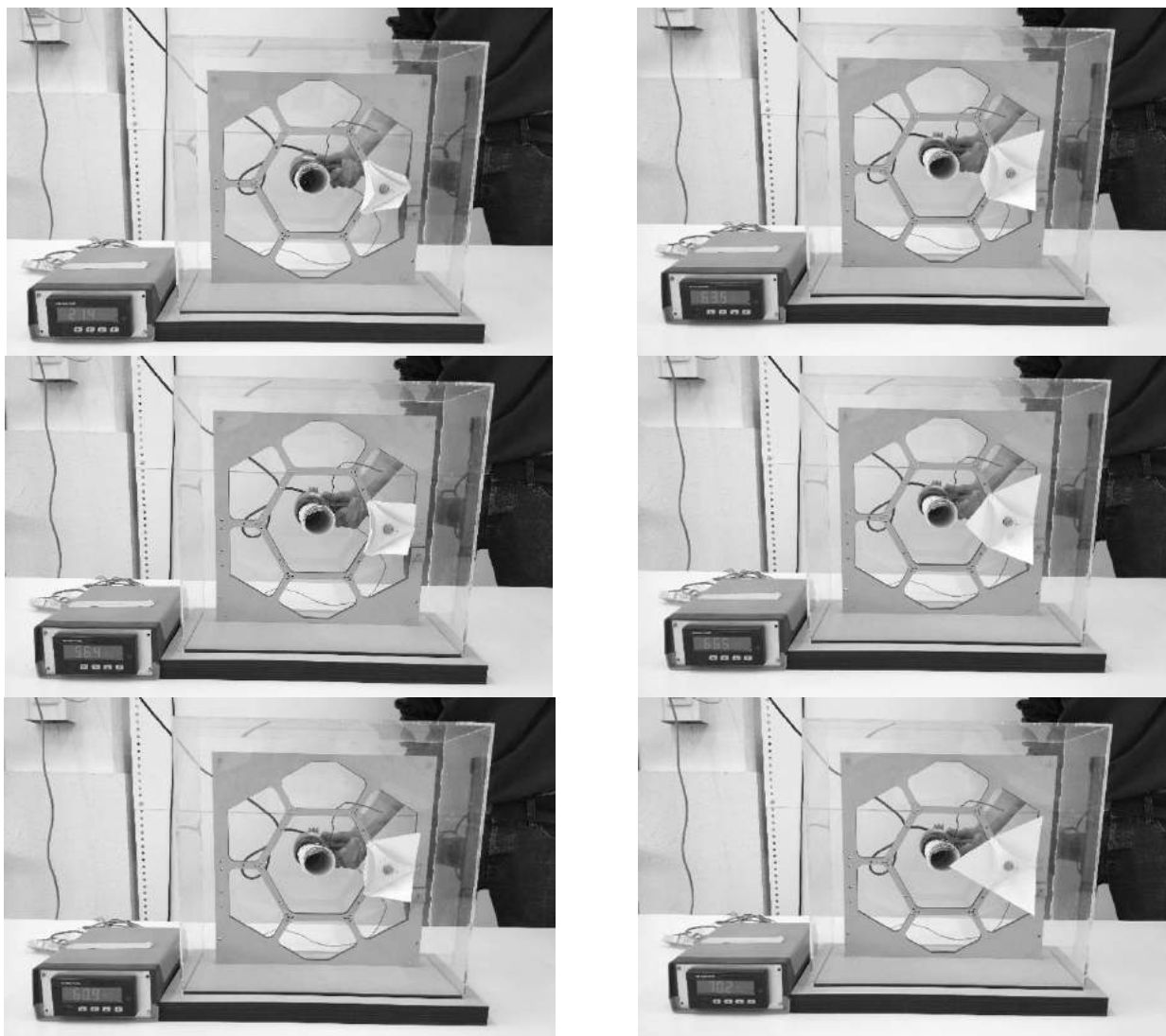
**Figure D- 8:** Motion sequence of the curved-line folding element with a pre-bent spine under a vertical point load in frontal and top view. The bottom-right image shows the bi-stable position from which the element cannot return without mechanical effort.



**Figure D - 9:** Motion sequence of the curved-line folding element actuated by electrical current. The time interval between the pictures is 10 s and the bottom-right is taken at 30 s after application of current.



**Figure D - 10:** Burning of the heated actuator wire in the central hole of the pre-bent spine. The right image shows the plastic deformation of the spine due to excessive pulling of the wire when actuated.



**Figure D - 11:** Motion sequence of the curved-line folding element actuated by ambient heat in an acrylic glass box. The experiment starts at room temperature, the element starts to unfold at  $\pm 50^\circ\text{C}$  and reaches a bi-stable state at  $\pm 70^\circ\text{C}$ . At this point, the element requires mechanical effort to return to its folded state.